



<https://theses.gla.ac.uk/>

Theses Digitisation:

<https://www.gla.ac.uk/myglasgow/research/enlighten/theses/digitisation/>

This is a digitised version of the original print thesis.

Copyright and moral rights for this work are retained by the author

A copy can be downloaded for personal non-commercial research or study, without prior permission or charge

This work cannot be reproduced or quoted extensively from without first obtaining permission in writing from the author

The content must not be changed in any way or sold commercially in any format or medium without the formal permission of the author

When referring to this work, full bibliographic details including the author, title, awarding institution and date of the thesis must be given

Enlighten: Theses

<https://theses.gla.ac.uk/>  
[research-enlighten@glasgow.ac.uk](mailto:research-enlighten@glasgow.ac.uk)

**THE EFFECT OF REACTIVE NITROGEN INTERMEDIATES  
ON *LEISHMANIA MEXICANA MEXICANA*.**

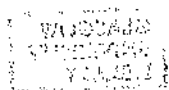
**William Hugh Hathorn Reece**

**A thesis submitted for the degree of Doctor of Philosophy to the  
Faculty of Science at the University of Glasgow.**

University of Glasgow,  
Department of Immunology,  
Western Infirmary,  
Glasgow, G11 6NT

© William H. H. Reece

June 1997



ProQuest Number: 10390898

All rights reserved

INFORMATION TO ALL USERS

The quality of this reproduction is dependent upon the quality of the copy submitted.

In the unlikely event that the author did not send a complete manuscript and there are missing pages, these will be noted. Also, if material had to be removed, a note will indicate the deletion.



ProQuest 10390898

Published by ProQuest LLC (2017). Copyright of the Dissertation is held by the Author.

All rights reserved.

This work is protected against unauthorized copying under Title 17, United States Code  
Microform Edition © ProQuest LLC.

ProQuest LLC.  
789 East Eisenhower Parkway  
P.O. Box 1346  
Ann Arbor, MI 48106 – 1346





Thesis  
10930  
copy 2

## Summary

*Leishmania mexicana mexicana* is a protozoan parasite that causes local and diffuse cutaneous leishmaniasis. There are no effective current vaccines, and current drugs have serious side effects. There is a wealth of evidence, both *in vitro* and *in vivo*, to suggest that the protective murine immune response involves the production of a set of partially oxidised products of nitrogen called Reactive Nitrogen Intermediates (RNI). RNI are synthesised during a protective murine immune response by the enzyme inducible Nitric Oxide Synthase (iNOS) and are extremely diverse both in their possible chemical targets and in their biological effects. Inhibition of RNI production in murine cutaneous leishmaniasis allows the parasite to survive in normally resistant hosts, and it is believed that they are the final effector mechanism in the protective T<sub>H</sub>1-type immune response.

Very little was known about the targets of RNI in *Leishmania*. This thesis aims to investigate the processes by which RNI kill *L. m. mexicana*. This species was chosen because it has recently become possible to grow it as amastigotes axenically *in vitro*. [<sup>3</sup>H]-thymidine uptake and transformation efficiency viability assays were optimised for use with these axenic amastigotes. In addition, because of the unusual culture conditions for amastigotes - Schneider's Drosophila Medium, pH 5.5, with 20% (v/v) foetal calf serum - it was necessary to develop suitable methods for RNI production and detection.

Production of RNI by S-nitroso-N-acetyl penicillamine and by acidified nitrite was used.

Little work has been done on the role of RNI in the immune response to *L. m. mexicana*. Therefore, the susceptibility of this species to RNI produced by murine macrophages was determined. The kinetics of toxicity in axenic culture showed that RNI were cytotoxic rather than cytostatic to this species, and that RNI can take up to several hours to kill the parasite. RNI did not affect, and were not affected by various other

components of the macrophage defence mechanism, namely  $\beta$ -glucuronidase, cathepsin D and hydrogen peroxide.

*L. m. mexicana* amastigotes were shown not to be particularly resistant to RNI compared to promastigotes, *Escherichia coli*, and the murine macrophage cell line J774. Low levels of RNI were also shown to be insufficient to induce a resistant phenotype in the parasite.

There have been many suggestions of the possible antileishmanial targets of RNI, based on the action of RNI in other cell types. These include inhibition of the mitochondrial electron transport chain and other iron-containing proteins, damage to lipids, damage to DNA, damage of membrane components held on to the membrane by glycosyl-phosphatidylinositol (GPI) anchors, and inhibition of proteins that contain sulphhydryl groups or tyrosine residues. The effect of RNI on the GPI-anchored glycoinositolphospholipids (GIPLs), DNA and mitochondrion of *L. m. mexicana* was examined. Of these, only the mitochondrion was affected by RNI at concentrations which approximated to the toxic concentrations, though DNA and GIPLs could be damaged by much higher concentrations of RNI. Inhibition of the mitochondrion was sufficient to account for all the toxicity of RNI to the parasite, since uncoupling the mitochondrial membrane with 2,4-dinitrophenol (DNP) caused similar kinetics of toxicity to RNI. It was also possible to inhibit the DNase activity of serum, and the implications of this to other biological systems are discussed.

The involvement of the mitochondrion in the toxicity of RNI to amastigotes is not surprising given the evolutionary conservation of the enzymes in the mitochondrial electron transport chain, and given the involvement of these enzymes in RNI toxicity to *E. coli* and mammalian cells. However, since *L. m. mexicana* normally reside in low oxygen

tensions, one might have expected that they would not be so reliant on their mitochondrion.

## Acknowledgements

There are many people who helped me with this thesis, to all of whom I am eternally grateful. Professor Foo "Eddy" Liew has provided me with invaluable supervision throughout all three and a half years of this project, and I would like to thank him for sharing with me his scientific experience and wisdom, and for his almost limitless patience with me. Dr Lorna Proudfoot's supervision has also been of inestimable help, she has come up with some of the great ideas in this project, run with me through the highs, kept my head level through the lows, and been a good friend throughout. A big thank you as well to Professor Graham Coombs without whose supervision, I would have been totally at sea, who has so unselfishly given up his time at often far too short notice to help me out, and who has provided the most excellent insight into the project.

Dr Billy Sands has also throughout this project provided extremely useful advice, and insight into almost every single aspect of my work, most especially anything that involved fluorescence, or required a knowledge of other parasites. I would like to thank him for his interest, enthusiasm, and disgusting sense of humour. A big thank you also to Dr Jeremy Mottram of the Wellcome Unit of Parasitology in Glasgow for his help, both in the initial assessment of the project, and in much of the work on DNA. Dr Damo Xu and Dr Xiao-Qing Wei were also wonderfully helpful with the DNA work, and helped make some of the very hard times actually enjoyable.

I would also like to thank Dr Lawrence Tetley and Margaret Mullen for preparing all the electron microscopy specimens and pictures, as well as their extremely useful help in interpreting the results. Thanks also to Christina Ross, Dr Charles McSharry and Eric Galloway for their kind supervision, care and attention during all the FACS work. Thanks

also to June Freel for her help in setting up the Oxygen electrode. Thanks also to David Laughland for his preparation of much of the media used in this thesis, looking after the laboratory, and for providing me with some of the worst jokes that I now have in my repertoire.

Finally, a big thank you to all my colleagues and friends in the Immunology Department and the Laboratory for Biochemical Parasitology, or whatever it will be called by the time you read this thesis. Without their friendship and support, this could never have happened.

# Index

	<b>Page</b>
Title.....	i
Summary.....	ii
Acknowledgements.....	v
Index.....	vii
List of Figures and Tables.....	xiv
Declaration.....	xix
Publications.....	xx
Abbreviations.....	xxi
1. Introduction.....	1
1.1 Leishmaniasis .....	2
1.1.1 Prevalence .....	2
1.1.2 Pathology.....	2
1.1.3 Species classification.....	3
1.1.4 Treatment .....	4
1.2 <i>Leishmania</i> life cycle.....	5
1.3 The composition of RNI.....	7
1.4 Production of RNI in biological systems.....	9

1.5 Inhibition of RNI production .....	10
1.5.1 Prevention of RNI production .....	10
1.5.2 Reduction of reactive RNI concentrations .....	11
1.6 The role of RNI in <i>Leishmania</i> infection.....	12
1.6.1 <i>In vivo</i> RNI production.....	12
1.6.2 <i>In vitro</i> RNI production and leishmanicidal activity.....	12
1.6.3 Studies on the factors required for iNOS induction compared to those for resistance to <i>Leishmania</i> . .....	15
1.6.4 Other macrophage defence mechanisms. ....	19
1.7 RNI production by humans.....	20
1.8 Delivery of RNI to the parasitophorous vacuole .....	21
1.9 Possible targets for RNI.....	22
1.9.1 Primary chemical targets.....	22
1.9.2 Secondary effects of RNI .....	27
1.10 The interaction of RNI with ROI.....	28
1.11 Defence against RNI.....	29
1.12 Aims of this thesis. ....	30
2. Materials and methods .....	32
2.1 Materials .....	33
2.2 Cell culture.....	39

2.2.1 Macrophages .....	39
2.2.2 <i>Leishmania</i> .....	39
2.2.3 Amastigotes .....	39
2.2.4 Promastigotes .....	40
2.2.5 <i>Tritrichomonas foetus</i> .....	40
2.2.6 <i>Escherichia coli</i> and <i>Salmonella typhimurium</i> .....	41
2.3 Animal subpassage of <i>L. m. mexicana</i> .....	41
2.4 Transformation efficiency assay of amastigote viability .....	42
2.5 Measurement of RNI production .....	42
2.6 Macrophage killing of amastigotes .....	43
2.7 Amastigote proliferation using [ <sup>3</sup> H]-Thymidine .....	44
2.8 Treatment with S-Nitrosothiols .....	44
2.9 Treatment with Sodium Nitrite .....	45
2.10 Measurement of ATP levels .....	47
2.11 Measurement of Rhodamine 123 uptake .....	47
2.12 Labelling and preparation of glycoinositol phospholipids (GIPLs) .....	48
2.12.1 Labelling: .....	48
2.12.2 Extraction: .....	48
2.12.3 Purification: .....	48
2.12.4 Treatment with RNI: .....	49

2.12.5 Determination of the amount of deglycosylation:.....	49
2.13 Electron microscopy .....	49
2.14 Oxygen uptake measurement.....	50
2.15 DNA assays .....	51
2.15.1 Buffers used: .....	51
2.15.2 Preparation of DNA from amastigotes:.....	52
2.15.3 Fluorimeter measurement of DNA concentration:.....	52
2.15.4 Nicking of DNA with DNase 1:.....	53
2.15.5 Nick translation:.....	54
2.15.6 Detection of labelled DNA:.....	54
3. Optimisation of assays for <i>L. m. mexicana</i> viability and <i>in vitro</i> production and detection of RNI.....	56
3.1 Introduction.....	57
3.2 Development of viability assays .....	58
3.2.1 Thymidine assay.....	58
3.2.2 Transformation assay. ....	59
3.3 Production and measurement of RNI. ....	62
3.3.1 Introduction .....	62
3.3.2 Absorption properties of the Griess reaction.....	63
3.3.3 Determination of the rate of release of RNI from SNAP .....	64

3.3.4 Release of RNI from SNAP in amastigote culture medium.....	70
3.3.5 The toxicity of SNAP to amastigotes.....	70
3.4 Production of RNI using acidified nitrite .....	74
3.5 <i>L. m. mexicana</i> infection of J774 cells at 32°C .....	79
3.6 Conclusions .....	83
4. Guideline experiments .....	86
4.1 Introduction.....	87
4.2 The interaction of RNI with other parasitophorous vacuole components .....	88
4.2.1 $\beta$ -glucuronidase and cathepsin D.....	88
4.2.2 Hydrogen peroxide .....	92
4.3 Comparative analysis of amastigote susceptibility to RNI.....	95
4.3.1 Comparison to promastigotes.....	95
4.3.2 Comparison to J774 cells .....	98
4.3.3 Comparison to <i>E. coli</i> , <i>S. typhimurium</i> , and <i>T. foetus</i> .....	98
4.4 The effect of low levels of RNI on <i>L. m. mexicana</i> amastigotes.....	104
4.5 Conclusions .....	107
5. RNI kill <i>Leishmania mexicana mexicana</i> .....	110
5.1 Introduction.....	111
5.2 Macrophage toxicity to <i>L. m. mexicana</i> amastigotes.....	111
5.3 The kinetics of RNI toxicity <i>in vitro</i> .....	114

5.3.1 Concentration curve of RNI toxicity .....	114
5.3.2 Time course of RNI toxicity.....	115
5.3.3 The effect of changing the concentration of amastigotes.....	119
5.4 Ultrastructural changes to amastigotes on treatment with RNI.....	122
5.5 Conclusions .....	127
6. The effect of RNI on glycoinositolphospholipids and DNA .....	130
6.1 Introduction.....	131
6.2 The effect of RNI on GIPLs .....	132
6.3 DNA damage .....	135
6.3.1 Development of the nick translation system .....	137
6.4 Detection of damage to amastigote DNA caused by RNI. ....	147
6.4.1 The effect of RNI on DNA in intact amastigotes.....	147
6.4.2 The direct effect of RNI on DNA <i>in vitro</i> .....	153
6.4.3 The effect of RNI on DNA in amastigote culture medium. ....	155
6.5 Conclusions .....	158
7. The effect of RNI on amastigote mitochondrial function. ....	161
7.1 Introduction.....	162
7.2 Axenically cultured amastigotes are susceptible to mitochondrial toxins.....	163
7.3 RNI inhibition of mitochondrial function.....	167
7.3.1 Oxygen consumption .....	167

7.3.2 The mitochondrial membrane potential .....	171
7.4 The effect of RNI on the concentration of ATP. ....	185
7.4.1 Development of the assay system .....	185
7.4.2 The effect of RNI on the concentration of ATP in amastigotes. ....	190
7.5 Discussion.....	196
8. General discussion .....	199
8.1 Viability assays.....	200
8.2 J774 toxicity to amastigotes. ....	202
8.3 The interaction of other PV toxins with RNI.....	203
8.4 Amastigote defence mechanisms against RNI.....	204
8.4.1 The kinetics of toxicity.....	208
8.5 The mechanism of killing. ....	209
8.6 <i>In vivo</i> relevance. ....	211
8.7 RNI inhibition of DNase in serum.....	212
8.8 Chemical targets of RNI in <i>Leishmania</i> . ....	214
8.9 RNI production by acidified nitrite.....	215
8.10 Future experiments .....	217
9. References .....	219

## List of figures and tables

### Chapter 1

Table 1.1: Species classification of the American <i>Leishmania</i> .	4
Table 1.2: The reactions by which RNI are formed.	7
Table 1.3: Stimuli for RNI production and leishmanicidal activity by macrophages.	14

### Chapter 3

Figure 3.1: [ <sup>3</sup> H]-thymidine uptake by amastigotes	60
Figure 3.2: Transformation efficiency assay.	61
Figure 3.3: Absorption spectrum for the Griess reaction.	65
Figure 3.4: Absorption spectrum for the Griess reaction in water	66
Figure 3.5: Absorption spectrum the Griess reaction in DMEM	67
Figure 3.6: The kinetics of the Griess reaction	68
Figure 3.7: Stability of the Griess reaction	69
Figure 3.8: The rate of release of RNI from SNAP in the Griess reagent.	71
Figure 3.9: Rate of release of RNI from SNAP in amastigote culture medium.	72
Figure 3.10: The effect of SNAP on amastigotes	73
Figure 3.11: The toxicity of a solution of sodium nitrite depends on the pH.	76
Figure 3.12: The toxicity of a solution of sodium nitrite correlates with the concentration of nitrous acid (HONO).	77
Figure 3.13: The effect of leaving the acidified nitrite solution for 24 h.	78

Table 3.1: Efficiency of the lysis protocol.	81
Figure 3.14: J774 macrophages can produce RNI and kill <i>L. m. mexicana</i> .	82
 <u>Chapter 4</u>	
Figure 4.1: The effect of $\beta$ -glucuronidase on [ $^3$ H]-thymidine uptake by amastigotes.	89
Figure 4.2: The effect of cathepsin D on [ $^3$ H]-thymidine uptake by amastigotes.	90
Figure 4.3: The effect of PV enzymes on RNI toxicity.	91
Figure 4.4: The effect of hydrogen peroxide on [ $^3$ H]-thymidine uptake by amastigotes.	93
Figure 4.5: Isobologram of the toxicity of RNI and hydrogen peroxide on amastigotes	94
Figure 4.6: Comparison of the susceptibility of amastigotes and promastigotes to RNI at pH 5.5.	96
Figure 4.7: Comparison of the susceptibility of amastigotes and promastigotes at pH 6.5.	97
Figure 4.8: Comparative susceptibility of amastigotes and J774s to RNI at pH 5.5	99
Figure 4.9: Comparison of the susceptibility to RNI of J774s and amastigotes at pH 6.5.	100
Figure 4.10: Uptake of [ $^3$ H]-thymidine by <i>E. coli</i> and <i>S. typhimurium</i> .	101
Figure 4.11: Uptake of [ $^3$ H]-thymidine by <i>Tritrichomonas foetus</i>	102
Figure 4.12: Comparison of the susceptibility of <i>E. coli</i> and <i>L. m. mexicana</i> amastigotes to RNI.	103
Figure 4.13: Attempt to induce amastigote resistance to RNI by prior exposure.	105

Figure 4.14: Low levels of RNI cause the parasites to take up more [<sup>3</sup>H]-thymidine 106

## Chapter 5

Figure 5.1: *L. m. mexicana* are susceptible to an arginine dependent macrophage killing mechanism 113

Figure 5.2: The effect of RNI on viability and [<sup>3</sup>H]-thymidine uptake by amastigotes. 116

Figure 5.3: Time course of RNI toxicity. 117

Figure 5.4: More RNI kill amastigotes faster. 118

Figure 5.5: Toxicity of RNI at graded concentrations of parasites. 120

Figure 5.6: Time course of RNI toxicity at different concentrations of amastigotes. 121

Figure 5.7: Electron microscopy of amastigotes treated with RNI 123

Table 5.1: Number of nuclei disrupted by RNI. 126

## Chapter 6

Figure 6.1: Structure of GIPL and where it is attacked by RNI (183,246) 132

Figure 6.2: The effect of RNI on GIPL integrity. 134

Figure 6.3: Overview of the nick translation procedure. 136

Figure 6.4: Nick translation of amastigote DNA. 138

Figure 6.5: Time course of the nick translation reaction with 3.5  $\mu$ M dATP 140

Figure 6.6: Nick translation of amastigote DNA with 80  $\mu$ M dATP. 141

Figure 6.7: The effect of DNase 1 on DNA labelling in the nick translation reaction. 143

Figure 6.8: DNase 1 standard curve with the amastigote DNA being nicked before the translation reaction. 145

Figure 6.9: Standard curve of DNase 1.	146
Figure 6.10: Nick translation of amastigote DNA using the modified nick translation assay.	149
Figure 6.11: DNase 1 standard curve and nick translation of amastigote DNA	150
Figure 6.12: Standard curve of ethidium bromide fluorescence.	151
Figure 6.13: The effect of RNI on nick translation of amastigote DNA.	152
Figure 6.14: The direct effect of RNI on amastigote DNA.	154
Figure 6.15: The effect of RNI on degradation of DNA in amastigote culture medium.	156
Figure 6.16: Degradation of DNA by serum in amastigote culture medium	157
 <u>Chapter 7</u>	
Figure 7.1: The effect of sodium azide on [ <sup>3</sup> H]-thymidine uptake by amastigotes.	165
Figure 7.2: The effect of FCCP on [ <sup>3</sup> H]-thymidine uptake by amastigotes.	166
Figure 7.3: The effect of DNP on [ <sup>3</sup> H]-thymidine uptake by amastigotes.	167
Figure 7.4: Oxygen consumption by amastigotes.	169
Figure 7.5: Inhibition of amastigote oxygen consumption by SNAP.	170
Figure 7.6: The effect of fixation on Rh123 retention by amastigotes.	172
Figure 7.7: Uptake of Rh123 over time.	174
Figure 7.8: Concentration curve of the effect of DNP on Rh123 uptake.	175
Figure 7.9: Time course of the effect of RNI on Rh123 uptake.	178
Figure 7.10: Arbitrary division of particles into four sizes.	179

Figure 7.9: Time course of the effect of RNI on Rh123 uptake.	178
Figure 7.10: Arbitrary division of particles into four sizes.	179
Figure 7.11: Analysis of the time course of Rh123 uptake in terms of the different sizes of particles.	180
Figure 7.12: The effect of RNI on Rh123 uptake by amastigotes.	181
Figure 7.13: Comparison of the effect of RNI on Rh123 and [ <sup>3</sup> H]-thymidine uptake.	183
Figure 7.14: The effect of DNP on Rh123 and [ <sup>3</sup> H]-thymidine uptake.	184
Table 7.1: Determination of the detectable concentration of ATP.	187
Figure 7.15: The luminometer reading decays with time.	188
Figure 7.16: Construction of a standard curve of ATP in SDM + FCS.	188
Figure 7.17: Detection of ATP in 10 <sup>6</sup> amastigotes.	189
Figure 7.18: Time course of the effect of RNI on the concentration of ATP in amastigotes.	192
Figure 7.19: The effect of different concentrations of RNI on the concentration of ATP.	193
Figure 7.20: Higher concentrations of DNP kill amastigotes faster.	194
Figure 7.21: The effect of different concentrations of DNP on amastigote viability and ATP concentrations.	195

## **Declaration**

These studies represent original work carried out by the author, and have not been submitted in any form to any other University. Where use has been made of material provided by others, due acknowledgement has been made.

June 1997

William Hugh Hathorn Reece

## Publications

Parts of this thesis have been included in the following publication:

Reece, W. H. H., L. Proudfoot, G. H. Coombs and F.-Y. Liew. 1996.

Quantification and characterisation of the effect of Reactive Nitrogen Intermediates on *Leishmania mexicana*. In "The Biology of Nitric Oxide Part 5" p. 169. S. Moncada, J. Stamler, S. Gross and E. A. Higgs, Editors. Portland Press.

## Abbreviations

ATP, ADP, AMP	Adenosine tri-, di-, mono-phosphate
BCG	Bacille Calmette-Guerin
BH <sub>4</sub>	Tetrahydrobiopterin
cGMP	cyclic Guanidine Monophosphate
DMEM	Dulbecco's Modified Eagle's Medium
DNA	Deoxyribonucleic acid
DNP	2,4-dinitrophenol,
GIPL	Glycoinositolphospholipid
GM-CSF	Granulocyte/Macrophage Colony Stimulating Factor
GPI	Glycosyl Phosphatidyl Inositol
GSNO	S-nitroso glutathione
HONO	Nitrous acid
IFN	Interferon
IL	Interleukin
iNOS	Inducible Nitric Oxide Synthase
nNOS	Neuronal Nitric Oxide Synthase
eNOS	Endothelial Nitric Oxide Synthase
MAF	Macrophage Activating Factor
NAD(P)(H)	Nicotinamide adenine dinucleotide (phosphate) (reduced)
NAP	N-acetyl penicillamine
NIO	N-imino ornithine
NMMA	N-monomethyl arginine
NO	Nitric oxide

NTP	Nucleotide Triphosphate (a mixture of ATP, CTP, TTP and GTP)
OD	Optical Density
PBS	Phosphate Buffered Saline
RNA	Ribonucleic acid
RNI	Reactive Nitrogen Intermediates
ROI	Reactive Oxygen Intermediates
RT	Room Temperature
SNAP	S-nitroso-N-acetyl penicillamine
TGF	Transforming Growth Factor
TNF	Tumour Necrosis Factor

## **1. Introduction**

## **1.1 Leishmaniasis**

### **1.1.1 Prevalence**

Leishmaniasis is a set of diseases caused by protozoan parasites of the genus *Leishmania*. The number of infected people in the world at present is estimated to be 12 million, and 350 million live in areas where the disease may be caught (1). In all, leishmaniasis was responsible for approximately 75 thousand deaths in 1991 (1). The disease is present on all continents except Australia, and can be found in a band across the globe that extends from Texas, the South of France and China down to Argentina, South Africa, and Thailand (1,2). It is found both in rural and urban populations (1).

The parasite is carried by sandflies of the genera *Lutzomyia* or *Phlebotomus* (2-4), and is maintained in urban areas by reservoirs mainly in dogs and humans, and in rural areas by reservoirs in rodents (1,5).

### **1.1.2 Pathology**

Leishmaniasis may be grouped into four main types of disease: local cutaneous, diffuse cutaneous, muco-cutaneous, and visceral (1,6).

Local cutaneous leishmaniasis is rarely fatal, but is often disfiguring (1,5). A lesion develops at the site of the sandfly bite, and is usually self-healing after several months (6), though it may ulcerate, leaving the site of the lesion open to secondary infections.

Diffuse Cutaneous Leishmaniasis (2,7,8) is a condition in which the initial lesion can spread over much of the body. The disseminated lesions do not ulcerate, but are full of parasites, mainly in highly vacuolated macrophages. The condition progresses slowly and becomes chronic.

Muco-cutaneous leishmaniasis is almost never self-healing (6). It occurs as a result of the parasite spreading from an initial lesion at the sandfly bite to the mucosal membranes. The lesions that develop can restrict airways and be grossly disfiguring, often requiring plastic surgery to repair (6).

Visceral leishmaniasis is rarely self-healing, and is usually fatal if untreated (1,6). The parasites spread throughout the body, most notably to the liver, spleen, and bone marrow, causing hepato- and spleno-megaly followed by multiple organ failure.

Patients with immune disorders, for example Acquired Immunodeficiency Syndrome (AIDS), often present with unusual symptoms of leishmaniasis (9), including infection of the digestive tract (10), parasite filled Kaposi's sarcoma (11), and polyarthritis (12).

### **1.1.3 Species classification**

Leishmaniasis is caused by single celled eukaryotic parasites of the genus *Leishmania*, class Zoomastigophora, order Kinetoplastida, suborder Trypanosomatina (5). Species of the parasite are grouped primarily according to their geographical distribution, and the types of disease that they are likely to cause.

In the Old World (Eurasia and Africa), visceral leishmaniasis is caused by two species of parasite, *L. donovani* and *L. infantum*, and cutaneous leishmaniasis by *L. tropica*, *L. major*, and *L. aethiopica*.

In the New World, American visceral leishmaniasis is caused by *L. chagasi*, mucocutaneous leishmaniasis by members of the *L. brasiliensis* complex, and cutaneous leishmaniasis by members of the *L. brasiliensis* and the *L. mexicana* complexes (2). *L. brasiliensis* and *L. mexicana* are divided into subspecies described in Table 1.1 (2).

**Table 1.1: Species classification of the American *Leishmania*.**

<i>Leishmania brasiliensis</i> complex	<i>Leishmania mexicana</i> complex
<i>L. brasiliensis brasiliensis</i>	<i>L. mexicana mexicana</i>
<i>L. b. guyanensis</i>	<i>L. m. amazonensis</i>
<i>L. b. panamensis</i>	<i>L. m. garnhami</i>
<i>L. peruviana</i>	<i>L. m. venezuelensis</i>
	<i>L. m. pifanoi</i>

The disease caused by each species of parasite has been oversimplified in the description outlined above. Many of the parasites can cause less severe, or more severe diseases depending on the host immune status (2,5,6,8).

The species with which this thesis is mainly concerned is *L. m. mexicana*. Normally, this species causes ulcerating simple cutaneous lesions, though occasionally it can cause diffuse cutaneous leishmaniasis in hosts with an unusual immune response (2,8)

**1.1.4 Treatment**

First-line treatments are still based on the pentavalent antimonial drugs such as sodium antimony gluconate (Pentostam) and antimony-N-methyl-glutamine (Glucantime)

(1,6), developed over 40 years ago. Second-line drugs are amphotericin B or pentamidine, but these are toxic, and require prolonged treatment. The side effects of the drugs are such that they are only used when the disease is unlikely to regress spontaneously, or is likely to cause permanent scarring (6). Some cutaneous lesions, and diffuse cutaneous lesions are only slightly affected by treatment (7), so the indicated treatment for these leishmaniasis is to do nothing, while for the other forms, treatment is indicated.

Immunotherapy, in which a parasite preparation is injected along with an appropriate immunomodulator to induce a protective immune response has sometimes been found to be as effective a treatment as the conventional treatments (13,14).

There is currently no safe, effective vaccine available. Several vaccine formulations are at present being developed (2,14), ranging from peptide vaccines to killed *Leishmania* in conjunction with BCG. The effectiveness of the risky practice of deliberate infection with a strain that causes cutaneous leishmaniasis in an area of the body that is not normally visible, indicates that a suitable vaccine is a realistic prospect (2,14,15). However, none of the present formulations are currently effective enough to be prescribed routinely.

## **1.2 *Leishmania* life cycle.**

All members of the genus have a digenetic life cycle, being transmitted between a variety of mammalian hosts by sandflies of the genera *Lutzomyia* or *Phlebotomus* (2-4).

The generally accepted life cycle of *Leishmania* (5,16,17) is one in which the parasite lives in the mammalian host as an amastigote in a parasitophorous vacuole (PV) of the mammalian macrophage. In the PV, the amastigote divides, until the macrophage bursts, releasing amastigotes to infect other macrophages. When the sandfly takes a blood

meal from near the lesion, it collects *Leishmania*-infected macrophages. In the gut of the sandfly, the amastigotes transform to promastigotes, where they attach to the gut wall of the sandfly, and mature from procyclic promastigotes to metacyclic promastigotes as they migrate to the sandfly mouthparts. The cycle is completed when the infective metacyclic promastigotes are injected into the mammal, where they infect macrophages and transform to amastigotes again.

The evidence that amastigotes were obligate intralysosomal parasites was based on the findings that it was impossible to grow amastigotes extracellularly at the temperature of the mammalian host (18), that it was unusual to find *Leishmania* in cells other than mononuclear phagocytes, and nonphagocytic cells do not support the growth of amastigotes (19).

Recently, however, this simple view has been challenged. *L. major* can not only reside in macrophages, but also in dendritic cells (20,21), which may protect the parasite from immune attack, and/or may serve to continually provide the immune system with material for maintenance of immunological memory (22). On top of this, during *L. major* infection of C57BL/6 mice, only 30-40 % of the parasites were found in cells with typical markers for macrophages (F4/80<sup>+</sup>, BM-8<sup>+</sup> and/or MOMA-2<sup>+</sup>) or dendritic cells (NLDC-145<sup>+</sup>) (22). This meant that 60-70 % of the amastigotes were actually in an unidentified cell type.

It has now also become possible to grow amastigotes from some species of *Leishmania* at the temperature of the mammalian host for several sub-passages. Methods have been described for *L. m. mexicana*, *L. m. pifanoi*, *L. b. panamensis*, *L. b. braziliensis*, *L. donovani* (reviewed by Bates, 23).

The work presented in this thesis focuses on *L. m. mexicana* since this species was the one in which the culture conditions for amastigotes were most similar to those of the PV, in that they were at pH 5.5 and not pH 7.2. Axenically cultured *L. m. mexicana* amastigotes are very similar to amastigotes isolated directly from a lesion (24,25). They are the same size and shape (3-5  $\mu\text{m}$  on the major axis), and have the same ultrastructure as lesion amastigotes. They have megasomes, which are lysosome-like structures which are not present in promastigotes, and they have a short, non-emergent flagellum in a flagellar pocket. Their cysteine protease pattern is similar to lesion amastigotes and they are almost as infective as lesion amastigotes.

An important factor in murine resistance to leishmaniasis is the production of Reactive Nitrogen Intermediates (RNI). In order to understand the role that RNI play, it is first necessary to explain what RNI are, and the mechanism of their production.

### 1.3 The composition of RNI.

RNI are a group of partially oxidised products of nitrogen. They are extremely diverse, and the different RNI all have different reactivities. It is not known which of the RNI are the most physiologically significant in any of the biological systems that have been studied. The reactions by which they are created are summarised in Table 1.2 .

**Table 1.2: The reactions by which RNI are formed.**

RNI molecule	Creation Reaction
NO	Arginine + O <sub>2</sub> → Citrulline + NO (26)
(Nitric oxide)	RS-NO → RS + NO (27,28)
	[Fe(CN) <sub>5</sub> NO] <sup>2-</sup> + H <sub>2</sub> O + hν → [Fe(CN) <sub>5</sub> H <sub>2</sub> O] <sup>2-</sup> + NO (28)

NO <sup>+</sup>	HONO + H <sup>+</sup> → NO <sup>+</sup> + H <sub>2</sub> O (28)
NO <sup>•</sup>	NO + e <sup>-</sup> → NO <sup>•</sup> (Reduction by cytochrome a <sub>3</sub> ) HNO → H <sup>+</sup> + NO <sup>•</sup> (28)
HONO (Nitrous acid)	NO <sub>2</sub> <sup>-</sup> + H <sup>+</sup> → HONO (28) NO <sup>+</sup> + H <sub>2</sub> O → HONO + H <sup>+</sup> (28)
H <sub>2</sub> NO <sub>2</sub> <sup>+</sup>	HONO + H <sup>+</sup> → H <sub>2</sub> NO <sub>2</sub> <sup>+</sup> (28)
HNO	RSNO + R SH → R-R + HNO (29)
OONO <sup>•</sup> (Peroxynitrite)	O <sub>2</sub> <sup>-</sup> + NO → OONO <sup>•</sup> (30) NO <sup>+</sup> + H <sub>2</sub> O <sub>2</sub> → OONO <sup>•</sup> + 2 H <sup>+</sup> (30)
RSNO (S-nitrosothiol)	NO <sup>+</sup> + RSH → RSNO + H <sup>+</sup> (28) RSH + NO in oxygenated solution → RSNO (Mechanism unknown) (31) R SNO + RSH → R SH + RSNO (27-29)
Transition metal - NO complexes	Chelation of NO by transition metals.
NO <sub>2</sub> <sup>-</sup> (Nitrite)	2 NO + O <sub>2</sub> → 2 NO <sub>2</sub> THEN 2 NO <sub>2</sub> → N <sub>2</sub> O <sub>4</sub> THEN N <sub>2</sub> O <sub>4</sub> + H <sub>2</sub> O → NO <sub>2</sub> <sup>-</sup> + NO <sub>3</sub> <sup>-</sup> (32) NO + NO <sub>2</sub> → N <sub>2</sub> O <sub>3</sub> THEN N <sub>2</sub> O <sub>3</sub> + H <sub>2</sub> O → 2 NO <sub>2</sub> <sup>-</sup> (32)
NO <sub>3</sub> <sup>-</sup> (Nitrate)	2 NO + O <sub>2</sub> → 2 NO <sub>2</sub> THEN 2 NO <sub>2</sub> → N <sub>2</sub> O <sub>4</sub> THEN N <sub>2</sub> O <sub>4</sub> + H <sub>2</sub> O → NO <sub>2</sub> <sup>-</sup> + NO <sub>3</sub> <sup>-</sup> (32) NO + Oxy-haemoglobin → NO <sub>3</sub> <sup>-</sup> + Met-Haemoglobin (33)

## 1.4 Production of RNI in biological systems

RNI are produced mainly by a group of enzymes called the nitric oxide synthases (NOS). NOS catalyses the reaction  $L\text{-Arginine} + O_2 \rightarrow \text{Citrulline} + NO$  (26,32). NO is very short lived in biological media, with a half life of 0.1 s (34), and quickly reacts with oxygen, iron and amine groups to form many of the other RNI via the creation reactions described in Table 1.2.

There are three isoforms of NOS in mammals, endothelial (eNOS), neuronal (nNOS) and inducible (iNOS) (35). eNOS and nNOS are often grouped together as cNOS (constitutive NOS). This is because the regulation of their activity differs from iNOS in that post-translational regulation is important. They are affected by calcium levels and by phosphorylation. Their  $V_{max}$  is well below that of iNOS (36), and they are primarily involved in the regulation of vascular tone and neural organisation and communication.

iNOS, on the other hand is regulated primarily pretranslationally at the level of transcription (35-38), and the stability of its mRNA can be affected by  $TGF\beta$  (36). Like the other two isoforms, it requires NADPH and tetrahydrobiopterin ( $BH_4$ ) as cofactors (35) and is a member of the cytochrome  $P_{450}$  class of enzymes to which cytochrome  $a_3$ , the last enzyme in the mitochondrial electron transport chain belongs. It binds calmodulin too tightly to be responsive to physiological changes in calcium levels (39), although calcium may be involved in its induction, since the calcium ionophore A23187 can synergise with lipopolysaccharide (LPS) to induce iNOS in murine macrophages (40,41). iNOS can be found in hepatocytes, macrophages, chondrocytes, adenocarcinoma cells, keratinocytes, and respiratory endothelia (36). iNOS is the enzyme that produces the RNI involved in the murine immune response against *Leishmania*.

## 1.5 Inhibition of RNI production

RNI levels may be reduced in biological systems by preventing the production of NO by iNOS, or by mopping up the RNI produced.

### 1.5.1 Prevention of RNI production

RNI production by iNOS is usually experimentally inhibited by the addition to the solution of arginine analogues, eg N-monomethyl-L-arginine (L-NMMA) (43-53), N-iminoethyl-L-ornithine (L-NIO) (54), or N-amino-L-arginine (55). These inhibitors compete with L-arginine for the active site of iNOS (42), so their effects may be reversed by the addition of more L-arginine.

It is often mistakenly assumed, however, that these molecules are specific for the nitric oxide synthases. They are all taken up by cells via the amino acid transport systems  $y^+$  and  $y^+L$  (51,56). These systems are also responsible for the uptake of many other amino acids (eg ornithine, lysine, arginine and citrulline), and the addition of the arginine analogues can cause efflux of these other molecules (51). The half saturation concentration ( $K_t$ ) of L-NMMA for the transport systems (151  $\mu$ M for  $y^+$  and 7.5  $\mu$ M for  $y^+L$ ) (51) is well below the concentration at which it inhibits RNI production in intact cells (100-500  $\mu$ M) (43-53). Therefore, while any biological effect L-NMMA may correlate with inhibition of RNI production, the analogue also disrupts the amino acid balance in cells.

The  $K_t$  of arginine for system  $y^+$  is 55.7  $\mu$ M and for  $y^+L$ , it is 2.4  $\mu$ M (51). In most *in vitro* media, the concentration of arginine is very high (in DMEM it is 400  $\mu$ M, in RPMI it is 2 mM), compared to the concentration in serum (~60  $\mu$ M). The transporters are

therefore normally saturated with arginine in media, which explains why such high concentrations of analogues are needed to see a biological effect.

In addition, L-NMMA and L-NIO may also exert their effects by chelating iron, or directly inhibiting the transfer of electrons to cytochrome c (57).

However, in many systems, L-NMMA can increase murine T-cell proliferation that has been inhibited by RNI-producing cells (58-60), indicating that it may be able to affect RNI production without inhibiting the underlying cellular activity.

RNI production may also be inhibited by reducing the concentration of L-arginine in the medium or depleting arginine in medium with arginase (40,47,61-64). Up to one third of all the arginine taken up by a macrophage is used for RNI production (63), and any reduction in the rate of uptake will reduce the production of RNI.

### **1.5.2 Reduction of reactive RNI concentrations**

RNI may be mopped up by adding excess iron (40), which chelates NO, and releases it only slowly (28). However, NO bound to iron also has chemical reactivity of its own as NO<sup>+</sup> (28), so this treatment is likely only to shift the balance of the different RNI, rather than remove RNI totally. Mixing iron with ascorbate, though, produces superoxide which can react with nitric oxide to produce peroxynitrite. Peroxynitrite has a very short half life in biological media, and in some instances this process inhibits the effects of RNI.

RNI may also be mopped up by haemoglobin (65,66). In this system, NO reacts with the oxygen in the iron-containing centre of haemoglobin to produce the stable nitrate anion and met-haemoglobin (33). This reaction forms the basis of the haemoglobin detection method for RNI and has been used to determine the role of RNI in *Trypanosoma brucei* infection (55,66) which is described later in this introduction.

## **1.6 The role of RNI in *Leishmania* infection.**

RNI play a fundamental role in the protective murine immune response to *Leishmania*. It is believed that they are the final effector molecules in a T<sub>H</sub>1-type immune response. There is a wealth of evidence, both *in vivo* and *in vitro*, supporting this view. This section will explain the *in vivo* evidence that RNI are important, then the evidence that the role that they play is as a final effector molecule.

### **1.6.1 *In vivo* RNI production.**

RNI production from iNOS *in vivo* is important in the production of a protective immune response to *Leishmania*. In *Leishmania* resistant mice, RNI production may be inhibited either by the injection of the arginine analogues L-NMMA (67) into the footpad, or by the inclusion of L-NMMA in the animals' drinking water (68). C3H/HeN mice fed L-NMMA and then challenged in the footpad with *L. major*, produced less RNI, (detected as nitrite and nitrate in urine), had larger footpad swelling, and a greater parasite burden in draining lymph nodes than control mice (68). CBA/T6T6 mice injected with L-NMMA directly into the footpad had a smaller footpad swelling than those injected with the biologically inert enantiomer D-NMMA or phosphate buffered saline (PBS) (67).

Targeted disruption of the iNOS gene also led to an increase in susceptibility to *L. major*, measured both as footpad swelling and as parasite burden in the footpad (69)

### **1.6.2 *In vitro* RNI production and leishmanicidal activity.**

*In vitro* *Leishmania* infection of murine macrophages has revealed that macrophages can produce RNI and kill the parasites. Many different stimuli in many different macrophages can induce RNI production and leishmanicidal activity. In all

systems where both have been measured together, the two effects correlate with each other, (as summarised in Table 1.3). Different stimuli for macrophages can produce different responses (70), but it is only those stimuli that induce production of RNI that cause the macrophages to kill *Leishmania*.

In addition the amount of RNI produced by peritoneal macrophages from different in-bred strains of mice in response to IFN $\gamma$  correlated with the ability of the mice to resist infection (71)

Those sets of cytokines described in Table 1.3 are the only ones for which a direct comparison has been made between RNI production and leishmanicidal activity. Many other stimuli can induce RNI production e.g. IL-1 $\alpha$  (72), GM-CSF and TNF $\alpha$  (73), IFN $\alpha$  and IFN $\beta$  (70), BCG (74), TNF $\alpha$  or TNF $\beta$  in synergy with IFN $\gamma$  (70). Others still can inhibit RNI production, most notably IL-4 (37), IL-10 (75,76), and TGF $\beta$  (77). IL-4 can, however, synergise with IFN $\gamma$  to stimulate leishmanicidal activity of macrophages (78), though it should be noted that its effects on RNI production depend very much on the timing of the exposure of the macrophage to IL-4 and the stimulating agent (Feng, G.-J., personal communication). It is surprising that no attempt has been made to correlate the cytokine inhibition of RNI production with an inhibition of leishmanicidal activity in murine macrophages.

**Table 1.3: Stimuli for RNI production and leishmanicidal activity by macrophages.**

Stimulus	Macrophage cell type	Ref
IFN $\gamma$ + <i>L. major</i> or LPS. Inhibitable with L-NMMA or anti-TNF $\alpha$	Resident peritoneal cells.	(79)
IFN $\gamma$ inhibitable with L-NMMA	Resident peritoneal cells	(62)
IFN $\gamma$ inhibitable with L-NMMA	Peritoneal exudate cells.	(67)
TNF $\alpha$ inhibitable by L-NMMA	Peritoneal exudate cells	(80)
IFN $\gamma$ + TNF $\alpha$	Peritoneal exudate cells	(81)
IFN $\gamma$ + LPS, inhibitable by L-NMMA or guanidine. MAF + LPS, inhibitable by depleting L-arginine.	Peritoneal exudate cells and bone-marrow derived macrophages	(64)
IFN $\gamma$ + LPS, inhibitable by L-NMMA or anti-TNF $\alpha$	Resident peritoneal cells and bone-marrow derived macrophages	(82)
Ca <sup>2+</sup> ionophore A23187 + LPS, inhibitable by L-NMMA or depleting L-arginine	Bone-marrow derived macrophages	(40,41)
A23187 + IFN $\gamma$	Bone-marrow derived macrophages	(83)
IFN $\gamma$ + LPS	Bone marrow derived macrophages	(54)
IFN $\gamma$ + Lipophosphoglycan	J774 cell line	(84)
IFN $\gamma$ + LPS, inhibitable by glycoinositolphospholipids	J774 cell line	(85,86)

### **1.6.3 Studies on the factors required for iNOS induction compared to those for resistance to *Leishmania*.**

CD4<sup>+</sup> T-cells can be divided into at least two subsets, T<sub>H</sub>1 or T<sub>H</sub>2, according to their cytokine secretion pattern in *in vitro* culture. T<sub>H</sub>1 cells secrete IL-2, IFN $\gamma$  and TNF $\beta$ , T<sub>H</sub>2 cells secrete IL-4, IL-5 and IL-10, while they both secrete IL-3, GM-CSF and TNF $\alpha$  (87, and reviewed in 88). They are presumed to come from the same progenitor, the T<sub>H</sub>0 cell, and differentiate into their respective subsets during an immune response.

As described above, the cytokines required to stimulate RNI production from murine macrophages come primarily from the T<sub>H</sub>1 response, while the T<sub>H</sub>2 cytokines inhibit RNI production. There is a wealth of evidence (15,89) to show that a T<sub>H</sub>1 response is protective in murine leishmaniasis, while a T<sub>H</sub>2 response is not, and this correlation is a major reason for believing that RNI are part of the protective immune response to *Leishmania*. This section will therefore deal with the evidence that resistance to cutaneous leishmaniasis is dependent upon CD4<sup>+</sup> T cell responses, and then that it is dependent on a T<sub>H</sub>1 response.

#### **1.6.3.1 The importance of T-cell responses in leishmaniasis.**

The evidence for B-cells playing a role in the protective response to leishmaniasis is slim. Complement-mediated lysis of *L. donovani* promastigotes and their uptake by macrophages can be enhanced by antileishmanial antibodies (90), and F<sub>ab</sub> fragments of an anti-LPG monoclonal prevented establishment of *L. major* infection in susceptible BALB/c mice (91). Other parasite-specific monoclonals could protect against *L. m. mexicana* (92), *L. major* or *L. m. amazonensis* infection (93).

This implies that a sufficiently high anti-*Leishmania* antibody titre could affect parasite survival in a susceptible host. However, the natural immune response does not appear to rely on antibodies. Antibody levels or isotype differences in murine cutaneous infection of different mouse strains do not correlate with resistance to *L. tropica* (94). Passive transfer of serum or antibody fraction from immune mice does not affect infection of BALB/c mice (95). In addition, Biozzi AB/L mice, which have defective antibody responses, are still resistant to *L. major* infection (96). Although one group reported that B-cell depletion exacerbated the disease, resistance to the disease was restored by T cells alone, and the authors concluded that the B-cells were simply required for an effective T cell response (97). Later attempts at B-cell depletion, however, did not confirm the original finding (98), and in BALB/c mice, B-cell depletion reduced the infection rather than exacerbating it (99).

In contrast to experiments with B-cells, the evidence for T-cell involvement is strong. Athymic nude CBA or C57BL/6 mice, which are T-cell deficient are susceptible to *L. major* or *L. tropica* infection (100) and adoptive transfer of syngeneic T-cells to these mice restores their ability to resist infection (100). Thymectomised, or irradiated mice also display reduced ability to resolve disease (101). Protective immunity can also be transferred to susceptible mice from syngeneic mice that have cured a primary infection with simply the T-cell population (102), and transferred from susceptible mice that have been protectively immunised against infection to syngeneic naive recipients (103).

Thus protection against *Leishmania* infection is dependent upon T-cell responses.

### 1.6.3.2 The role of CD4<sup>+</sup> cells in protective immunity

The evidence that CD4<sup>+</sup> cells are primarily responsible for controlling infection comes also from adoptive transfer experiments. CD4<sup>+</sup> cells from resistant mice that have resolved a primary infection can transfer immunity to naive recipients (102-104). It is possible to immunise susceptible BALB/c mice with repeated intravenous or intraperitoneal injections of irradiated, heat-killed or sonicated promastigotes (95). This immunity was transferable to naive BALB/c mice by the CD4<sup>+</sup> population only (103).

However, not all CD4<sup>+</sup> responses are effective in clearing infection. In fact, an incorrect T cell response can be detrimental. For instance, susceptible BALB/c mice can be made resistant to infection by whole-body  $\gamma$ -irradiation, anti-CD4 or cyclosporine A treatment (105-107). These mice mount a CD4<sup>+</sup> protective response which can be transferred to naive susceptible mice, but CD4<sup>+</sup> cells from naive susceptible mice can also transfer susceptibility to resistant mice (105). CD4<sup>+</sup> T-cell lines from BALB/c mice could also suppress protective immunity in resistant and immunised susceptible mice (108,109).

### 1.6.3.3 T<sub>H</sub>1 and T<sub>H</sub>2 responses in immunity

It was soon realised that the reason for the differences in CD4<sup>+</sup> responses was due to the ability of CD4<sup>+</sup> cells to produce either a T<sub>H</sub>1 or a T<sub>H</sub>2 type response. These differences in CD4<sup>+</sup> responses could account for the differences in susceptibility to experimental *L. major* infection (110,111). T<sub>H</sub>1 responses predominate in *L. major* resistant C57BL/6 mice, whereas in susceptible BALB/c mice, a T<sub>H</sub>2 response predominates (111). Adoptive transfer of T-cell lines that express T<sub>H</sub>1 or T<sub>H</sub>2 cytokines can also provide evidence for the role of a T<sub>H</sub>1/T<sub>H</sub>2 balance in regulating *L. major* resistance (112). IL-2 and IFN $\gamma$  secreting cells transfer resistance, while IL-4 secreting

cells transfer exacerbation in both BALB/c and SCID mice (113). However, there was a single report of a  $T_H1$  cell line that confers susceptibility (108).

Further evidence for a role for the  $T_H1$  response in resistance to infection comes from cytokine depletion studies. Resistant C3H/HeN mice can be made susceptible by IFN $\gamma$  depletion using a neutralising IFN $\gamma$  monoclonal antibody (114). And anti-IL-4 treatment of BALB/c mice confers protection on them, since it decreases the IL-4 response (115). The production of another  $T_H2$  cytokine, IL-10, also correlates with susceptibility to leishmaniasis, since mRNA for it can be found in the draining lymph nodes of susceptible mice (111). However, neutralisation of this cytokine did not affect the progression of disease in BALB/c mice (116).

Transgenic and knockout mice have also been important in providing evidence for the importance of a  $T_H1$  response. 129/Sv mice, which are normally resistant to leishmaniasis could be rendered susceptible by overexpression of IL-4 (117), or by targeted disruption of the IFN $\gamma$ -receptor (118). Disruption of the IFN $\gamma$  gene in C57BL/6 mice causes the immune response to default to a  $T_H2$  pathway, and the mice become susceptible to *L. major* infection (119). Normally susceptible IL-4 knockout mice, however, are able to control *L. mexicana* infection (120), though the gene disruption has no effect on their ability to clear *L. donovani* infection. IL-4 knockout BALB/c mice are also able to resist infection with *L. major* (121), and although another group reported that IL-4 knockout BALB/c mice were still susceptible to *L. major* infection, the knockout mice still did not show the rapidly progressive disease of the control mice (122).

So a  $T_H1$  response is important for the *in vivo* resolution of *Leishmania* infection, but the cytokines alone are not sufficient to cure the infection since iNOS knockout mice have an increased  $T_H1$  response, but are still unable to cure an *L. major* infection (69). As

described above, *in vitro* iNOS production by macrophages is induced by T<sub>H</sub>1 cytokines and inhibited by T<sub>H</sub>2 cytokines, suggesting that the final effector mechanism may be this induction of iNOS.

#### 1.6.4 Other macrophage defence mechanisms.

Further evidence for the role of RNI as a final effector mechanism of the T<sub>H</sub>1 response to *Leishmania* comes from *in vitro* experiments which show that the other defence mechanisms of murine macrophages are not particularly effective.

Infected bone marrow-derived macrophages can kill *L. major* if stimulated with IFN $\gamma$  and LPS, which induce RNI production (54). However production of the oxidative burst for example by zymosan in bone marrow derived macrophages does not correlate with killing (54,64). Furthermore, it was not possible to inhibit toxicity using superoxide dismutase, and superoxide production actually slightly inhibited killing (54). Though killing of *L. donovani* (123) and *L. major* (81) correlated with production of reactive oxygen intermediates (ROI), this production of ROI increased with the addition of L-NMMA, while killing decreased (81), indicating that the two processes were separable.

Other components of macrophage defence are also ineffective. Even in an unstimulated macrophage, *Leishmania* live in an acidic compartment that has many of the lysosomal degradative enzymes in it (16). It is formed by the fusion of phagocytic vacuole containing the parasite with secondary lysosomes (124-126). The parasitophorous vacuole contains both macrophage- and *Leishmania*- derived products. The macrophage derived products include acid phosphatase, arylsulfatase, and trimetaphosphatase (127), cathepsins B, D, H and L,  $\beta$ -glucuronidase (128,129), and macrophage acid phosphatase (128). The parasite does not inhibit the acidification of the vacuole (128), but instead is best adapted

to growing at this pH in the amastigote form (25). This acidification, however, is important for killing in an activated macrophage, since inhibition of the acidification using bafilomycin A1 inhibited leishmanicidal activity (130).

Finally, evidence for a toxic role of RNI comes from the fact that RNI can be directly toxic to *Leishmania*. Addition of SNAP (54), or culturing the parasites in acidified nitrite (64) is toxic to the *L. major* and *L. enriettii* promastigotes.

RNI are not solely involved in the response to *Leishmania* infection. They are involved in the response to myriad other organisms (reviewed in 26,42,138), including intracellular organisms (43,44,52,131-133), extracellular organisms (55), viruses (45), bacteria (47,134,135), worms (136), and fungi (137). RNI are therefore a quite universal toxic mechanism.

### **1.7 RNI production by humans**

Until now, I have concentrated on murine production of RNI since this is the system in which RNI production by immune system cells is best understood. However, iNOS has also been found in bovine (139), rat (140,141), rabbit (141), and human cells (58,142-144).

However, while it has proved simple to get detectable levels of RNI from murine macrophages, it has proved harder in human cells. Comparing human and murine peritoneal macrophages with similar stimuli, it was possible to induce detectable RNI from mouse and not human cells (145,146). However, there have been reports of detectable RNI from human peripheral blood mononuclear cells (73,147), and in a rheumatoid arthritic joint, it was possible to detect co-staining of human iNOS with the macrophage markers nonspecific esterase and CD68 (143).

However, the human response to *L. donovani* infection does correlate with ROI production (148,149). There is, however, an oxygen-independent killing mechanism as well, since macrophages from patients with Chronic Granulomatous Disease (CGD), which lack an efficient respiratory burst, are still able to kill the parasite (149), albeit not as efficiently as control people.

The  $T_H1/T_H2$  dichotomy is also not as clear in the human disease as in mice, since self-healing cutaneous lesions often contain mRNA for  $IFN\gamma$ , IL-4, IL-5 and IL-10 at the same time (150). In addition, during a fulminating visceral infection of *L. donovani*, humans often produce extremely high levels of  $IFN\gamma$  (150). The mouse model may also be very different from the human since the same species of parasite cause different disease severities in the different mammals.

Currently, not enough is known therefore about the human system to extrapolate from the murine experiments to say that RNI play a fundamental role in the human response to *Leishmania*.

### **1.8 Delivery of RNI to the parasitophorous vacuole**

RNI may enter the PV as any of the neutral molecules in the group, many of which are neutrally charged, and thus are able to diffuse freely through lipids as well as water. Still, some nitrosothiols have been described as possible transporters of RNI, eg S-nitroso-cysteine or S-nitroso-glutathione (GSNO), which are formed when  $NO^+$  reacts with cysteine or glutathione (151).

## 1.9 Possible targets for RNI

### 1.9.1 Primary chemical targets

RNI have diverse reactions, and can react with several different targets in cells. These include iron, sulphhydryl groups, amine groups, tyrosine residues, lipids, sugars and oxygen.

#### 1.9.1.1 Iron

RNI affect many enzymes with iron sulphur centres. Inhibition of complexes I and II of the mitochondrial electron transport chain has been described both as targets of activated macrophages (152) and in cells treated with authentic NO gas *in vitro* (153). NO inhibited O<sub>2</sub> uptake that was dependent on malate and succinate, but not  $\alpha$ -glycerophosphate or tetramethylphenylenediamine, indicating that the inhibition was specific for complexes I and II in the transport chain. Mitochondrial aconitase, the rate limiting step in the Krebs cycle, is also inactivated by RNI (61,154-156). Cytosolic aconitase, however, is activated by the release of iron so that it binds iron responsive element motifs in DNA, decreasing the transcription of ferritin mRNA to regulate iron metabolism in murine elicited peritoneal macrophages (49)

The labile iron in the [4Fe4S]<sup>2+</sup> cluster may also be removed by oxidising RNI such as ONOO<sup>-</sup>, leaving a [3Fe4S]<sup>1+</sup> cluster (157).

RNI can also react with iron in heme (158), found for instance in the cytochrome P<sub>450</sub> family of enzymes (159) which includes NOS (160), cytochrome c oxidase, and superoxide dismutase. Different members of the family have different susceptibility to NO gas (158), and the inhibition is characterised by a fast, reversible inhibition of the

enzyme, followed by a slow phase with variable reversibility. NO can also react with the oxygen in oxy-haemoglobin to produce nitrate and met-haemoglobin (33).

### 1.9.1.2 Sulphydryl groups

S-nitrosothiols can be formed by any of the reactions shown in Table 1.2. They will prevent formation of disulphide bonds in proteins, and may inhibit DNA binding by many proteins that require sulphydryl groups for binding (29). This reaction is very common, and occurs under physiological conditions (161). Over 96 % of the RNI in human plasma was reported to circulate as S-nitroso adducts of proteins (162). S-nitroso-haemoglobin has been reported as playing a major role in maintenance of vascular pressure, and the nitrosation reaction has been reported to regulate the rate at which oxygen is released from haemoglobin (163).

Numerous example of RNI inhibiting enzymes through reaction with thiols have been described, including the NMDA receptor, cathepsin B, the calcium activated potassium channel, NADPH oxidase, G proteins/p21<sup>ras</sup> (164), adenylyl cyclase, bacterial membranc SH group target proteins, glyceraldehyde-3-phosphate dehydrogenase (165), tissue plasminogen activator (166), aldolase, aldehyde dehydrogenase,  $\gamma$ -glutamylcysteinyl synthetase, actin, AP-1 (167), NF $\kappa$ B (168), O-methylguanine-DNA methyltransferase (169), and albumin (29).

S-nitrosylation can also increase the rate at which the cysteine residue is ADP-ribosylated (29,165), leading to a more permanent deactivation of the enzyme.

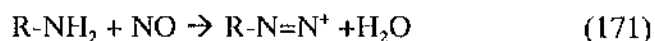
The half life of the nitrosothiol varies greatly from over 24 h for S-nitroso- bovine serum albumin to less than 1 h for SNAP (161). This means that many of the compounds could be considered to be “carriers” for RNI, or long-term stores. Furthermore, it provides

evidence that RNI other than nitric oxide are involved in biological systems, since NO itself will not react with sulphhydryl groups, while NO<sup>+</sup> or NO in the presence of oxygen will.

Once S-nitrosothiols are formed, they can directly donate the NO moiety to other sulphhydryl groups (28), or they can release NO or NO<sup>+</sup> forming a sulphur radical or an RS<sup>-</sup> group respectively. There is also evidence for them releasing NO<sup>-</sup> (170). However, no detection method has yet been able to detect the formation of the RS<sup>-</sup> radical that should be formed from release of NO, suggesting that they probably exert their effects by direct reaction with their targets.

### 1.9.1.3 Amine groups

RNI can react with primary amine groups on either DNA or proteins. The initial diazotisation reaction is common between the two:



This intermediate can then either release nitrogen leading to deamination of the target, or cross-link the target to another organic molecule. Both reactions occur in DNA treated with RNI (171). Cross-linking requires the immediate proximity with another molecule and, in the case of DNA, this reaction occurs approximately six times slower than the deamination reaction (171).

Not all amine groups are equally reactive. The susceptibility of the different bases of DNA to deamination depends on the pH, whether the DNA is denatured, and the base sequence (171). At pH 4.2 adenine and guanine in RNA react at comparable rates, and cytosine slower, while in calf thymus DNA, guanine is deaminated faster than cytosine,

which in turn is faster than adenine. This variability makes it impossible to predict which bases are likely to be most affected *in vivo*.

RNI increase the rate of mutation in DNA treated both outside cells (172-174) and in whole human cells (175). Damage to pancreatic islet cells treated with RNI could not be inhibited by endonuclease inhibitors, suggesting that RNI may be acting directly on these cells' DNA as well (53). In addition, RNI may also damage DNA indirectly, since they can inhibit DNA repair and synthesis enzymes (178).

Amines in amino acids are also susceptible, and RNI attack on the NH<sub>2</sub> terminus of hemoglobin has been reported (176), as well as on free amino acids (31):

Deamination and cross-linking are irreversible reactions, and any damaged molecules will need to be replaced rather than repaired by a damaged cell.

#### **1.9.1.4 Tyrosine**

The RNI molecules peroxynitrite and NO<sub>2</sub> can irreversibly react with the phenolic ring of tyrosine to produce nitrotyrosine (177). This nitration reaction may inhibit the phosphorylation of tyrosine, which is involved in intracellular signalling. In addition, this reaction may play a part in the inactivation of the ribonucleotide reductase both with *in vitro* inhibition using RNI donors (178) and in targets of macrophage activation (179,180). Ribonucleotide reductase catalyses the rate limiting step in DNA synthesis, and since macrophage cytostasis can be reversed by adding back deoxyribonucleosides (180), inhibition of this enzyme may be an important part of the RNI attack.

### 1.9.1.5 Oxygen depletion

RNI react with oxygen to produce nitrite and nitrate in biological solutions (28).

There are many demands on the oxygen supply to a peripheral site of an immune response, including the rapid respiration of immune system cells, the production of a respiratory burst, and the fact that there is very little vascularisation of a *Leishmania* lesion.

Production of RNI may therefore starve cells of oxygen.

To counteract this, RNI, in their capacity as the endothelium derived relaxing factor (65), have an arteriodilatory effect, thereby increasing the blood flow, and therefore the oxygen supply to tissues involved in an immune response.

### 1.9.1.6 Lipid peroxidation

Peroxynitrite rapidly oxidises lipids (181). The reaction is extremely fast and is diffusion limited. The free radicals formed by the peroxidation reaction set up a chain reaction that can spread throughout the lipid bilayer, similar to that caused by ROI. NO can form adducts that stop this chain reaction (181). The chain reaction can also be inhibited by glutathione with superoxide dismutase (182). However, both of these enzymes are also subject to attack by RNI, and may therefore be inhibited, allowing a chain reaction to continue.

Membrane components attached by glycosyl-phosphatidylinositol (GPI) anchors can also be removed by RNI (183). Such components on *Leishmania* include glycoinositol phospholipids (GIPLs), lipophosphoglycan (LPG), and the membrane protein gp63 (183).

## 1.9.2 Secondary effects of RNI

### 1.9.2.1 Effects on proliferation and cell activation.

Proliferation of many cell types is inhibited by RNI (26,185). These include EMT-6 mammary carcinoma cells (61,72), fungi (63), murine skin cancer cells (184), murine splenocytes (60), peritoneal exudate cells (48), *Trypanosoma cruzi* (133). However, in some endothelial cells, low levels of RNI can enhance proliferation (186).

The toxic effects of RNI *in vitro*, however, do not always correlate with effects *in vivo*. For instance, *T. brucei* proliferation can be inhibited by RNI from macrophages *in vitro* (66), but under *in vivo* conditions RNI are not effective. Indeed the inhibitory effects of RNI on the immune system mean that *in vivo* inhibition of RNI production leads to reduced parasitemia (55).

RNI can also activate immune system cells. With human peripheral blood mononuclear cells, SNAP increased glucose uptake, altered the tyrosine phosphorylation pattern, increased NF $\kappa$ B translocation, and TNF $\alpha$  production (187). The effects could not be mimicked by 8-bromo-cGMP, a metabolically stable cGMP analogue, but the effects could have been due to G-protein activation (164).

The specific anti-proliferative effects of RNI could be due to inhibition of energy production, effects on intracellular signalling, or inhibition of ribonucleotide reductase which will inhibit production of DNA precursors without inhibiting production of RNA precursors.

### 1.9.2.2 Cell death

RNI can stimulate apoptosis or cause necrosis. Apoptosis is a programmed cell death in which the cell self-destructs, digesting its own cytoplasm, and then cutting up its DNA first into fragments several kilobases long, and then into fragments that are multiples of length that is wrapped around its histones (approximately 200 bp), forming a ladder if separated on an ethidium bromide gel (188,189).

Low concentrations of RNI can sometimes provide the signal for apoptosis in pancreatic  $\beta$ -cells (190), murine thymocytes (191), human epithelial cells and murine macrophages (192). How RNI provide the signal is unknown, but RNI treatment can be accompanied by an increase in Fas gene expression (191) which can provide the signal for apoptosis.

In contrast, higher concentrations of RNI can cause necrosis. Necrosis is a form of death caused by the cells losing their energy reserve, and being unable to maintain their osmotic balance. The cell swells and both internal and external membranes become disrupted (188,193,194). This effect is seen in oligodendrocytes (193) and cortical cell cultures (194) treated with high levels of RNI. *In vivo* evidence for RNI induced necrosis comes from inhibition of RNI production by L-NMMA during focal ischemia in the rat brain, where necrotic cell death was inhibited, but apoptotic death was not (195).

### 1.10 The interaction of RNI with ROI.

RNI can react with the ROI superoxide anion ( $O_2^-$ ) and hydrogen peroxide ( $H_2O_2$ ) to produce peroxynitrite. Peroxynitrite is extremely short lived in biological solutions, with a half life of less than 1 s, since it is such a strong oxidant. It breaks down to the

hydroxyl radical HO and  $\text{NO}_2^-$  (181). Whether effects attributable to RNI are inhibited or exacerbated by ROI depends on the concentration of RNI, ROI, and the target reactions.

Instances in which the effects of RNI are exacerbated by ROI include lipid peroxidation (181), inhibition of aconitase (156), and the iron-sulphur centres of the electron transport chain (196). However, in other experiments, the effects of RNI can be inhibited by ROI, for instance the effect of NO gas on mitochondrial respiration of macrophages could be inhibited by  $\text{FeSO}_4$ /ascorbate mixture (153).  $\text{FeSO}_4$  on its own had no effect, suggesting that it was not mopping up the RNI.

RNI can also increase the oxidative capacity of ROI, increasing dihydrorhodamine oxidation by  $\text{O}_2^-$  (197), and lipid peroxidation (198). The chain reactions set up by lipid peroxidation, however, may also be inhibited by NO, indicating that the ratio of concentrations of  $\text{NO}:\text{O}_2^-$ :target can heavily influence whether synergy or inhibition are important. In contrast, RNI can also inhibit the cytotoxicity of both superoxide and hydrogen peroxide (199).

### 1.11 Defence against RNI.

*Leishmania* have several mechanisms that can protect them from RNI. They can modulate the immune response to prevent the macrophage from producing RNI either by preventing the induction of a  $\text{T}_\text{H}1$  response, or by inhibiting the induction of RNI in the macrophage itself.

*L. donovani* infection of macrophages down-regulates expression of the costimulatory molecule B7-1 (200), which means that macrophages are more likely to induce anergy than activation in T-cells. *L. major* infected macrophages also provide better stimulation to  $\text{T}_\text{H}2$  cells than  $\text{T}_\text{H}1$  cells (38). Promastigotes from *L. major* and *L.*

*mexicana* and amastigotes from *L. mexicana* enter macrophages silently, without the macrophages producing IL-12, which would normally induce a T<sub>H</sub>1 type response.

Amastigotes from *L. major*, however, do induce the production of IL-12 on infection of macrophages (201).

*L. major* can also down-regulate production of RNI by secreting GIPLs (84) or LPG (86) which inhibit transcription of iNOS. However, LPG can also synergise with IFN $\gamma$  to produce RNI if given after IFN $\gamma$  to murine macrophages (86), so the timing of the exposure to the different stimuli is important.

Though there have been no reports of *Leishmania* resistance to RNI itself, there are two strains of *Mycobacterium intracellulare* (46) and *M. avium* (50) that have been reported resistant (46), *Brucella abortus* is also resistant to RNI produced by macrophages (202). The mechanism of resistance is unknown, but could be the production of thiols, uptake of iron, or production of ROI.

### **1.12 Aims of this thesis.**

This project aimed to characterise some of the biochemical pathways that are affected in *L. m. mexicana* amastigotes when they are treated with RNI, and examine the interaction of RNI with other components of the PV. The main aims were:

1. To develop suitable systems for producing RNI, and assessing their effect on the viability of axenically grown *L. m. mexicana* amastigotes.
2. To determine how RNI interact with other components of the parasitophorous vacuole, such as  $\beta$ -glucuronidase, cathepsin D, and ROI, and whether this is important in the killing of *L. m. mexicana*.

3. To determine whether *L. m. mexicana* amastigotes are particularly susceptible to RNI, and whether resistance could be induced by low levels of RNI.
4. To determine whether GPIs, DNA or the mitochondria in live parasites were affected by RNI and whether they could be the primary targets of RNI.

## **2. Materials and methods**

## 2.1 Materials

Chemical	Supplier
[ <sup>3</sup> H]-Glucosamine	NEN Dupont, Stevenage, Hertfordshire, UK
[ <sup>3</sup> H]-Methyl-thymidine	Amersham International plc, Buckinghamshire, UK
1-Propanol	Fisons, Loughborough, UK
2,4-Dinitrophenol	Sigma, Poole, Dorset, UK
96 % Ethanol	Western Infirmary, Glasgow, Scotland
Acetic acid	Fisher Scientific International, Loughborough, UK
Agarose	Biogene Ltd, Kimbolton, Cambridgeshire, UK
$\alpha$ -Naphthylamine	Sigma, Poole, Dorset, UK
Araldite	Agar Scientific
Autoradiography films	Sigma, Poole, Dorset, UK
Benzyl penicillin	Sigma, Poole, Dorset, UK
Boric acid	Fisher Scientific International, Loughborough, UK
Chloroform	BDH Ltd, Poole, Dorset, UK
Culture plates (24 and 48 well)	Costar, Cambridge, Massachusetts, USA
Disodium hydrogen phosphate	BDH Ltd, Poole, Dorset, UK
Dithioerythritol	Boehringer-Mannheim, East Sussex, UK (from diluting enzyme buffer L)

DNA molecular weight markers	Gibco BRL, Paisley, Scotland
DNA polymerase (Kornberg fragment)	Boehringer-Mannheim, East Sussex, UK
DNase 1	Boehringer-Mannheim, East Sussex, UK
Ecoscint scintillation fluid	Fisher Scientific International, Loughborough, UK
Enhance spray	NEN Dupont, Stevenage, Hertfordshire, UK
Ethidium bromide	Sigma, Poole, Dorset, UK
Ethylenediaminetetraacetic acid (EDTA)	Sigma, Poole, Dorset, UK
FACSFlow	Becton Dickinson, Cowley, Oxford, UK
Fluorimeter 96 well plates	Porvair filtronics, King's Lynn, Norfolk, UK
Foetal calf serum (FCS)	For J774 - Gibco BRL, Paisley, Scotland  For <i>L. m. mexicana</i> promastigotes and amastigotes -  Labtech batch no. 206  Always heat inactivated by heating to 56°C for 45 min.
Formaldehyde	BDII Ltd, Poole, Dorset, UK
Gentamicin sulphate	Sigma, Poole, Dorset, UK and The Wellcome Foundation, Beckenham, Kent, UK
Glass filters	Whatman, Maidstone, Kent, UK

Glutaraldehyde (25% grade)	Sigma, Poole, Dorset, UK
Hemocytometers	Weber Scientific International, Teddington, Middlesex, UK
HOMEM medium	Prepared on site.  EMEM/Spinners salts plus L-glutamine, MEM amino acids, MEM non-essential amino acids from Gibco BRL, Paisley, Scotland. Sodium Bicarbonate and sodium pyruvate from BDH Ltd, Poole, Dorset, UK. Para-aminobenzoic acid, biotin, HEPES from Sigma, Poole, Dorset, UK.
Horse Serum	Gibco BRL, Paisley, Scotland
Hydrochloric acid (HCl)	Fisons, Loughborough, UK
Interferon gamma (IFN $\gamma$ )	A kind gift from Dr G. Adolf, Ernst-Boehringer Institut f r Arznmittel-Forschung, Vienna, Austria
L-Arginine	Sigma, Poole, Dorset, UK
L-Glutamine	Gibco BRL, Paisley, Scotland
Lipopolysaccharide from <i>Salmonella enteridis</i> .	Sigma, Poole, Dorset, UK
Lithium chloride	Sigma, Poole, Dorset, UK
L-Monomethyl arginine (L- NMMA)	The Wellcome Foundation, Beckenham, Kent, UK

Luminometer tubes	Sterilin, Teddington, Middlesex, UK
Luria Broth agar	Gibco BRL, Paisley, Scotland
Magnesium chloride	Boehringer-Mannheim, East Sussex, UK (from diluting enzyme buffer L)
Methanol	Fisher Scientific International, Loughborough, UK
Minimal Essential Medium without arginine, cysteine, leucine methionine, inositol, glucose, or glutamine	Gibco BRL, Paisley, Scotland
Modified Diamond's Medium (MDM)	Made on site using:  Trypticase from Gibco BRL, Paisley, Scotland,  Yeast extract from DIFCO, ascorbic acid, KCl,  KHCO <sub>3</sub> , KH <sub>2</sub> PO <sub>4</sub> , K <sub>2</sub> HPO <sub>4</sub> , FeSO <sub>4</sub> .2H <sub>2</sub> O from  Sigma, Poole, Dorset, UK.
Nylon membrane for DNA	Boehringer-Mannheim, East Sussex, UK
Nylon mesh	Cadisch Precision Meshes Ltd, Finchley, UK
Opti-Flow Scintillation fluid	Fisons, Loughborough, UK
Osmium tetroxide	In-house supplies
Penicillin	Gibco BRL, Paisley, Scotland
Phenol Blue	Sigma, Poole, Dorset, UK

Phenol/chloroform/isoamyl alcohol (25:24:1)	Sigma, Poole, Dorset, UK
Phosphoric acid	Sigma, Poole, Dorset, UK
Potassium Chloride (KCl)	Sigma, Poole, Dorset, UK
Potassium dihydrogen phosphate	Fisher Scientific International, Loughborough, UK
Proliferation plates (96 well)	Nunclon, Roskild, Denmark
Propylene oxide	Merck Ltd, Poole, Dorset, UK
Rhodamine 123	Sigma, Poole, Dorset, UK
Ribonuclease A	Sigma, Poole, Dorset, UK
RPMI 1640 medium	Flow laboratories, Kent, UK
Salmon sperm DNA	Sigma, Poole, Dorset, UK
Schneider's Drosophila medium	Gibco BRL, Paisley, Scotland
S-nitroso-N-acetylpenicillamine (SNAP)	The Wellcome Foundation, Beckenham, Kent, UK
Sodium borohydride	Sigma, Poole, Dorset, UK
Sodium chloride	Fisher Scientific International, Loughborough, UK
Sodium citrate	Fisons, Loughborough, UK
Sodium dihydrogenphosphate	BDH Ltd, Poole, Dorset, UK
Sodium hydroxide	Fisher Scientific International, Loughborough, UK

Sodium Lauryl Sulphate (SDS)	Gibco BRL, Paisley, Scotland
Sodium nitrite (NaNO <sub>2</sub> )	Sigma, Poole, Dorset, UK
Sterilisation filters	Gelman sciences, Ann Arbor, Michigan USA
Streptomycin	Gibco BRL, Paisley, Scotland
Streptomycin	Sigma, Poole, Dorset, UK
Sucrose	BDH Ltd, Poole, Dorset, UK
Sulphanilamide	Sigma, Poole, Dorset, UK
Syringe needles	Becton Dickinson, Cowley, Oxford, UK
Syringes	Becton Dickinson, Cowley, Oxford, UK
<i>tetra</i> -Sodium pyrophosphate	BDH Ltd, Poole, Dorset, UK
Thin layer chromatography (TLC)	Merck Ltd, Poole, Dorset, UK
Kieselgel 60 plates	
Trichloroacetic acid (TCA)	BDH Ltd, Poole, Dorset, UK
TRIS	Gibco BRL, Paisley, Scotland
TRIS HCl	Gibco BRL, Paisley, Scotland
Triton X-100	Sigma, Poole, Dorset, UK
Trypan Blue	BDH Ltd, Poole, Dorset, UK
Uranyl acetate	Agar Scientific
Xylene cyanol FF	Sigma, Poole, Dorset, UK

## 2.2 Cell culture

### 2.2.1 Macrophages

J774 macrophages (from The Wellcome Foundation, Beckenham, Kent, UK) were cultured in tissue culture treated flasks in RPMI medium with 10% FCS (v/v) + L-glutamine (2 mM), Penicillin (100 U/ml) and Streptomycin (100 µg/ml). The cells were subpassaged every 2-3 days by scraping the adherent monolayer off with a cell scraper and inoculating some of the cells into new flasks.

### 2.2.2 *Leishmania*

The strain of *L. m. mexicana* that was used was MNYC/BZ/62/M379.

### 2.2.3 Amastigotes

Amastigotes were cultured according to the method of Bates *et al.* (24), in Schneider's *Drosophila* medium with 20% FCS (v/v) and gentamicin sulphate (25 µg/ml), pH 5.4-5.7. Amastigotes were subpassaged every 4-5 days by aspirating a portion of the culture through a 19G needle, and ejecting it through a 26G<sup>3</sup>/<sub>8</sub> needle. The cultures were grown at 32°C under air.

## 2.2.4 Promastigotes

Promastigotes were cultured in HOMEM medium (203), prepared as follows by

D. Laughland:

E-MEM/Spinners Salts with L-glutamine	1 Litre pack
Glucose	2 g
Sodium bicarbonate	0.3 g
Sodium pyruvate	0.11 g
<i>para</i> -aminobenzoic acid	1 mg
Biotin	0.1 mg
HEPES	5.96 g
MEM amino acids (50x)	10 ml
MEM non-essential amino acids (100x)	10 ml
pH 7.4-7.8	

Promastigotes were prepared by inoculating amastigotes into HOMEM with 10% FCS (v/v), and grown at 28°C in air. The culture was subpassaged every 3-5 days.

## 2.2.5 *Tritrichomonas foetus*.

*T. foetus* strain F2 was cultured at 37°C in Modified Diamond's Medium (MDM) with 10% (v/v) Heat Inactivated Horse Serum and 1 mg ml<sup>-1</sup> streptomycin and 1000 U ml<sup>-1</sup> benzyl penicillin. MDM was prepared as follows by D. Laughland:

For 1 litre of MDM:

20 g Trypticase  
10 g Yeast extract  
5 g Maltose hydrate  
1 g L-Ascorbic acid  
1 g KCl  
1 g KHCO<sub>3</sub>  
1 g KH<sub>2</sub>PO<sub>4</sub>  
0.5 g K<sub>2</sub>HPO<sub>4</sub>  
0.1 g FeSO<sub>4</sub>·2H<sub>2</sub>O  
900 ml Water  
pH 6.3-6.4

**2.2.6 *Escherichia coli* and *Salmonella typhimurium*.**

*S. typhimurium* strain BAD509 and *E. coli* strain C600 were scraped off Luria Broth agar plates. The concentration was estimated using OD<sub>600</sub>, assuming that OD<sub>600</sub>=0.2 when they were at 10<sup>10</sup> per ml.

**2.3 Animal subpassage of *L. m. mexicana*.**

BALB/c mice were infected subcutaneously in the rump with 10<sup>6</sup> *L. m. mexicana* amastigotes in HOMEM medium without FCS. After two months, when the lesion was visible, the mice were killed, and amastigotes prepared by pushing the lesion through a tea strainer into amastigote culture medium. Clumps of amastigotes were broken up by aspirating the suspension through a 19G needle into a syringe, and ejecting it through a 26G<sup>3/8</sup> needle. The suspension was centrifuged at 1600 g for 5 min at room temperature (RT), and resuspended in 5 ml culture medium. Clumps were broken up by pushing the

suspension three times through a 26G<sup>3</sup>/<sub>8</sub> needle, and amastigotes were resuspended to 0.5 - 2 x 10<sup>6</sup> ml<sup>-1</sup> in 10 ml culture medium.

#### **2.4 Transformation efficiency assay of amastigote viability**

Amastigote viability was assayed by their efficiency of transforming to promastigotes. Amastigotes were inoculated into 500 µl or 1 ml of HOMEM with 10% (v/v) FCS, at a density of  $\leq 10^6$  ml<sup>-1</sup>.

After 24 or 48 hr incubation at 28°C, many of the viable amastigotes had transformed to promastigotes. At this point, clumps were broken up by pushing the culture three times through a 26G<sup>3</sup>/<sub>8</sub> needle, and an aliquot of 100-200 µl was mixed with an equal volume of 4% formaldehyde in PBS to fix them. The numbers of parasites were counted on a hemocytometer. Cells were counted as promastigotes if they were > 5 µm in length, and had a flagellum at least as long as their body length. Thus a cell was only counted as viable if it had fully transformed to a promastigote. A sufficient number of squares were counted on the hemocytometer to include over 100 promastigotes in the control wells.

#### **2.5 Measurement of RNI production**

RNI production by macrophages and SNAP was measured by the accumulation of nitrite in the medium using the Griess reaction. The Griess reagent was made by mixing equal volumes of 0.1% (w/v)  $\alpha$ -naphthylamine in water and 1% (w/v) sulfanilamide in 5% (v/v) phosphoric acid. 100 µl of Griess reagent was added to 100 µl sample and after 10 min the absorbance at 545 nm was measured on a Titertek Multiscan MCC 340 96-well plate spectrometer. In other experiments, the measurement was at 490 nm with a reference

at 630 nm on a Dynatech MR5000 96-well plate spectrometer. Absorption spectra were measured on an LKB Ultrospec 4050 spectrophotometer.

## 2.6 Macrophage killing of amastigotes

Viable macrophages were counted using trypan blue exclusion (20  $\mu$ l macrophages mixed with 80  $\mu$ l of 4% (w/v) trypan blue in phosphate buffered saline pH 7.4 (PBS)), and cultured at  $2 \times 10^5$  ml<sup>-1</sup> in 1 ml medium in a 24 well plate. They were allowed to adhere at 32°C, 5% CO<sub>2</sub>, for 2-3 h. Axenically grown amastigotes were centrifuged at 1600g for 5 min at RT, and resuspended in 1 ml macrophage culture medium. The clumps of amastigotes were dispersed by pushing the suspension three times through a 26G<sup>3/8</sup> needle, and the amastigotes were resuspended to  $2 \times 10^6$  ml<sup>-1</sup>. The 1 ml medium of the macrophage cultures was replaced with 1 ml of this amastigote suspension (giving an infection ratio of 10:1). The amastigotes were allowed to infect the macrophages for 3 h at 32°C, 5% CO<sub>2</sub>/95% air. The non-adherent amastigotes were then washed off the macrophages with three changes of warm RPMI without FCS. 1 ml of macrophage culture medium was then added. Adherent amastigotes were then allowed to invade the J774 cells by incubation overnight at 32°C, under 5% CO<sub>2</sub>/95% air.

Infected J774s were stimulated with lipopolysaccharide (LPS) (2  $\mu$ g ml<sup>-1</sup>) + interferon- $\gamma$  (IFN $\gamma$ ) (500 U ml<sup>-1</sup>), with or without L-NMMA (2 mM), and excess L-Arginine (2-10 mM). They were cultured for 48 h at 32°C under 5% CO<sub>2</sub>/95% air. 100  $\mu$ l of supernatant was then removed to measure RNI production using the Griess reaction.

The macrophages were then lysed to release the amastigotes using a variation on the method of Kiderlen and Kaye (198). The cultures were scraped in the 1 ml incubation

medium using a yellow tip, and the suspension was then added to a 1.5 ml eppendorf. Two washes of the wells with 250  $\mu$ l of HOMEM without FCS were added to the same eppendorfs. Then 12.5  $\mu$ l of 1% (w/v) SDS was added to the suspension. The suspension was centrifuged for 5 min at 1600 g RT, the supernatant removed, and 200  $\mu$ l of 0.008% SDS in warm HOMEM without FCS was added to the pellet. The solution was left for 5 min at 32°C, and the weakened macrophages were lysed by pushing the suspension six to seven times through a 26G<sup>3</sup>/<sub>8</sub> needle.

The viability of the released amastigotes was then assayed by their transformation efficiency (see section 2.4).

### **2.7 Amastigote proliferation using [<sup>3</sup>H]-Thymidine.**

Amastigotes were incubated at  $1-2 \times 10^6$  ml<sup>-1</sup> in 100-200  $\mu$ l of culture medium in 96 well plates. Each well contained 1  $\mu$ Ci of [<sup>3</sup>H]-thymidine. The plate was cultured for 24 hr at 32°C under air, then harvested on a 1295 Beta-plate harvester (Wallac). 10 ml Betaplate scintillation fluid (Wallac) was subsequently added, and the filters were counted on a 1205 Betaplate counter (Wallac).

### **2.8 Treatment with S-Nitrosothiols.**

Amastigotes at  $5 \times 10^6$  ml<sup>-1</sup> were treated in 2 ml culture medium with freshly dissolved S-nitroso-N-acetyl penicillamine (SNAP). After 30 min, 10 ml HOMEM without FCS was added and the suspension was centrifuged at 1600g for 5 min at RT. The culture was washed twice with 1 ml HOMEM without FCS, and resuspended in 1 ml HOMEM with 10% (v/v) FCS. Clumps of amastigotes were dispersed by passing the suspension three times through a 26G<sup>3</sup>/<sub>8</sub> needle. Three aliquots of 50  $\mu$ l were taken and the

cell density determined immediately. The cultures were then incubated for 48 hr at 26°C under air in 24 well plates to assay transformation efficiency.

## 2.9 Treatment with Sodium Nitrite

RNI were produced by adding sodium nitrite to the amastigote culture medium. Since the medium was already acidic, this provided a very good method for producing RNI (see section 8.9).

The concentration of nitrous acid (HONO) in the solution could be calculated using the formula:

$$[\text{HONO}] = \frac{[\text{sodium nitrite added}]}{\left(1 + 10^{(\text{pH} - 3.4)}\right)} \quad (\text{Eqn 1})$$

This formula was derived using the following series of equations:



Which means that the  $K_a$  is defined by:

$$K_{a(\text{HONO})} = \frac{[\text{NO}_2^-] [\text{H}^+]}{[\text{HONO}]} \quad (\text{Eqn 3})$$

The  $\text{p}K_a$  for HONO is already known:

$$\text{p}K_{a(\text{HONO})} = 3.4 \quad (\text{Eqn 4})$$

By definition:

$$K_a = 10^{-\text{p}K_a} \quad (\text{Eqn 5})$$

$$\Rightarrow \frac{[\text{NO}_2^-][\text{H}^+]}{[\text{HONO}]} = 10^{-3.4} \quad (\text{Eqn 6})$$

The concentration of HONO present can be calculated, given that the pH and the total sodium nitrite added were known. To do this, it is necessary to express  $[\text{NO}_2^-]$  in terms of [total sodium nitrite added] and to express  $[\text{H}^+]$  in terms of the pH.

Assuming that the concentration of RNI is small compared to the concentration of the nitrite anion and HONO:

$$[\text{NO}_2^-] = [\text{total sodium nitrite added}] - [\text{HONO}] \quad (\text{Eqn 7})$$

And by definition:

$$[\text{H}^+] = 10^{(-\text{pH})} \quad (\text{Eqn 8})$$

So, by substitution of these equations into Eqn 6:

$$\Rightarrow 10^{-3.4} = \frac{([\text{total sodium nitrite added}] - [\text{HONO}]) \times 10^{(-\text{pH})}}{[\text{HONO}]} \quad (\text{Eqn 9})$$

Which can be rearranged to give:

$$\Rightarrow \frac{10^{-3.4}}{10^{(-\text{pH})}} = \frac{([\text{total sodium nitrite added}] - [\text{HONO}])}{[\text{HONO}]} \quad (\text{Eqn 10})$$

By further rearrangement, we get:

$$10^{(\text{pH}-3.4)} = \frac{[\text{total sodium nitrite added}]}{[\text{HONO}]} - 1 \quad (\text{Eqn 11})$$

$$\Rightarrow \frac{10^{(\text{pH}-3.4)} + 1}{[\text{total sodium nitrite added}]} = \frac{1}{[\text{HONO}]} \quad (\text{Eqn 12})$$

$$\Rightarrow \frac{[\text{total sodium nitrite added}]}{10^{(\text{pH}-3.4)} + 1} = [\text{HONO}] \quad (\text{Eqn 13})$$

Which is the same as Eqn 1.

## 2.10 Measurement of ATP levels.

ATP was measured using a method based on Churchill *et al.* (204) and Strehler (205). Amastigotes were cultured at  $2 \times 10^7 \text{ ml}^{-1}$  in medium containing HONO. To lyse the cells, 100  $\mu\text{l}$  of culture was rapidly mixed with 900  $\mu\text{l}$  of ice cold 5.56% (w/v) TCA in water. The sample was kept on ice, and then centrifuged at 13000g for 20 min at 4°C to remove the precipitated protein. 500  $\mu\text{l}$  of the supernatant was neutralised with 55  $\mu\text{l}$  of 3 M KOH/0.4 M Tris/0.3 M KCl. 50  $\mu\text{l}$  of this was warmed to 25°C in a water bath, and mixed in a luminometer tube with 50  $\mu\text{l}$  luciferase reaction mixture prepared from a kit from Sigma. Light emissions were measured in a Wallac LKB 1250 luminometer, and readings were integrated over the period 30 to 40s after mixing the sample with the reaction mixture.

## 2.11 Measurement of Rhodamine 123 uptake.

A Becton Dickinson Fluorescence Analysis Cell Sorter (FACS) was used in all experiments. Amastigotes were filtered through a 100  $\mu\text{m}$  nylon mesh at the start of the experiment to prevent debris from clogging the FACS.

Amastigotes were cultured at  $2 \times 10^6 \text{ ml}^{-1}$  in culture medium containing 13  $\mu\text{M}$  Rhodamine 123. At each time point, 20  $\mu\text{l}$  of the labelled suspension was put into 980  $\mu\text{l}$

FACSFlow buffer and immediately acquired on the FACS. 2000 amastigotes were normally acquired.

## **2.12 Labelling and preparation of glycoinositol phospholipids (GIPLs).**

### **2.12.1 Labelling:**

GIPLs were labelled by incubating  $4 \times 10^7$  amastigotes in 4 ml Minimal Essential Medium (MEM) containing 100  $\mu\text{Ci/ml}$  of [ $^3\text{H}$ ]-glucosamine, pH 5.5 for 4 hr.

### **2.12.2 Extraction:**

GIPLs were extracted by centrifuging the amastigotes at 12000g for 5 min at RT, and resuspending in 500  $\mu\text{l}$  of a mixture of chloroform/methanol/water (1:2:0.5). The suspension was vortexed, sonicated, and left for over 2 hr at RT. The mixture was centrifuged at 12000g for 5 min at RT, and the pellet extracted again. The extract was dried under nitrogen.

### **2.12.3 Purification:**

GIPLs were desalted by resuspending in 300  $\mu\text{l}$  of water-saturated butanol, and adding 100  $\mu\text{l}$  water. The mixture was vortexed, and centrifuged at 12000g for 15 s at RT. The top phase containing the GIPLs was removed, and the water phase again extracted with a further 300  $\mu\text{l}$  butanol. The mixed butanol phases were then back-extracted with 200  $\mu\text{l}$  water. The GIPLs were then dried under vacuum, and resuspended in either 3M sodium acetate buffer pH 4.0 or amastigote culture medium.

#### **2.12.4 Treatment with RNI:**

GIPLs were incubated for 24 hr at 33°C in nitrite acidified with sodium acetate (pH 4.0) or amastigote culture medium in a final volume of 22.5 µl. 5 µl 0.4 M boric acid was then added and neutralised to pH 9 with 2 M sodium hydroxide (approximately 3 µl). The carbohydrate aldehydes released were reduced by adding 10 µl sodium borohydride in 1 mM sodium hydroxide, and incubating overnight at RT. The reduction was stopped with 20 µl 1 M acetic acid, and the volume made to 100 µl with water.

#### **2.12.5 Determination of the amount of deglycosylation:**

The GIPL suspensions were extracted twice with 300 µl water-saturated butanol, and then the butanol phase was back-extracted once with 200 µl water, as described in the preparation procedure. The volumes of the phases were measured, and 10% of each phase was assessed for radioactivity using 5 ml Ecoscint scintillation fluid in a Minaxi Tri-Carb 4000 series scintillation counter.

#### **2.13 Electron microscopy**

Samples for electron microscopy were processed, sectioned and stained by Margaret Mullen and Dr Lawrence Tetley.

0.2 M phosphate buffer pH 7.4 was made by the addition of 19 ml of 27.2 g/l potassium dihydrogen phosphate and 81 ml of 28.4 g/l disodium hydrogen phosphate.

Amastigotes at  $2 \times 10^6$  ml<sup>-1</sup> (axenically cultured or fresh from a lesion) were cultured with various concentrations of sodium nitrite or 2,4-dinitrophenol, and at each time point, 3 ml was spun at 1600g for 5 min at RT. The pellets were fixed in 2.5% (v/v)

glutaraldehyde in 0.1 M phosphate buffer for 30 min at RT. The sample was then washed with 1ml 0.2 M phosphate buffer, and placed in 1% osmium tetroxide for 1 h. After washing three times in distilled water over 30 min, it was placed in 0.5 % uranyl acetate for 1 hr in the dark, and then rinsed with distilled water. The sample was dehydrated in gradually increasing concentrations of ethanol (30%, 50%, 70%, 90%, Absolute (twice), Dried Absolute Ethanol) for 10 min in each wash.

The sample was washed for five minutes three times in propylene oxide, and embedded in propylene oxide/Araldite (1:1).

Araldite:

10 ml Dodecenyl succinic anhydride

10 ml Araldite CY212

0.4 ml Benzyl dimethylamine

After drying overnight in a rotator, the samples were embedded in fresh Araldite and baked at 60°C for 48 hr. They were sectioned on a Reichert:Jung Ultratome into 60-80 nm sections onto copper grids, and stained with 2% methanolic uranyl acetate for 5 min. Samples were viewed on a Ziess 902 transmission electron microscope.

## **2.14 Oxygen uptake measurement**

Amastigotes (axenically cultured or fresh from a lesion) were cultured at  $2 \times 10^6$  ml<sup>-1</sup> in a 70% ethanol-sterilised temperature-controlled chamber. Readings were taken with a model 1302 oxygen electrode and recorded on a 781B oxygen meter, both from Strathkelvin Instruments. An SE120 pen recorder from Belmont Instruments recorded the trace, with the paper moving at 12 cm/hr. Rates of oxygen consumption were measured at a given time after addition of the sample in to the chamber (usually 20 min). Calibration

was by bubbling air through the medium to achieve 100% saturation, and 0% oxygen was measured using a dilute solution of sodium sulphite.

## **2.15 DNA assays**

All methods were based on Sambrook *et al.* (2006), Promega protocols and applications guide 1990, and Fehsel *et al.* (53)

### **2.15.1 Buffers used:**

TELT buffer:

- 50 mM Tris HCl pH 8.0
- 62.5 mM EDTA pH 9.0
- 2.5 M lithium chloride
- 4% v/v Triton X-100

TE buffer:

- 10 mM Tris HCl pH 7.5
- 1 mM EDTA

Gel Loading buffer:

- 25 mM Tris HCl pH 7.5
- 1 mM EDTA
- 40% (w/v) sucrose
- 0.025% (w/v) Phenol Blue
- 0.025% (w/v) xylene cyanole FF

20 x SSC

175.3 g l<sup>-1</sup> sodium chloride

88.2 g l<sup>-1</sup> Sodium citrate

pH 7.0

5 x Tris/Borate/EDTA (TBE) buffer (in 1 litre)

54 g TRIS base

25.7 g boric acid

20 ml 0.5 M EDTA (pH 8.0)

### **2.15.2 Preparation of DNA from amastigotes:**

0.5-2 x 10<sup>7</sup> amastigotes were centrifuged at 1600g for 5 min at RT, and lysed in 500 µl TELT buffer. After 5 min incubation at RT, proteins were denatured and extracted with an equal volume of phenol/chloroform/isoamyl alcohol (ratio 25:24:1), and then once with chloroform. After precipitation with two volumes of 100% ethanol for 5 min on ice, and centrifuging at 13000 g for 5 min at 4°C, the pellets were vacuum dried and resuspended in TE buffer containing 20 µg/ml of pancreatic ribonuclease A. The DNA was left at 4°C overnight to rehydrate before measuring the concentration using either the OD<sub>260</sub>/OD<sub>280</sub> ratio of a 1:50 dilution of DNA in a TE buffer on a Beckman spectrophotometer or using the fluorimeter (see section 2.15.3).

### **2.15.3 Fluorimeter measurement of DNA concentration:**

2 µl amastigote DNA was mixed with 50 µl TE buffer containing 2 µg/ml ethidium bromide in a fluorimeter 96 well plate. A standard preparation of amastigote DNA was used, the concentration of which was determined using the OD<sub>260</sub>. Fluorescence was measured using a Perkin Elmer Luminescence Spectrometer LS50B with an excitation

wavelength of 254 nm and an emission wavelength of 605 nm with a slit width of 15 nm. The integration time was 1 s, though there was little difference in the reading if 0.1 s or 10 s were used (data not shown).

#### **2.15.4 Nicking of DNA with DNase 1:**

DNase 1 nicking buffer:

50 mM Tris HCl  
10 mM Magnesium chloride  
0.1 mM Dithioerythritol

0.3 µg amastigote DNA was mixed with DNase 1 and incubated for 2 hr at 37°C.

A sample was then run on a 0.8% agarose gel, and a sample was added to the nick translation reaction.

### 2.15.5 Nick translation:

Reaction mixture:

50 mM Tris HCl  
10 mM Magnesium chloride  
0.1 mM Dithioerythritol  
56  $\mu$ M dATP  
56  $\mu$ M dCTP  
56  $\mu$ M dGTP  
56  $\mu$ M dTTP  
1  $\mu$ Ci [ $^{32}$ P]- $\alpha$ -dATP  
1U DNA polymerase (Kornberg polymerase)  
Final volume: 20  $\mu$ l

A typical reaction proceeded for 2 hr, and was stopped by putting 10  $\mu$ l into 290  $\mu$ l 0.2 M EDTA for quantification using TCA precipitation. The rest of the reaction was mixed with 10  $\mu$ l of a Gel Loading Buffer/0.2 M EDTA (ratio 3:7) for gel electrophoresis.

### 2.15.6 Detection of labelled DNA:

#### 2.15.6.1 Trichloroacetic Acid (TCA) precipitation:

10  $\mu$ l of the stopped reaction mixture (see section 2.15.5) was spotted onto a glass filter to measure the total radiation, and 10  $\mu$ l was mixed with 90  $\mu$ l denatured salmon sperm DNA. To this was added 1.3 ml 10% (w/v) TCA/1% (w/v) *tetra*-sodium pyrophosphate. After 20 min on ice, the whole reaction was filtered through a glass filter, and washed three times with 5 ml 10% TCA/1% *tetra*-sodium pyrophosphate, then once with 5 ml 96% Ethanol. Both sets of filters were air dried, mixed with 5 ml Opti-Flow Scintillation fluid, and counted in a LS 6500 Beckman Scintillation counter.

### 2.15.6.2 Electrophoresis:

Samples were run on a 0.8% 0.5 x TBE agarose gel containing 0.5 µg/ml ethidium bromide. Radioactive markers were made by adding 5 µl of the markers to 15 µl of the nick translation mixture. The gels were photographed, denatured in 0.4 M NaOH/1 M NaCl for 40 min, and blotted overnight onto a nylon membrane using 20 x SSC buffer and capillary action. The membrane was washed in 0.5 M Tris/1 M NaCl pH 7.5, then air dried and autoradiographed.

**3. Optimisation of assays for *L. m. mexicana* viability and *in vitro* production and detection of RNI.**

### 3.1 Introduction

To study the effect of RNI on *L. m. mexicana* amastigotes *in vitro*, both viability assays for the parasite and adequate methods of RNI production needed to be developed.

Methods for axenically culturing amastigotes from any species of *Leishmania* have only recently become available (23), so there are no standard viability assays for them. Assessment of amastigote viability in macrophages has either been by Giemsa staining of fixed macrophages (62,128), or by lysing the macrophages, transforming the amastigotes to promastigotes and assaying viability by [<sup>3</sup>H]-thymidine uptake (85,207), or MTT reduction (198). [<sup>3</sup>H]-thymidine uptake and MTT reduction are used after transforming amastigotes to promastigotes, so have only been used to assess promastigote viability. Since promastigote metabolism is different from amastigote metabolism (208), an assessment of whether either of these methods was suitable for amastigote viability was required.

RNI detection and production with the equipment available required an assessment of the standard chemical reactions. The normal assay for the Griess reaction requires measurement at 540 nm (33), while the closest filters available for the departmental 96 well spectrometer were 490 nm and 570 nm. Furthermore, the effect of some of the dyes (eg Phenol Red) in the media used on the absorption spectrum of the Griess reaction product needed to be assessed.

One method for production of RNI is the addition of S-nitroso-N-acetyl penicillamine (SNAP) to the medium. The release of RNI from this molecule can be affected by temperature, pH, presence of sulphhydryl groups and metal ions (27,28), all of which are dependent on the medium and foetal calf serum (FCS) used. To determine the

rate of RNI production for the systems used here, it was necessary to determine how SNAP interacted with the Griess reagents and amastigote culture medium.

Another method for RNI production is acidification of sodium nitrite to form nitrous acid, which then decays to form the other RNI (64). It was necessary to determine both the stability of this system and whether the toxicity of such a system was due to RNI production, to nitrite itself or to the sodium ions.

Finally, to study the mechanisms whereby J774 cells, a murine macrophage-like cell line, kill amastigotes, it was necessary to develop methods for stimulating the line to produce RNI at 32°C, and to develop a method for lysing the J774 cells to release intact amastigotes. This chapter describes the initial experiments to determine the optimal conditions for the viability assays, production and measurement of RNI *in vitro*, and the stimulation of J774 cells.

## **3.2 Development of viability assays**

Two viability assays were studied - [<sup>3</sup>H]-thymidine uptake, and transformation efficiency. To show that the assays were suitable for *L. m. mexicana* amastigotes, it was necessary to show that increasing the concentration of amastigotes at the start of the experiment increased both [<sup>3</sup>H]-thymidine uptake and the number of promastigotes after the transformation.

### **3.2.1 Thymidine assay**

Amastigotes were cultured for 24 h in the presence of thymidine, as described in Materials and Methods. [<sup>3</sup>H]-thymidine uptake increased with increasing initial concentrations of amastigotes up to  $1 \times 10^7$  ml<sup>-1</sup> (Figure 3.1). Since readings from

thymidine uptake were obtainable down to  $2 \times 10^6 \text{ ml}^{-1}$ , most thymidine uptake experiments were performed at this concentration of parasites. Though the uptake of [ $^3\text{H}$ ]-thymidine was much less, the readings were still high enough to give reproducible results.

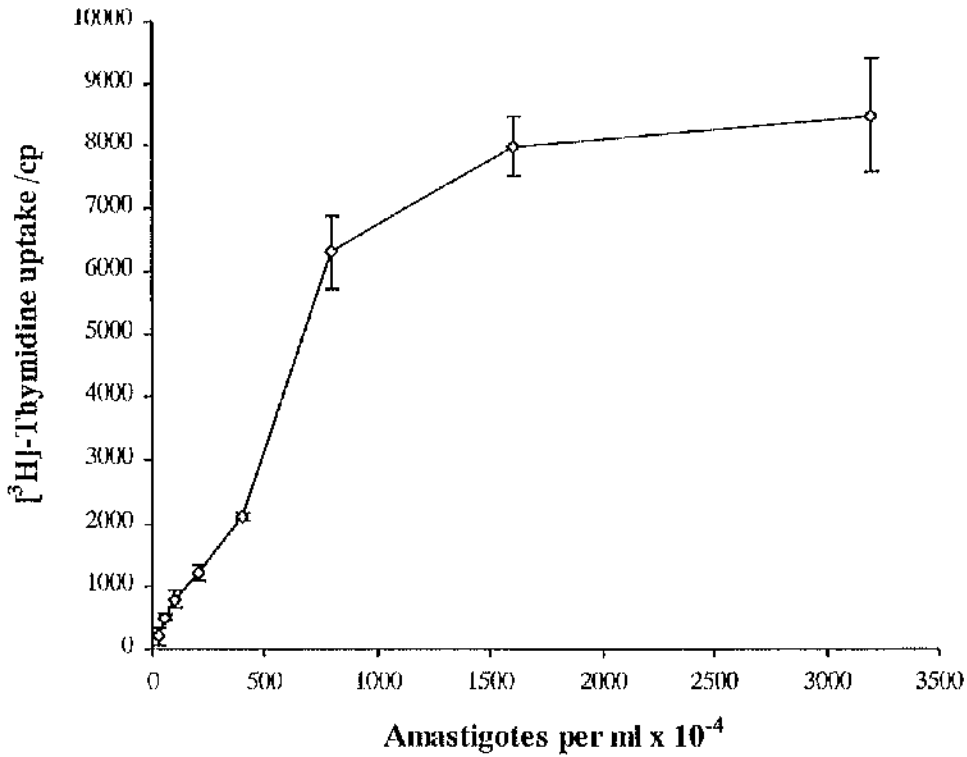
### 3.2.2 Transformation assay.

Amastigotes are very different from promastigotes. The former are small ( $3 \times 5 \mu\text{m}$ ), aflagellate, and non-motile. The latter are very varied in shape and size, but characteristically are flagellate, motile, and up to  $60 \mu\text{m}$  in length. The protein and surface glycolipid profiles are also very different, and the transformation process involves a division step. This means that in order to transform to promastigotes, the amastigote must have its protein, glycolipid, and DNA synthesising systems intact.

The extracellular signals required to transform from amastigotes to promastigotes have not been clearly defined, but amastigote growth is sustained in Schneider's *Drosophila* Medium, pH 5.4-5.7, with 20% (v/v) FCS at  $32\text{-}33^\circ\text{C}$  (24). Amastigotes will transform to promastigotes in HOMEM medium (203) containing 10% (v/v) FCS, and grown at  $26\text{-}28^\circ\text{C}$  (25). The transformation process can take 48 h, though often 24 h was sufficient. Because of the often rapid growth of promastigotes after transformation, it was preferable to sample the number of transforming promastigotes after 24 h.

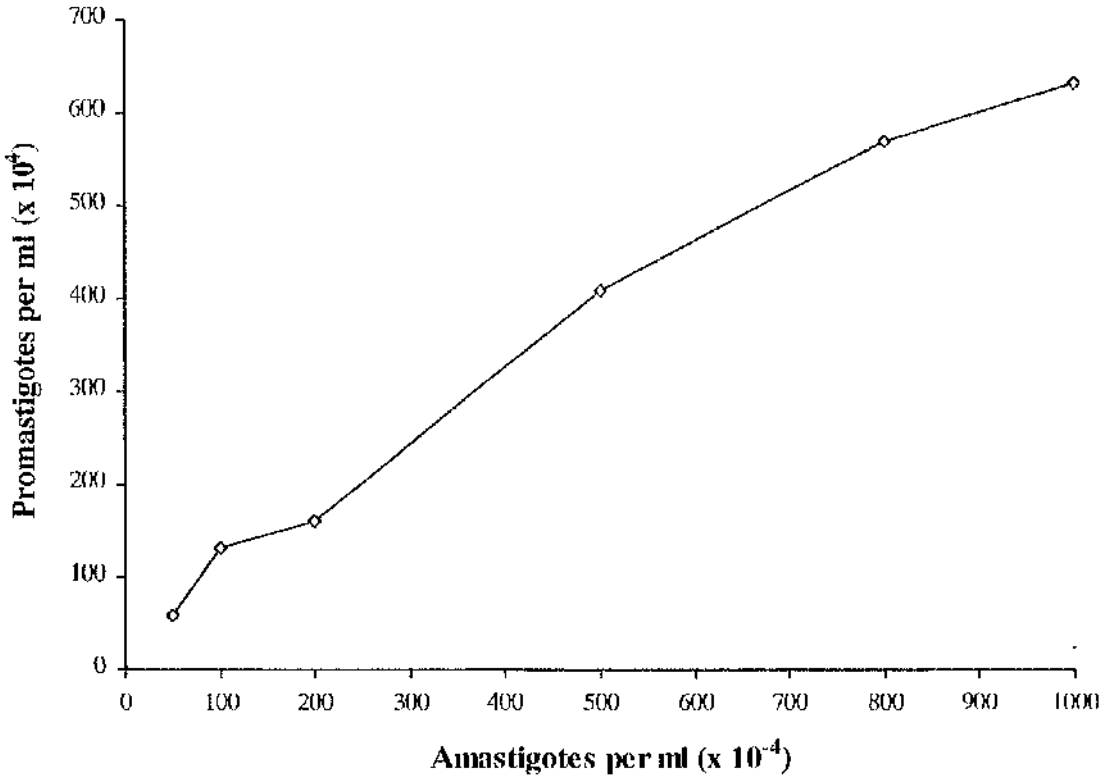
Figure 3.2 shows that the number of promastigotes after transformation increased with increasing initial concentrations of amastigotes up to a starting concentration of  $1 \times 10^7 \text{ ml}^{-1}$ . In future experiments, it appeared that the transformation efficiency could vary greatly, so most transformation assays were set up at below  $1 \times 10^6 \text{ ml}^{-1}$  to ensure that at the end of the assay, the promastigotes had not reached stationary phase.

**Figure 3.1: [<sup>3</sup>H]-thymidine uptake by amastigotes**



[<sup>3</sup>H]-thymidine uptake by amastigotes over 24 h was assayed at 32°C. Results are expressed as the mean ± SEM. The results shown are representative of two separate experiments.

**Figure 3.2: Transformation efficiency assay.**



Axenically cultured amastigotes were seeded at different concentrations in HOMEM medium with 10% (v/v) FCS, and cultured at 26°C for 48 h. A sample was then fixed, and the density of promastigotes was determined.

### 3.3 Production and measurement of RNI.

#### 3.3.1 Introduction

Several methods have been used for the production of RNI *in vitro*, including bubbling of nitric oxide gas through medium, addition of chemicals that produce RNI, and production from the enzyme nitric oxide synthase. One problem with most methods is that the half life of the production system is often extremely short (28), which is unsuitable for mimicking the *in vivo* situation where a population of macrophages will produce RNI over a period of many hours (160).

Another problem is the measurement of the concentration of RNI present. The only method suitable for quantifying the individual RNI species is electron spin resonance, which cannot give localised information on the concentrations of RNI that might surround a parasite in the parasitophorous vacuole (PV). Furthermore, the debate continues as to which of the RNI species account for most of the toxicity. In addition, the proportions of the different species of RNI are likely to depend upon the environment of the production system. The kinetics of the reactions between the different RNI are likely to depend on the redox potential, the pH, the concentration of sulphhydryl groups and metal ions, the concentration of oxygen, and probably many other unknown factors.

The most common way to overcome this problem is to circumvent it, by adding a chemical that releases some RNI. Frequently S-nitroso-N-acetyl-penicillamine (SNAP) has been used, which releases NO and NO<sup>+</sup> as well as reacting directly with other compounds. The amount of RNI present is then expressed simply as a concentration of the chemical added. A complication of this method is that the production of RNI from these

compounds depends very much on the medium that is being used (209). Since amastigote culture medium is acidic, with the  $[H^+]$  being almost two orders of magnitude higher than in other media in which these chemicals have routinely been used, the kinetics of release of RNI from SNAP were assessed using the Griess reaction which was first optimised for the system.

### 3.3.2 Absorption properties of the Griess reaction

Measurement of RNI production is often made by the Griess reaction. This involves the diazotisation of two aromatic amines, the progress of the reaction being measured by absorbance of the product at 540 nm. Since a 540 nm filter was not available, the suitability of other filters was assessed.

The absorption spectrum for the Griess reaction (Figure 3.3) shows that the absorption maximum of the product is 520 nm whether it is in DMEM, RPMI or water. Thus the dyes in the media do not affect the absorption maxima and minima, though in DMEM they may affect the absorption coefficient, so that standard curves should be constructed in DMEM for measurements of the concentration of RNI in DMEM.

The filters that could be used on the Dynatech MR5000 spectrometer were 490 nm or 570 nm. The absorption coefficient at 490 nm was not far below that at 520 nm, indicating that this may be a suitable filter (Figure 3.3). A reference wavelength of 630 nm could be used to normalise for non-specific diffraction

In water there is no dye that may produce a background reading (Figure 3.4), but in DMEM the optical density below 560 nm may be affected by a dye that is present in the medium (Figure 3.5). Without a detailed chemical analysis it is impossible to say whether

macrophages or SNAP might affect the absorbance of this dye. Therefore, although the absorbance at 490 nm may be stronger, the absorbance at 570 nm is less likely to be affected by changes in this dye.

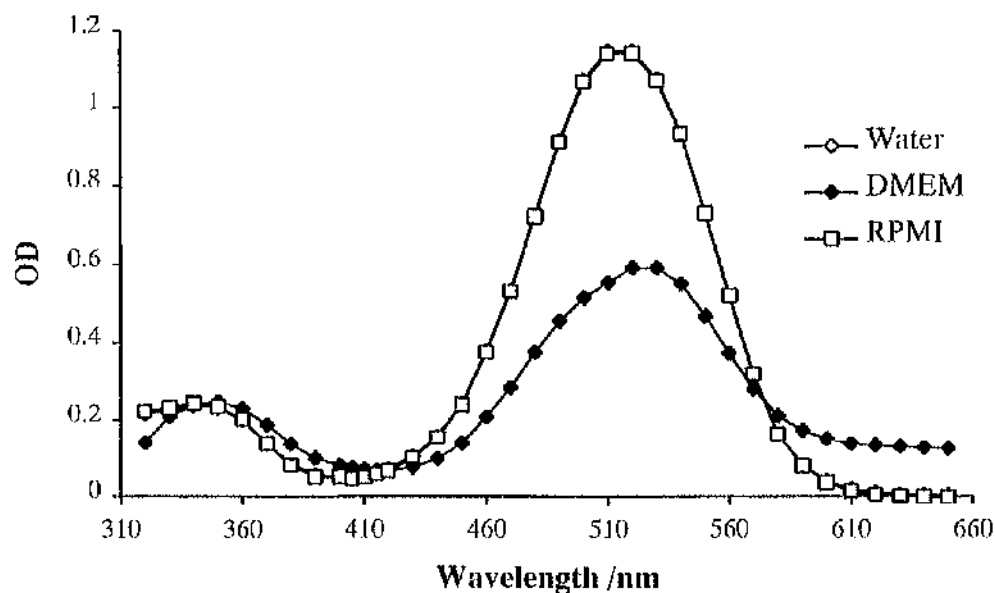
Therefore, absorbance at 570 nm was generally used with the Dynatech MR5000, and 545 nm with the Titertek Multiscan MCC 340 spectrometer.

### **3.3.3 Determination of the rate of release of RNI from SNAP**

#### **3.3.3.1 Release of RNI from SNAP in Griess reagent**

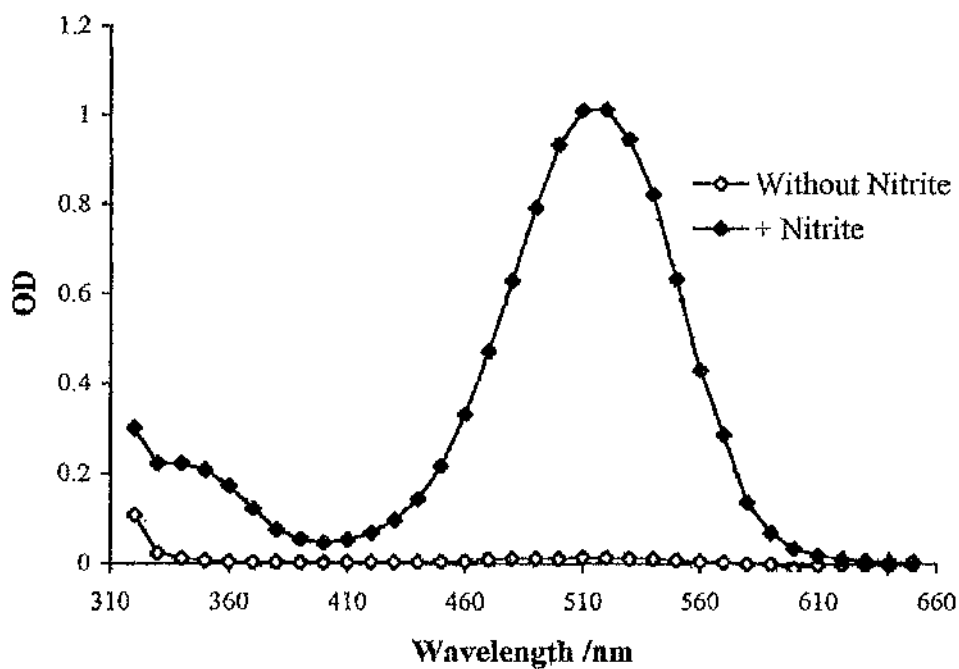
To determine the rate of release of RNI from SNAP in any medium using the Griess reagent, it was necessary to assess RNI release from SNAP in the Griess reagent, which in turn required knowledge of how quickly the Griess reagent could detect RNI production. The Griess reagent responded very quickly to sodium nitrite (Figure 3.6), and the reading for a given concentration of nitrite stayed stable for almost two hours (Figure 3.7). Therefore, if SNAP released RNI for several hours, which would be a suitable rate for analysing its effects on amastigotes, the Griess reagent would respond quickly enough to be useful in measuring the rate of RNI release from SNAP.

**Figure 3.3: Absorption spectrum for the Griess reaction.**



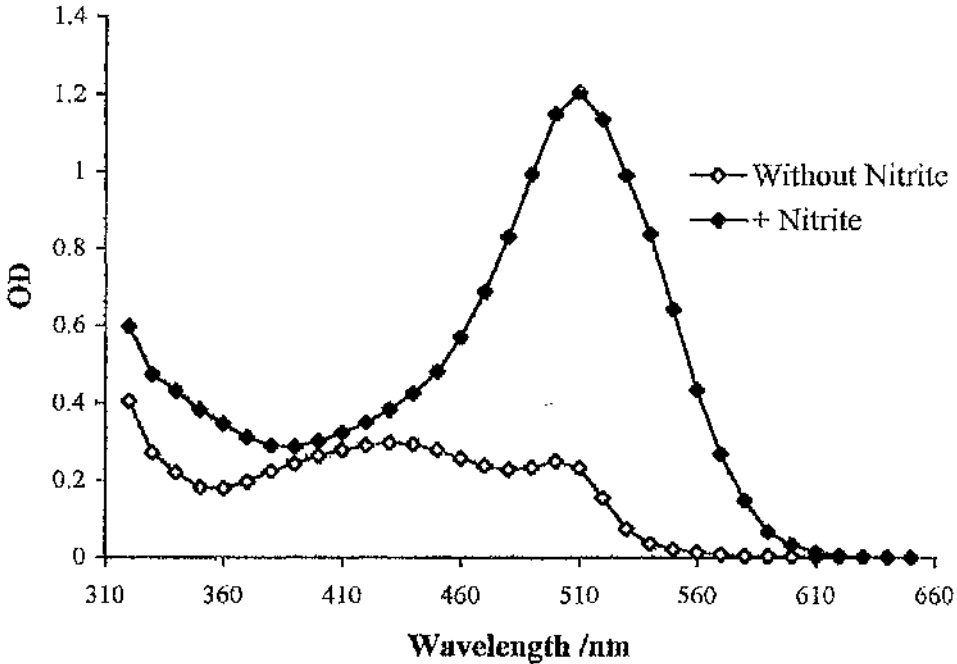
Sodium nitrite was dissolved to 72.5  $\mu\text{M}$  in 500  $\mu\text{l}$  medium and mixed with 500  $\mu\text{l}$  of the Griess reagent for at least 10 min at room temperature. The spectrum of the products was then determined. The results for the measurement in water are so close to those for RPMI that the symbols are hidden behind the symbols for RPMI.

Figure 3.4: Absorption spectrum for the Griess reaction in water



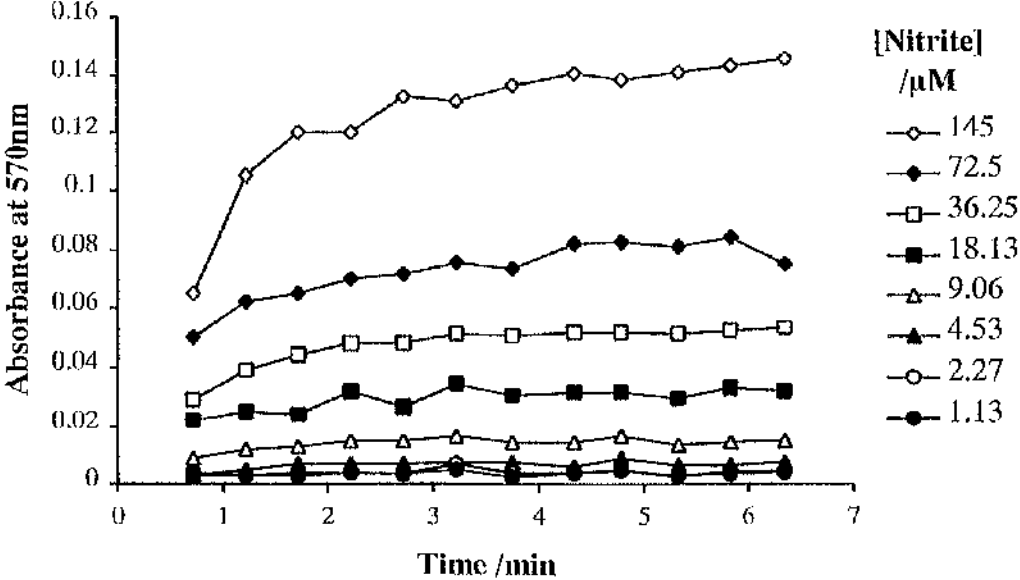
Sodium nitrite was dissolved to 72.5  $\mu\text{M}$  in 500  $\mu\text{l}$  water and mixed with 500  $\mu\text{l}$  of the Griess reagent for at least 10 min at room temperature.

**Figure 3.5: Absorption spectrum the Griess reaction in DMEM**



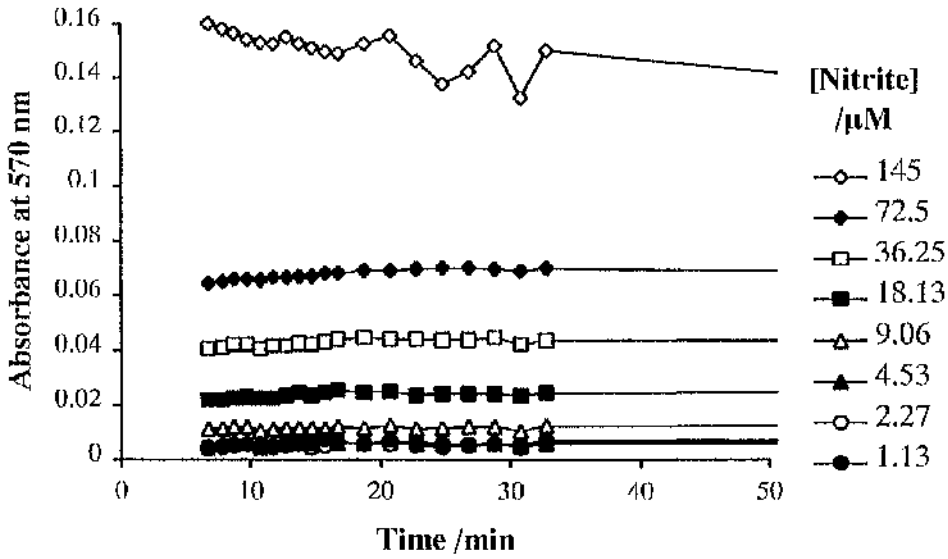
Sodium nitrite was dissolved to 72.5  $\mu$ M in 500  $\mu$ l DMEM and mixed with 500  $\mu$ l of the Griess reagent for at least 10 min at room temperature.

**Figure 3.6: The kinetics of the Griess reaction**



Serial dilutions of sodium nitrite were made in 50  $\mu\text{l}$  RPMI, and mixed with 50  $\mu\text{l}$  Griess reagent at RT.

Figure 3.7: Stability of the Griess reaction



Serial dilutions of sodium nitrite were made in 50  $\mu$ l RPMI, and mixed with 50  $\mu$ l Griess reagent at RT.

### **3.3.4 Release of RNI from SNAP in amastigote culture medium**

SNAP does not immediately release all its RNI in the Griess reagents (Figure 3.8), so it is meaningful to use the Griess reaction to measure the rate of nitrite release from SNAP in culture medium.

The rate of release of RNI from SNAP in amastigote culture medium is nearly the same as the rate of release in Griess reagent (Figure 3.8 and Figure 3.9). 1 mM SNAP will release approximately  $1 \mu\text{M min}^{-1}$  nitrite in amastigote culture medium.

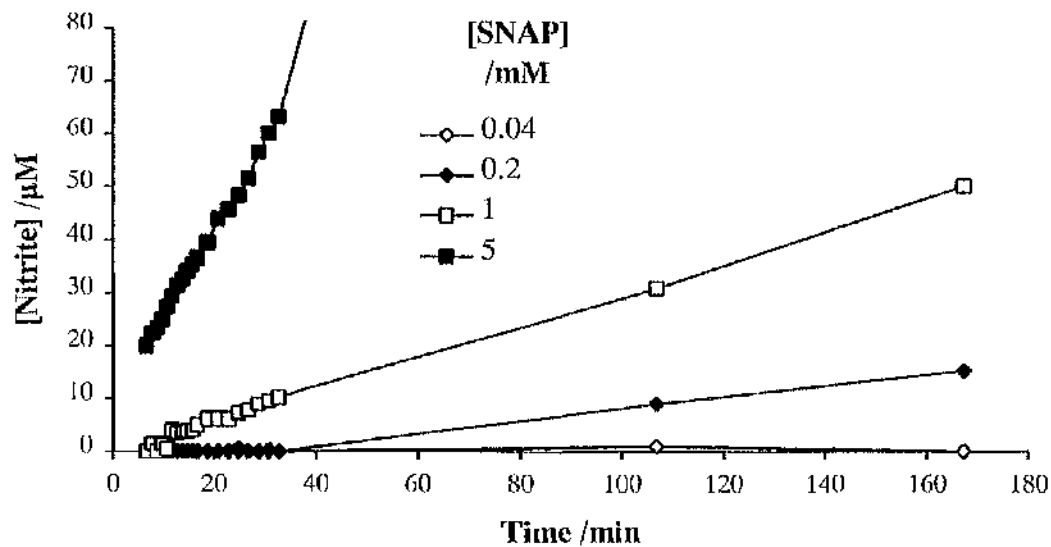
This meant that a solution of SNAP in amastigote culture medium would continue to produce RNI for a few hours. This is a reasonable length of time when compared to the several hours over which macrophages release RNI in culture. SNAP can therefore reasonably be used to produce RNI to assess the toxicity to *L. m. mexicana* amastigotes.

The rate of release of RNI release from SNAP was then measured in every experiment using SNAP.

### **3.3.5 The toxicity of SNAP to amastigotes.**

SNAP is toxic to amastigotes in a half hour incubation (Figure 3.10). 1 mM SNAP usually killed just some of the cells, whereas 10 mM SNAP was normally lethal to all cells by 30 min. The toxicity was not due to the N-acetyl-penicillamine (NAP) moiety of SNAP since NAP at 10 mM was not toxic.

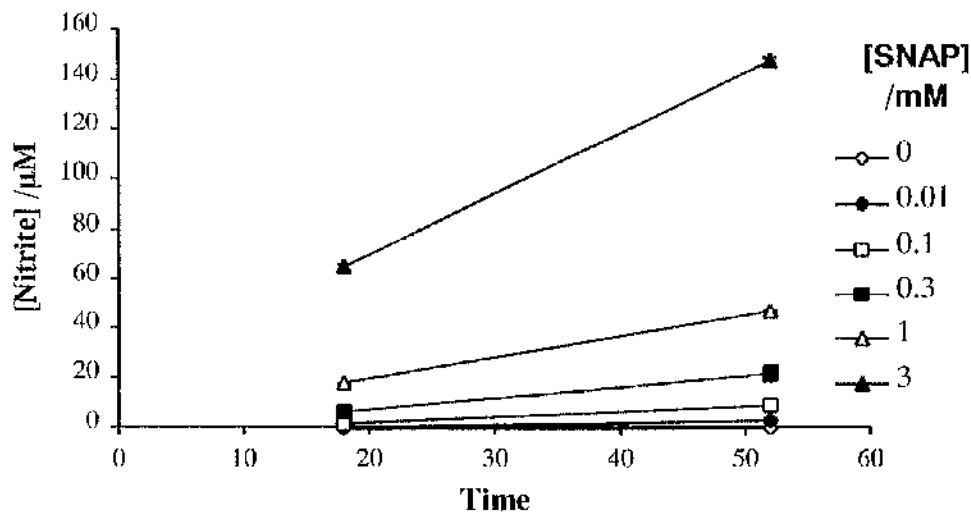
Figure 3.8: The rate of release of RNI from SNAP in the Griess reagent.



SNAP was dissolved in RPMI with 20% (v/v) FCS, and placed in 50  $\mu$ l in a 96 well plate.

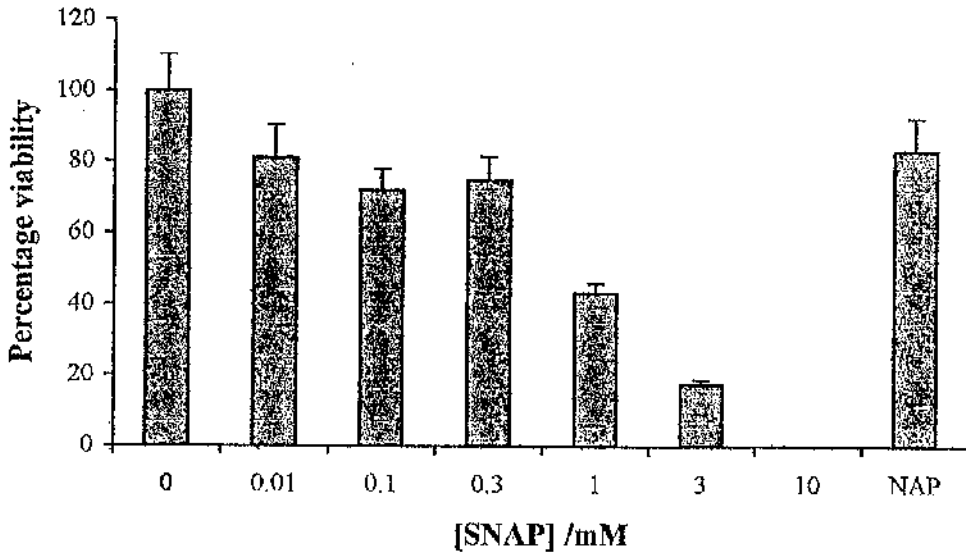
50  $\mu$ l of Griess reagent was added, and compared to a standard of sodium nitrite.

**Figure 3.9: Rate of release of RNI from SNAP in amastigote culture medium.**



50  $\mu$ l SNAP in amastigote culture medium was mixed with 50  $\mu$ l Griess reagent at the times shown, incubated at RT for 10 min, and read at 540 nm against a sodium nitrite standard curve. Results are expressed as the mean  $\pm$  SEM, and is representative of five separate experiments.

**Figure 3.10: The effect of SNAP on amastigotes**



Axenically grown amastigotes were treated with freshly dissolved SNAP or 10 mM NAP for 30 min at 32°C in air. Viability was assayed by transformation efficiency. Results are expressed as the mean  $\pm$  SEM, and are representative of five separate experiments.

### 3.4 Production of RNI using acidified nitrite

Another method for producing RNI *in vitro* is by acidification of the nitrite anion. In distilled water, most of the reactions of such a solution can be attributed to RNI that behave like  $\text{NO}^+$  (J. Reglinski, personal communication). However, in complex biological media, almost all of the RNI can be formed by the complex series of reactions involving sulphhydryl groups and iron-containing enzymes.

A solution of acidified nitrite can form an equilibrium between the nitrite and RNI that is more likely to mimic the *in vivo* system of a steady production of NO by nitric oxide synthase (NOS) than simply adding SNAP (see section 3.6).

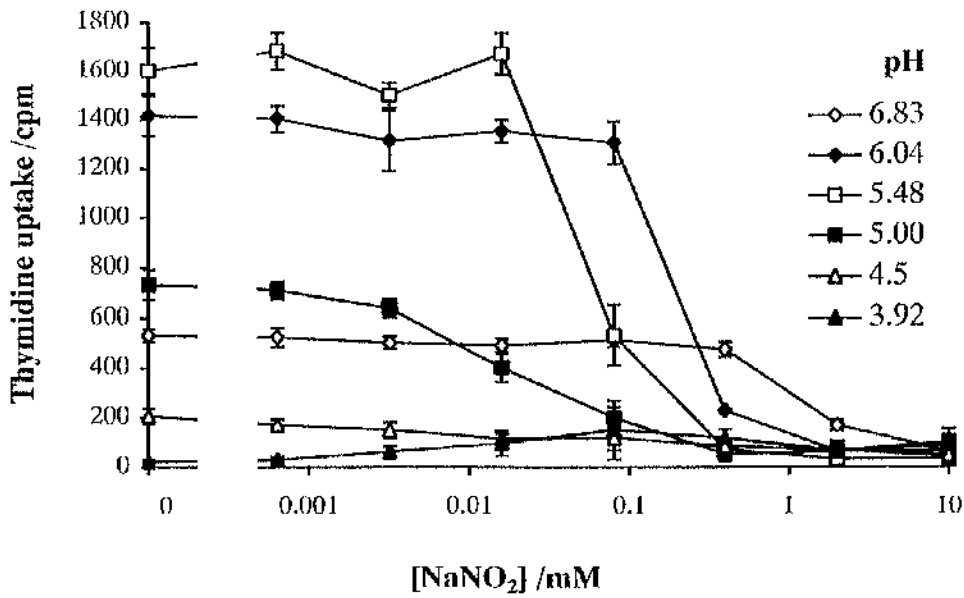
Acidified nitrite produces RNI by protonation of the nitrite anion to form nitrous acid (HONO). HONO will then spontaneously decay to form the other RNI. To prove that the toxicity of such a solution is due to RNI production rather than direct toxicity of the nitrite anion or the sodium ion, we compared the toxicity of a solution of nitrite at different pH's (Figure 3.11).

In such a solution, the toxicity depends both on the concentration of nitrite and on the pH. It is possible, however, to calculate the concentration of HONO using the equations described in Materials and Methods (Section 2.9). The toxicity of the solution can thereby be shown to correlate with the concentration of HONO.

This does not mean that HONO is necessarily the toxic moiety in the solution, but rather that its calculated concentration correlates with toxicity (Figure 3.12). It is therefore a good measure of the concentration of whatever is toxic.

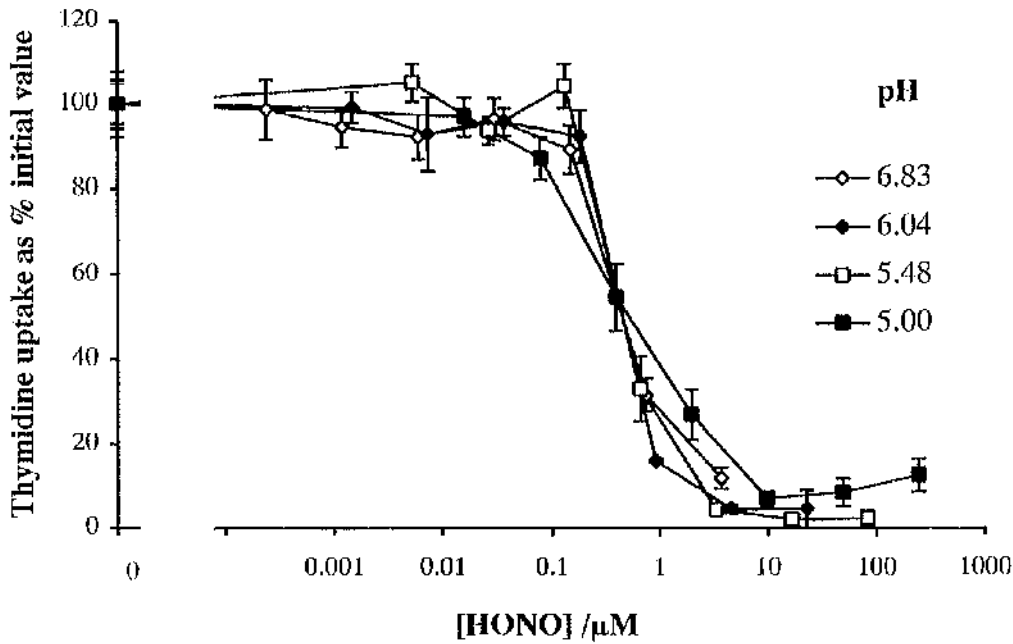
Such a solution maintains most of its toxicity for at least 24 h (Figure 3.13). Thus the concentration of RNI after 24 h is only slightly lower than the concentration when the equilibrium is set up fresh. This is particularly important, because it is imperative not to study the toxic effects of an extremely high short dose of RNI, which may be different from the toxic effects of a long exposure to RNI.

Figure 3.11: The toxicity of a solution of sodium nitrite depends on the pH.



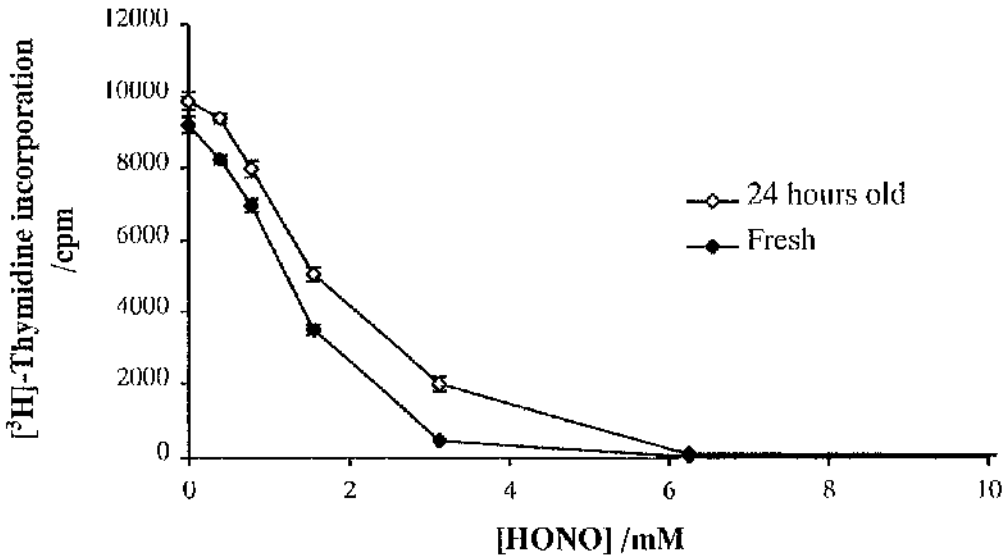
$[^3H]$ -thymidine uptake by amastigotes was assayed in the presence of sodium nitrite in medium acidified with 1 M hydrochloric acid. Results are expressed as the mean  $\pm$  SEM (n=4), and are representative of three separate experiments.

**Figure 3.12: The toxicity of a solution of sodium nitrite correlates with the concentration of nitrous acid (HONO).**



Data from Figure 3.11. Results normalised for the effects of pH on control proliferation, by taking the proliferation in the absence of sodium nitrite as 100 %. The concentration of HONO was calculated from the concentration of sodium nitrite and the pH. Results are expressed as the mean  $\pm$  SEM (n=4), and are representative of three separate experiments.

Figure 3.13: The effect of leaving the acidified nitrite solution for 24 h.



Serial dilutions of sodium nitrite were made in amastigote culture medium, and either kept at 32°C in air overnight or used immediately. Amastigotes were added to a final concentration of  $2 \times 10^6 \text{ ml}^{-1}$  in the presence of thymidine, and cultured for a further 24 h before harvesting.

### 3.5 *L. m. mexicana* infection of J774 cells at 32°C

Assays of macrophage killing of amastigotes have either been based on microscopic examination of Giemsa-stained macrophages or lysis of macrophages followed by a viability assay such as [<sup>3</sup>H]-thymidine uptake or MTT reduction. One problem with Giemsa staining is that it is not possible to determine whether the amastigote is alive or dead. The major problem with many of the viability assays is that they do not distinguish between macrophages and *Leishmania*, so that if the macrophages are not completely lysed, the results could be attributed to the macrophages that are left rather than the parasites.

The transformation efficiency viability assay overcomes both these problems when used to measure the relative number of live or dead amastigotes that could be recovered from a population of macrophages. This method does not give an absolute number of viable parasites per cell, but simply a relative measure of percentage viability between infected populations. Amastigotes taken from an unstimulated macrophage culture were therefore defined as 100 % viable.

Since there is only a small difference in the concentrations of sodium lauryl sulphate (SDS) that are required to lyse amastigotes from *L. donovani* and macrophages (198), a method for specifically lysing J774s rather than amastigotes was developed. This involved a combination of SDS and shearing induced by pushing the macrophage suspension through a 26G<sup>3</sup>/<sub>8</sub> needle. The efficiency of the protocol was assessed by the final number of macrophages and the number of amastigotes recovered (Table 3.1).

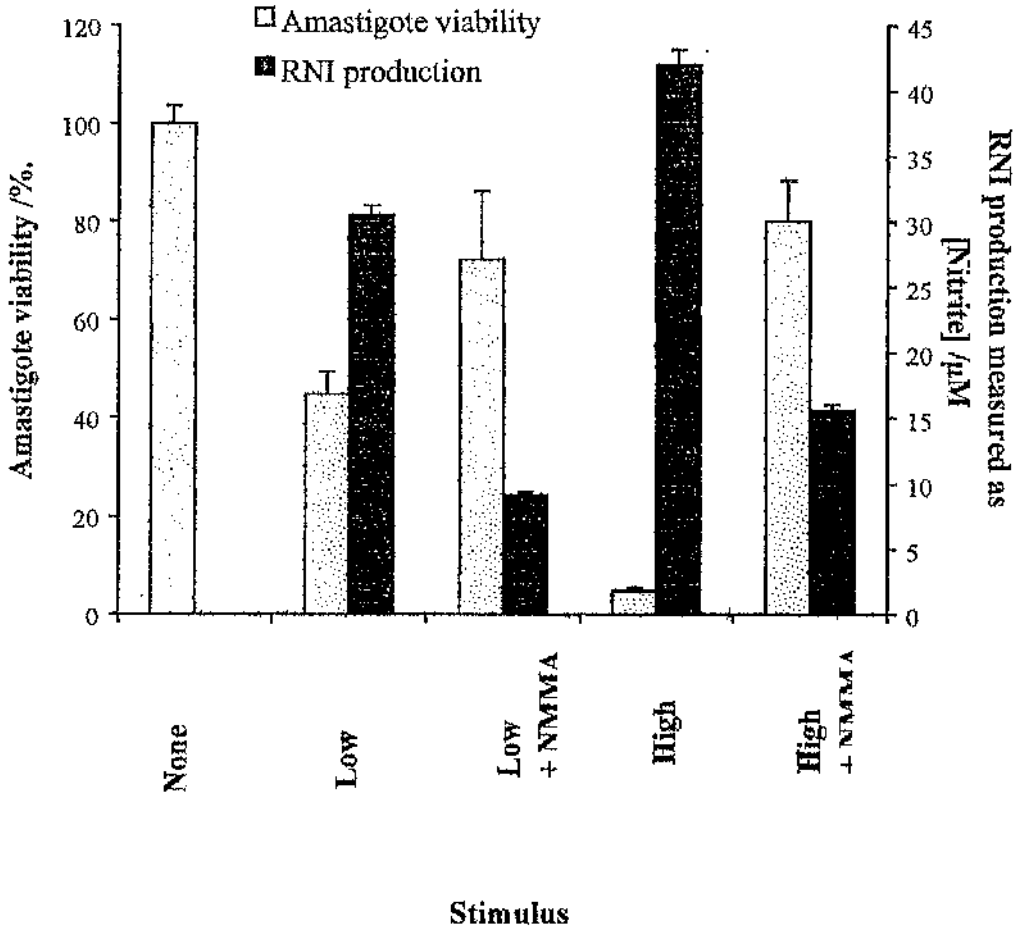
Having established that it was possible to lyse J774s without lysing *L. m. mexicana* amastigotes, the conditions required for J774s to produce RNI at 32°C were examined. Figure 3.14 shows that J774s could produce RNI and kill *L. m. mexicana* at 32°C. RNI production and some of the leishmanicidal activity could be inhibited by NOS inhibitor L-NMMA. More RNI was produced from J774s stimulated with the high stimulus (500 U ml<sup>-1</sup> IFN $\gamma$  + 2  $\mu$ g ml<sup>-1</sup> LPS).

**Table 3.1: Efficiency of the lysis protocol.**

	<b>Treatment</b>	<b>Macrophages in total</b>	<b>Amastigotes</b>
(i)	Scraping wells with a yellow tip	$(5.3 \pm 0.6) \times 10^4$	N.D.
(ii)	(i) followed by centrifugation at 1600g for 5 min at 23°C. Resuspend in 100 µl 0.1% SDS for a up to 15 min.	After 7 min: $4.3 \times 10^4$ After 10 min: $1.5 \times 10^4$ After 15 min: $2.9 \times 10^4$	N.D.
(iii)	(ii) followed by five times through a yellow tip.	$1.9 \times 10^4$	N.D.
(iv)	(iii) followed by 4 x through a 26G <sub>3/8</sub> needle	$1 \times 10^3$	N.D.
(v)	As (iii) followed by 3 x through 26G <sub>3/8</sub> needle	$5 \times 10^3$	N.D.
(vi)	As (iv) but 0.01% SDS for 7 min.	$1 \times 10^3$	$9 \times 10^5$
(vii)	As (iii), but before centrifugation, added 15 µl of 1% SDS	0 (n=2)	$3.1 \times 10^5$ and $3.7 \times 10^5$
(viii)	As (vii), but using 0.008% SDS, instead of 0.01% SDS	2 and 0	$5.8 \times 10^5$ and $5.4 \times 10^5$

$2 \times 10^5$  J774 cells were infected overnight with  $2 \times 10^6$  amastigotes as described in Materials and Methods. Cells were lysed as described, and the efficiency assayed by counting the number of amastigotes and J774s immediately after lysis. N.D. - Not Determined.

Figure 3.14: J774 macrophages can produce RNI and kill *L. m. mexicana*.



J774s were infected with amastigotes, then stimulated for 48 h with either Low stimulus ( $40 \text{ U ml}^{-1} \text{ IFN}\gamma + 10 \text{ ng ml}^{-1} \text{ LPS}$ ) or High stimulus ( $500 \text{ U ml}^{-1} \text{ IFN}\gamma + 2 \text{ }\mu\text{g ml}^{-1} \text{ LPS}$ ) in the presence of  $1 \text{ mM L-NMMA}$ . J774s were lysed using protocol (viii) (Table 3.1), and amastigote viability was assayed by transformation efficiency. Results are expressed as the mean  $\pm$  SEM (n=4).

### 3.6 Conclusions

The viability assays, [<sup>3</sup>H]-thymidine uptake and transformation efficiency, are both suitable for use with amastigotes from *L. m. mexicana* (Figure 3.1 and Figure 3.2). [<sup>3</sup>H]-Thymidine uptake has the advantage that it is easy to use, and several different measurements can be made in the same experiment.

Transformation efficiency has the advantage that the results are unequivocally a measure of amastigote viability. For instance, unlike thymidine uptake, it will distinguish between death and a temporary inhibition of pyrimidine uptake across the membrane, or any effect on pyrimidine synthesis. Another advantage of this assay is that it can take a 'snapshot' of viability, which is suitable for time course experiments of toxicity, whereas [<sup>3</sup>H]-thymidine uptake requires a 24 h incubation. It is, however, a much more cumbersome assay.

Of the filters available for the Griess reaction, it is best to use 570 nm for absorption, and 630 nm for reference when detecting nitrite production, to ensure that there was no interference from dyes in the medium.

1 mM SNAP produces nitrite at a rate of approximately 1  $\mu\text{M min}^{-1}$  in medium. These measurements were not confounded by a sudden release of nitrite when SNAP was added to the Griess reagent, or by the decay product of SNAP mopping up nitrite on addition of the Griess reagents, both of which scenarios are conceivable given the varied, and poorly characterised, reactions of RNI.

The high concentrations of SNAP (3 mM and 10 mM) required to kill amastigotes in 30 min released enough nitrite in that time for the nitrite itself to be toxic in the

amastigote culture medium (compare the toxic concentrations in Figure 3.11 to the amount of nitrite released by 3 mM SNAP in Figure 3.9). This meant that the concentrations of the different RNI species would be changing constantly during the period of the exposure.

The toxicity of the solution of sodium nitrite, on the other hand, remains stable for up to 24 h (Figure 3.13). Since RNI is formed by an equilibrium between nitrite and RNI, exposure to RNI is constant over this time period. The toxicity correlates with the concentration of HONO (Figure 3.11 and Figure 3.12), which is therefore a useful measure of the concentration of RNI in the solution.

Since amastigotes are routinely cultured at pH 5.4-5.7, the addition of sodium nitrite to the medium is the best way of producing RNI. The method will produce many of the forms of RNI that are likely to be present in the macrophage - from the small oxides of nitrogen (eg NO, NO<sup>+</sup>, HNO<sup>+</sup>, H<sub>2</sub>NO<sup>+</sup>, NO<sup>-</sup>, HONOO) to the larger complexes with organic molecules (eg S-nitrosothiols and NO ligated to iron in proteins). Although RNI are produced in a macrophage from a completely different route (Arginine + O<sub>2</sub> → Citrulline + NO), a similar set of RNI are likely to be present in the parasitophorous vacuole to the species set up by acidification of RNI in proteinaceous media. This is because the reactions that interconvert the different RNI species are fast.

It was possible to lyse infected J774s preferentially to release viable amastigotes using a combination of shearing and SDS (Table 3.1), and protocol (viii) became the standard protocol for preparation of amastigotes from macrophages.

J774s could produce RNI and kill amastigotes at 32°C (Figure 3.14), and both effects were inhibitable by L-NMMA, an arginine analogue, hinting at a role for RNI in macrophage killing of amastigotes. This phenomenon is investigated further in Chapter 4.

In conclusion, assays were developed for the determination of amastigote viability, and for RNI detection and production. A protocol for the preferential lysis of J774s was developed and the conditions required to stimulate J774s to kill amastigotes and produce RNI at 32°C were determined.

#### **4. Guideline experiments**

## 4.1 Introduction

To study the effect of RNI on *L. m. mexicana*, it is important to consider the overall picture in which macrophages simultaneously produce a variety of responses during an infection, and to examine a possible protective response that amastigotes may have developed to RNI.

The effect of RNI in many systems can be affected by the presence of other molecules, such as proteins or oxygen radicals (27,28). These are both present in activated macrophages, and in order to study the effect of RNI on *L. m. mexicana* amastigotes, the interaction of RNI with some of the macrophages' other defence systems was examined.

A study of amastigote resistance to RNI was also undertaken. It is impossible to correlate the concentrations of RNI that we are studying with concentrations that could be produced *in vivo*. However, if amastigotes were extremely resistant to RNI, then the toxic concentrations of RNI may be too high to be physiologically relevant.

Amastigote susceptibility to RNI was compared to that of promastigotes, J774 macrophages, *Escherichia coli*, *Salmonella typhimurium* and *Tritrichomonas foetus*. Promastigotes were examined to see whether amastigotes had a life-cycle stage dependent resistance. J774s were examined to see whether the amount of RNI produced by a macrophage would kill amastigotes without killing the macrophage itself. *E. coli* was examined as a totally unrelated extracellular organism, while *S. typhimurium* was examined as an unrelated intracellular organism. *T. foetus* was examined because it does not have a mitochondrion, which we believed may be a potential target of RNI.

Amastigotes were either taken directly from lesions in susceptible BALB/c mice, or grown axenically *in vitro*. In both cases, they were probably not exposed to high concentrations of RNI. Organisms are often able to develop resistance to toxic molecules if they are exposed to small amounts of the toxins, so induction of an RNI resistant phenotype was attempted in amastigotes using exposure to low levels of RNI.

## **4.2 The interaction of RNI with other parasitophorous vacuole components**

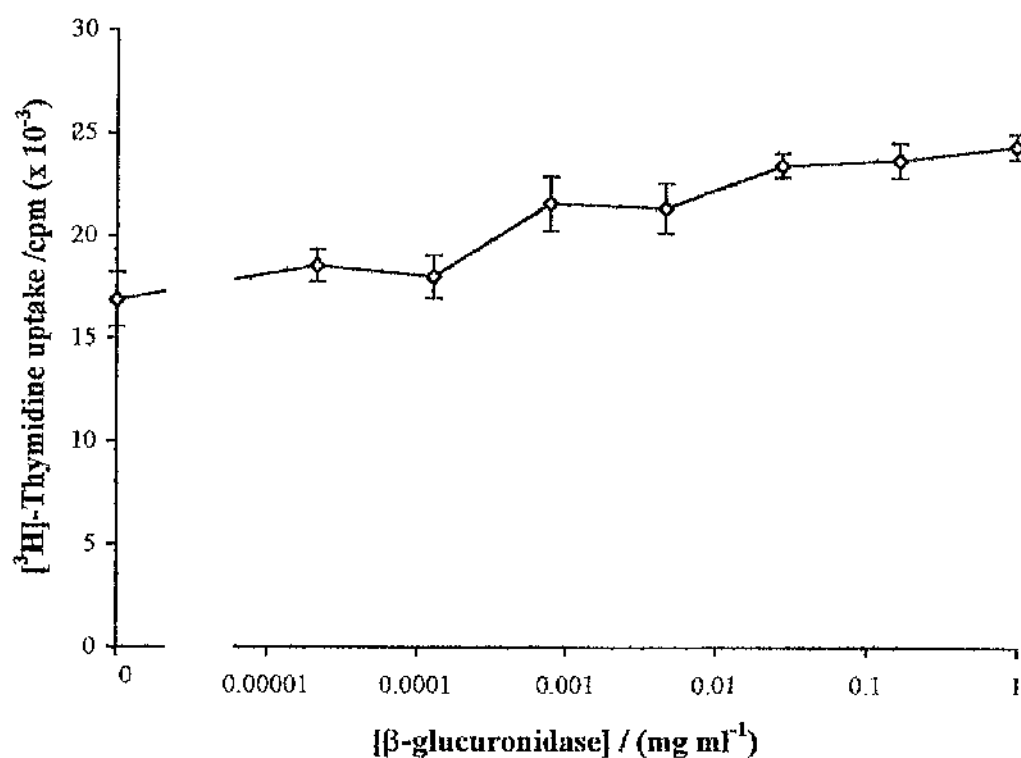
The interaction of RNI with three other defence components present in the parasitophorous vacuole (PV) was studied. The compounds selected were  $\beta$ -glucuronidase, cathepsin D and hydrogen peroxide.

### **4.2.1 $\beta$ -glucuronidase and cathepsin D**

To determine the concentration of PV enzymes that should be used to assess toxicity, a concentration curve of the toxicity of the enzymes alone towards amastigotes was set up. Neither of the two enzymes studied had any toxicity of their own (Figure 4.1 and Figure 4.2), so the effect of the highest concentration of each enzyme on RNI toxicity was determined.

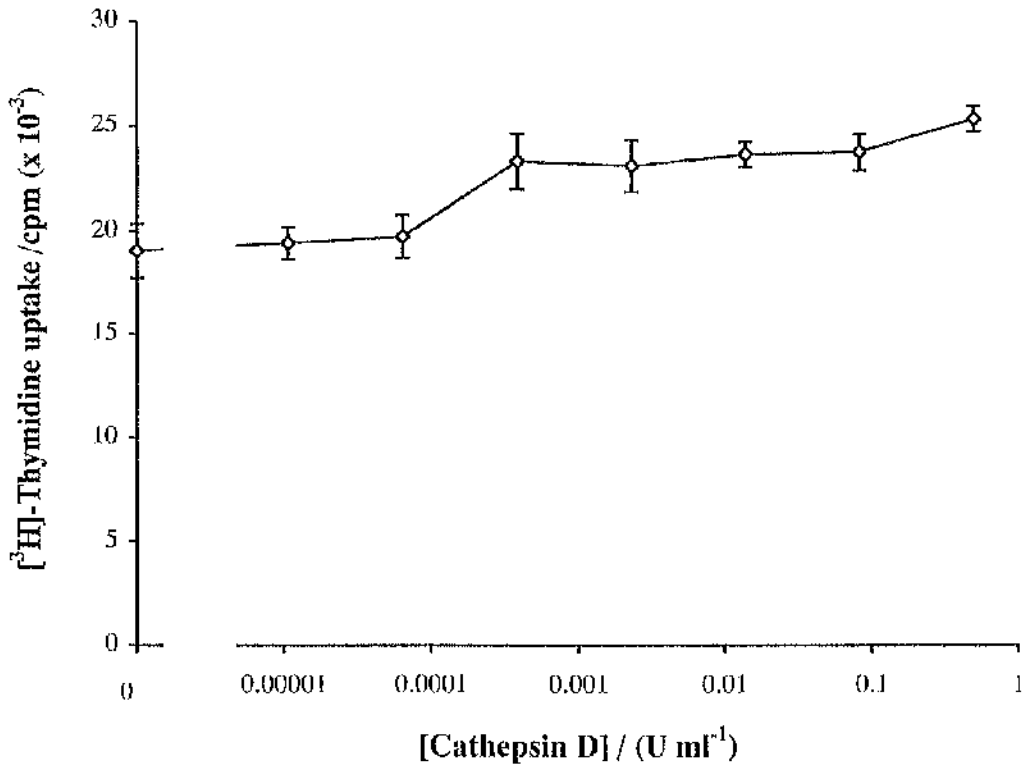
Neither enzyme had any effect on the toxicity of RNI (Figure 4.3). Therefore, RNI is likely to work independently of these enzymes.

Figure 4.1: The effect of  $\beta$ -glucuronidase on [ $^3\text{H}$ ]-thymidine uptake by amastigotes.



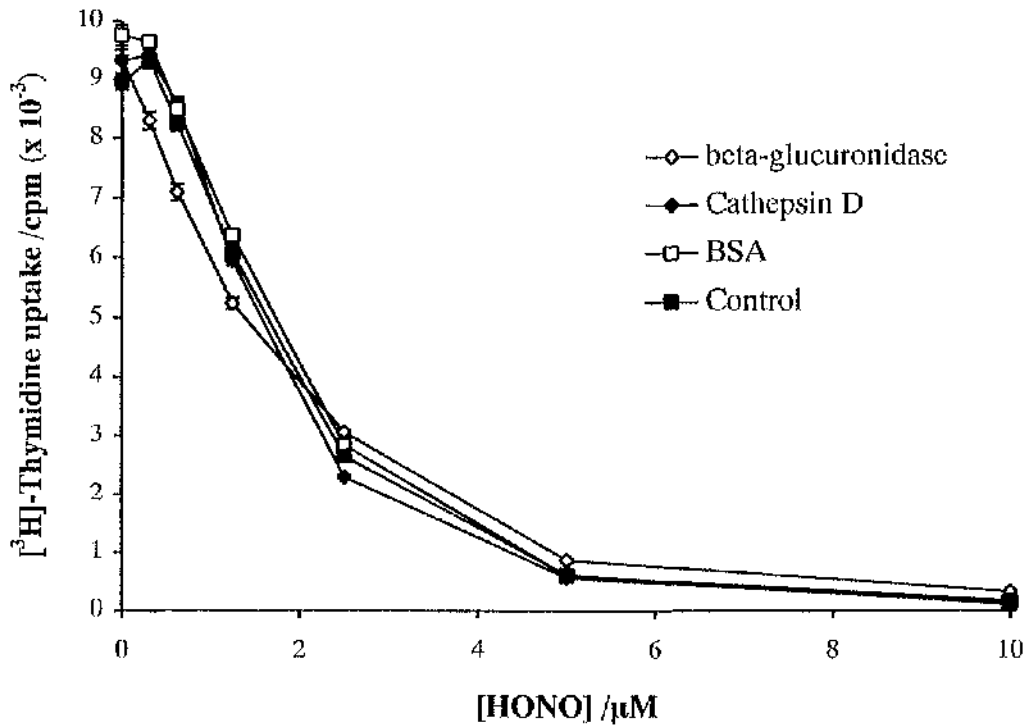
[ $^3\text{H}$ ]-thymidine uptake by amastigotes ( $2 \times 10^6 \text{ ml}^{-1}$ ) was assayed in the presence of different concentrations of  $\beta$ -glucuronidase at  $32^\circ\text{C}$ . Results are expressed as the mean  $\pm$  SEM ( $n=4$ ).

Figure 4.2: The effect of cathepsin D on [<sup>3</sup>H]-thymidine uptake by amastigotes.



[<sup>3</sup>H]-thymidine uptake by amastigotes ( $2 \times 10^6 \text{ ml}^{-1}$ ) was assayed in the presence of different concentrations of cathepsin D at 32°C. Results are expressed as the mean  $\pm$  SEM (n=4).

Figure 4.3: The effect of PV enzymes on RNI toxicity.



[<sup>3</sup>H]-Thymidine uptake by amastigotes ( $2 \times 10^6 \text{ ml}^{-1}$ ) was assayed in the presence of sodium nitrite and either  $1 \text{ mg ml}^{-1}$   $\beta$ -glucuronidase, or  $0.5 \text{ U ml}^{-1}$  Cathepsin D, or  $1 \text{ mg ml}^{-1}$  BSA (as a negative control), or medium alone at  $32^\circ\text{C}$ . Results are expressed as the mean  $\pm$  SEM ( $n=4$ ).

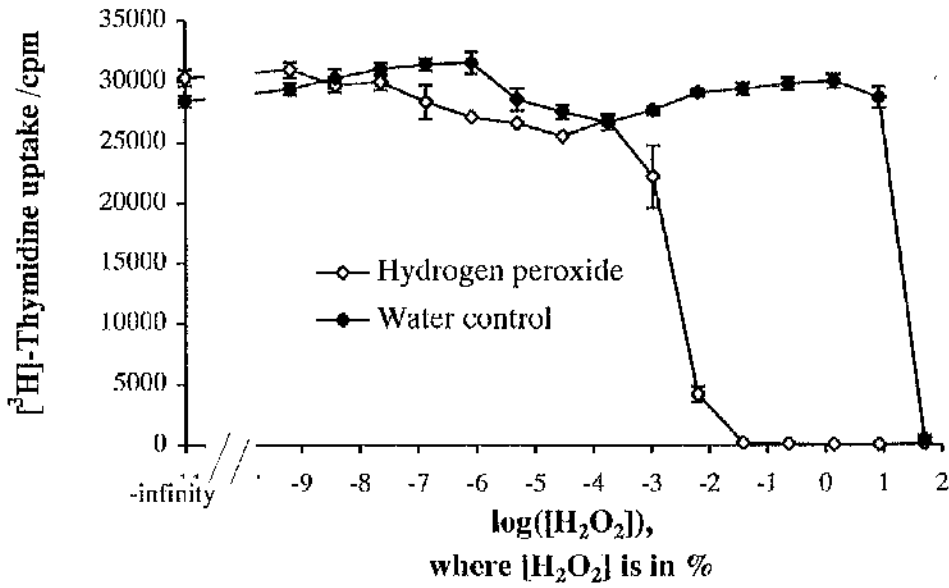
#### 4.2.2 Hydrogen peroxide

Hydrogen peroxide is itself toxic to amastigotes in the concentration range 0.0001 to 0.1 % (Figure 4.4).

To determine how RNI and hydrogen peroxide interact, an isobologram was plotted (Figure 4.5). An isobologram plots the 50% inhibitory concentration ( $IC_{50}$ ) of RNI at each concentration of hydrogen peroxide, and the  $IC_{50}$  of hydrogen peroxide at each concentration of RNI. If the effects of the toxins are antagonistic, then at intermediary concentrations of hydrogen peroxide the  $IC_{50}$  for RNI would be raised, and *vice versa*. So, the graph would be skewed towards the dashed line. If the toxins were synergistic, the graph would be skewed towards the dotted line, since the  $IC_{50}$  at the intermediary concentrations would be lowered.

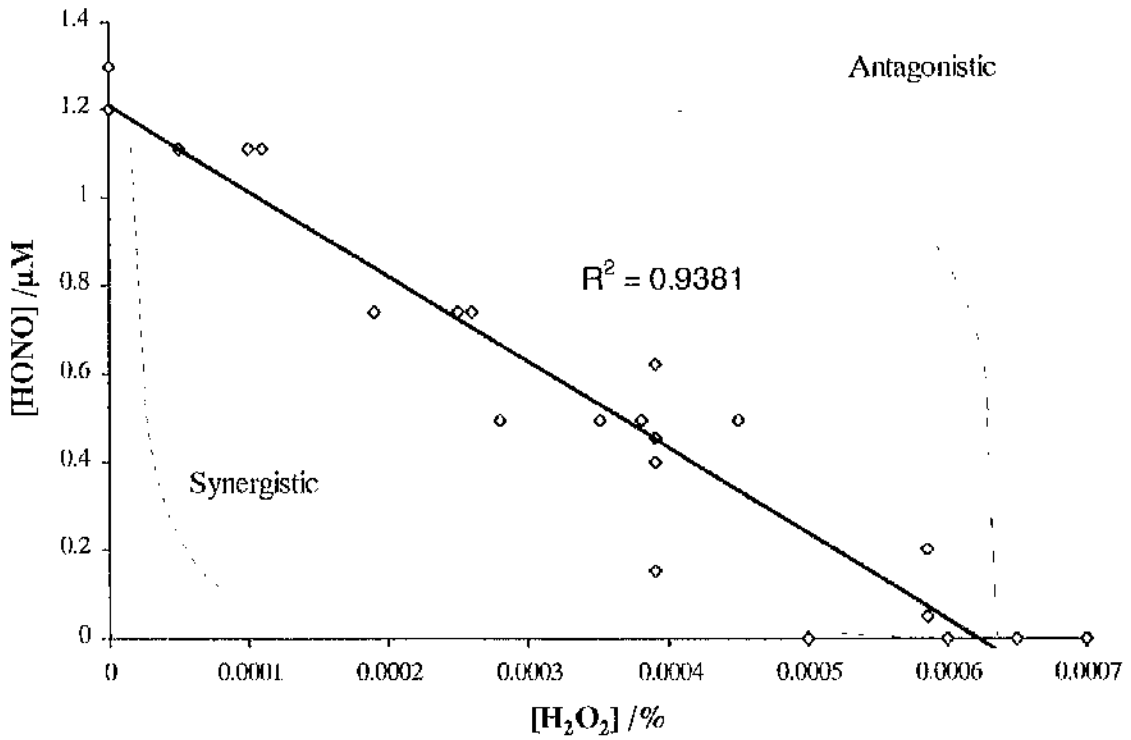
Since the line is straight, the effects of the two toxins are additive, suggesting that they act independently of one another.

**Figure 4.4: The effect of hydrogen peroxide on [<sup>3</sup>H]-thymidine uptake by amastigotes.**



[<sup>3</sup>H]-thymidine uptake by amastigotes ( $2 \times 10^6 \text{ ml}^{-1}$ ) was measured at different concentrations of hydrogen peroxide. A control of water was used to account for the possible effect of the water in which the hydrogen peroxide was dissolved. Results are expressed as the mean  $\pm$  SEM (n=4).

**Figure 4.5: Isobologram of the toxicity of RNI and hydrogen peroxide on amastigotes**



$[^3H]$ -thymidine uptake by amastigotes ( $2 \times 10^6 \text{ ml}^{-1}$ ) was measured at different concentrations of hydrogen peroxide and sodium nitrite. The  $IC_{50}$  at each concentration of toxin was plotted at each concentration of the other toxin.

### 4.3 Comparative analysis of amastigote susceptibility to RNI

The toxicity of RNI to amastigotes was compared to the toxicity to promastigotes, J774s, and *E. coli*, and development of suitable assays for *S. typhimurium* and *T. foetus* was attempted.

Since promastigotes and J774s normally grow in very different media to amastigotes, the toxicity of RNI at both pH 5.5 and 6.5 was examined. It was impossible to compare the toxicity of RNI at pH 7.5, because that would have necessitated using molar concentrations of sodium nitrite, which would almost certainly have had an associated osmotic toxicity as well as any toxicity due to RNI.

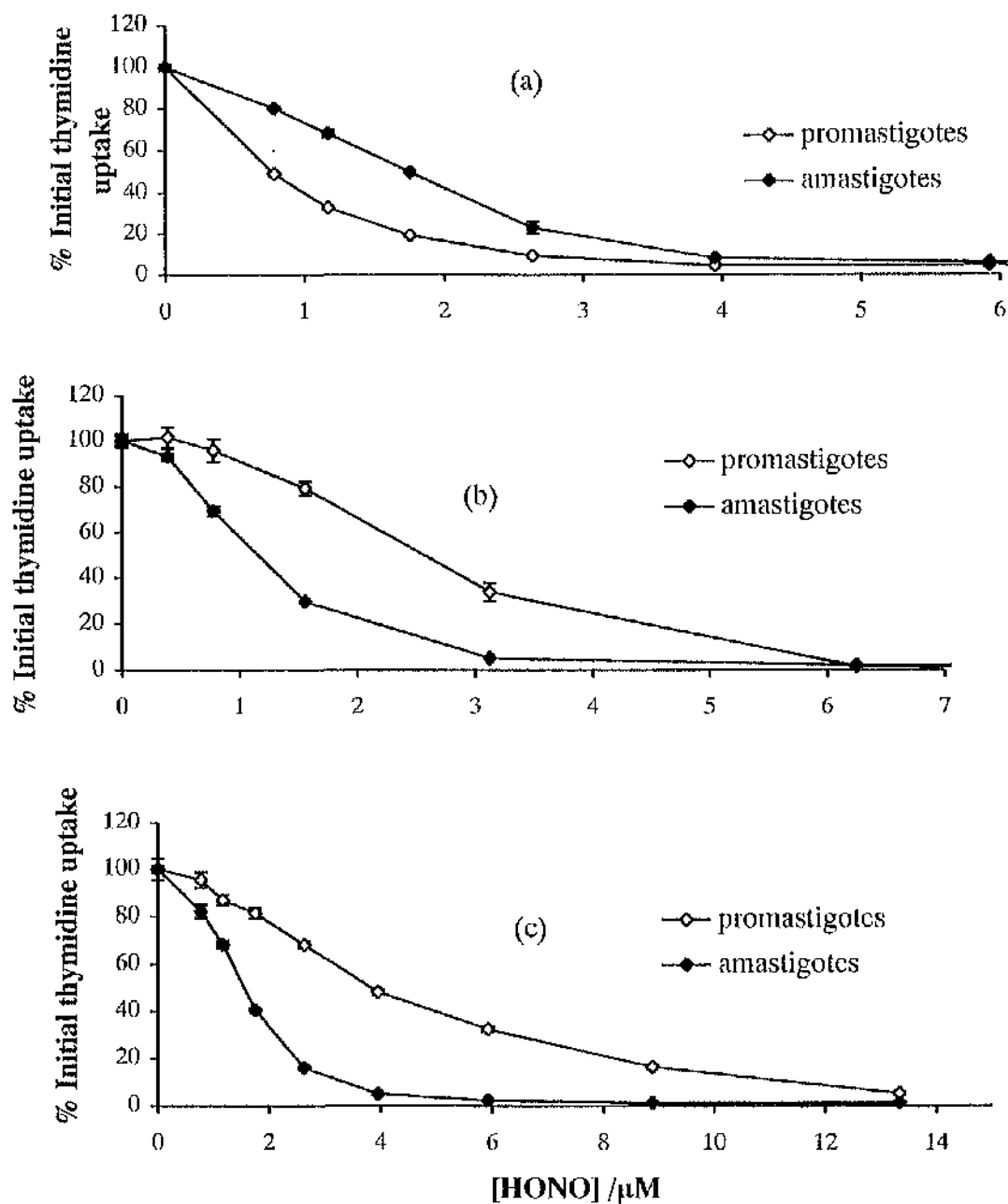
#### 4.3.1 Comparison to promastigotes

Amastigotes were not more resistant than promastigotes, either at pH 5.5 (which is similar to the pH in the PV (128)) (Figure 4.6), or at pH 6.5 (which is close to the pH of insect cell media) (Figure 4.7). Results from all experiments done are shown, because of the variability between experiments.

During the experiments at pH 6.5, control amastigotes had often transformed to promastigotes by the end of the 24 h incubation, and at pH 5.5, the promastigotes had often transformed to amastigotes by the end of the incubation.

Amastigotes were not particularly resistant to RNI compared to promastigotes, though in some instances, promastigotes may have been more resistant than amastigotes, though since this was not repeatable in all experiments, it would be rash to conclude that this was a real difference (Figure 4.6 (b) and (c) and Figure 4.7 (a) and (b)).

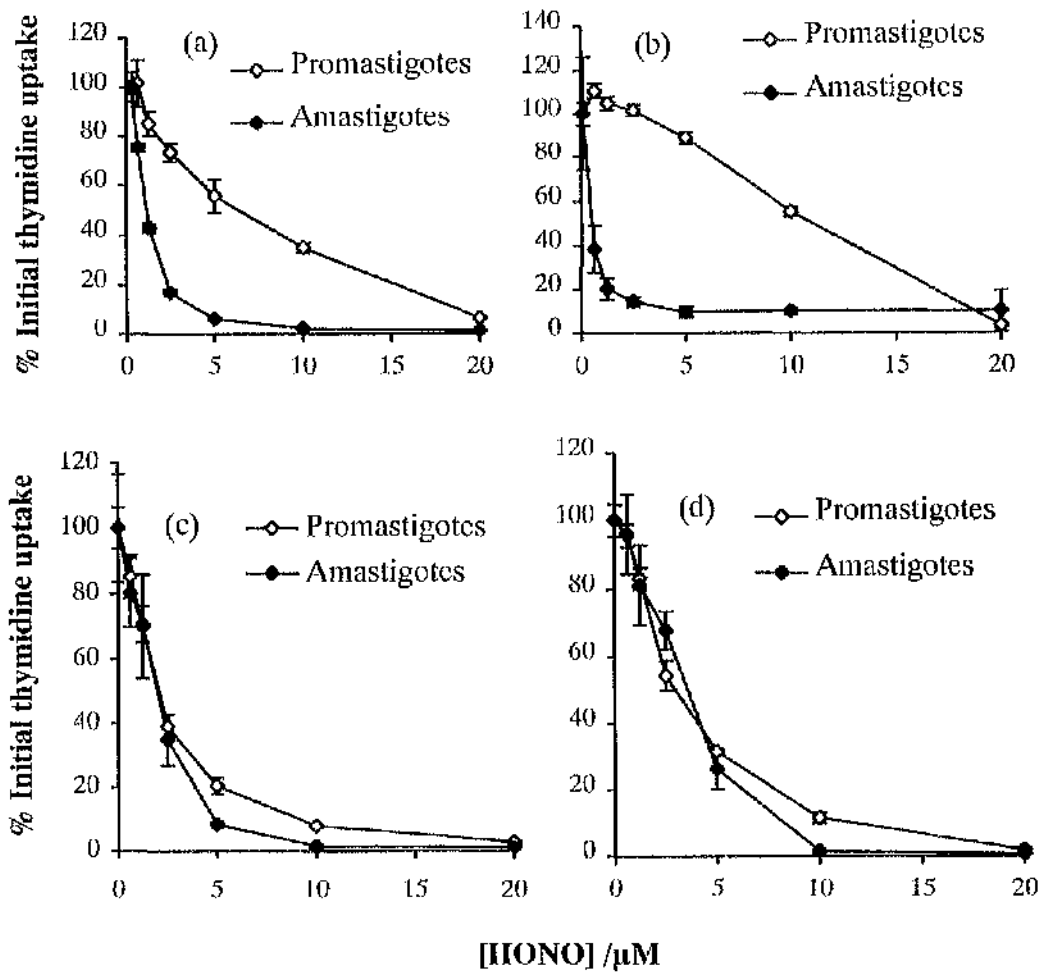
**Figure 4.6: Comparison of the susceptibility of amastigotes and promastigotes to RNI at pH 5.5.**



$^3\text{H}$ -thymidine uptake by amastigotes and promastigotes ( $1 \times 10^6 \text{ ml}^{-1}$ ) was assayed in amastigote culture medium at pH 5.5 for 24 hr  $32^\circ\text{C}$ . Results from three separate experiments are shown. Results are expressed as means  $\pm$  SEM ( $n=4$ ).

**Figure 4.7: Comparison of the susceptibility of amastigotes and promastigotes at pH**

**6.5.**



$[^3\text{H}]$ -thymidine uptake by amastigotes and promastigotes ( $1 \times 10^6 \text{ ml}^{-1}$ ) in amastigote culture medium pH 6.5  $28^\circ\text{C}$  was assayed in the presence of RNI. Results from 4 separate experiments are shown. The mean  $\pm$  SEM ( $n=4$ ) are shown.

### 4.3.2 Comparison to J774 cells

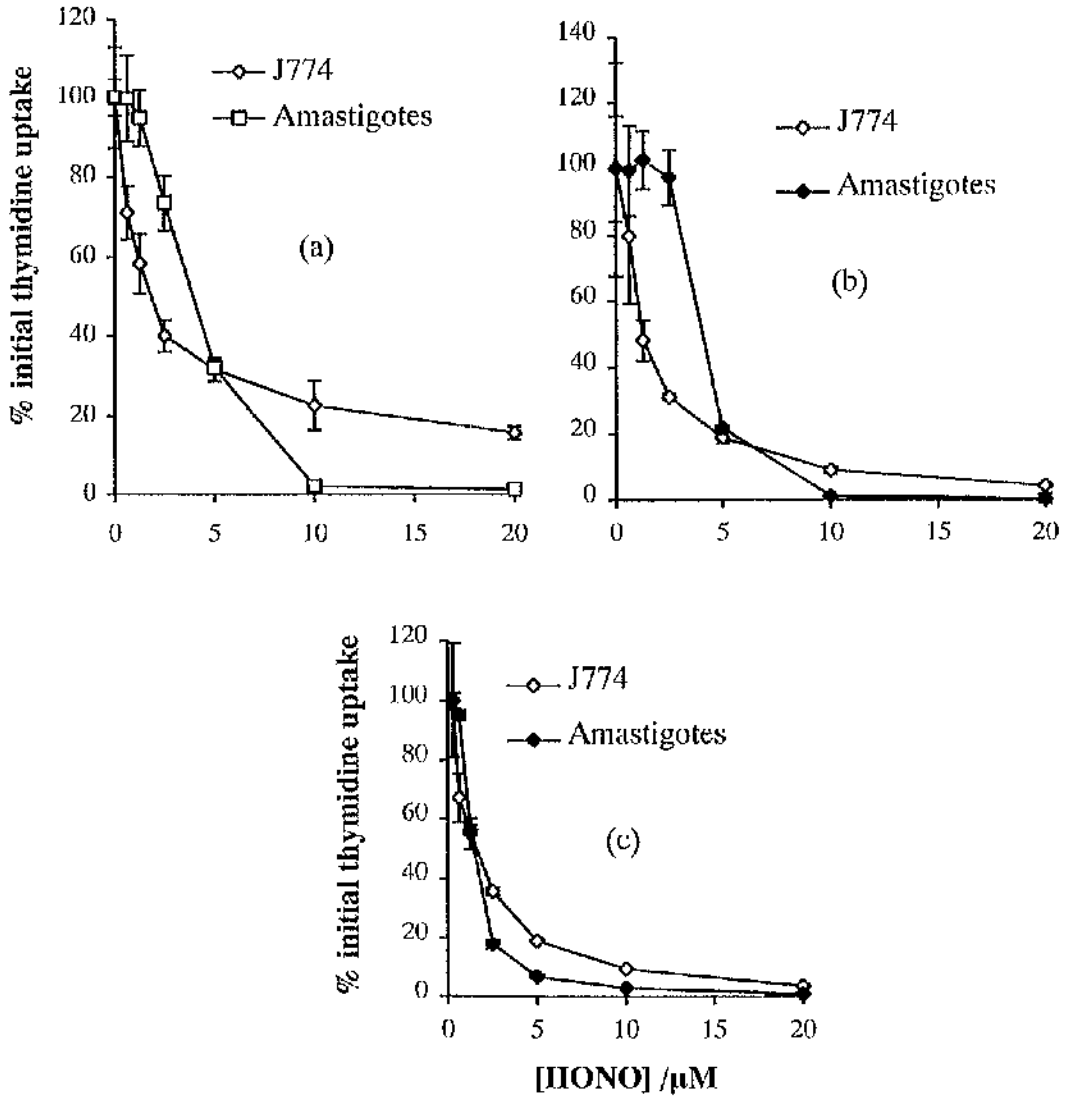
The concentrations of RNI that were toxic were similar in both J774s and amastigotes at both pH 5.5 and pH 6.5 (Figure 4.8 and Figure 4.9). Amastigotes were not particularly resistant to RNI when compared to J774s, and any difference was not repeatable between experiments.

### 4.3.3 Comparison to *E. coli*, *S. typhimurium*, and *T. foetus*

Neither *Salmonella typhimurium*, *Tritrichomonas foetus* nor *E. coli* took up [<sup>3</sup>H]-thymidine in amastigote culture medium in a dose-dependent manner (Figure 4.10 and Figure 4.11). *E. coli* was the only one of these organisms that grew in amastigote culture medium at all, and hence was the only organism with which it was possible to make a reasonable comparison to *L. m. mexicana* amastigotes.

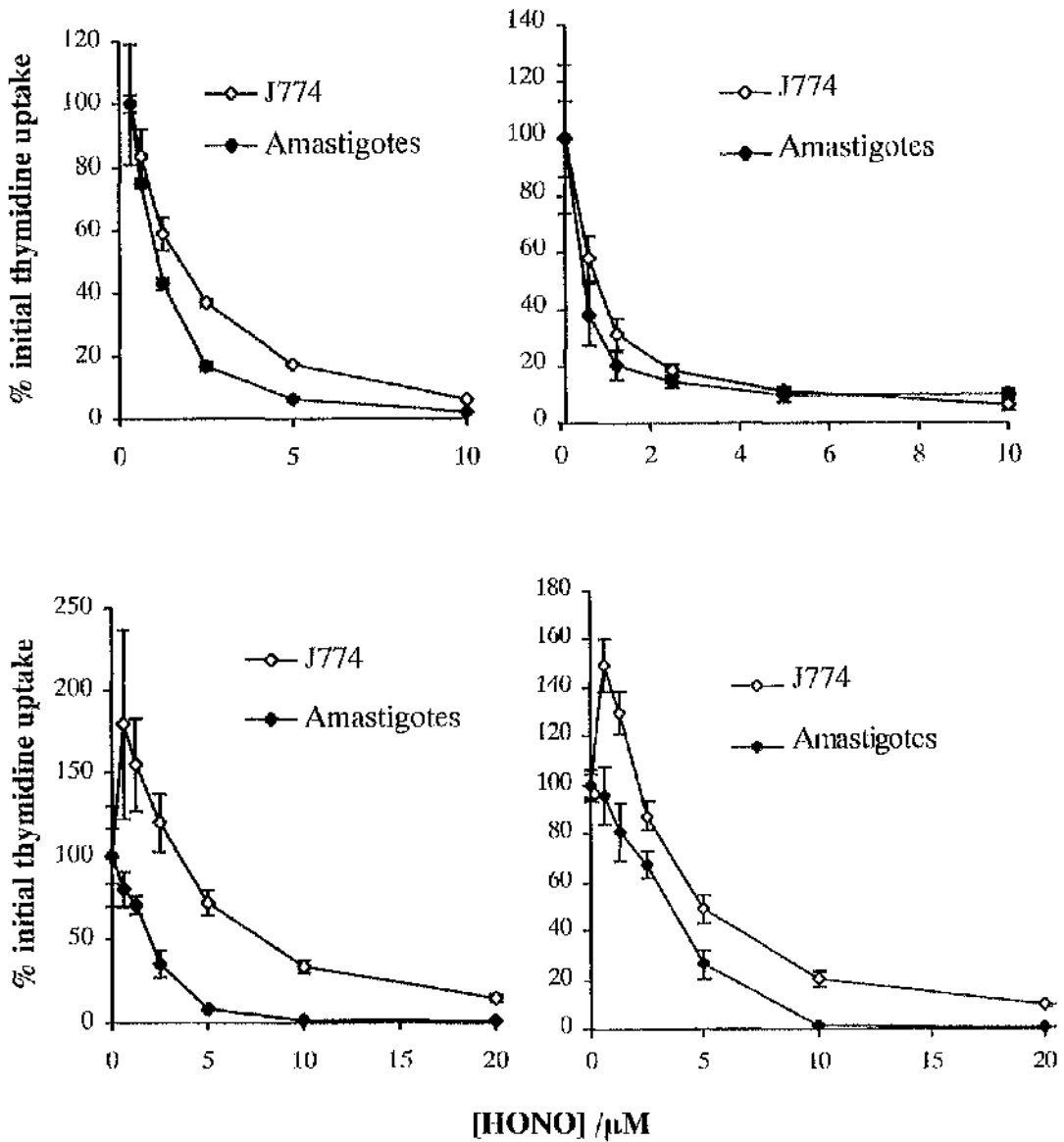
The comparison of the susceptibility *E. coli* to amastigotes needed to be done over a similar time scale of exposure for each organism. *E. coli* viability was assessed by the OD<sub>600</sub>. The concentration of RNI that killed *E. coli* outright in 18 h was comparable to that which killed amastigotes in 24 h (Figure 4.12). The lower concentrations may only have seemed to have an effect on *L. m. mexicana* and not *E. coli*, because even small numbers of *E. coli* may have outgrown the top end of the assay system. Though the assay system was therefore inadequate to say that *E. coli* was more resistant than *L. m. mexicana* amastigotes to RNI, Figure 4.12 suggests that *L. m. mexicana* were not more resistant than *E. coli*.

**Figure 4.8: Comparative susceptibility of amastigotes and J774s to RNI at pH 5.5**



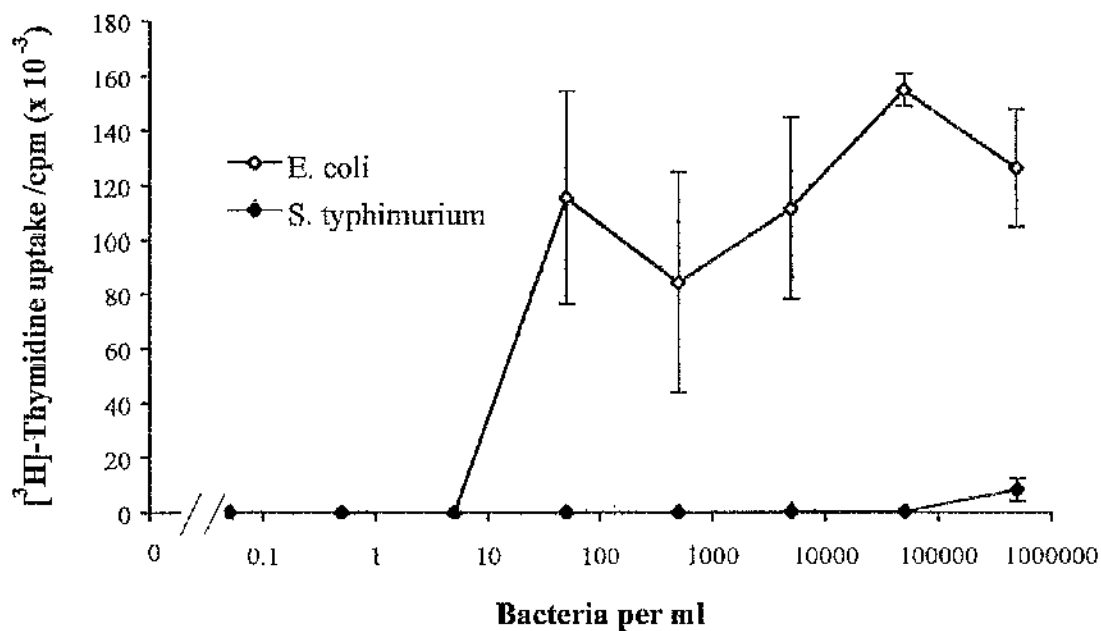
Amastigotes ( $1 \times 10^6 \text{ ml}^{-1}$ ) and J774 ( $2 \times 10^5 \text{ ml}^{-1}$ ) were cultured in amastigote culture medium at pH 5.5 for 24 h at  $32^\circ\text{C}$  in the presence of  $[^3\text{H}]$ -thymidine and sodium nitrite. Results are expressed as the mean  $\pm$  SEM ( $n=4$ ), and results from three separate experiments are shown.

**Figure 4.9: Comparison of the susceptibility to RNI of J774s and amastigotes at pH 6.5.**



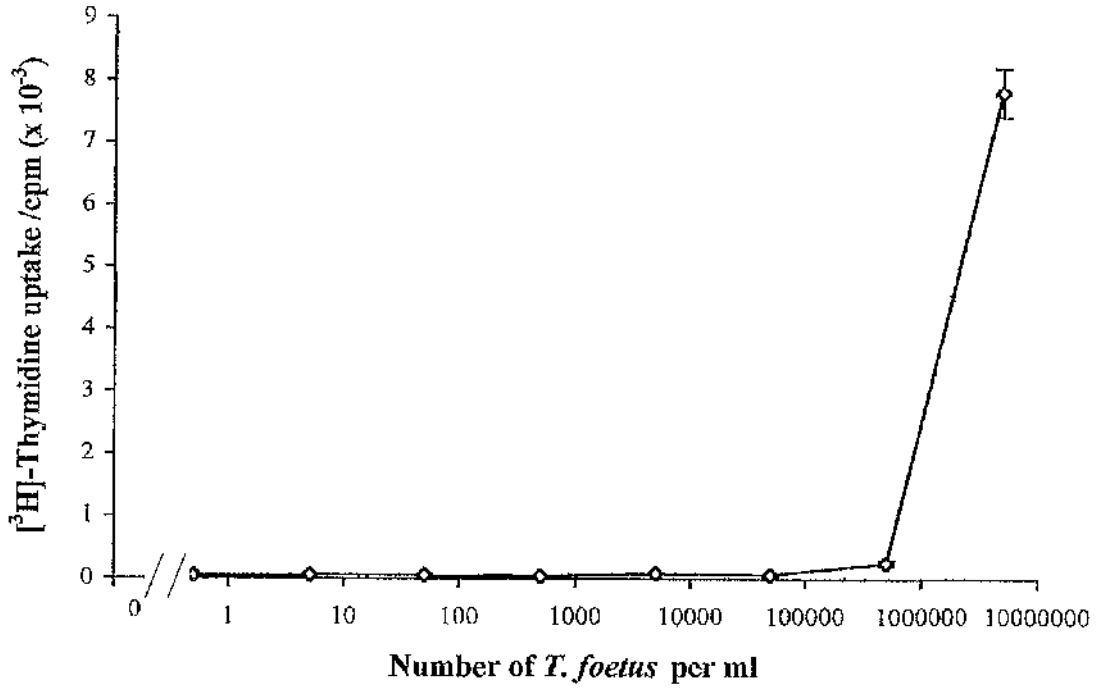
Amastigotes ( $1 \times 10^6 \text{ ml}^{-1}$ ) and J774 ( $2 \times 10^5 \text{ ml}^{-1}$ ) were cultured in amastigote culture medium pH 6.5 for 24 h at  $32^\circ\text{C}$ . Results from four separate experiments are shown, and are expressed as the mean  $\pm$  SEM ( $n=4$ ).

Figure 4.10: Uptake of [<sup>3</sup>H]-thymidine by *E. coli* and *S. typhimurium*.



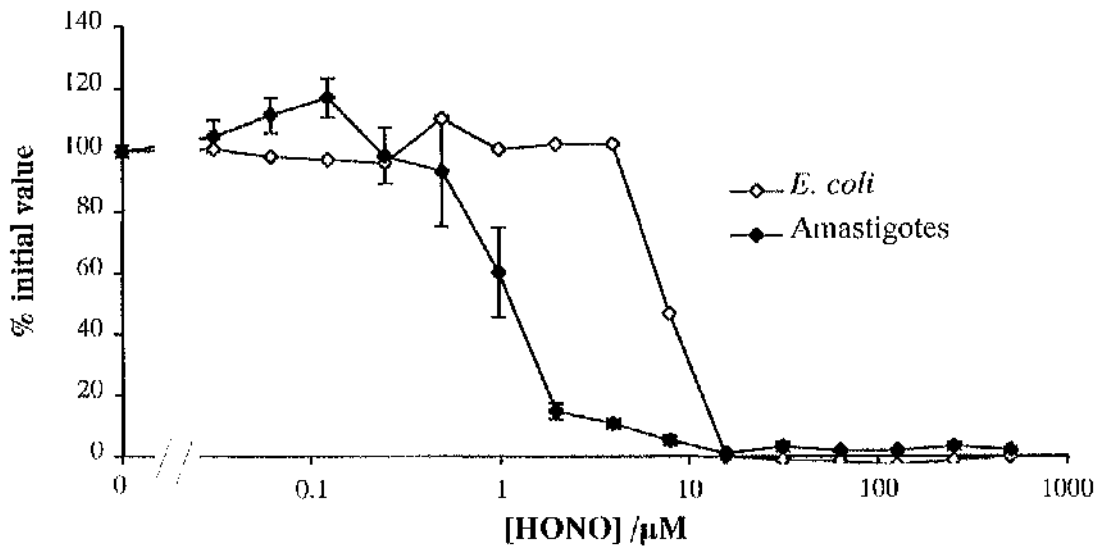
*E. coli* and *S. typhimurium* were cultured for 24 h in amastigote culture medium pH 5.5 at 33°C in the presence of [<sup>3</sup>H]-thymidine. Results are expressed as the mean ± SEM (n=4).

Figure 4.11: Uptake of [<sup>3</sup>H]-thymidine by *Tritrichomonas foetus*



*T. foetus* were cultured in amastigote culture medium at 32°C for 24 h in the presence of [<sup>3</sup>H]-thymidine. Results are expressed as the mean ± SEM (n=4).

**Figure 4.12: Comparison of the susceptibility of *E. coli* and *L. m. mexicana* amastigotes to RNI.**



Amastigotes ( $1 \times 10^6 \text{ ml}^{-1}$ ) and *E. coli* ( $\text{OD}_{600} = 0.01$ ) were cultured in amastigote culture medium pH 6.5 for 24 h at 33°C. Amastigote proliferation was measured by [ $^3\text{H}$ ]-thymidine incorporation (mean  $\pm$  SEM), and *E. coli* proliferation by the  $\text{OD}_{600}$ .

#### 4.4 The effect of low levels of RNI on *L. m. mexicana* amastigotes.

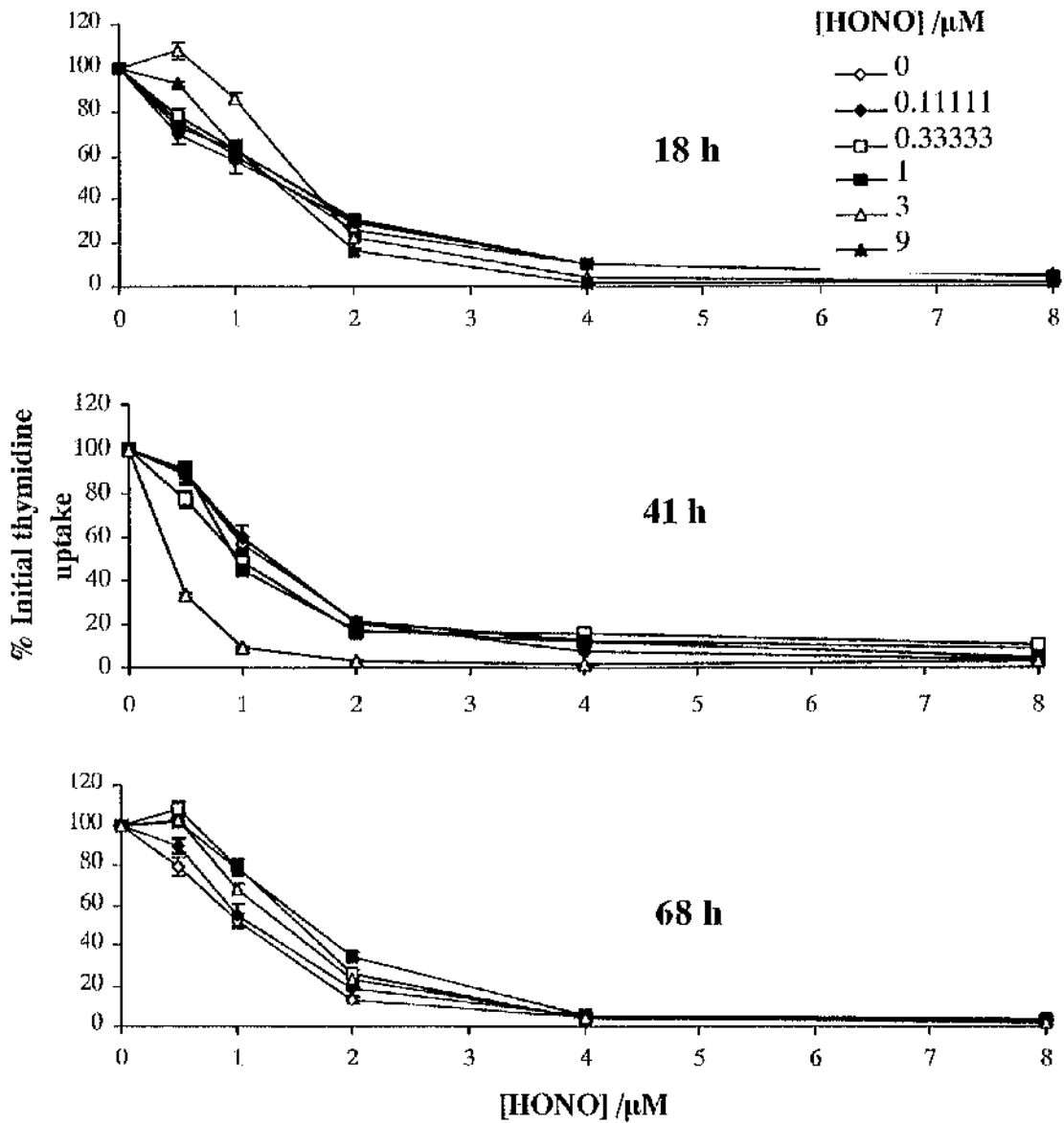
When *Leishmania* amastigotes first invade macrophages they encounter a small amount of RNI produced by one of the constitutive isoforms of nitric oxide synthase (eNOS or nNOS), before being exposed to higher concentrations produced by the cytokine-inducible isoform (iNOS).

To see whether these initial small doses of RNI induced resistance to a later larger dose of RNI, *L. m. mexicana* amastigotes were exposed to RNI for up to three days, before susceptibility to RNI was assayed by [<sup>3</sup>H]-thymidine uptake. This should have been a long enough exposure to attempt to induce a phenotypic change in susceptibility - equivalent to five generations in the control cultures.

The low levels of RNI did not induce any resistance to a later large exposure (Figure 4.13). Therefore low level RNI exposure is not sufficient to induce resistance to RNI.

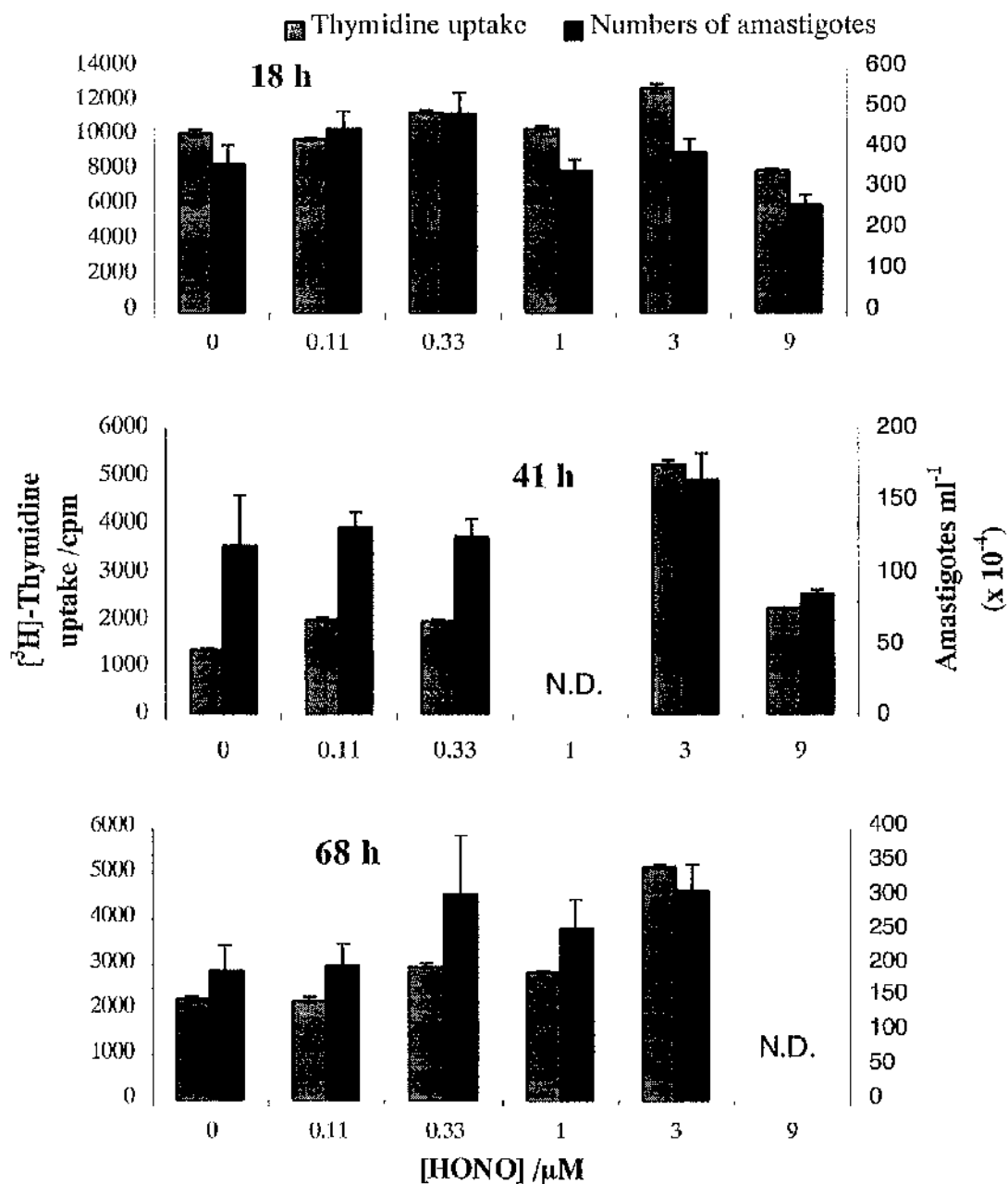
Data from the same experiments showed that low levels of RNI cause the parasites to incorporate up to five times more [<sup>3</sup>H]-thymidine than cultures that had been cultured without RNI for two or three days (Figure 4.14). This additional uptake was not accompanied by a similar increase in parasite numbers (Figure 4.14), suggesting that the parasites may have been synthesising DNA without dividing. It is also possible that they were simply taking up [<sup>3</sup>H]-thymidine more efficiently compared to their rate of *de novo* pyrimidine synthesis.

**Figure 4.13: Attempt to induce amastigote resistance to RNI by prior exposure.**



Amastigotes were cultured at  $2 \times 10^6 \text{ ml}^{-1}$  for up to 68 h at  $32^\circ\text{C}$  with various concentrations of RNI. Each line represents the concentration of RNI to which they were exposed during this initial exposure. The amastigotes were then washed, and exposed to freshly prepared RNI at the concentrations shown on the x-axis for 24 h in the presence of [ $^3\text{H}$ ]-thymidine. Results are expressed as the mean  $\pm$  SEM, and are representative of two separate experiments.

**Figure 4.14: Low levels of RNI cause the parasites to take up more [<sup>3</sup>H]-thymidine after two days**



Data from Figure 4.13, expressing the amount of [<sup>3</sup>H]-thymidine taken up by cultures that were exposed to RNI, washed, and then cultured for 24 h in the absence of RNI. Results are expressed as the mean ± SEM and are representative of two separate experiments.

(N.D. = Not determined).

## 4.5 Conclusions

RNI work independently of some of the other factors present in the PV. The toxicity is not affected by cathepsin D, or  $\beta$ -glucuronidase (Figure 4.3). Since the toxicity is additive to hydrogen peroxide (Figure 4.5), any additional hydrogen peroxide or RNI that the macrophage could produce would not affect the toxicity of the other at concentrations below those at which they killed the parasite.

The other ROI species involved in the oxidative burst is the superoxide anion. This molecule is extremely difficult to produce *in vitro*, and all the methods available produce short bursts of superoxide. These bursts would have been made even shorter since amastigote culture medium is buffered with a carbonate buffer, which reacts with superoxide to produce carbon dioxide. An assessment of this molecule's interaction with RNI would probably have required physiologically irrelevant high concentrations of superoxide. In addition, since superoxide is negatively charged, the anion would have difficulty entering the membrane enclosed PV, so any studies *in vitro* would probably have been meaningless. Therefore, it is meaningful to study the effect of RNI on *L. m. mexicana* without adding additional hydrogen peroxide or the other PV enzymes.

There was no evidence to suggest that amastigotes were particularly resistant to RNI when compared to *E. coli*, J774s or promastigotes. From an evolutionary aspect, this may be surprising, since RNI are probably so important in murine resistance to *Leishmania* infection.

In some instances, amastigotes may have been more susceptible to RNI than promastigotes (Figure 4.7). There could have been a multitude of reasons for this, including the possibility that promastigotes contained RNI scavenging molecules, or that they affected the pH of the medium differently to amastigotes, or that promastigotes were larger than amastigotes, or that promastigotes were routinely cultured in pH 7.4, and may have retained some of the phosphate buffer during the washing process, or that the [ $^3\text{H}$ ]-thymidine uptake assay was overloaded with parasites in these experiments.

In addition, promastigotes are not normally exposed to RNI, and any resistance mechanisms that they might have would therefore probably have occurred serendipitously. Therefore the possibility that promastigotes may be more resistant to RNI than amastigotes was not investigated further.

Low levels of RNI alone were not capable of inducing resistance to a later challenge of RNI in amastigotes within three days. This exposure was not aimed at inducing an RNI resistant genotype in the amastigotes, only a phenotype, to see if they were capable of responding to these low levels of RNI. If they do respond to low levels, then it takes them longer than three days, which is several generations of parasites, and may be too late for them to fight off an immune attack.

Low levels of RNI (1-3  $\mu\text{M}$  HONO) cause the parasites to take up more [ $^3\text{H}$ ]-thymidine after being washed off (Figure 4.14). The large (up to 5-fold) increases [ $^3\text{H}$ ]-thymidine uptake were not accompanied by a corresponding increase in parasite number. This would suggest that the parasites were taking up [ $^3\text{H}$ ]-thymidine without dividing.

This [ $^3\text{H}$ ]-thymidine uptake could be an indication of DNA damage being repaired by the parasite. The added incorporation could also be due to a change in the balance of

pyrimidine uptake compared to *de novo* pyrimidine biosynthesis. The issue of DNA damage is examined in Chapter 6.

In summary, there was no evidence to suggest that RNI interact with any of the other components of the macrophage defence against *Leishmania*, nor that amastigotes were particularly resistant to RNI. It was not possible to induce an RNI resistant phenotype using low levels of RNI alone.

**5. RNI kill *Leishmania mexicana mexicana***

## 5.1 Introduction

Most of the work that has suggested a role for RNI in murine resistance to leishmaniasis has been done using the *L. major* model (62,64,68,69,85,127,210). Before examining RNI toxicity to *L. m. mexicana in vitro*, it was necessary to determine whether this species was also susceptible to the amounts of RNI that could be produced by a murine macrophage.

This chapter is concerned with establishing the macroscopic nature of the toxicity of RNI. That is, establishing whether RNI are cytotoxic or cytostatic, whether the toxic mechanism is saturable, and whether the toxicity can be affected by the concentration of amastigotes.

Finally, the amastigotes' ultrastructure after treatment with RNI was examined, bearing in mind that often ultrastructural changes are secondary to any biochemical effects.

## 5.2 Macrophage toxicity to *L. m. mexicana* amastigotes.

To assay murine macrophage toxicity to amastigotes, the macrophage-like cell line J774 was infected with *L. m. mexicana* amastigotes, and stimulated for 48 h with interferon gamma (IFN $\gamma$ ) and lipopolysaccharide (LPS) from *Salmonella enteritidis*.

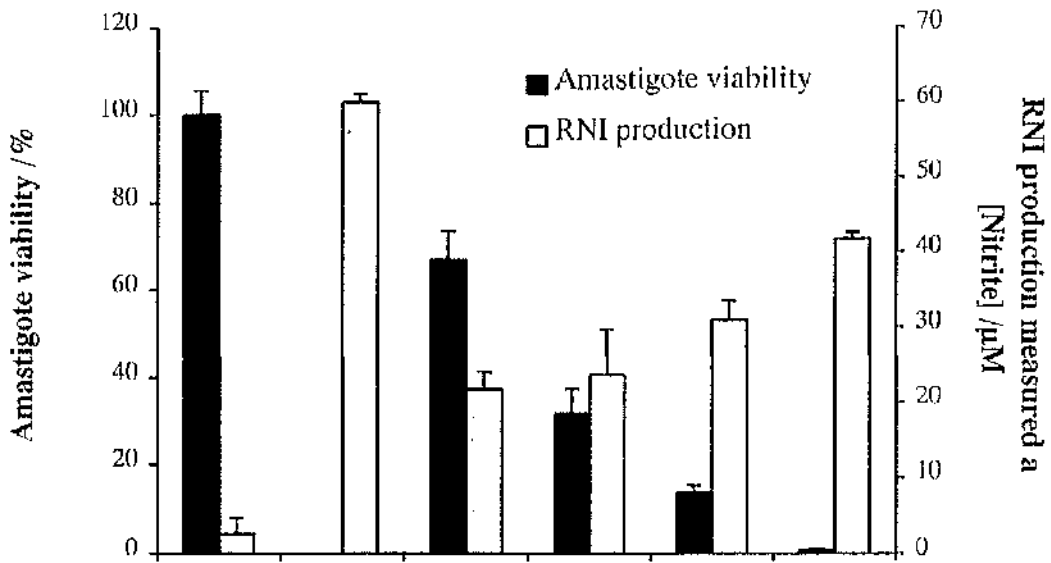
J774 macrophages can kill amastigotes with RNI (Figure 5.1). This toxicity is inhibitable by the arginine analogue L-NMMA. The inhibition can be reversed by adding back extra arginine.

Killing of amastigotes correlates with the inhibition of RNI production, suggesting that RNI can account for macrophage toxicity.

When J774s are stimulated to the extent that they kill all the invading amastigotes, it is only necessary to inhibit RNI production by approximately seventy to eighty percent in order to rescue most of the amastigotes (Figure 5.1). This means that the amount of RNI produced from an activated macrophage is only a few times more than it takes to kill the parasites and is not orders of magnitude greater.

Therefore, it is physiologically relevant to study concentrations of RNI within one order of magnitude of the concentrations that kill *L. m. mexicana* amastigotes.

**Figure 5.1: *L. m. mexicana* are susceptible to an arginine dependent macrophage killing mechanism**



LPS + IFN $\gamma$	-	+	+	+	+	+
2 mM L-NMMA	-	-	+	+	+	+
[L-Arginine] /mM	-	-	-	1	3	10

*J774s* were infected with amastigotes (infection ratio 10:1) overnight, and stimulated with IFN $\gamma$  (500 U ml<sup>-1</sup>) and LPS (2  $\mu$ g ml<sup>-1</sup>) for 48 h. RNI production was measured by the accumulation of nitrite in the medium using the Griess reaction. The *J774s* were lysed and amastigote viability was measured using transformation efficiency in which amastigotes from control macrophages were defined as 100% viable.

### 5.3 The kinetics of RNI toxicity *in vitro*.

#### 5.3.1 Concentration curve of RNI toxicity

Experiments in Chapter 3 revealed the concentration of RNI that inhibited thymidine incorporation. However, RNI have been variously described as cytotoxic (133,134) or cytostatic (135) to different organisms. [<sup>3</sup>H]-thymidine uptake is probably a measure of DNA synthesis, so it may be a measure of cytostasis rather than cytotoxicity.

A more accurate measure of the toxic concentrations of RNI is shown in Figure 5.2. The shape of the graph in Figure 5.2 indicates that even at concentrations of RNI below those that are toxic, an increase in RNI concentration will lead to fewer viable amastigotes. Therefore the more RNI that a macrophage can produce, the more amastigotes it will kill.

Amastigotes treated with RNI disintegrate - note the loss of amastigotes before transformation in Figure 5.2. It was possible, however, to see "ghosts" of amastigotes that looked like they had lost their internal organelles, and were translucent, yet retained the external shape of amastigotes.

The loss of amastigotes before transformation that was seen in Figure 5.2 was not due to a slight instability in the structure that led to parasite disintegration during the washing and fixing process. Ghosts of amastigotes could be seen even before the amastigotes had been washed, indicating that the collapse of the structure was due not to shearing forces caused by the centrifugation, but to the amastigotes disintegrating on their own.

There is no long plateau of concentrations where the parasites have stopped dividing, but are still viable, suggesting that for axenically grown amastigotes, RNI are best described as cytotoxic rather than cytostatic in a 24 h exposure.

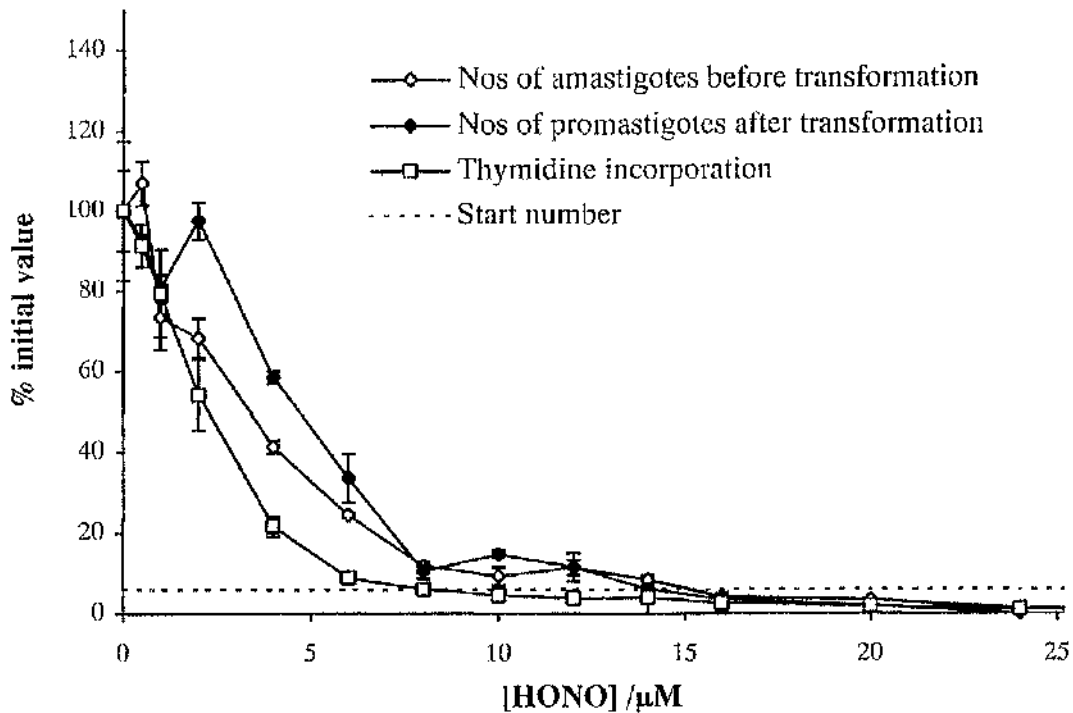
[<sup>3</sup>H]-thymidine uptake is also not inhibited long before the parasites die, suggesting that it is a reasonable viability assay for RNI toxicity.

### 5.3.2 Time course of RNI toxicity

RNI are produced from J774s over a period of several hours (54, Feng G.J. personal communication). The cells usually start producing RNI approximately six hours after stimulation with IFN $\gamma$  and LPS, with peak production at approximately 16 h, then slowing down over the next two days (Feng G.J., personal communication).

The rate at which RNI kill amastigotes depends on the amount of RNI present. The amount of RNI needed to kill amastigotes in 24 h is in the order of magnitude of 20  $\mu$ M HONO (Figure 5.3). We found that above that concentration, more RNI killed the amastigotes faster (Figure 5.4). This suggests that the target of RNI is not saturated at concentrations of RNI below 20  $\mu$ M.

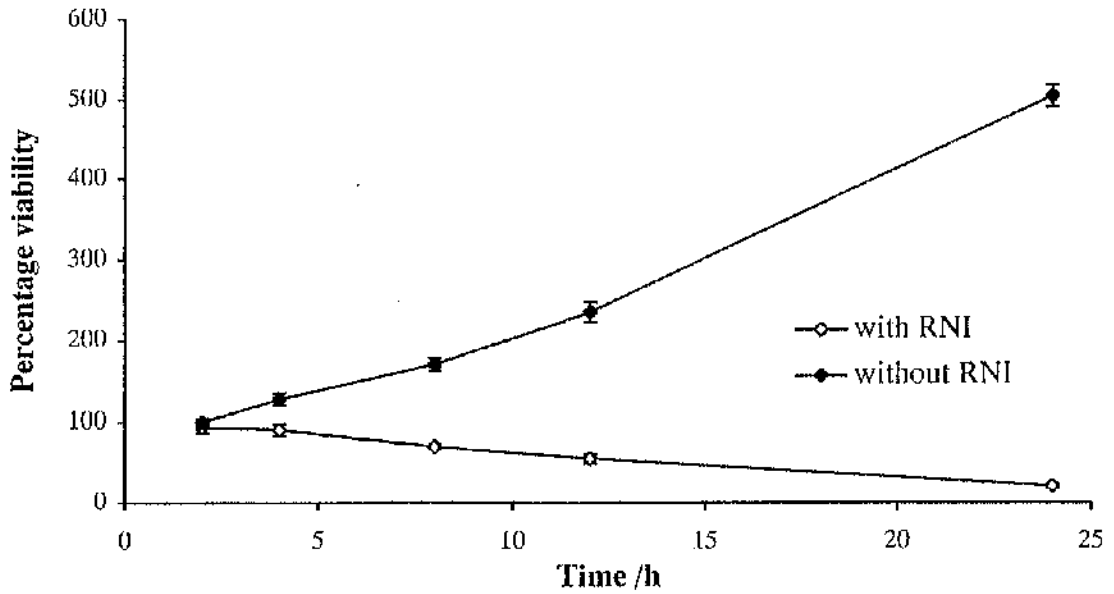
Figure 5.2: The effect of RNI on viability and [<sup>3</sup>H]-thymidine uptake by amastigotes.



Amastigotes ( $2 \times 10^6 \text{ ml}^{-1}$ ) were cultured with sodium nitrite for 24 h at  $32^\circ\text{C}$ . During this period, [<sup>3</sup>H]-thymidine incorporation was measured ( $n=4$ ). The number of amastigotes was then counted ( $n=3$ ), and the number of viable amastigotes was measured using the transformation assay ( $n=3$ ). 100% viability was defined as the efficiency of transformation of parasites that had not been treated with RNI. The start number is the concentration of amastigotes before treatment with RNI expressed as a percentage of the concentration of amastigotes before transformation, to show how the amastigotes had grown over the 24 h treatment.

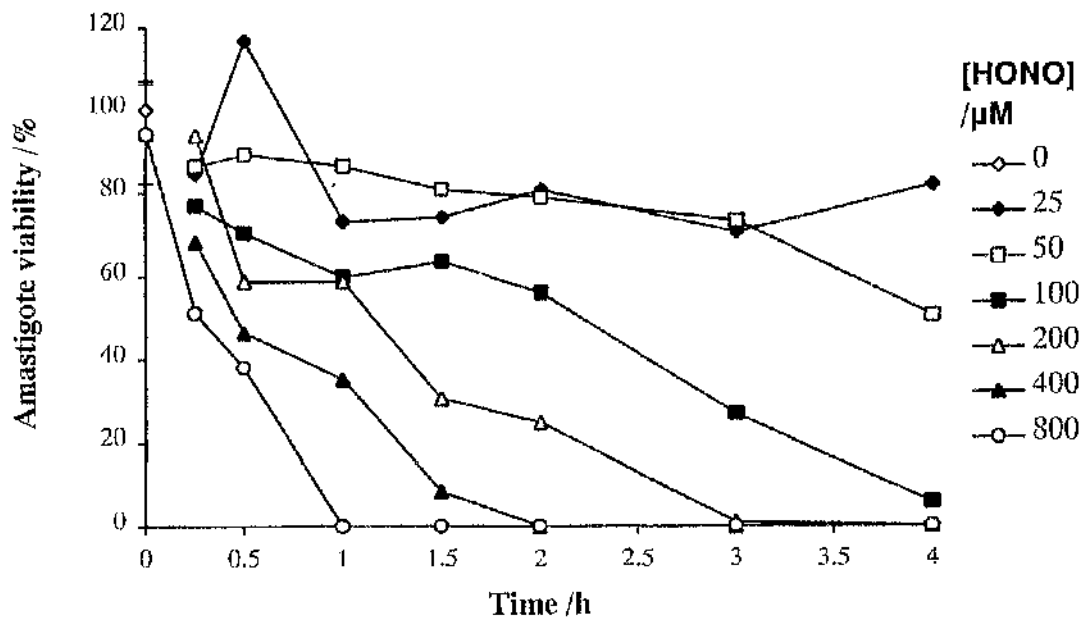
Results are expressed as the means  $\pm$  SEM, and are representative of three separate experiments.

Figure 5.3: Time course of RNI toxicity.



Axenically grown amastigotes ( $2 \times 10^6 \text{ ml}^{-1}$ ) were cultured with RNI at pH 5.5 with  $20 \mu\text{M}$  HONO for the times shown. At each time point, a sample was removed and viability assayed by transformation efficiency. Results are expressed as the mean  $\pm$  SEM ( $n=3$ ), and are representative of three separate experiments.

Figure 5.4: More RNI kill amastigotes faster.



Amastigotes ( $2 \times 10^6 \text{ ml}^{-1}$ ) were treated with sodium nitrite at pH 5.5. At each time point, a sample was taken, washed, and viability assayed by transformation efficiency. The mean is shown, and the results are representative of three separate experiments.

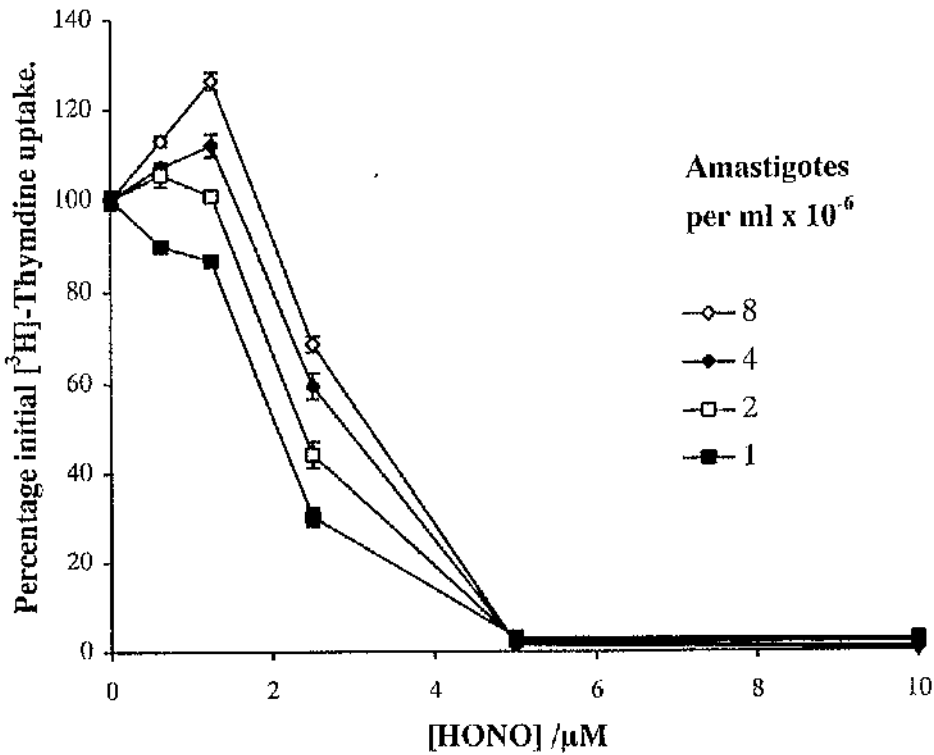
### 5.3.3 The effect of changing the concentration of amastigotes

It was possible that RNI were altering the metabolism of amastigotes in such a way that the amastigotes secreted a toxic product. The concentration of amastigotes used in most experiments was  $1-4 \times 10^6 \text{ ml}^{-1}$ . The concentration of amastigotes in a lesion is of the order  $10^{10} \text{ ml}^{-1}$ . It was necessary to determine, therefore, whether the interaction between parasites was important in determining RNI toxicity.

The susceptibility of different concentrations of parasites to RNI was assayed, both in terms of the concentration of RNI to which they were susceptible, and in terms of the rate at which they died.

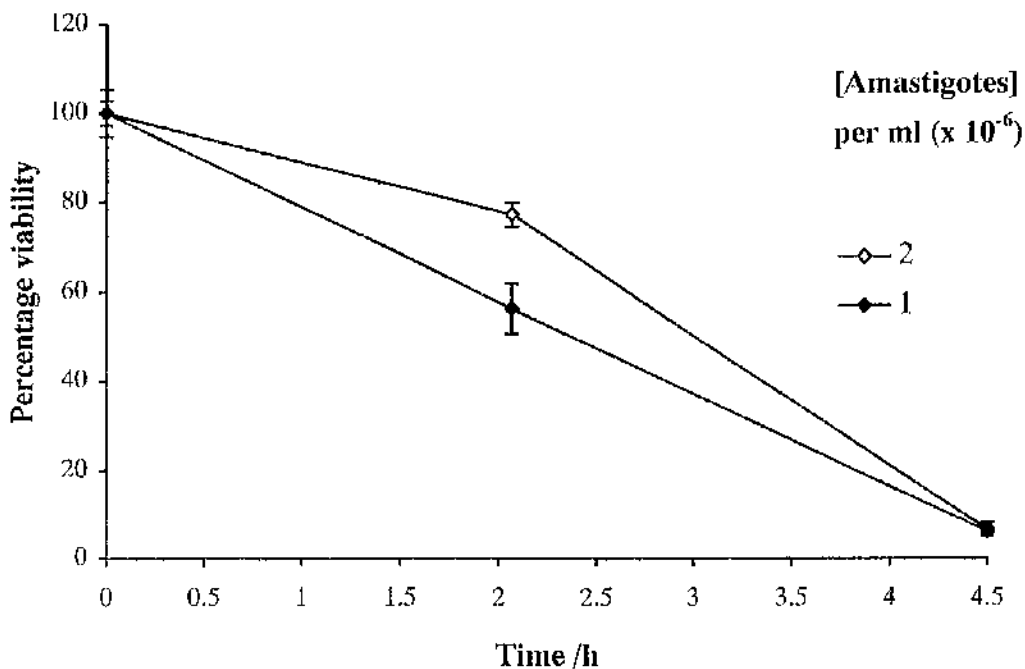
Higher concentrations of parasites were neither susceptible to lower concentrations of RNI (Figure 5.5), nor did they die faster (Figure 5.6). These two figures in fact showed that there was very little difference between the susceptibility of high concentrations and low concentrations of parasites.

Figure 5.5: Toxicity of RNI at graded concentrations of parasites.



Amastigotes were cultured at different concentrations with sodium nitrite for 24 h, and viability was assayed by  $[^3\text{H}]$ -thymidine uptake during that period. Results are expressed as the mean  $\pm$  SEM ( $n=4$ ), and are representative of three separate experiments.

Figure 5.6: Time course of RNI toxicity at different concentrations of amastigotes.



Amastigotes were cultured in the RNI at 100  $\mu\text{M}$  HONO, and viability was assayed at each time point by transformation efficiency. Results are expressed as the mean  $\pm$  SEM (n=4).

#### 5.4 Ultrastructural changes to amastigotes on treatment with RNI.

To see if there were any ultrastructural changes visible before the parasites started to disintegrate, amastigotes were treated with RNI at 100  $\mu$ M HONO, fixed in glutaraldehyde, and examined using a heavy metal stain with transmission electron microscopy.

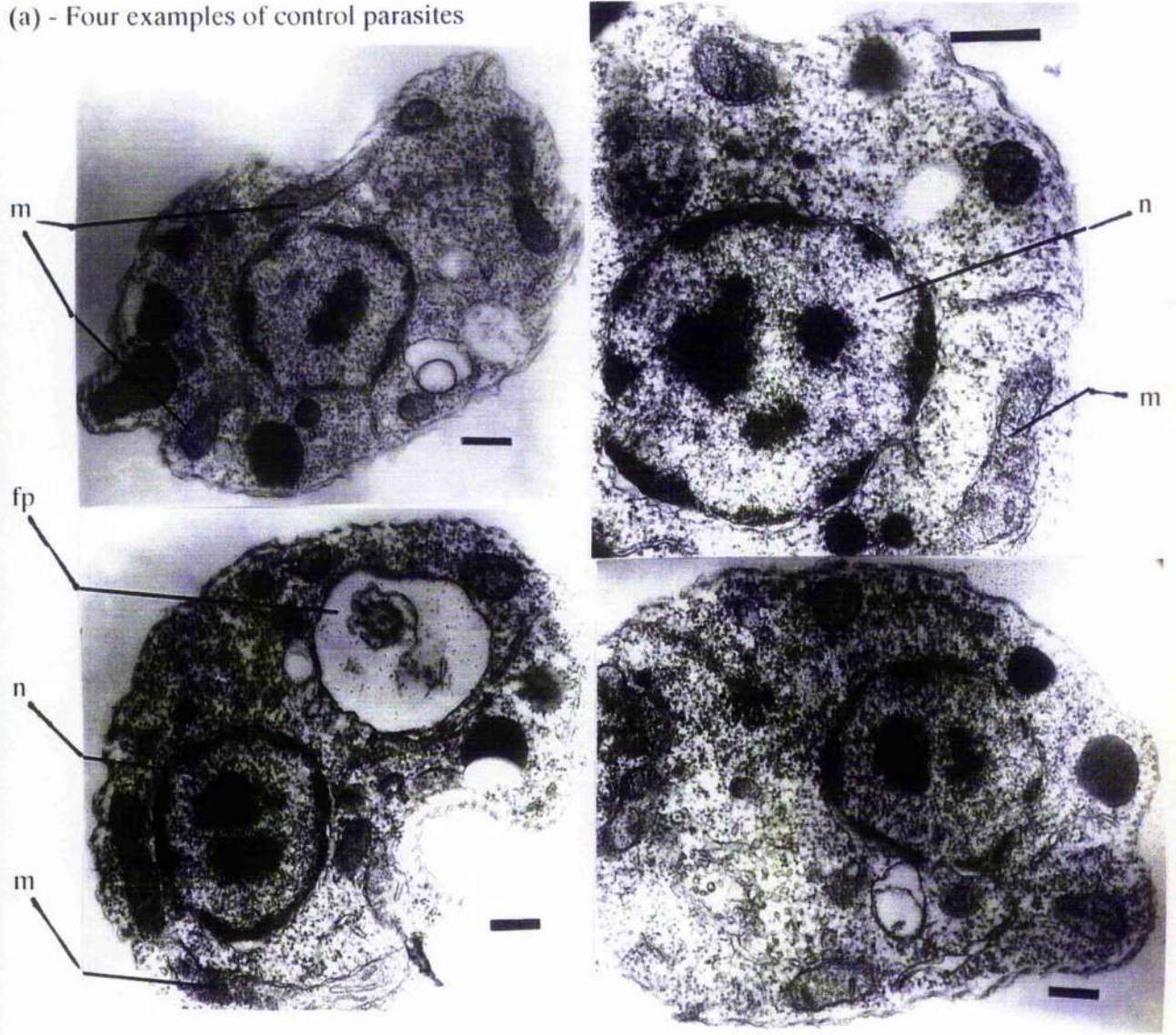
No ultrastructural changes were visible within 17 min 30 s of treatment. After 2 h, however, there were changes visible in the nucleus, and in the mitochondrion (Figure 5.7(c)).

In many cases, after 2 h, the nucleus had begun to disintegrate, and the chromatin had come away from part of the nuclear membrane (Figure 5.7(c)). Where the chromatin had left the nuclear membrane, the membrane had begun to form whorls, almost half of the nuclei examined showed this effect (Table 5.1). Swelling of the mitochondria was also visible after 2 h treatment. The internal structure of the mitochondrion was less dense, and the internal organisation of the mitochondrion was disrupted.

**Figure 5.7: Electron microscopy of amastigotes treated with RNI.**

Amastigotes ( $2 \times 10^6 \text{ ml}^{-1}$ ) were treated with RNI at  $100 \mu\text{M}$  HONO for 0 min (a), 17 min 30 s (b), or 2 h (c). At each time point, the amastigotes were centrifuged and fixed for 20 min in glutaraldehyde, before processing for electron microscopy.

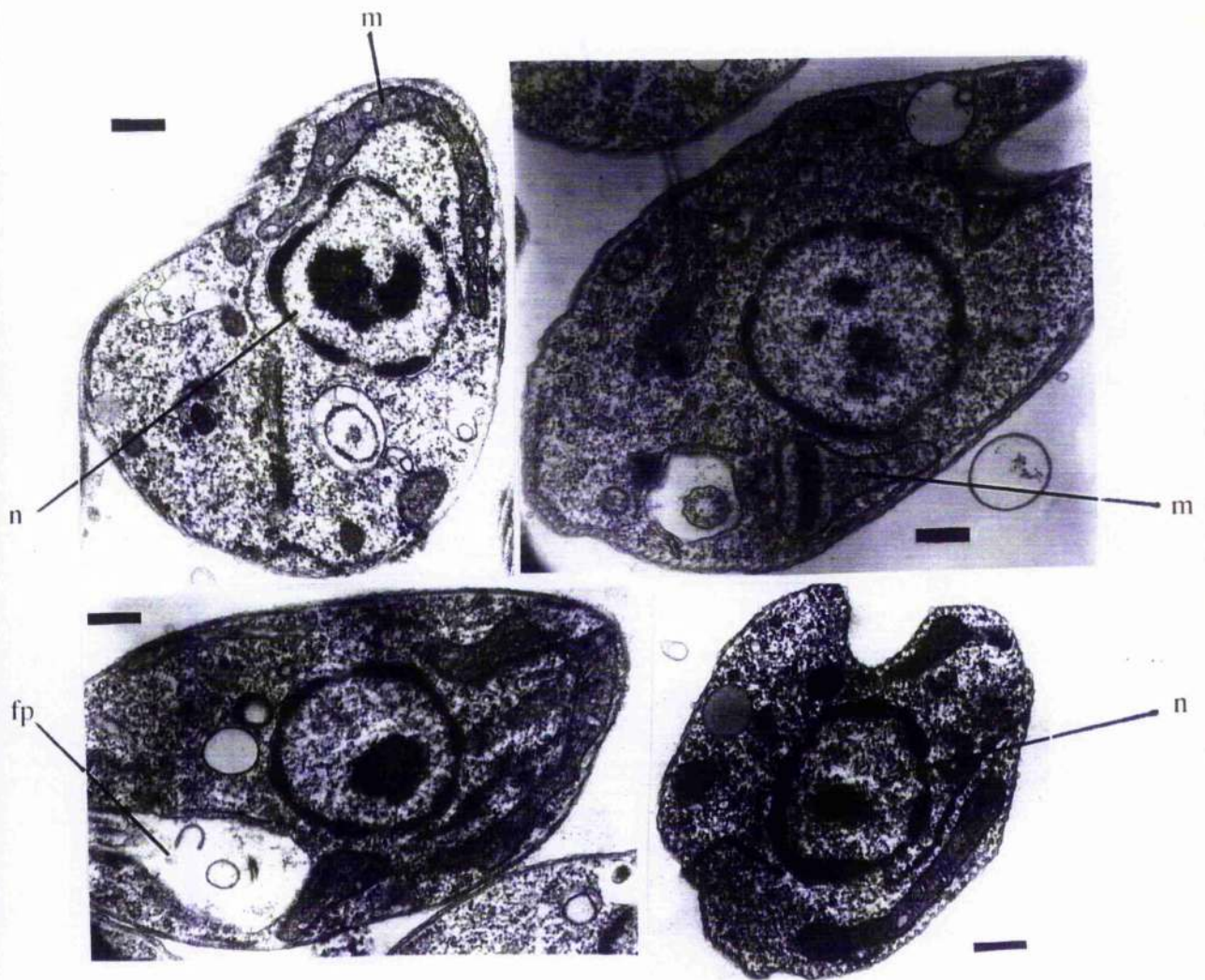
(a) - Four examples of control parasites



n - nucleus, with dark staining chromatin. m - mitochondrion. fp - flagellar pocket.

The bars represent  $0.4 \mu\text{M}$

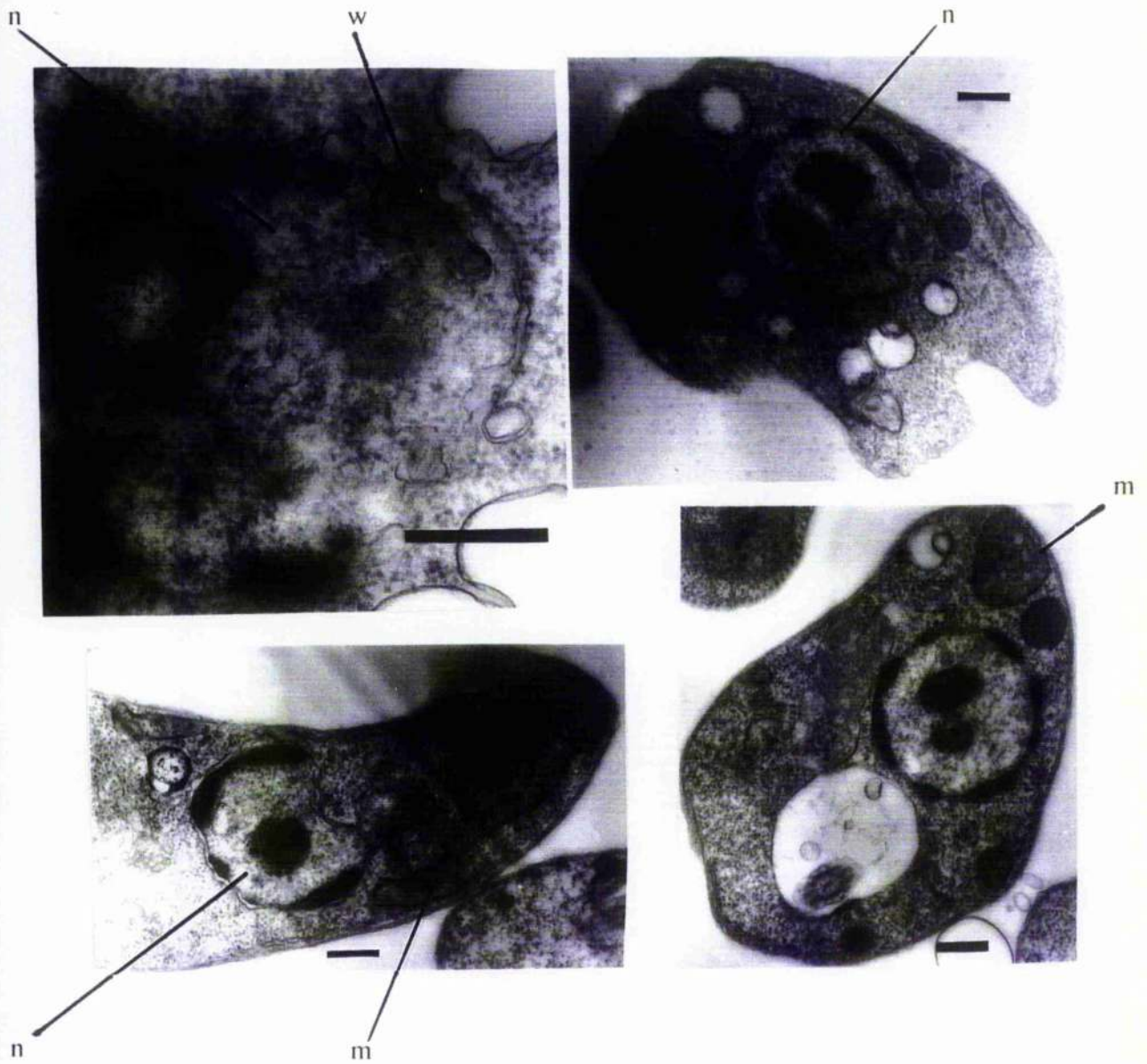
Figure 5.7 (b): Four examples of amastigotes treated with RNI for 17 min 30 s.



m - mitochondrion. fp - flagellar pocket. n - nucleus.

The bars represent 0.4  $\mu\text{m}$ .

**Figure 5.7 (c):** Four examples of amastigotes treated with RNI for 2 h.



n - nucleus that has been disrupted. w - nuclear membrane whorls. m - unusually swollen mitochondrion.

The bars represent 0.4 μm

**Table 5.1: Number of nuclei disrupted by RNI.**

Time	Total number of nuclei counted	Total number of undisrupted nuclei
0	102	100
17 min 30 s	102	93
2 hr	100	54

Nuclei from the sections photographed in Figure 5.7(c) were counted and scored as “disrupted” if the nucleus contained abnormal chromatin structures, or nuclear membrane whorls.

## 5.5 Conclusions

J774, a murine macrophage-like cell line, was able to produce enough RNI to kill amastigotes from *L. m. mexicana*. Killing of amastigotes and RNI by J774s was inhibited by the arginine analogue L-NMMA, and reversed by adding back arginine.

However, L-NMMA not only inhibits nitric oxide synthase, but also the cationic amino acid transporter systems  $y^+$  and  $y^+L$ . This will affect the uptake of not only arginine, but lysine, and probably ornithine (51,211). Adding excess arginine would compete for this transport system still further, decreasing the intracellular availability of the other cations, but increasing the intracellular availability of arginine. Therefore, since the inhibition of killing could be reversed by addition of excess arginine (Figure 5.1), the inhibition of the uptake of the other cationic amino acids is unlikely to be the mechanism by which the J774s kill *L. m. mexicana*.

The J774 toxicity assay detected killing of parasites that had already invaded macrophages, and did not assay toxicity to extracellular organisms, or inhibition of invasion, both of which are other potential areas of macrophage interaction with *L. m. mexicana*, but are beyond the scope of this thesis.

RNI are best described as cytotoxic rather than cytostatic to *L. m. mexicana* amastigotes. This does not mean that there are not cytostatic concentrations of RNI, as have been described for *Achromobacter*, *Flavobacterium*, *Pseudomonas*, *Micrococcus*, *Escherichia*, *Aerobacter*, *Torula* (212), *Plasmodium falciparum* (132), *Mycobacterium leprae* (47) and *Toxoplasma gondii* (213). A classically cytostatic molecule would, however, have a large range of concentrations over which it inhibits growth of the parasite

without killing the parasite. This is not the case with RNI and *L. m. mexicana* amastigotes (Figure 5.2).

Inhibition of [<sup>3</sup>H]-thymidine uptake by RNI takes place over the cytotoxic concentration range of RNI. Therefore, [<sup>3</sup>H]-thymidine uptake is a measure of viability, and not simply of stasis, when used to assay RNI toxicity on *L. m. mexicana* amastigotes.

The time course of toxicity is several hours (Figure 5.3 and Figure 5.4), and lower concentrations of RNI (20 μM HONO) can sometimes take over 24 h to kill amastigotes.

The toxicity is reversible, so that if the RNI are washed off, the parasites are able to recover sufficiently to transform to promastigotes (Figure 5.2). This is similar to the effect seen in mammalian mitochondria (141,158,214) where there is an initial fast, reversible inhibition of energy production by the cells, followed by an irreversible damage to the electron transport chain of the mitochondrion.

The rate of killing contrasts with the fast rate of killing of organisms by ROI. The difference may be in that ROI are reported to act by damaging membranes, which are presumably repaired quickly, so that a low amount of ROI for a long period will not have a toxic effect. While the target(s) of RNI remain(s) unknown, it is impossible to speculate why RNI should take a long time.

More RNI kill amastigotes faster. This means that the target(s) of RNI in amastigotes is(are) not saturable. This also means that if there is one vital but unsaturable target that is affected by low concentrations, whilst there is another that is affected at slightly higher concentrations, it will be very difficult to pick a concentration of RNI that affects one without the other.

The toxicity of RNI is not affected by the concentration of amastigotes. RNI are therefore not working by altering the metabolism of amastigotes so that they produce a toxic molecule that kills neighbouring cells. This is important, since the concentration of amastigotes in a lesion (up to  $10^{10} \text{ ml}^{-1}$ ) is much higher than the concentrations of amastigotes used here ( $1.4 \times 10^6 \text{ ml}^{-1}$ ). Since the toxicity is not dependent upon amastigotes interacting with each other, the assay systems used in this thesis probably reflect the effect of RNI on amastigotes.

No ultrastructural changes are visible in amastigotes within 17 min 30 s of initial exposure to RNI (Figure 5.7 (b)). The nuclei, mitochondria, surface membranes, flagellar pocket, and golgi apparatus are all intact.

There are ultrastructural changes in the parasites after 2 h of treatment with RNI (Figure 5.7(c)). The nucleus and mitochondrion may both be disrupted, though the nuclear changes are more easily discernible than the changes to the mitochondrion. The changes to the nucleus are not similar to the condensation of chromatin seen in apoptotic mammalian cells (see for example (215)), they look more like the nucleus is simply falling apart. Up to half of the nuclei are affected in this way (Table 5.1).

The changes to the mitochondrion are characteristic of necrotic cell death. In a necrotic cell, the cell loses energy and is unable to maintain its osmotic balance, eventually lysing. Shortly before lysis, the necrotic mammalian cell will swell and both internal and external membranes are disrupted (188). This ultrastructural description is similar to what is seen in the dying amastigotes (Figure 5.7(c)).

In conclusion, the amastigotes are killed by RNI produced both by a macrophage and axenically *in vitro*. The target(s) is(are) not saturable, and the ultrastructural changes are reminiscent of mammalian necrosis.

## **6. The effect of RNI on glycoinositolphospholipids and DNA**

## 6.1 Introduction

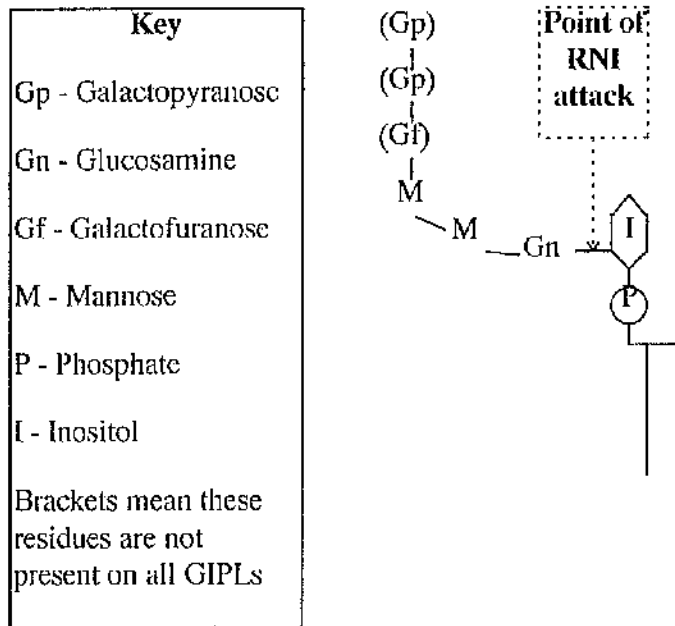
In previous chapters, the kinetics of RNI toxicity were established. In this chapter the effect of RNI on two postulated targets of RNI are examined - glycoinositolphospholipids (GIPLs) and the deoxyribonucleic acid (DNA) of *L. m. mexicana* amastigotes.

GIPLs are a major surface membrane component of amastigotes. The structure of GIPLs is shown schematically in Figure 6.1. Acidified nitrite is routinely used in the preparation of the sugar moiety from many different glycosyl-phosphatidylinositol anchored membrane components including GIPLs, and is able to cleave the sugar moiety from this family of molecules (183).

It was reasonable to suppose that GIPLs may therefore be a major target of RNI in amastigotes, especially as amastigote death was characterised by the parasites disintegrating.

Another possible target of RNI is the DNA. Given the disruption to the nuclear structure that seen in electron micrographs, and the increase in [<sup>3</sup>H]-thymidine incorporation seen by treating amastigotes for a long time with low levels of RNI, this was considered quite a likely target.

**Figure 6.1: Structure of GIPL and where it is attacked by RNI (183,246)**



The assay system (nick translation) that was used for detecting DNA damage by RNI was developed from a paper in which rat pancreatic islet cells were treated with the RNI producer sodium nitroprusside (SNP) (53). This led to DNA damage that was not inhibitable by inhibitors of endogenous endonucleases, suggesting that the damage was therefore probably not due to apoptosis. The authors concluded that islet cell DNA was an early target of attack by nitric oxide.

## 6.2 The effect of RNI on GIPLs

GIPLs can be labelled on the sugar moiety by incubating amastigotes in glucosc-free medium supplemented with [<sup>3</sup>H]-glucosamine. The GIPLs may then be purified from amastigotes by chloroform:methanol:water extraction followed by butanol:water partition. If the sugar moiety is still attached to the inositol phospholipid moiety, then the label will partition in the butanol fraction. If the sugar moiety has detached, then the label will partition in the water fraction.

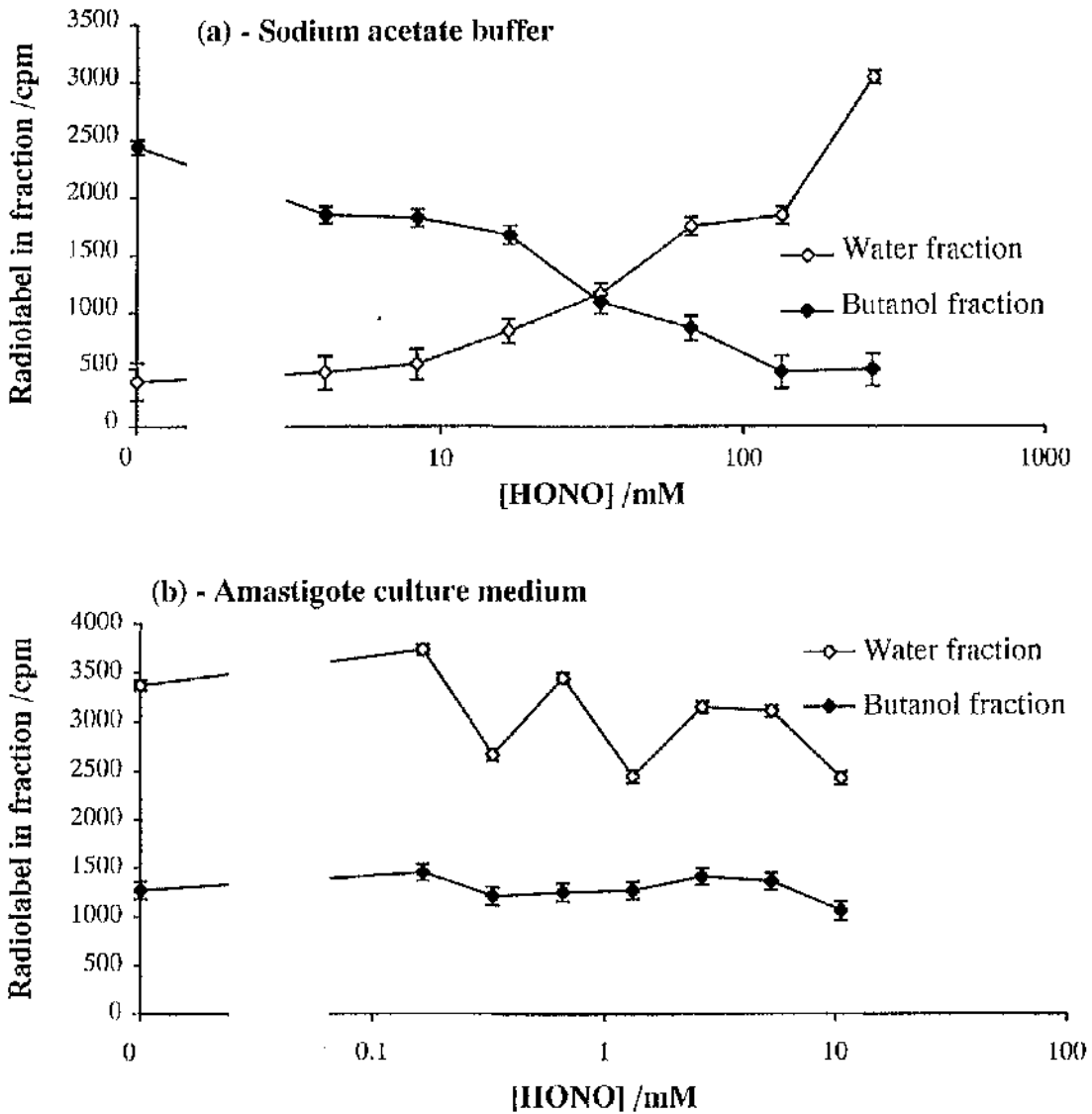
The concentration of RNI in sodium acetate buffer required to remove the sugar moiety from GIPLs is extremely high (mM range) compared to the concentration required to kill amastigotes (tens of  $\mu\text{M}$  range) (Figure 6.2(a)).

In amastigote culture medium, it was not possible to get the concentration of RNI to the concentrations attainable in sodium acetate buffer (Figure 6.2(b)). However, there was still no change in the partitioning of the label, and the concentration was still far above the toxic concentration of RNI.

When GIPLs were treated with RNI in amastigote culture medium, most of the label partitioned with the water phase in control cultures. There are two possible reasons for this. Either the salts and protein in the medium may have altered the solvent properties of the solution enough to prevent efficient partitioning. Or there may be an enzyme that breaks down GIPLs in serum. Whatever the reason for the anomaly in the control culture, there was no change in the partitioning characteristics with increasing RNI, and the ratio of counts in the water phase to counts in the butanol phase never reached as high as it did in sodium acetate buffer at the highest concentration of RNI. This suggests that the RNI are still not attacking the GIPLs in culture medium.

Therefore degradation of GIPLs is unlikely to be a major factor in the toxicity of RNI, since GIPL degradation occurs at much higher concentrations of RNI than it takes to kill amastigotes.

**Figure 6.2: The effect of RNI on GIPL integrity.**



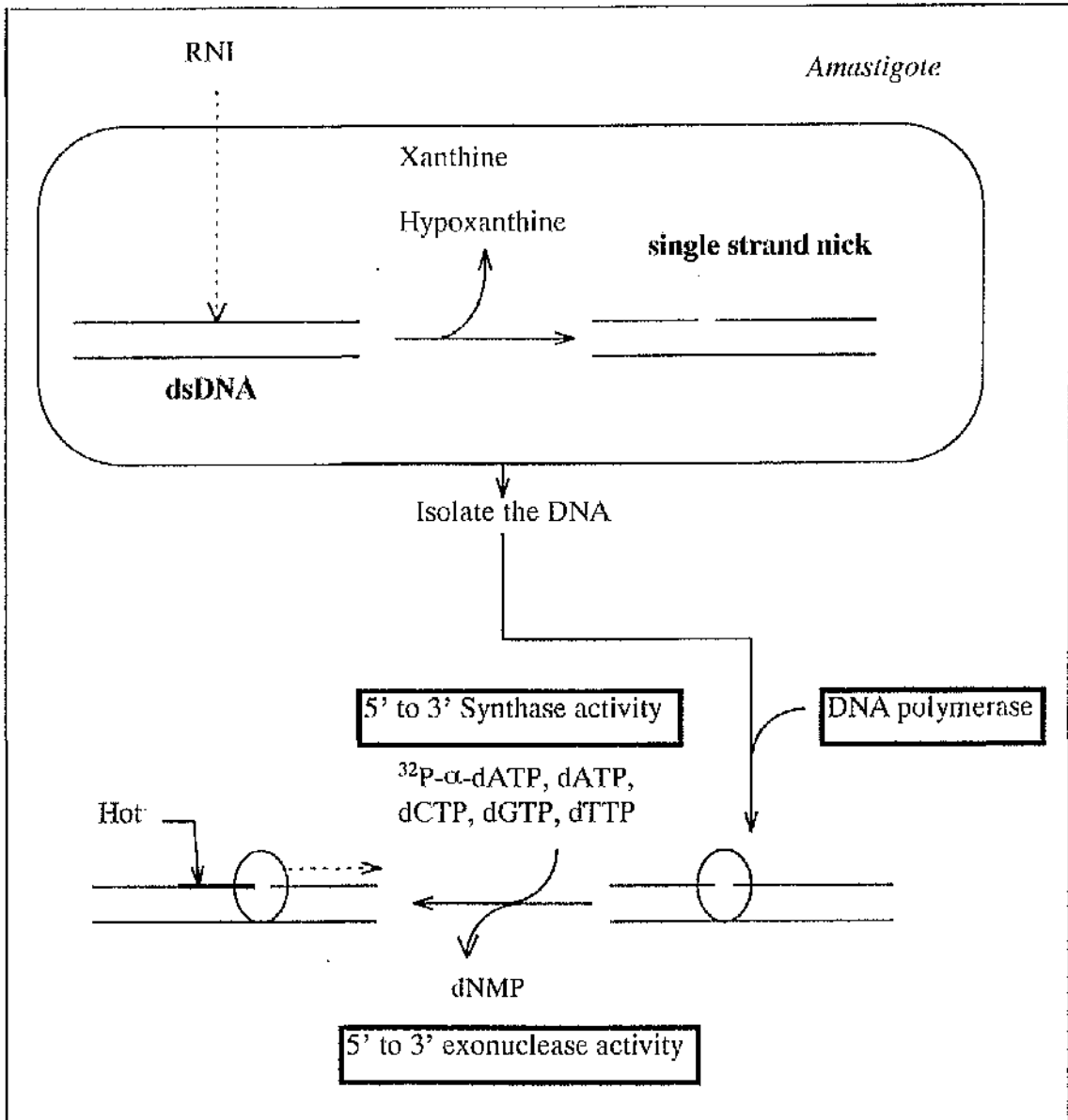
GIPLs were purified from amastigotes, and treated in either sodium acetate buffer pH 4.0 or amastigote culture medium (pH 5.5) for 24 h at 32°C, then partitioned between water and butanol. Where the label partitions in the water fraction, the sugar moiety has been cleaved from the inositol lipid moiety (open diamonds), where the label partitions in butanol, the sugar moiety is still attached to the inositol lipid moiety (closed diamonds).

### 6.3 DNA damage

RNI damage to DNA was assayed using nick translation. The principle behind this technique is shown schematically in Figure 6.3. The amastigotes were treated with RNI or 2,4-dinitrophenol (DNP) for up to 4 h. DNP was used as a control for killing amastigotes with a toxin that does not directly damage DNA. The DNA was then extracted and purified, and mixed with the Kornberg fragment of DNA polymerase and deoxyribonucleotides containing [ $^{32}\text{P}$ ]- $\alpha$ -dATP. Since the Kornberg fragment contains a 5'-3' exonuclease activity as well as a synthase activity, it translates single strand nicks along the double helix, replacing cold nucleotides with hot nucleotides (206).

Nick translation detects double strand breaks as well as single strand nicks in the DNA, since DNA polymerase can label the ends of both blunt-ended and overhanging DNA strands (206).

Figure 6.3: Overview of the nick translation procedure.



### 6.3.1 Development of the nick translation system

#### 6.3.1.1 The published assay system

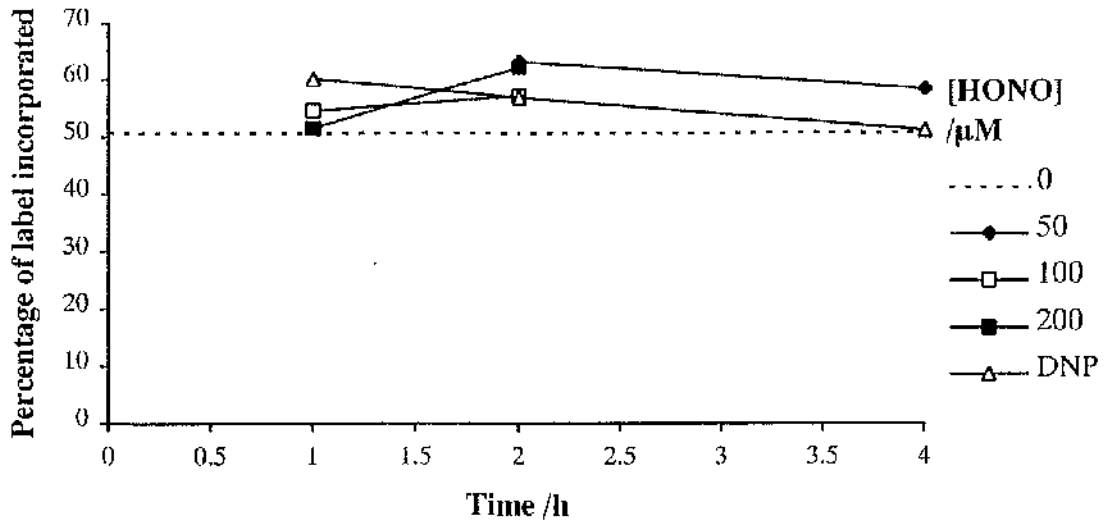
The published assay system used cold nucleotides with biotinylated dUTP in place of dTTP (53), and detected the incorporation of the labelled nucleotide using the peroxidase reaction with diaminobenzidine as enzyme substrate. In order to allow quantification of the damage, I used [<sup>32</sup>P]- $\alpha$ -dATP instead of biotinylated dUTP, and detected incorporation in some experiments by TCA precipitation and in others by agarose gel DNA electrophoresis followed by transferring the DNA to a nylon membrane for autoradiography.

Using amastigote DNA, approximately 50% of the radiolabel was incorporated into the DNA within 2 h (Figure 6.4). There was no change in the amount of label incorporated on addition of either RNI or DNP.

However, the lack of difference may simply have reflected the fact that so much of the radiolabel had been incorporated into the control DNA even without extra damage. The fact that this occurs in amastigote DNA, and not in the published control mammalian DNA, may have been due to the smaller fragment size of amastigote DNA compared to mammalian DNA. This would have meant that the end-labelling of the DNA strands may have used up all the dATP.

The published assay was therefore not suitable for studying amastigote DNA, since it was limited by the availability of dATP. So it became necessary to develop a system where the amount of radiolabel incorporated was dependent upon the number of nicks in the DNA, and not upon the concentration of dATP or any of the other nucleotides.

Figure 6.4: Nick translation of amastigote DNA.



Amastigotes ( $4 \times 10^6 \text{ ml}^{-1}$ ) were treated with RNI or DNP for up to 4 h at  $32^\circ\text{C}$ . At each time point, a sample was taken, DNA purified, and nick translated in a reaction containing a final 1.7 nM dATP for 120 min at room temperature. Label incorporation was detected by precipitating the DNA with TCA, and filtering the precipitate.

### 6.3.1.2 Increasing the cold dATP concentration.

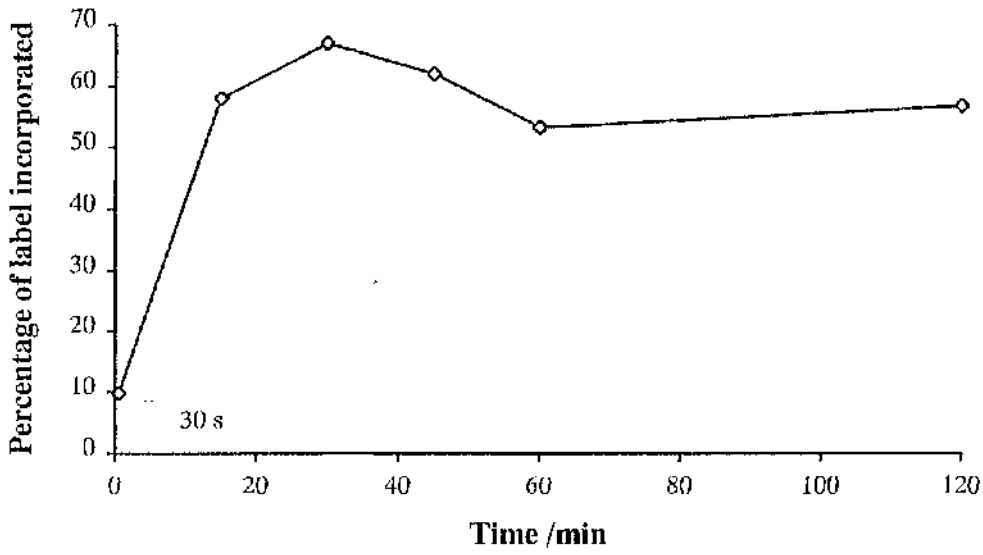
Since most of the [ $^{32}\text{P}$ ]- $\alpha$ -dATP was incorporated into control DNA, the rate of incorporation of [ $^{32}\text{P}$ ]- $\alpha$ -dATP into control DNA was assayed in the presence of an increased concentration of cold dATP (final [dATP] = 3.5  $\mu\text{M}$  as compared to 1.7 nM used previously).

Even with 3.5  $\mu\text{M}$  dATP, there was only an increase in label up to 15 min (Figure 6.5), indicating that the reaction was still limited by the availability of dATP.

The concentration of dATP had to be increased to 80  $\mu\text{M}$  to get a time course of incorporation which would be long enough to enable measurement of up to sixteen samples with reasonable reliability (Figure 6.6). The concentration of the other nucleotides was also increased to 80  $\mu\text{M}$ , so that they would not limit the rate of the reaction either.

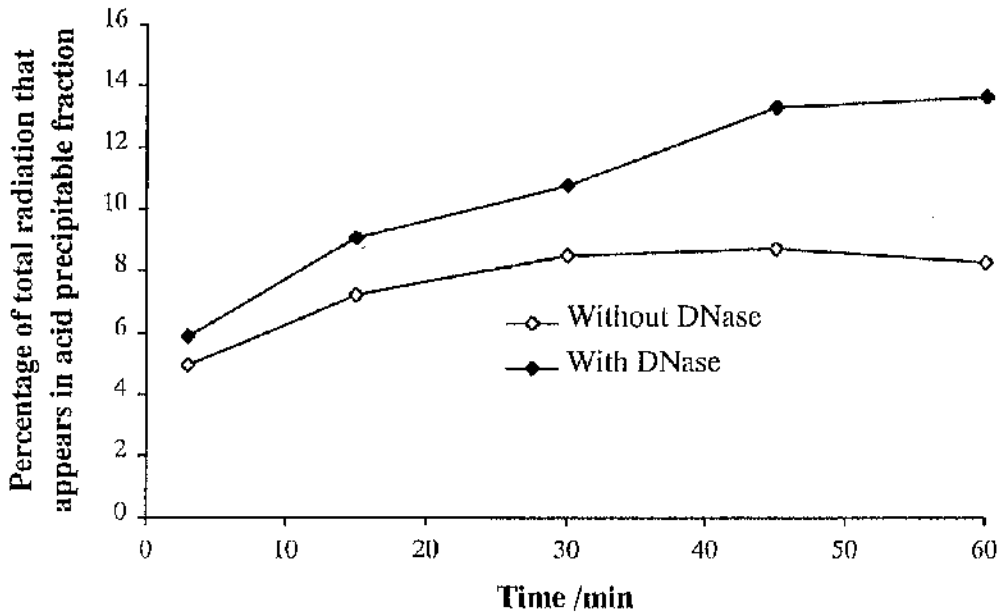
The addition of DNase 1 to the reaction demonstrated that more radiolabel would be incorporated if there were more nicks in the DNA (Figure 6.6). In the presence of  $\text{Mg}^{2+}$  ions, DNase 1 creates single strand nicks rather than double strand breaks in DNA (206), which is why the buffer contains  $\text{MgCl}_2$ .

**Figure 6.5: Time course of the nick translation reaction with 3.5  $\mu$ M dATP**



Amastigote DNA was incubated in the nick translation reaction mixture containing 3.5  $\mu$ M dATP at RT for up to 120 min. At each time point, a 2  $\mu$ l sample was removed, stopped with 0.2 M EDTA, and TCA precipitated to determine the amount of [ $^{32}$ P]- $\alpha$ -dATP incorporated into the DNA.

Figure 6.6: Nick translation of amastigote DNA with 80  $\mu\text{M}$  dATP.

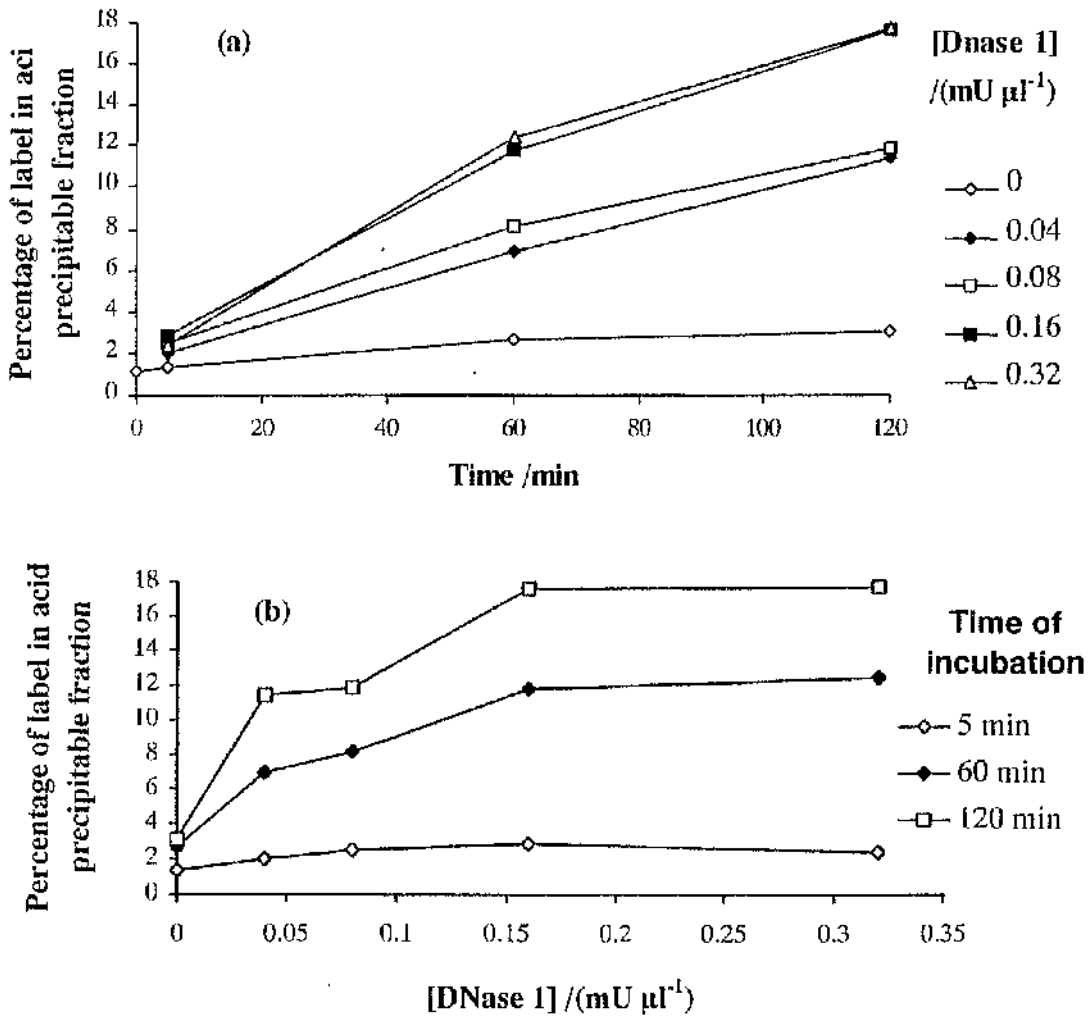


Amastigote DNA was treated with the nick translation mixture containing 80  $\mu\text{M}$  dATP, dCTP, dTTP and dGTP, and 90  $\mu\text{U } \mu\text{l}^{-1}$  DNase 1 at 15°C. At each time point, 20  $\mu\text{l}$  of the reaction was stopped in 580  $\mu\text{l}$  0.2 M EDTA, and the percentage of [ $^{32}\text{P}$ ]- $\alpha$ -dATP that was taken up by the DNA was assayed by TCA precipitation.

### 6.3.1.3 Construction of a standard curve with DNase 1

Having developed the assay system, it was possible to show that the more the DNA was nicked, the more label was incorporated into it (Figure 6.7). However, there was a bigger difference between the amount of labelling with DNase 1 and without DNase 1 after a two hour incubation than after a shorter incubation (Figure 6.7(b)). This suggests that the incubation period should be 120 min to get the maximum difference between labelled and unlabelled DNA.

**Figure 6.7: The effect of DNase 1 on DNA labelling in the nick translation reaction.**



Amastigote DNA was treated with nick translation reaction mixture containing 56  $\mu\text{M}$  dATP, dCTP, dGTP and dTTP, and various concentrations of DNase 1. At each time point, 20  $\mu\text{l}$  reaction was removed, and stopped with 580  $\mu\text{l}$  0.2 M EDTA, and the label incorporated was detected by TCA precipitation. Results are expressed both as the variation in labelling with time (a) and with the concentration of DNase 1 (b), and are representative of three separate experiments.

#### 6.3.1.4 Nicking control amastigote DNA before translation.

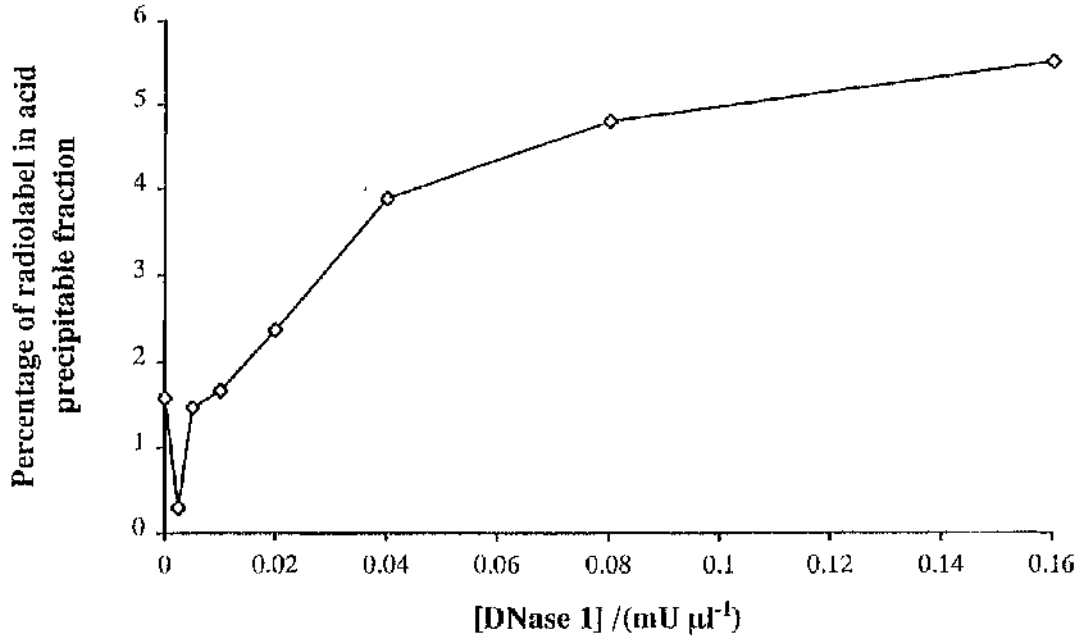
The previous experiments showed that more label gets incorporated into the DNA if the DNase 1 is included in the translation mixture with the DNA polymerase. However, it was important to be able to detect damage to DNA that had already been nicked. So, to determine that the technique could do this, a standard curve of DNase 1 nicked DNA was constructed.

The curve in Figure 6.8 was constructed by adding the DNase 1 to the DNA, and incubating at 37°C for 2 h. The translation reaction was then added to the nicking mixture, and incubated at 15°C. The dilution and the drop in temperature for the second incubation slow the rate of nicking down 160-fold (206). This means that over 99% of the nicking took place in the first incubation.

The modified technique detected damage to amastigote DNA below approximately 1 mU  $\mu\text{l}^{-1}$  DNase 1. Above this concentration, the amount of damage could sometimes be so much that the assay incorporated less [ $^{32}\text{P}$ ]- $\alpha$ -dATP with increasing DNase 1 (Figure 6.9).

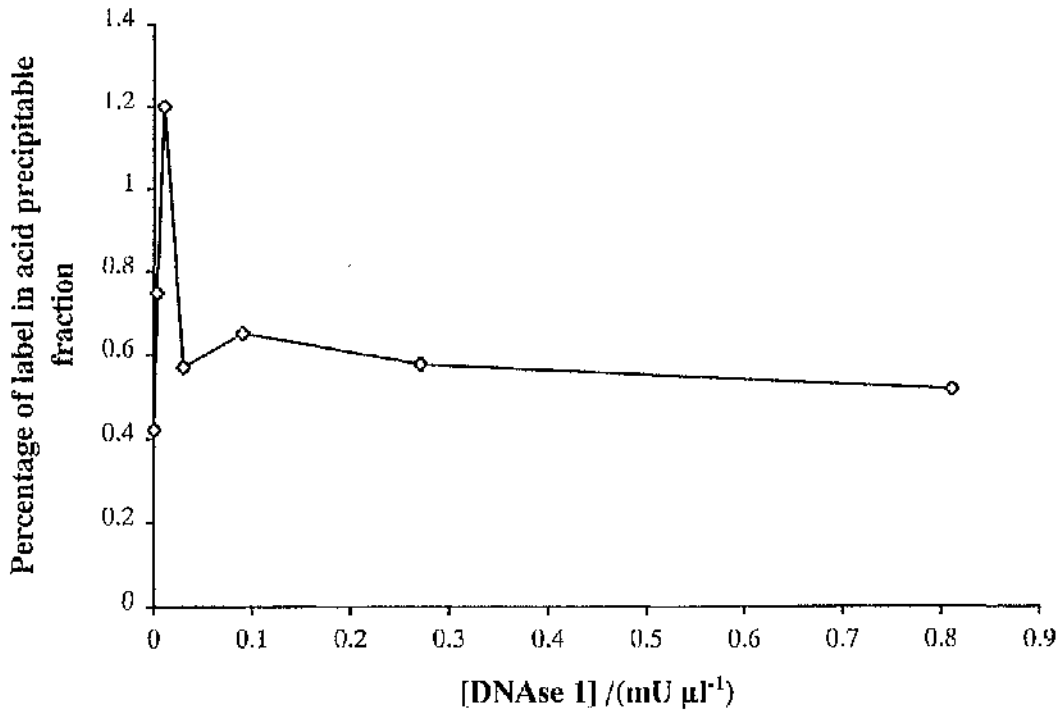
Additional damage leading to less label in the TCA precipitable fraction could be because smaller fragments did not precipitate as efficiently, or because the DNA polymerase could not work efficiently on badly damaged DNA.

Figure 6.8: DNase 1 standard curve with the amastigote DNA being nicked before the translation reaction.



Amastigote DNA was treated with DNase 1 for 2 h at 37°C. The translation reaction mixture containing 56 μM of all deoxyribonucleotides (final concentration) was then added, and incubated for a further 2 h at 15°C. The reaction was stopped with 580 μl 0.2 M EDTA, and [<sup>32</sup>P]-α-dATP incorporation was assayed by TCA precipitation.

Figure 6.9: Standard curve of DNase 1.



Amastigote DNA was treated with DNase 1 for 2 h at 37°C. The translation reaction mixture containing 56  $\mu\text{M}$  of all deoxyribonucleotides (final concentration) was then added, and incubated for a further 2 h at 15°C. The reaction was stopped with 580  $\mu\text{l}$  0.2 M EDTA, and [ $^{32}\text{P}$ ]- $\alpha$ -dATP incorporation was assayed by TCA precipitation. Note that the concentration range on the x-axis is higher than that in Figure 6.8.

## 6.4 Detection of damage to amastigote DNA caused by RNI.

### 6.4.1 The effect of RNI on DNA in intact amastigotes

Using the modified nick translation assay, damage caused by RNI to live amastigote DNA was assessed. There was little [ $^{32}\text{P}$ ]- $\alpha$ -dATP incorporated into any of the DNA prepared from amastigotes treated with RNI or DNP (Figure 6.10). This either suggests that there was no detectable damage to the DNA, or that the damage was so great that it was above the level detectable with TCA precipitation of the nick translation reaction (Figure 6.9).

The low amount of label probably represents little damage since running the standard curve on an agarose gel showed that additional label could be detected in the chromosomal DNA up until the point that smearing of the DNA appeared on the autoradiograph (Figure 6.11 (c)).

There was, however, a *caveat*. On running the sample DNA on a gel stained with ethidium bromide, it was discovered that different amounts of DNA had been loaded into each reaction (Figure 6.11(b)).

The reason for the variation was probably that measurement of the concentration of DNA using  $\text{OD}_{260}/\text{OD}_{280}$  is affected by even small concentrations of impurities in the preparation, rather than a pipetting error. The evidence for this was twofold. Firstly, the  $\text{OD}_{260}/\text{OD}_{280}$  had been measured in triplicate, and the variation in readings was not large. Secondly, the amount of DNA that had been loaded into the standard curve was reasonably similar in each lane (Figure 6.11(a)).

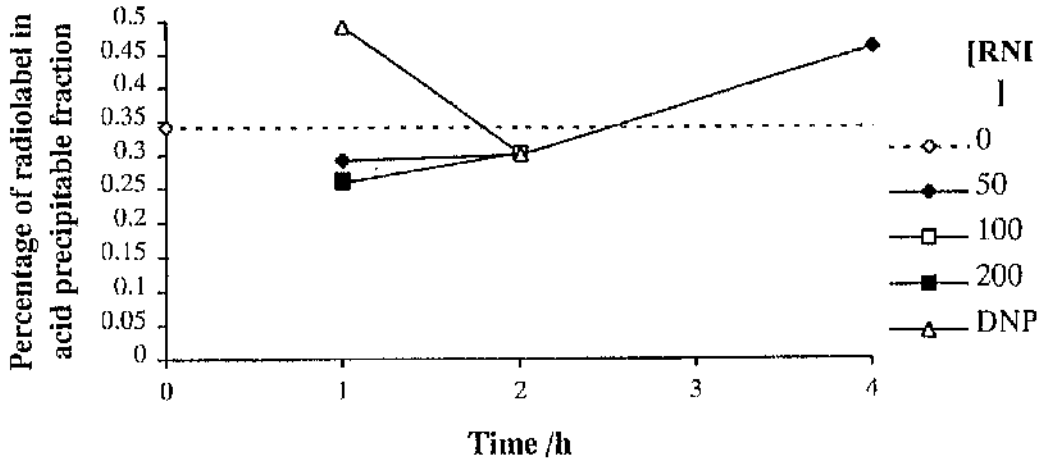
The amount of label incorporated into each tube in Figure 6.10 could therefore be explained by the different amounts of DNA. Despite this, the amount of label did not consistently change with increasing amounts of RNI (Figure 6.11(d)).

Therefore the concentration of DNA was normalised between samples with ethidium bromide fluorescence, by modifying a technique described in *Molecular Cloning - A Laboratory Manual* (2006) to make the technique quantitative.

Using amastigote DNA, whose concentration had been calculated using  $OD_{260}/OD_{280}$ , we were able to construct a standard curve of DNA in PBS containing  $2 \mu\text{g ml}^{-1}$  ethidium bromide (Figure 6.12). Reading the concentration of DNA from the different samples using this standard curve, it was possible to get slightly more even concentrations of DNA loaded into each sample of the nick translation reaction (Figure 6.13(a)).

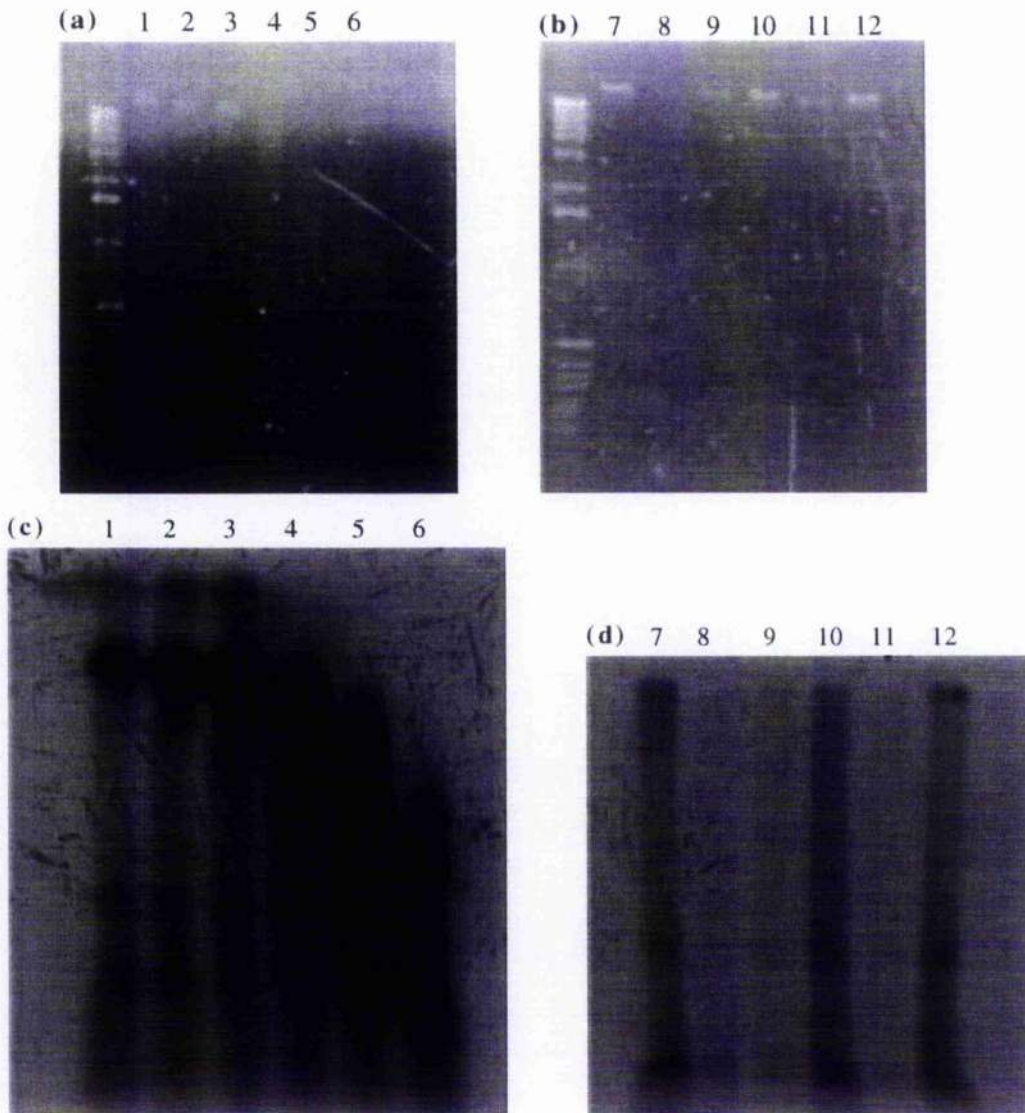
It was still not possible to detect any damage to the DNA with different treatments of RNI or DNP (Figure 6.13).

**Figure 6.10: Nick translation of amastigote DNA using the modified nick translation assay.**



Amastigotes were treated with RNI or DNP for the times shown, DNA was then extracted, and nick translated using the modified nick translation reaction (56  $\mu$ M dNTP). The amount of radiolabel incorporated into the DNA was assayed by TCA precipitation.

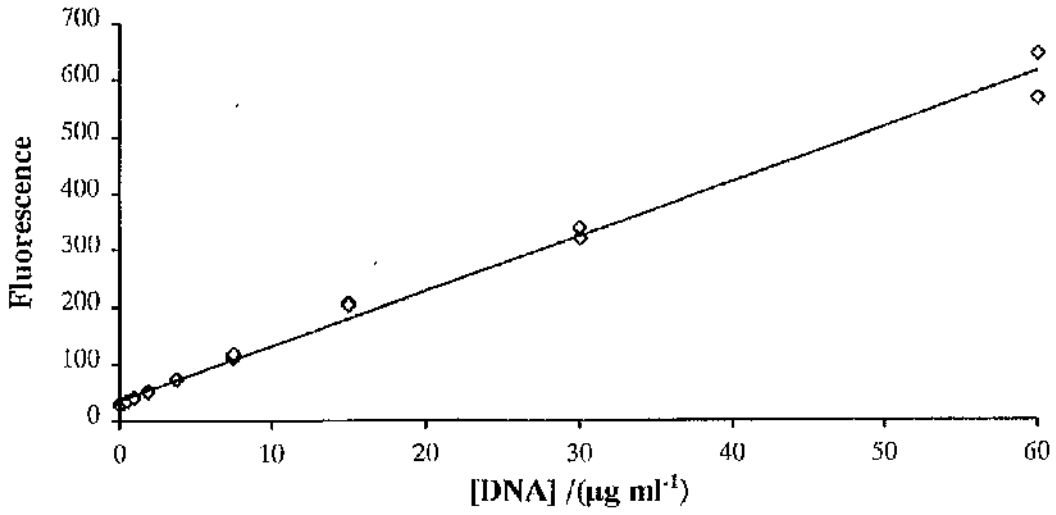
**Figure 6.11: DNase 1 standard curve and nick translation of amastigote DNA**



A standard curve was constructed by treating control amastigote DNA with increasing concentrations of DNase 1 (3-fold serial dilutions from 0.27 mU  $\mu\text{l}^{-1}$ ) (a) and (c).

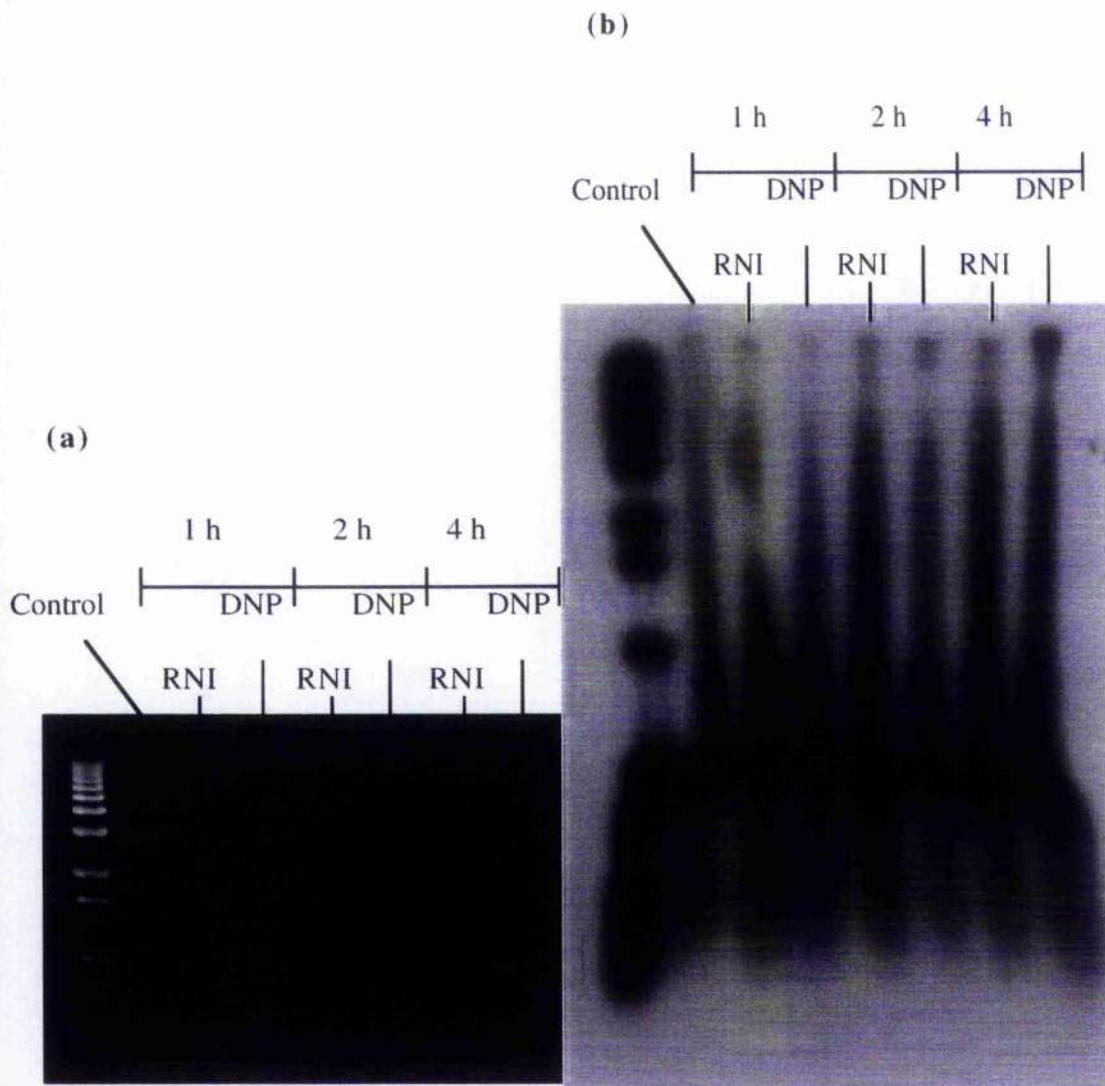
Amastigotes ( $4 \times 10^6 \text{ ml}^{-1}$ ) were treated with 100  $\mu\text{M}$  RNI or 200  $\mu\text{M}$  DNP for up to 4 h (7 - control, 8 - RNI 1 h, 9 - DNP 1 h, 10 - RNI 2 h, 11 - DNP 2 h, 12 - DNP 4 h) (b) and (d). DNA was purified, and damage was detected by nick translation followed by separation on a 0.8% agarose gel. The gels were stained with ethidium bromide (a) and (b), and then the DNA transferred to a nylon filter for autoradiography (c) and (d).

**Figure 6.12: Standard curve of ethidium bromide fluorescence.**



Serial dilutions of amastigote DNA were placed in  $50 \mu\text{l}$   $2 \mu\text{g ml}^{-1}$  ethidium bromide in PBS in a 96 well plate. The excitation wavelength was 254 nm, and the emission wavelength was 605 nm.

**Figure 6.13: The effect of RNI on nick translation of amastigote DNA.**



Amastigotes were treated with RNI (100  $\mu$ M HONO) or DNP (200  $\mu$ M) for up to 4 h at 32°C. The DNA was then extracted, normalised using ethidium bromide measurement, and treated with the nick translation mixture containing 56  $\mu$ M dNTP. The labelled DNA was run on a 0.8% agarose gel stained with ethidium bromide and photographed (a). The DNA was transferred to a nylon membrane by capillary action (b), for autoradiography. The molecular weight markers were labelled with the nick translation mixture that end-labels linear DNA.

#### 6.4.2 The direct effect of RNI on DNA *in vitro*.

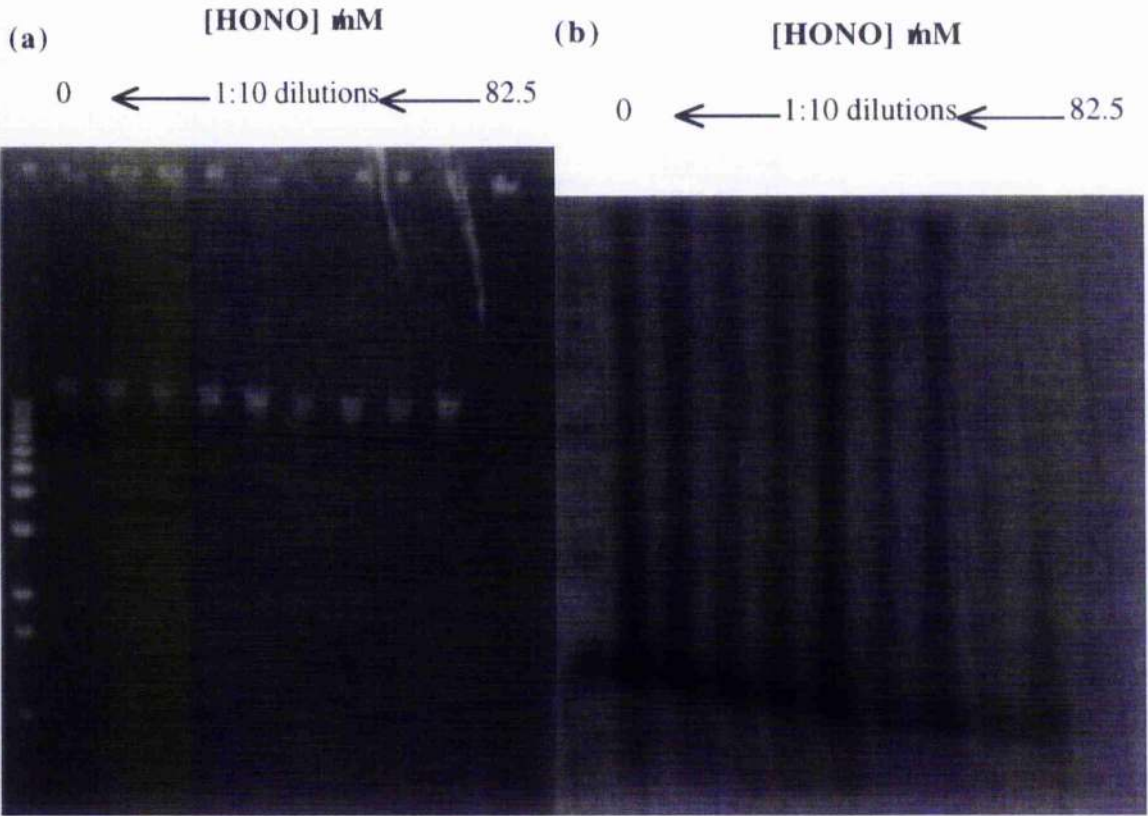
Since it had not been able to detect any damage to the DNA in amastigotes at concentrations of RNI that killed amastigotes, the concentrations of RNI at which it was possible to detect damage to DNA using nick translation were examined.

DNA was prepared from amastigotes, and incubated in sodium acetate buffer pH 4.0 for 4 h at 32°C. The incubation mixture was neutralised with 10 M sodium hydroxide, and labelled with the nick translation mixture. Damage was assayed by running the DNA on a 0.8 % agarose gel, photographing it, then transferring it to a nylon filter for autoradiography.

RNI did not cause damage directly to DNA that was detectable with nick translation (Figure 6.14). RNI did, however, damage the DNA in a way that makes the DNA stay in the well at high concentrations of RNI (82.5 mM HONO). At this concentration, a yellow residue was visible in the reaction mixture, confirming that the DNA and RNI had reacted.

This was consistent with a rare, though not unprecedented, type of damage in which the diazotisation reaction leads to cross-linking of DNA strands (216).

**Figure 6.14: The direct effect of RNI on amastigote DNA.**



Amastigote DNA was treated with sodium nitrite in sodium acetate buffer pH 4.0 for 4 h. It was then neutralised, labelled with the nick translation mixture, and run on a 0.8% agarose gel. It was then photographed (a), and transferred to a nylon filter for autoradiography (b).

### **6.4.3 The effect of RNI on DNA in amastigote culture medium.**

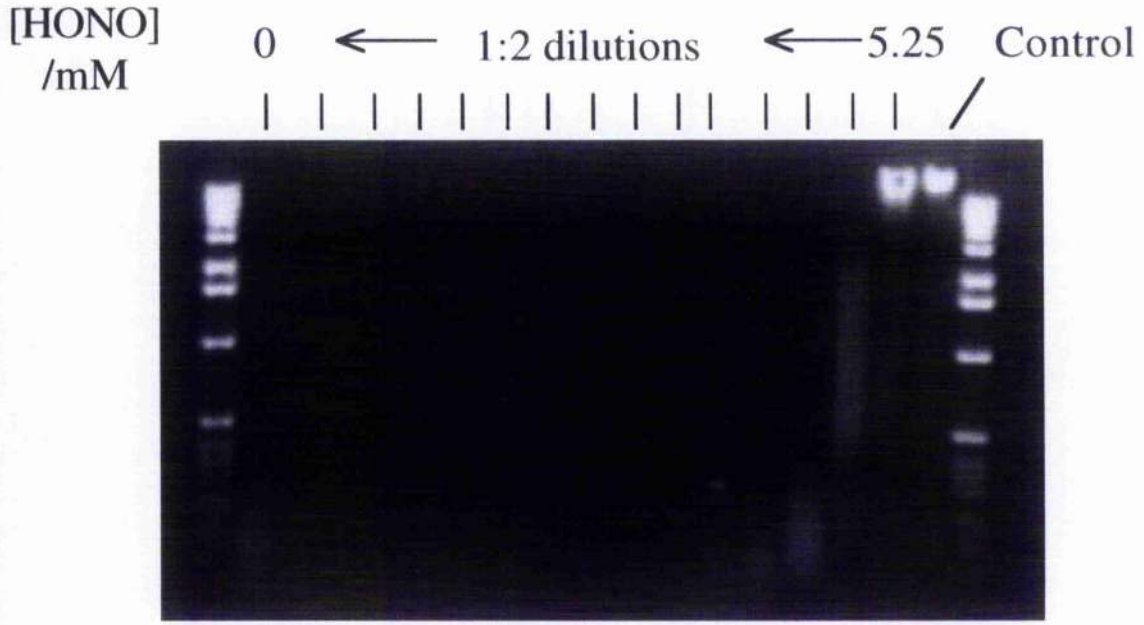
Since it was impossible to detect any damage to the DNA caused by RNI in sodium acetate buffer, damage to DNA caused by RNI in amastigote culture medium was assessed.

Amastigote DNA was incubated in serial dilutions of sodium nitrite in amastigote culture medium for 4 h (Figure 6.15). The concentration of RNI obtainable was not as high as those obtainable in sodium acetate buffer.

It was impossible to assay damage to DNA in this system since there was a DNase activity in amastigote culture medium that degraded amastigote DNA at low concentrations of RNI. However, high concentrations of RNI inhibited this DNase activity (Figure 6.15).

The DNase activity in amastigote culture medium was in the serum fraction of the medium (Figure 6.16)

**Figure 6.15: The effect of RNI on degradation of DNA in amastigote culture medium.**



Amastigote DNA was incubated in amastigote culture medium containing sodium nitrite for 4 h at 32°C. Control DNA was in TE buffer. The reaction was then neutralised and DNA separated run on a 0.8 % agarose gel containing ethidium bromide.

**Figure 6.16: Degradation of DNA by serum in amastigote culture medium**



Amastigote DNA was incubated in amastigote culture medium pH 5.5 containing 20% FCS (1), or no FCS (2), or in TE buffer (3) for 4 h. The DNA was run on a 0.8% agarose gel stained with ethidium bromide.

## 6.5 Conclusions

Neither DNA nor GIPLs are likely to be major early targets of RNI attack on *L. m. mexicana* amastigotes. Both components are susceptible to large concentrations of RNI, but it was not possible to detect any damage to either at concentrations of RNI that kill amastigotes.

Damage to both DNA and GIPLs involves a diazotisation reaction that can either continue by removing an amine group, or in some cases in DNA, cross-link the double helix (216). It may not be surprising that diazotisation reactions are not important *in vivo* since the reaction rate for diazotisation is up to  $10^6$  times slower than the reaction of RNI with sulphhydryl groups (31), which in turn react slower than the iron-sulphur centres of many enzymes.

On the other hand, RNI have been used as mutagens on living cells (171,175), suggesting that a diazotisation reaction with DNA may be significant at levels which are not completely toxic. However, it is much more common to find experimenters using RNI mutagenesis on DNA that has been purified from bacteria, and then added back to the bacteria or on viruses (171).

The published assay for mammalian DNA labels amastigote DNA extremely efficiently. It proved necessary to increase the concentration of competing cold dATP approximately  $10^4$  fold to stop dATP limiting the amount of incorporation into control DNA. The reason for this may be that amastigote DNA is in much smaller fragments than mammalian DNA, or that amastigote DNA already has many single strand nicks in it. On the basis of these results, it is only possible to speculate as to which is more likely.

It was necessary to develop the nick translation system to detect damage to amastigote DNA. There was a bigger difference between nicked DNA and undamaged DNA if the translation reaction was allowed to proceed for up to 2 h. This suggests that there were so many sites for binding of DNA polymerase in control DNA, that adding extra sites did not increase the amount of label incorporation until those initial sites had been repaired. In this case, the concentration of DNA polymerase would have limited the rate of the reaction, but the end-point would have been determined by the number of nicks.

The assay as developed detected damage caused by DNase I. The more damage, the more label was taken up. However if too high a concentration of DNase I was used, less label was taken up. With autoradiography, however, it was apparent that more label was incorporated into chromosomal DNA until the point at which it began to smear on the gel. It is therefore likely that the damage to amastigote DNA was not above the level detectable with nick translation, and that any damage caused by RNI was too small to be detected.

RNI inhibit the DNase activity in serum. In many inflammatory autoimmune diseases, RNI are produced at the site of inflammation, and often systemic  $\alpha$ -DNA antibodies can be detected. The concentrations of RNI that totally inhibit DNase in Figure 6.15 are much higher than the concentrations required to kill amastigotes and J774 cells, so are likely to be much higher than those found physiologically. Despite this, lower concentrations of RNI may slow down the rate of degradation of DNA in serum and our assay would not have detected such small changes in enzyme kinetics. In this case, the presence of RNI in an inflammatory lesion may prolong the half life of DNA released from necrotic cells, thereby contributing to the formation of  $\alpha$ -DNA antibodies.

In conclusion, DNA and GPIs are unlikely to be major early direct targets of RNI attack on amastigotes.

**7. The effect of RNI on amastigote mitochondrial function.**

## 7.1 Introduction

In *E. coli* and many mammalian systems, some of the targets of RNI are the iron-sulphur containing enzymes of the mitochondrial electron transport chain (26). To assess whether the mitochondrion in amastigotes was affected by RNI, and whether this could account for the toxicity of RNI, several measures of mitochondrial function were assayed - oxygen uptake, rhodamine 123 (Rh123) uptake, and the concentration of ATP.

Oxygen uptake is a measure of the ability of the electron transport chain to carry electrons, since oxygen reduction is the final step in this pathway. If the electron transport chain is disrupted at any point, oxygen uptake will be affected.

Rh123 provides a measure of the energy-production capacity of the mitochondrion. It is a positively charged fluorescent dye whose uptake is dependent on the membrane potential across the mitochondrial membrane (217). The larger the membrane potential, the more Rh123 is taken up.

Many organisms, as phylogenetically diverse as archaeobacteria and mammalian cells have a pump that can remove Rh123 from the mitochondrion (in the case of mammalian cells) or the bacterium (218). This pump can be inhibited by some of the mitochondrial uncouplers (e.g. FCCP), so that whereas some mitochondrial inhibitors decrease Rh123 uptake, others may increase it. Therefore, a positive control that inhibits Rh123 uptake was chosen - 2,4-dinitrophenol (DNP).

Another consideration when using Rh123 is that at high concentrations it auto-quenches. This means that in some instances, the more Rh123 that is taken up by a mitochondrion, the less fluorescent light will be emitted (219). At lower concentrations of Rh123, the more dye that is taken up, the more fluorescent light will be emitted.

The concentration of ATP is a measure of how effectively the mitochondrion actually provides energy to the amastigote cytoplasm. Many researchers measure the concentration of ADP and AMP as well, and express this energy availability in terms of the "Adenylate Energy Charge" (AEC) (204,220):

$$\text{AEC} = \frac{2 \times [\text{ATP}] + [\text{ADP}]}{[\text{ATP}] + [\text{ADP}] + [\text{AMP}]} \quad \text{Equation 1}$$

This was not, however, an appropriate measure for my purposes. The AEC would remain unchanged if the plasma membrane was damaged by RNI, allowing nucleotides to leak out of the amastigotes. Indeed [<sup>3</sup>H]-adenine release is often used in mammalian cells as a measure of cellular viability. The concentration of ATP alone therefore provided a better assessment of how much energy was available for reactions that require ATP than the AEC.

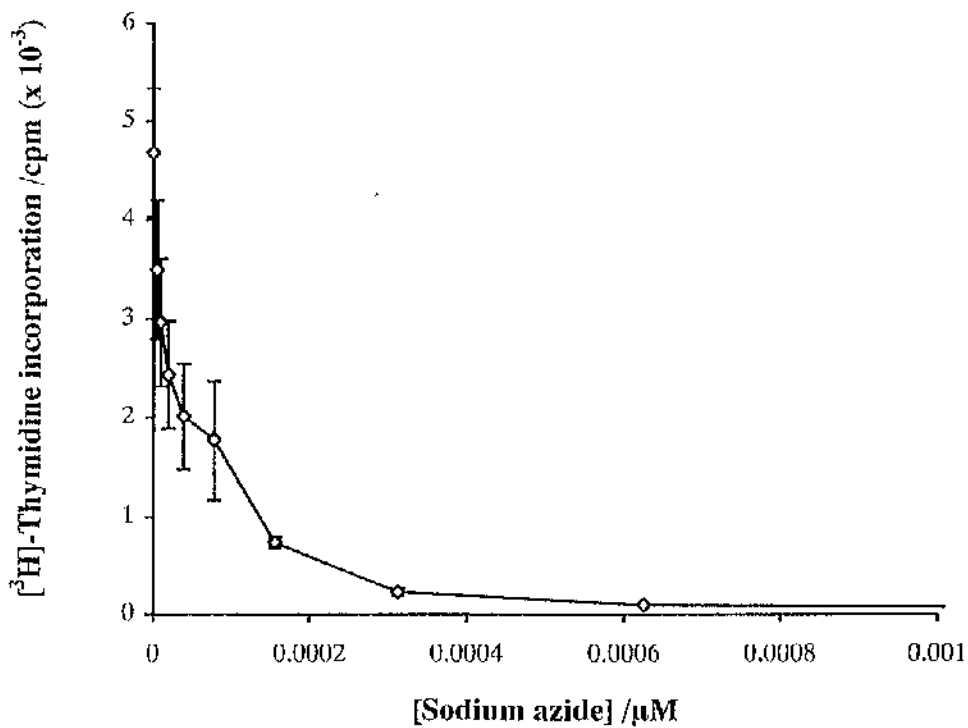
Initially, it was important to assess whether the axenically grown amastigotes were susceptible to any sort of mitochondrial toxin, and if so, to what concentrations they were susceptible.

## **7.2 Axenically cultured amastigotes are susceptible to mitochondrial toxins.**

[<sup>3</sup>H]-thymidine uptake by amastigotes was affected by all three mitochondrial toxins tested- sodium azide (Figure 7.1), carbonylcyanide P-trifluoromethoxyphenylhydrazone (FCCP) (Figure 7.2) and 2,4-dinitrophenol (DNP) (Figure 7.3). Sodium azide inhibits the electron transport chain, while FCCP and DNP are uncouplers.

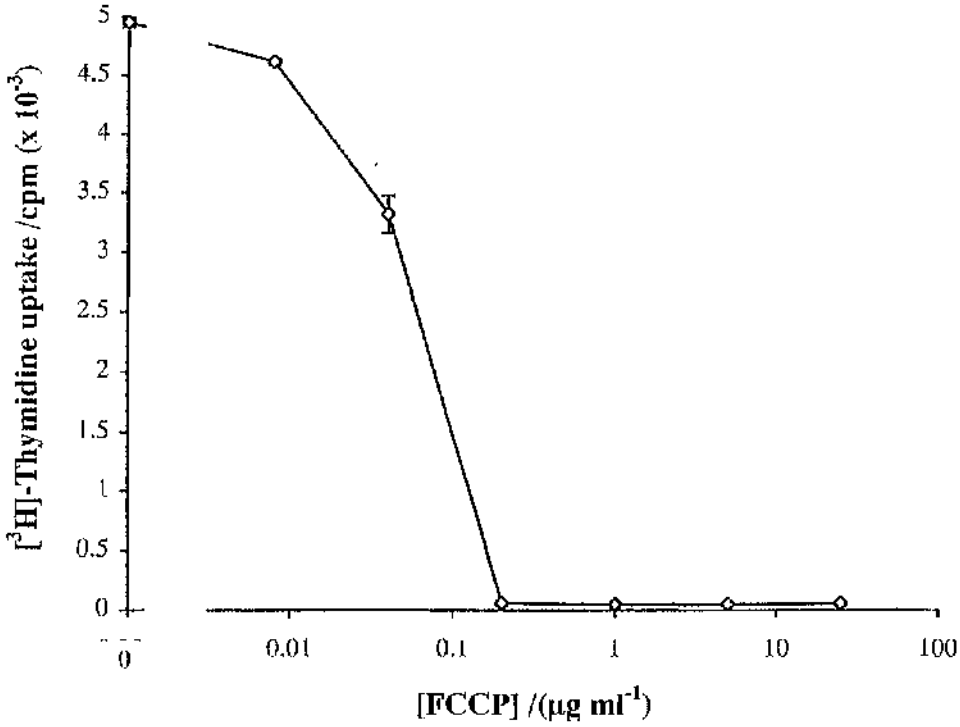
[<sup>3</sup>H]-thymidine uptake by amastigotes is therefore dependent on energy production by their mitochondrion.

Figure 7.1: The effect of sodium azide on [<sup>3</sup>H]-thymidine uptake by amastigotes.



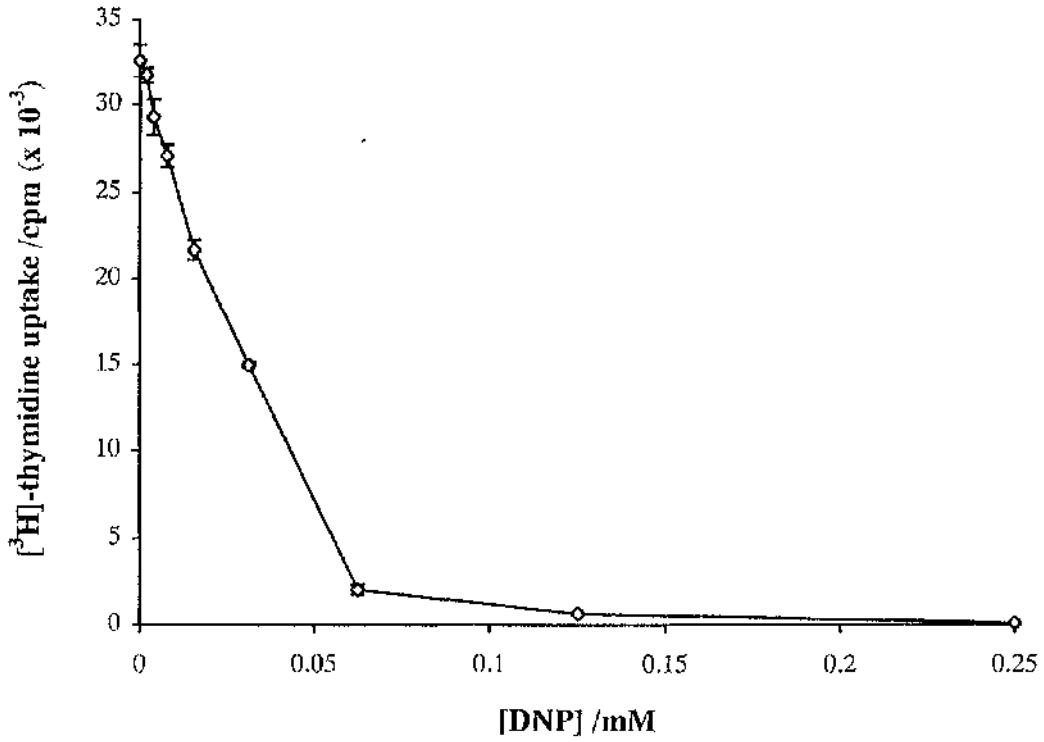
[<sup>3</sup>H]-thymidine uptake by amastigotes ( $1 \times 10^6 \text{ ml}^{-1}$ ) was assayed in the presence of sodium azide for 24 h at 32°C. Results are expressed as the mean  $\pm$  SEM (n=4).

Figure 7.2: The effect of FCCP on [<sup>3</sup>H]-thymidine uptake by amastigotes.



[<sup>3</sup>H]-thymidine uptake by amastigotes ( $1 \times 10^6 \text{ ml}^{-1}$ ) was assayed in the presence of FCCP for 24 h at 32°C. Results are expressed as the mean  $\pm$  SEM (n=4).

Figure 7.3: The effect of DNP on [<sup>3</sup>H]-thymidine uptake by amastigotes.



[<sup>3</sup>H]-thymidine uptake by amastigotes ( $1 \times 10^6 \text{ ml}^{-1}$ ) was assayed in the presence of FCCP for 24 h at 32°C. Results are expressed as the mean  $\pm$  SEM (n=4).

### 7.3 RNI inhibition of mitochondrial function.

#### 7.3.1 Oxygen consumption

Before the acidified nitrite system for assessment of RNI toxicity was developed, S-nitroso-N-acetyl penicillamine (SNAP) was used to produce RNI. During this period, mitochondrial function was assessed by the inhibition of oxygen uptake by amastigotes.

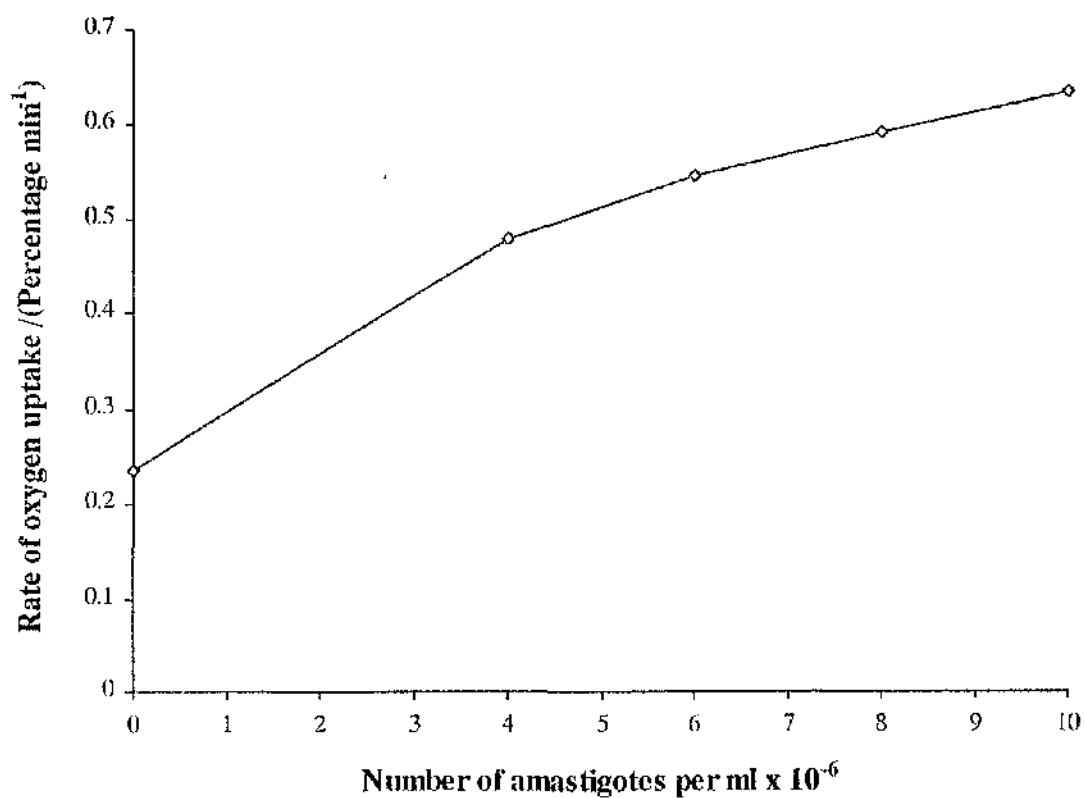
In all experiments, fully aerated amastigote culture medium was defined as 100 % saturation, and a dilute solution of sodium sulphite defined as 0 % saturation. Without a detailed analysis of the solubility of oxygen in amastigote culture medium, it was impossible to convert these figures to molar quantities.

Even in sterile amastigote culture medium, there was a baseline consumption of oxygen of approximately  $0.24\% \text{ min}^{-1}$  (Figure 7.4). As the concentration of amastigotes increased from  $10^6$  to  $10^7 \text{ ml}^{-1}$ , more amastigotes consumed oxygen more quickly. This covered the concentration range that we used for all experiments.

The rate of oxygen consumption by amastigotes was inhibited by concentrations of SNAP up to 1 mM (Figure 7.5). The oxygen consumed by SNAP concentrations above 1 mM obscured any effect on amastigote oxygen consumption. This effect was probably due to the reaction of nitric oxide with molecular oxygen in solution to produce nitrite and nitrate anions.

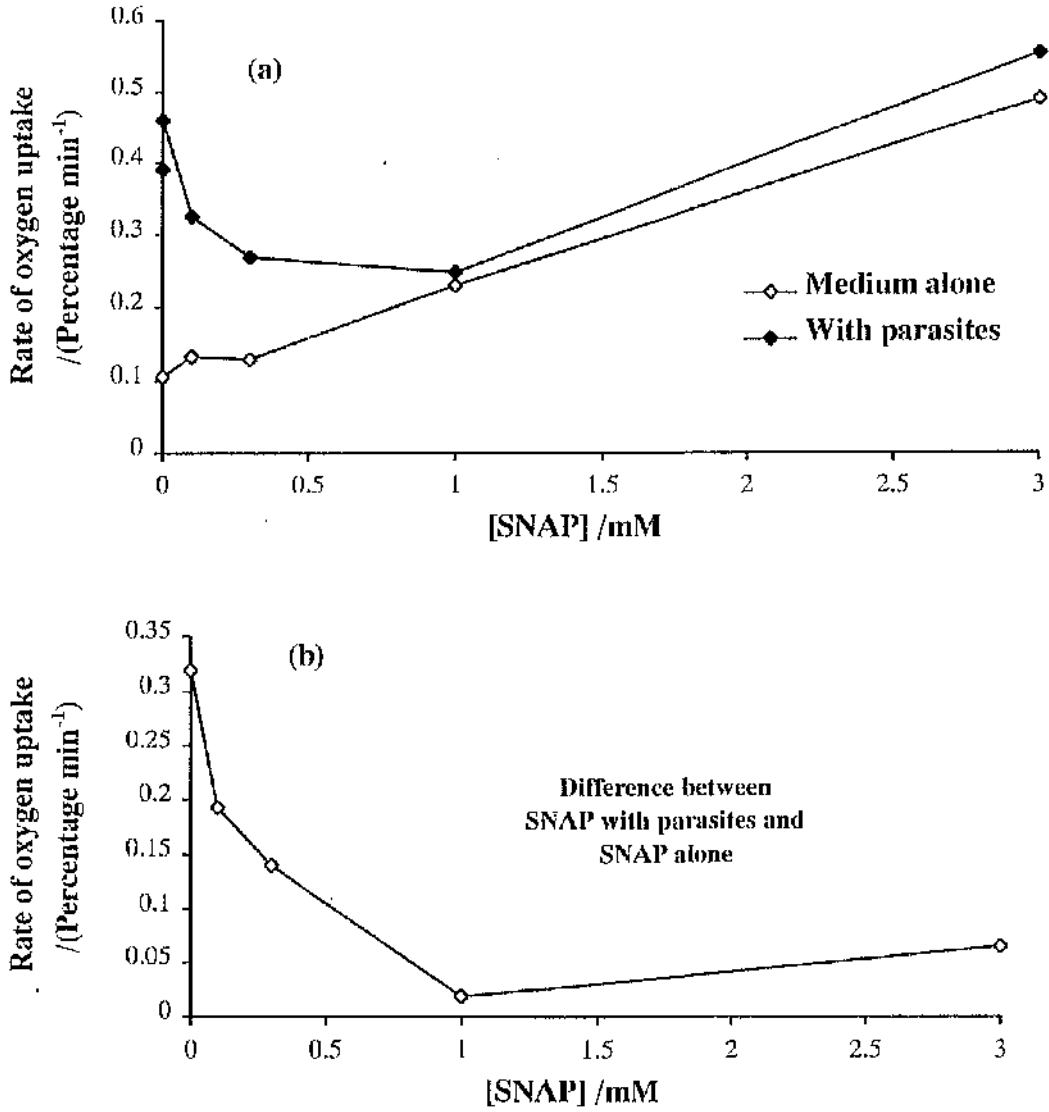
A half-hour exposure of amastigotes to 1 mM SNAP was not normally completely toxic (Figure 3.10). Therefore amastigotes were able to recover from this level of inhibition of oxygen consumption for this time period.

Figure 7.4: Oxygen consumption by amastigotes.



Oxygen uptake by different concentrations of amastigotes was measured in amastigote culture medium.

Figure 7.5: Inhibition of amastigote oxygen consumption by SNAP.



Oxygen uptake by amastigotes ( $2 \times 10^6 \text{ ml}^{-1}$ ) in amastigote culture medium was measured in the presence of SNAP. Results are representative of three separate experiments.

### **7.3.2 The mitochondrial membrane potential**

To assess the effect of RNI on the mitochondrial membrane potential, uptake of Rh123 was measured using a Fluorescence Activated Cell Sorter (FACS). As Rh123 accumulates in the mitochondrion, it initially leads to more fluorescence per parasite, but at higher concentrations, it auto-quenches, and more Rh123 uptake can lead to less fluorescence.

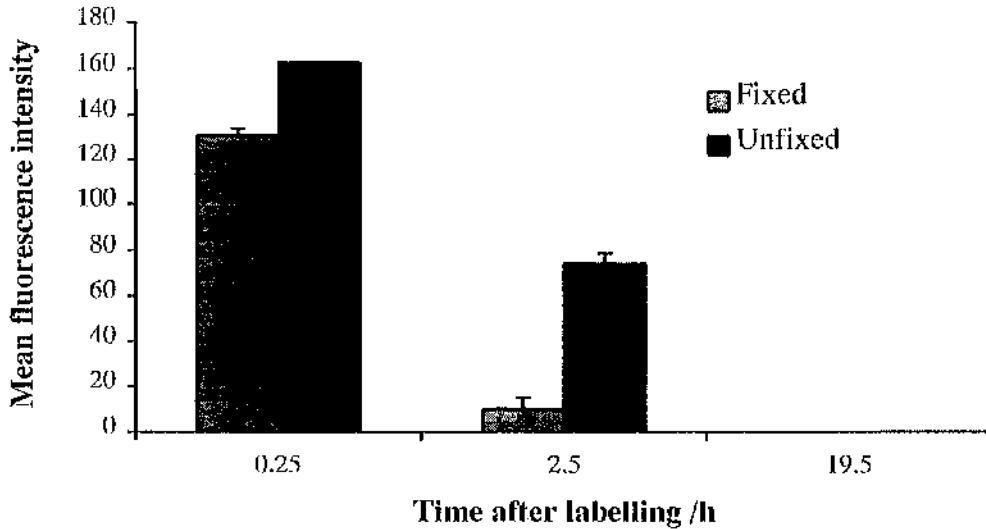
For safety considerations, it would have been preferable to fix the amastigotes before using the FACS. Rh123 in some cells can be retained for up to 24 h after fixation (217), but it is not chemically attachable to any mitochondrial components, so in most systems it leaches out quickly. It was therefore necessary to assess whether the dye was fixable in amastigotes.

#### **7.3.2.1 Development of the assay:**

##### **7.3.2.1.1 Assessment of the effect of fixation**

Amastigotes labelled with Rh123 before running through the FACS lose a significant amount of the label by 25 min compared to live amastigotes (Figure 7.6). After 2½ hours, most of the label has leached out of amastigotes. It is therefore not sensible to fix amastigotes after labelling with Rh123 before FACS analysis.

**Figure 7.6: The effect of fixation on Rh123 retention by amastigotes.**



Amastigotes ( $2 \times 10^6 \text{ ml}^{-1}$ ) were incubated in  $13 \mu\text{M}$  Rh123 for 15 min at  $32^\circ\text{C}$ . They were then spun at  $1600g$  5 min RT, and resuspended in FACSFlo<sup>w</sup> with or without 1% paraformaldehyde. Clumps of amastigotes were broken up by pushing the suspension three times through a  $26G^{3/8}$  needle, and 2000 particles were collected on the FACS. Results are expressed as the mean  $\pm$  SEM.

#### **7.3.2.1.2 Time course of Rh123 uptake by axenic amastigotes.**

13  $\mu\text{M}$  Rh123 is taken up by amastigotes over 21 min. A reading above background was obtainable after six minutes, which means we were able to assess mitochondrial function over a six minute period (Figure 7.7).

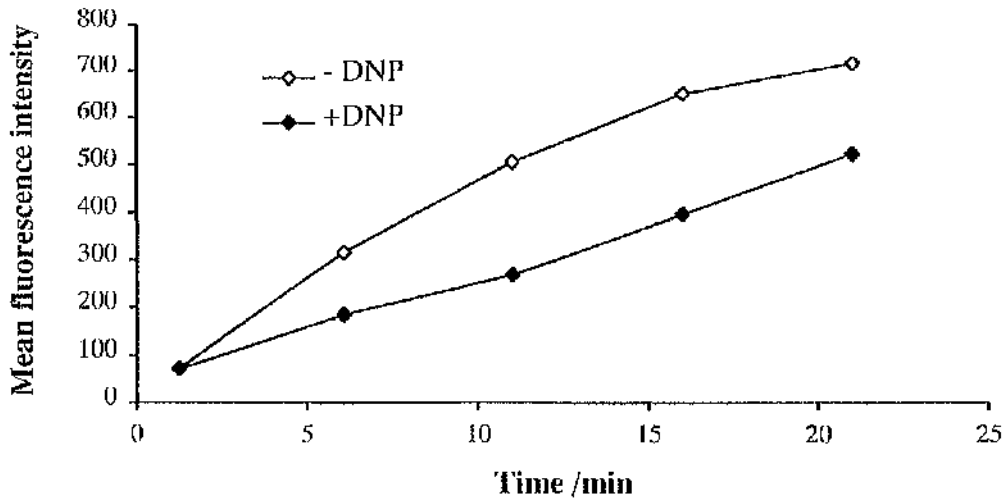
The fluorescence increase was not linear over the 20 min, presumably because of auto-quenching by Rh123, and possibly because the postulated efflux pump may have removed the Rh123 more efficiently at higher concentrations.

A six minute uptake of Rh123 is in the range in which more Rh123 uptake would lead to more fluorescence, while an inhibition of Rh123 uptake would lead to less fluorescence.

#### **7.3.2.2 Concentration curve of the effect of DNP**

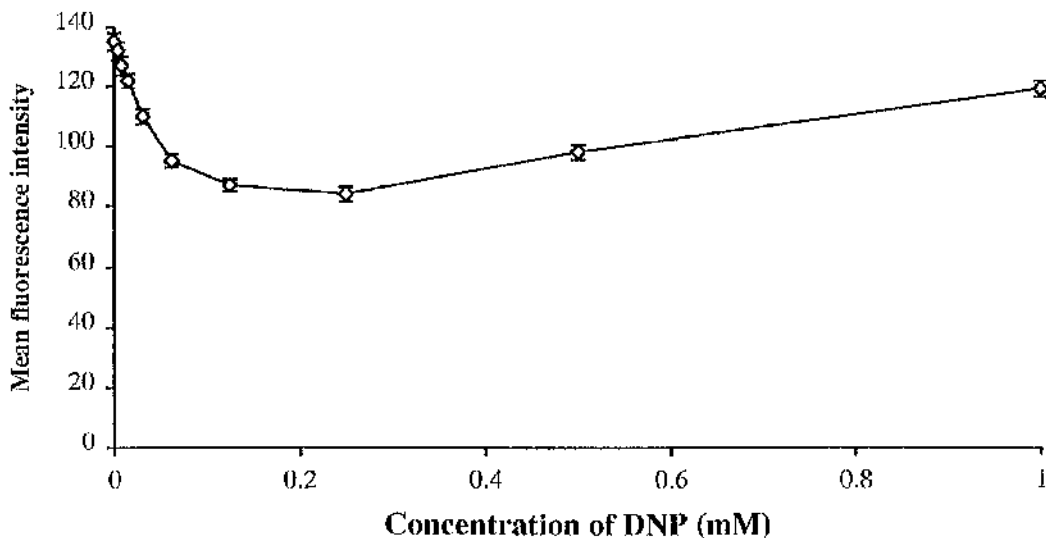
Below 100  $\mu\text{M}$ , DNP inhibited Rh123 uptake. Between 100  $\mu\text{M}$  and 1 mM DNP, however, Rh123 uptake increased (Figure 7.8). 200  $\mu\text{M}$  DNP was therefore used as a positive control for inhibition of Rh123 uptake.

Figure 7.7: Uptake of Rh123 over time.



Amastigotes ( $2 \times 10^6 \text{ ml}^{-1}$ ) were cultured in  $13 \mu\text{M}$  Rh123 with or without  $2 \text{ mM}$  DNP. At each time point,  $20 \mu\text{l}$  of the sample was placed in  $1 \text{ ml}$  FACSFlow, and 2000 particles were collected on the FACS.

**Figure 7.8: Concentration curve of the effect of DNP on Rh123 uptake.**



Amastigotes ( $2 \times 10^6 \text{ ml}^{-1}$ ) were incubated for 6 min in DNP containing  $13 \mu\text{M}$  Rh123. A sample of  $20 \mu\text{l}$  was then mixed with  $980 \mu\text{l}$  FACSFlow, and collected on the FACS. Results are expressed as the mean  $\pm$  SEM, and are representative of three separate experiments.

### 7.3.2.3 The effect of RNI on Rh123 uptake.

Having determined the conditions that would enable an assessment of the effect of RNI on Rh123 uptake, the time course and the concentration at which RNI had their effect on Rh123 uptake by *L. m. mexicana* amastigotes was investigated.

#### 7.3.2.3.1 Time course of inhibition

RNI at 100  $\mu\text{M}$  HONO inhibit the uptake of Rh123 very quickly (Figure 7.9). The first time point shown represents an exposure of six minutes to RNI, and already uptake is inhibited to the same extent as 200  $\mu\text{M}$  DNP. For the rest of the exposure to RNI (up to 7.1 h), the membrane potential remains low, indicating that the amastigotes do not find a way of combating the inhibition.

The mean fluorescence of control amastigotes increases with the amount of time that they are cultured before being exposed to Rh123 (Figure 7.9). This is probably due to the amastigotes clumping during the culture. The clumps of amastigotes were only broken up before the initial culture, and not just before they were exposed to Rh123.

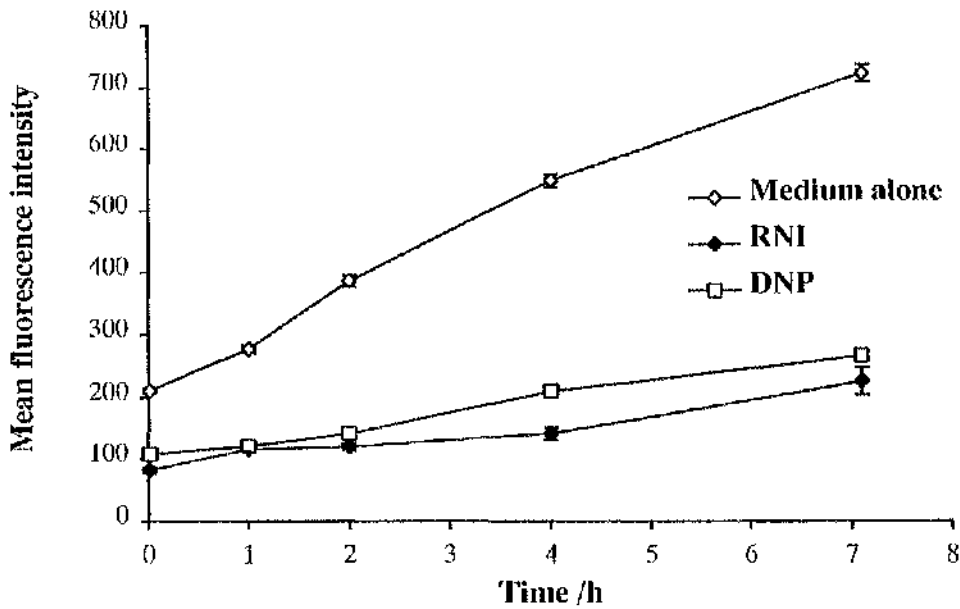
This hypothesis was tested by dividing the forward and side scatter region which contains amastigotes into four different regions of increasing size (Figure 7.10), and measuring the mean fluorescence per particle in each region (Figure 7.11(a)). Except in the case of the largest region, the mean fluorescence per particle in each region hardly changed. The mean fluorescence of the largest particle size would be expected to increase as the mean particle size increased.

The number of particles in each region, however, did change over the time course of the experiment (Figure 7.11(b)). On average, the particles increased in size. Amastigotes did not get bigger if observed under a microscope, but they were clumping. This suggested that the increase in particle size was probably due to clumping of amastigotes that remained the same size.

RNI inhibited the Rh123 uptake by all particle sizes (Figure 7.12), and so was not preventing the increase in fluorescence simply by stopping the amastigotes clumping.

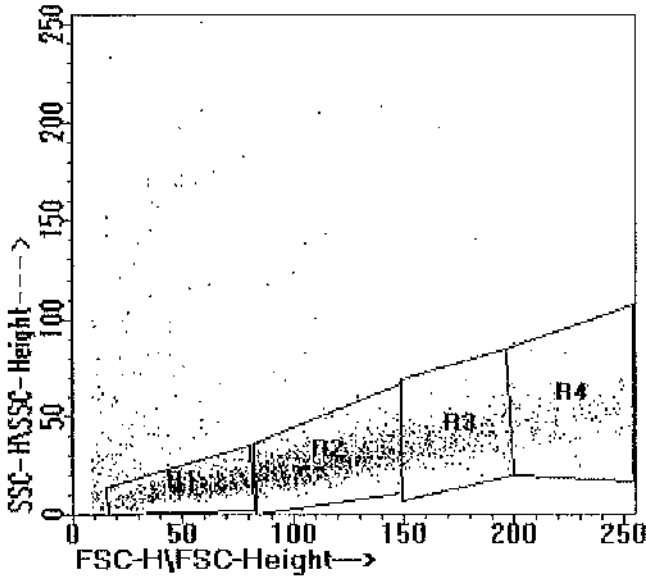
RNI therefore inhibits Rh123 uptake by axenic amastigotes quickly. The fast rate of inhibition contrasts markedly with the time course of killing of several hours seen in Figure 7.21 and in Figure 5.4.

**Figure 7.9: Time course of the effect of RNI on Rh123 uptake.**



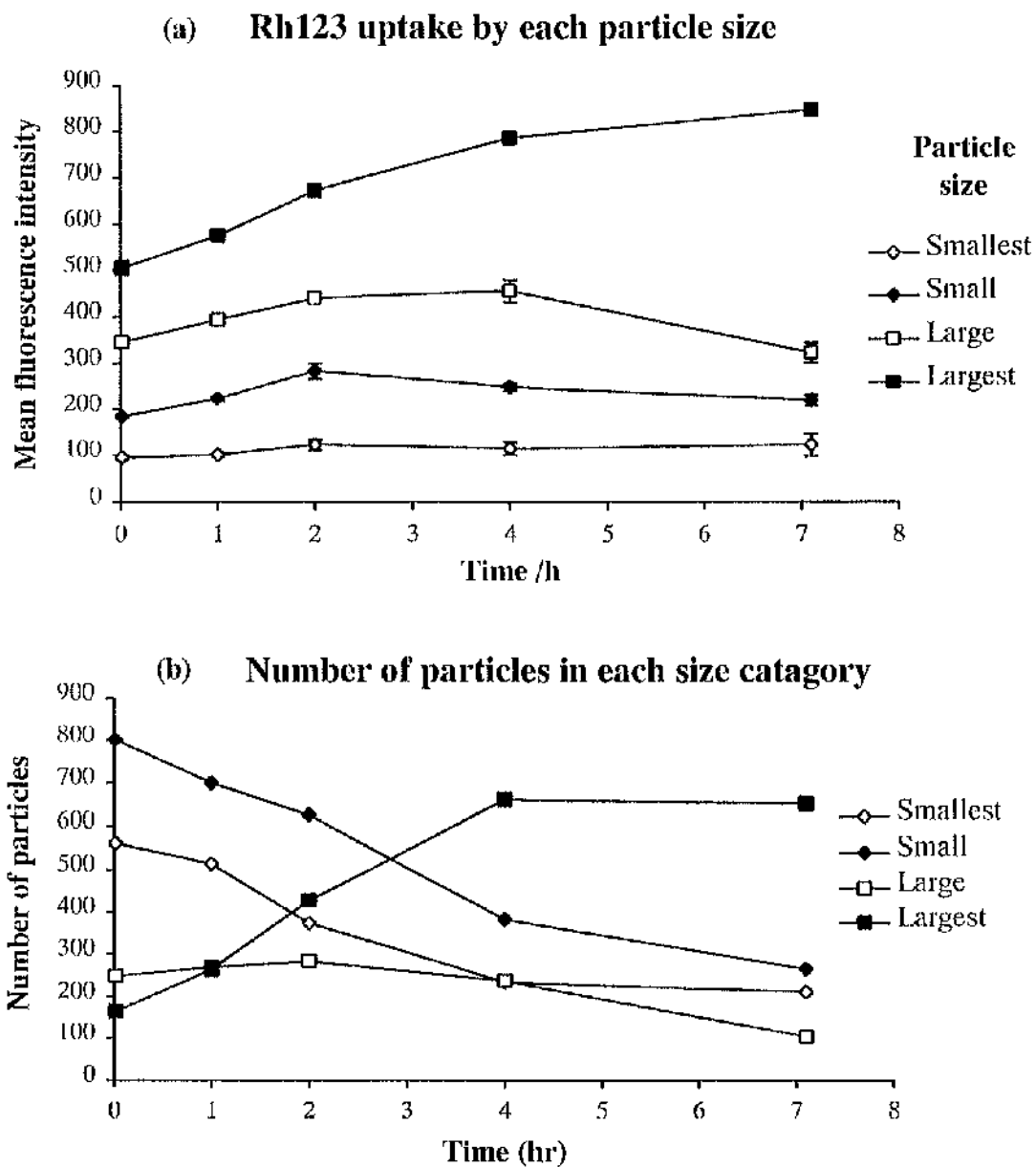
Amastigotes ( $2 \times 10^6 \text{ ml}^{-1}$ ) were cultured in medium containing either RNI (100  $\mu\text{M}$  HONO), 200  $\mu\text{M}$  DNP, or neither. At each time point, a sample was mixed with Rh123 (final concentration 13  $\mu\text{M}$ ) also containing RNI, DNP or neither, and incubated for 6 min  $32^\circ\text{C}$ . 20  $\mu\text{l}$  of this mixture was mixed with FACSFlow, and 2000 particles were collected on the FACS. Results are expressed as the mean  $\pm$  SEM and are representative of three separate experiments.

**Figure 7.10: Arbitrary division of particles into four sizes.**



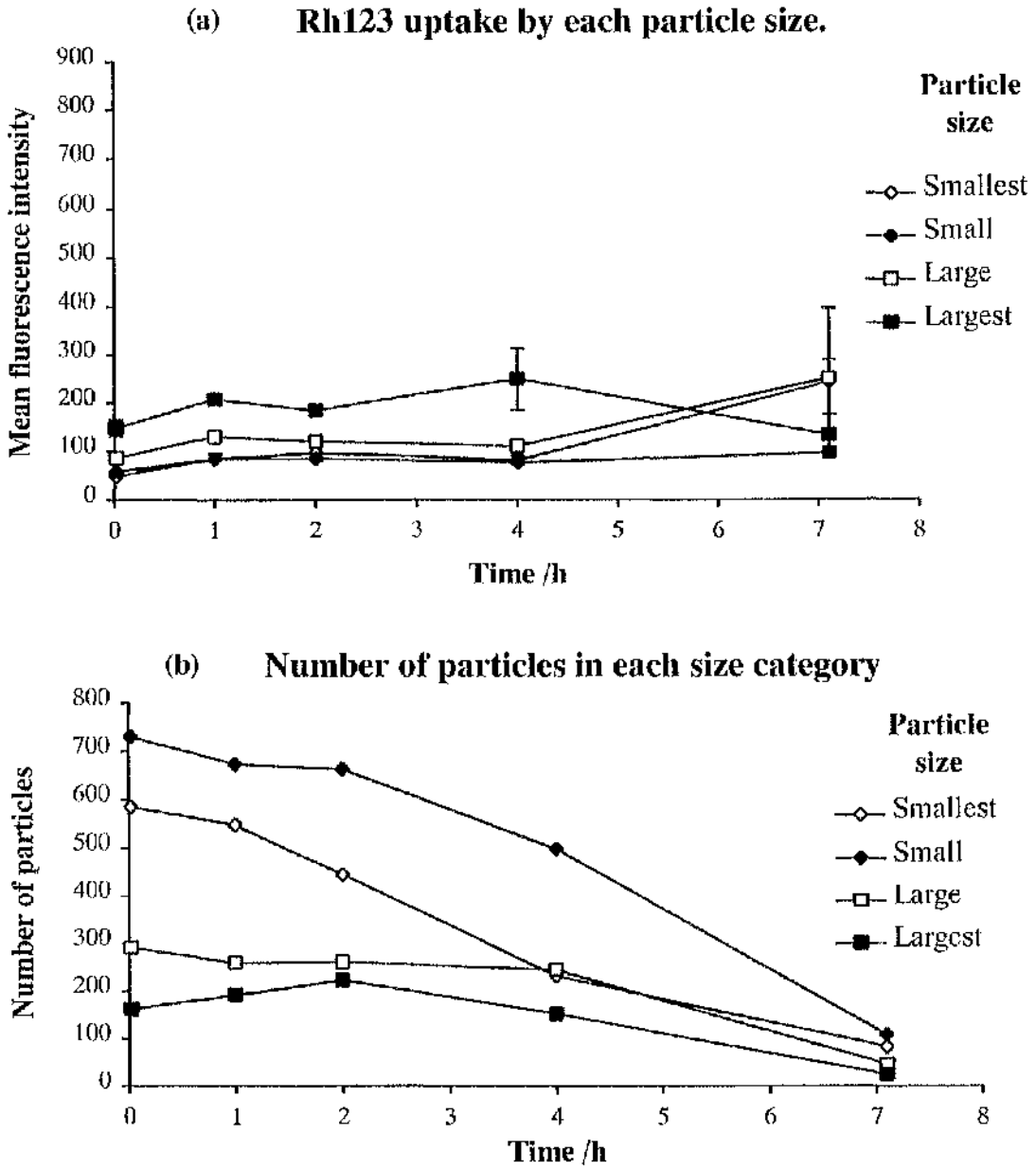
A dot plot showing the forward and side scatter data from control amastigotes after a 6 min incubation in Rh123 from Figure 7.9. Forward scatter increases with increasing particle size, while side scatter increases with increasing refractive index of each particle. The four regions were chosen arbitrarily, and were of increasing size (R1 - Smallest, R2 - Small, R3 - Large, R4 - Largest).

**Figure 7.11: Analysis of the time course of Rh123 uptake in terms of the different sizes of particles.**



Data from control treatment in Figure 7.9 reanalysed taking into account the four region sizes defined in Figure 7.10.

Figure 7.12: The effect of RNI on Rh123 uptake by amastigotes.



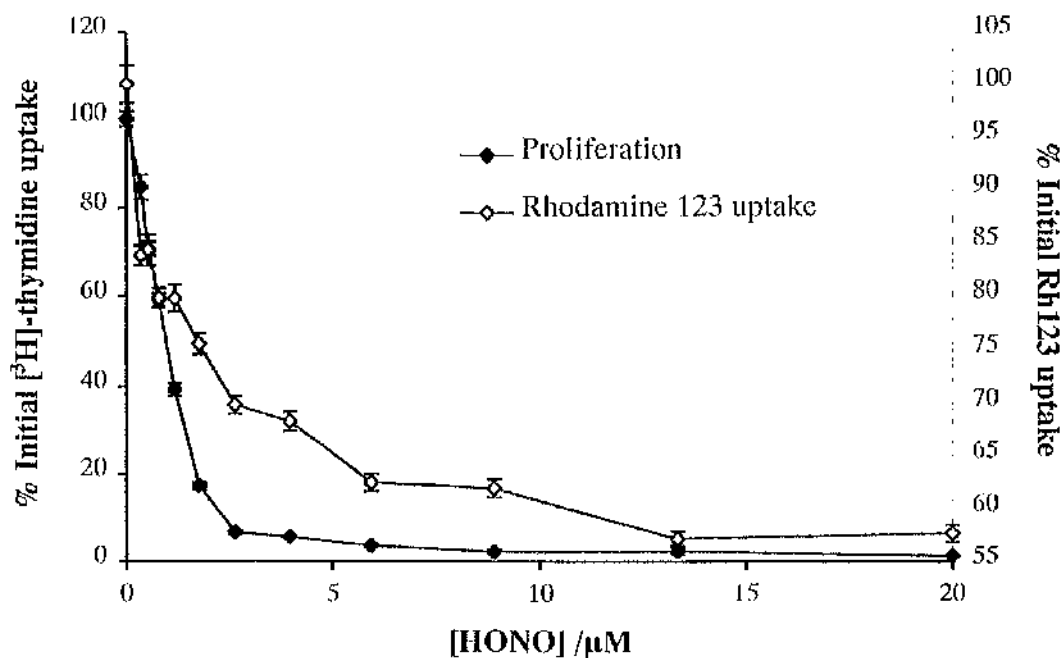
Data from RNI treatment in Figure 7.9 reanalysed taking into account the four region sizes defined in Figure 7.10.

### **7.3.2.3.2 Concentration curve of RNI inhibition of Rh123 uptake.**

The concentration of RNI required to inhibit Rh123 uptake was similar to the concentration required to inhibit [<sup>3</sup>H]-thymidine uptake by amastigotes (Figure 7.13). When compared to the concentrations required to deglycosylate GPIs or to damage DNA (Chapter 6), these concentrations are very similar to the toxic concentrations of RNI.

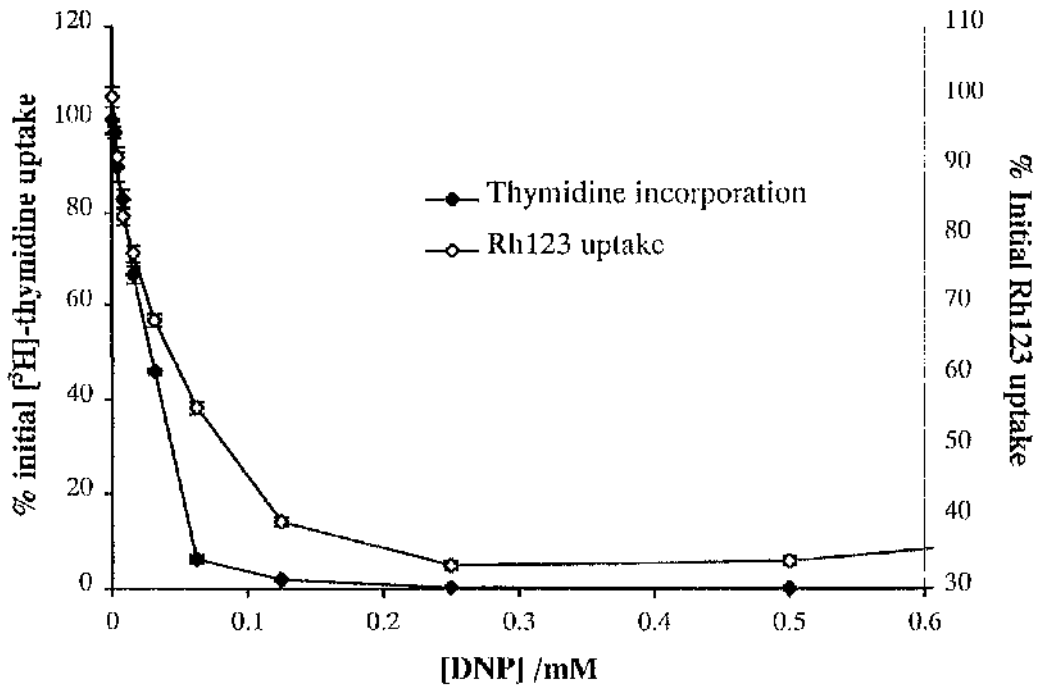
The inhibition of Rh123 uptake by DNP is also very similar to the concentration required for DNP to inhibit [<sup>3</sup>H]-thymidine uptake (Figure 7.14). This suggests that the inhibition of the mitochondrial membrane potential alone can account for the toxicity of RNI.

Figure 7.13: Comparison of the effect of RNI on Rh123 and [<sup>3</sup>H]-thymidine uptake.



[<sup>3</sup>H]-thymidine uptake by amastigotes ( $2 \times 10^6 \text{ ml}^{-1}$ ) was assayed over 24 h in the presence of RNI, and Rh123 ( $13 \mu\text{M}$ ) uptake was assayed over 6 min. Results are expressed as the mean  $\pm$  SEM, and are representative of two separate experiments.

Figure 7.14: The effect of DNP on Rh123 and [<sup>3</sup>H]-thymidine uptake.



[<sup>3</sup>H]-thymidine uptake by amastigotes ( $2 \times 10^6 \text{ ml}^{-1}$ ) was assayed over 24 h in the presence of DNP, and Rh123 ( $13 \mu\text{M}$ ) uptake was assayed over 6 min. Results are expressed as the mean  $\pm$  SEM, and are representative of two separate experiments.

## 7.4 The effect of RNI on the concentration of ATP.

*L. m. mexicana* amastigotes normally live in a subcutaneous lesion that has very little vascularisation. This might suggest that they normally live in very low oxygen tensions, and may be able to survive on ATP produced anaerobically. To test whether RNI attack does actually lead to a decrease in the amount of energy cytoplasmically available, we measured the concentration of ATP using luminescence from firefly luciferase.

Firefly luciferase cannot use dATP, NADH or NADPH as substrates, so the measurements here represent changes in the concentration of ATP alone.

Neutralised TCA lysates were prepared by mixing 100  $\mu$ l of the sample with 900  $\mu$ l of 5.56 % TCA, spinning at 12 000g for 20 min at 4°C, and neutralising 500  $\mu$ l of the supernatant with 51-55  $\mu$ l of 3 M KOH/0.4 M Tris/0.3 M KCl.

### 7.4.1 Development of the assay system

The amount of light emitted from luciferase in the presence of  $10^{-15}$  M ATP was detectable (Table 7.1). However, the luminometer reading decayed significantly with time (Figure 7.15), so it was necessary to make all measurements of the concentration of ATP at exactly the same time after mixing the samples. The period of 30 s to 40 s after mixing was therefore chosen for convenience.

It was also possible to construct a standard curve of ATP in amastigote culture medium under conditions which mimicked those for treatment of amastigotes with RNI (Figure 7.16). This revealed that the foetal calf serum did not contain sufficient ATP to disrupt the measurement nor did it contain a highly active ATPase. It also showed that the

high salt content of the final ATP preparation did not inhibit luciferase sufficiently to prevent the assay working.

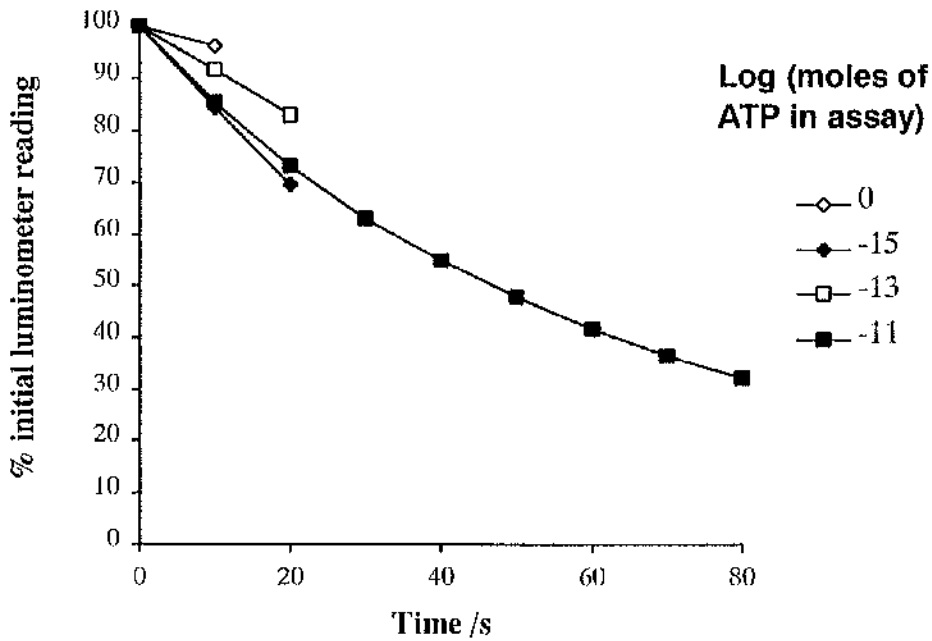
It was possible to detect the concentrations of ATP present in a culture of amastigotes at  $2 \times 10^7 \text{ ml}^{-1}$  (Figure 7.17). The light reading was sufficiently high at this concentration of amastigotes to allow a lower concentration of amastigotes to be used in later experiments. The luminometer reading did not change as quickly in this experiment as it did in water, probably because the higher salt concentration of the neutralised precipitate partially inhibited the luciferase.

**Table 7.1: Determination of the detectable concentration of ATP.**

<b>Amount of ATP in assay /moles</b>	<b>Luminometer reading</b>
0	-0.26
$10^{-15}$	0.89
$10^{-13}$	38.05
$10^{-11}$	8308

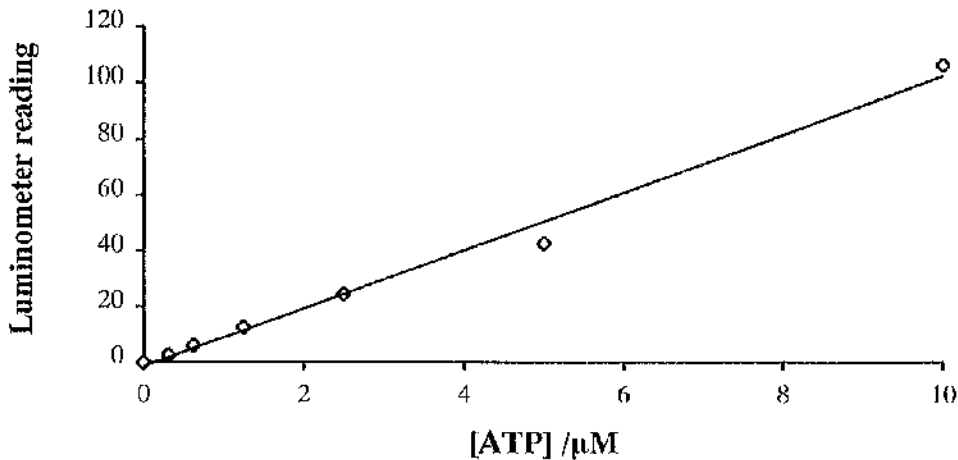
ATP was dissolved in water to the concentrations shown, 100  $\mu$ l was mixed with 100  $\mu$ l firefly luciferase, and the luminescence read at 25°C.

Figure 7.15: The luminometer reading decays with time.



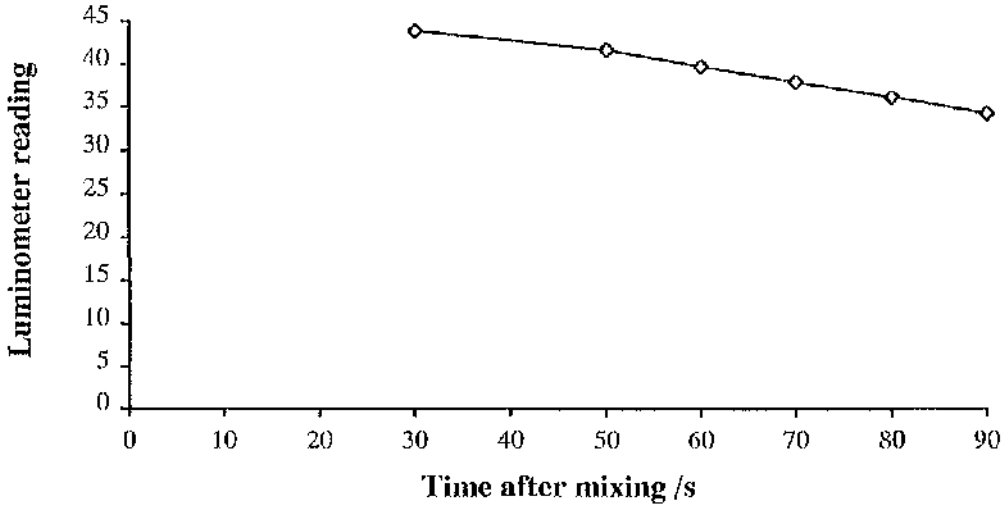
The samples from Table 7.1 were followed over time at 25°C.

Figure 7.16: Construction of a standard curve of ATP in SDM + FCS.



A standard curve of ATP was constructed in amastigote culture medium. The luminescence of a neutralised TCA lysate was measured at 25°C. Results are representative of five separate experiments.

**Figure 7.17: Detection of ATP in  $10^6$  amastigotes.**



The luminescence of a neutralised TCA lysate of amastigotes ( $2 \times 10^7 \text{ ml}^{-1}$ ) was measured at  $25^\circ\text{C}$ .

## **7.4.2 The effect of RNI on the concentration of ATP in amastigotes.**

### **7.4.2.1 Time course**

RNI decrease the concentration of ATP in amastigotes very quickly (Figure 7.18). The parasites then take up to a few hours to die. This suggests that the amastigotes do not have an alternative energy source to which they can turn once their mitochondrion has been inhibited.

The first time point shown in Figure 7.18 is 16 s. In this time, the concentration of ATP has fallen 50%, illustrating the extremely fast effect of RNI on the concentration of ATP.

### **7.4.2.2 The effect of increasing the concentration of RNI on the concentration of ATP.**

In Chapter 5 more RNI were shown to kill amastigotes faster. Figure 7.13 suggests that inhibition of Rh123 uptake was complete by a concentration of RNI of approximately 20  $\mu\text{M}$  HONO, whereas the rate of killing of amastigotes continues to increase even up to 800  $\mu\text{M}$  HONO (Figure 5.4). This may suggest that the energy production systems of amastigotes were still partially functional at these higher concentrations, but that the function was not detectable by Rh123 uptake.

This appears to be the case. Increasing the concentration of RNI causes the ATP levels to drop faster (Figure 7.19), suggesting that the ATP production system is inhibited still further at these higher concentrations.

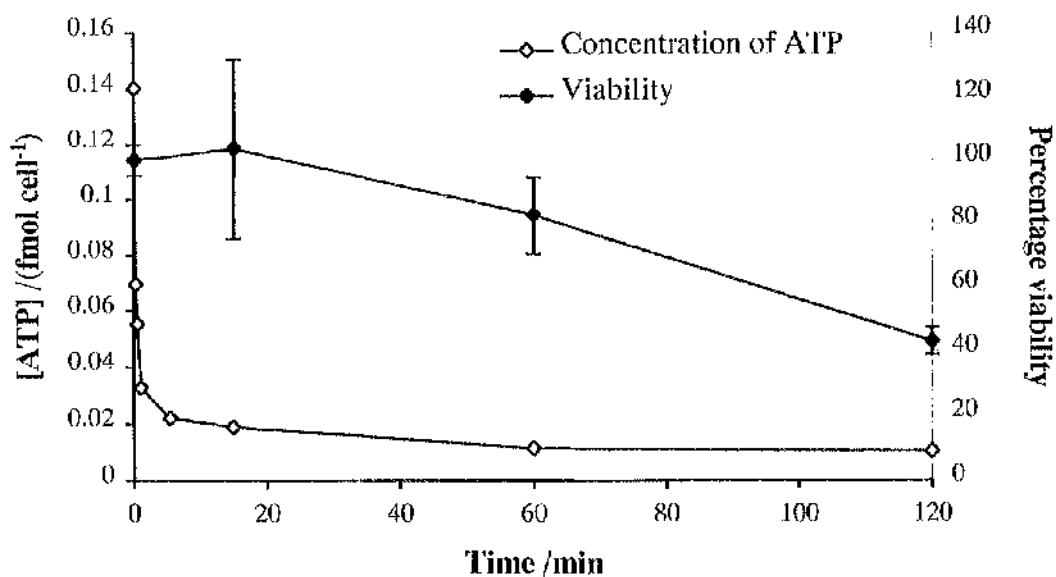
In addition, this provides evidence that it is an ATP production system, and not an ATP utilisation system that is the primary target of RNI. It also suggests that the ATP production system (be it the mitochondrion or glycolysis) does not need to be completely inhibited to kill amastigotes, since an incomplete inhibition of ATP production still kills the amastigotes, albeit more slowly.

Increasing the concentration of DNP above that which inhibited Rh123 uptake also led to a faster death (Figure 7.20). This suggests that partial inhibition of the mitochondrial membrane potential alone gradually leads to a depletion of ATP concentration and finally death. Inhibition of the mitochondrion by DNP leads to a fast drop in ATP concentrations (Figure 7.21).

The toxicity of RNI can therefore still be accounted for by the inhibition of the mitochondrion.

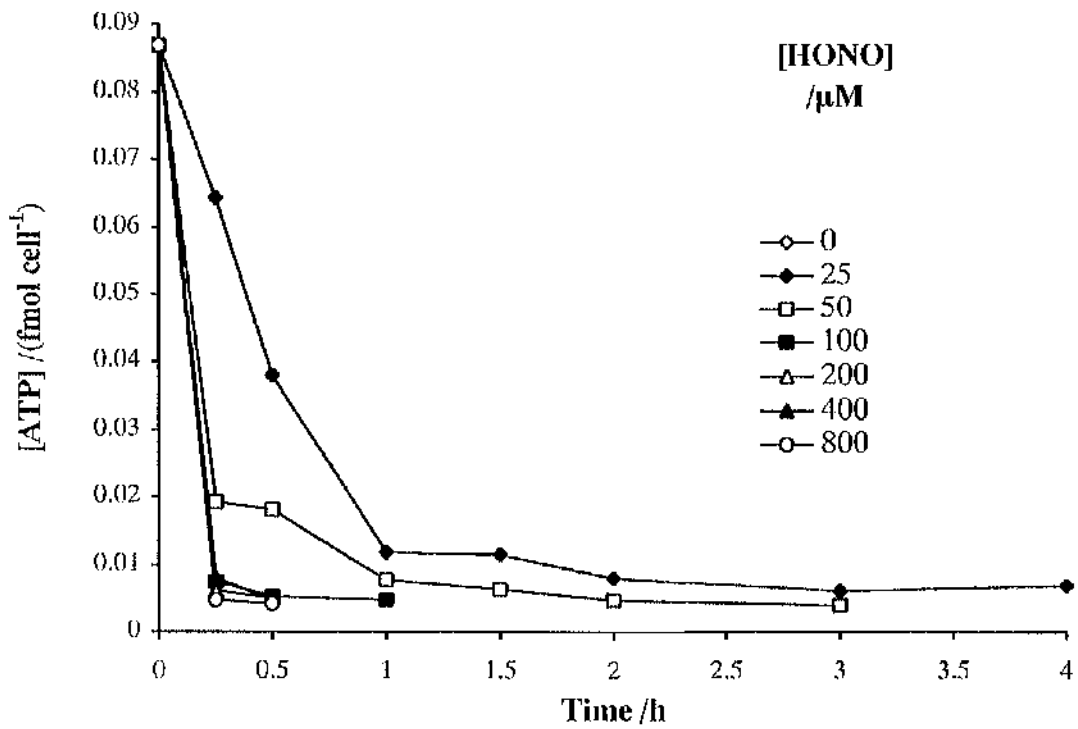
Rh123 uptake is not a perfect assay for detection of the inhibition of the mitochondrial membrane potential. A total inhibition of Rh123 uptake was observed at 100  $\mu\text{M}$  DNP and at RNI concentrations of 20  $\mu\text{M}$  HONO (Figure 7.13 and Figure 7.14). Increasing the concentration of both of these toxins above those levels speeds up death, indicating that the mitochondrion may be affected still further above the concentrations where inhibition could be detected by Rh123 uptake (Figure 7.20 and Figure 7.21).

**Figure 7.18: Time course of the effect of RNI on the concentration of ATP in amastigotes.**



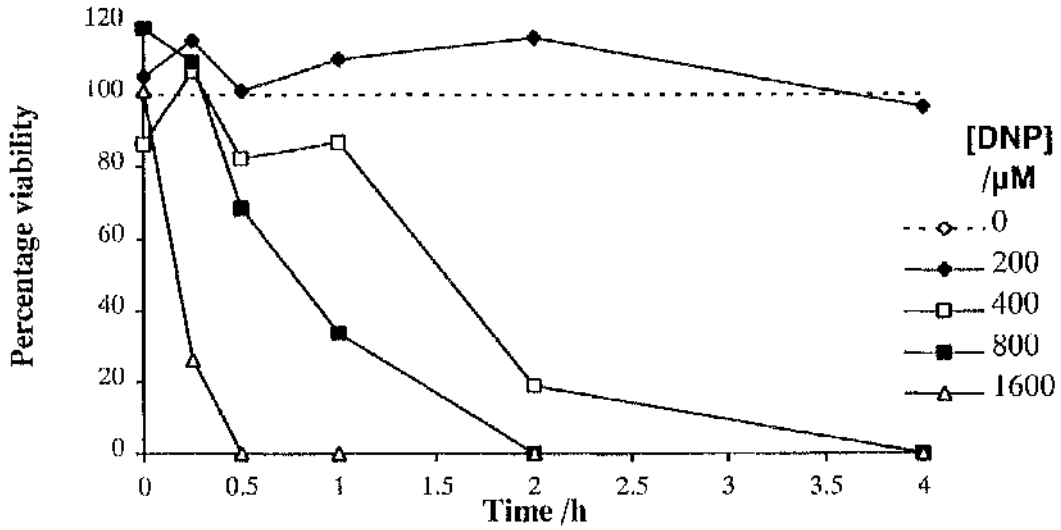
Amastigotes ( $4 \times 10^6 \text{ ml}^{-1}$ ) were treated with RNI ( $100 \mu\text{M HONO}$ ) for up to 2 h. the concentration of ATP was measured by luminescence, and percentage viability by transformation efficiency. Results are expressed as the mean ( $\pm$  SEM  $n=4$  for the viability measurements), and are representative of three separate experiments.

**Figure 7.19:** The effect of different concentrations of RNI on the concentration of ATP.



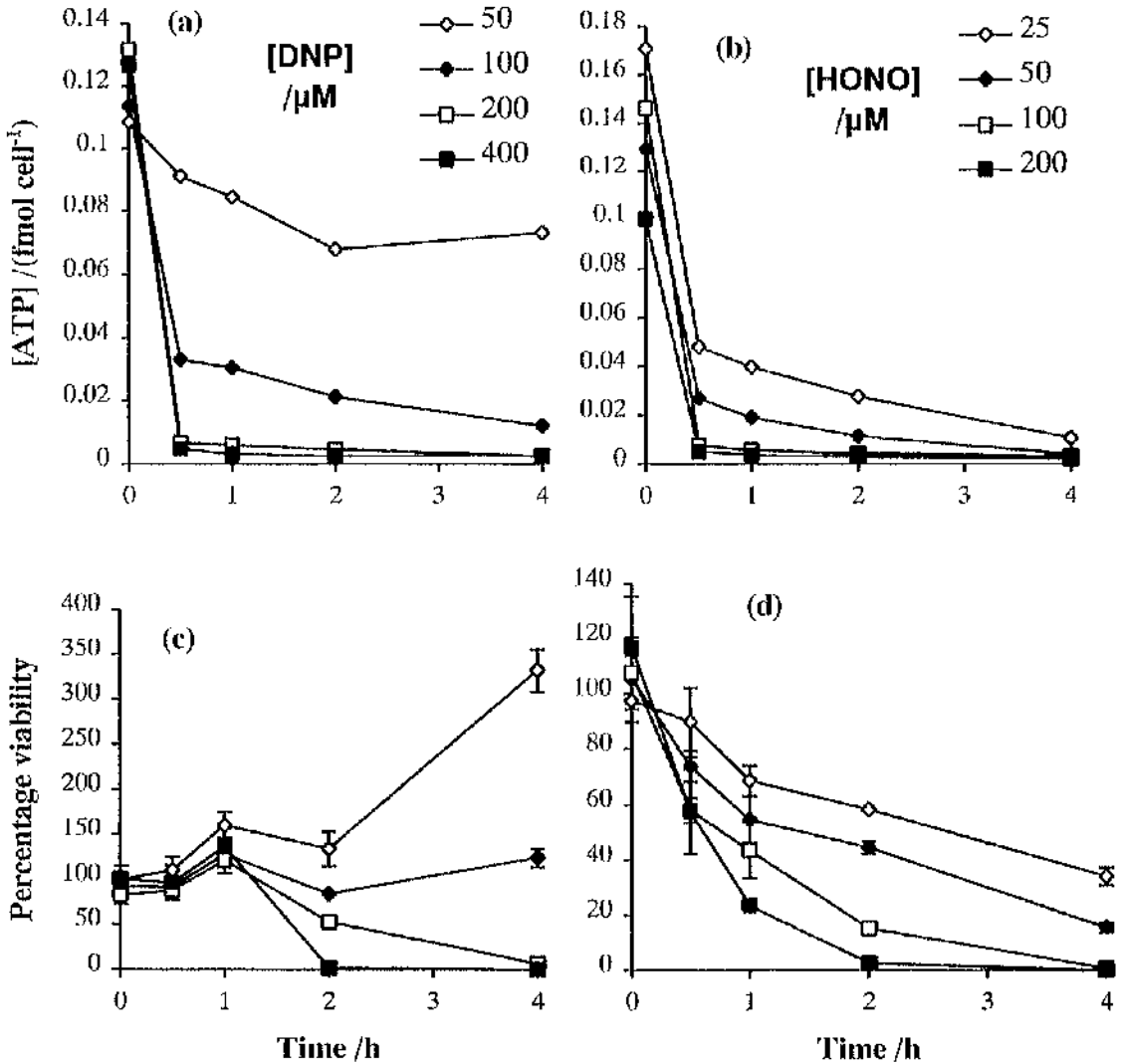
Amastigotes ( $4 \times 10^6 \text{ ml}^{-1}$ ) were cultured with RNI for up to 4 h. At each time point, the concentration of ATP was measured by luminometry of a TCA lysate.

Figure 7.20: Higher concentrations of DNP kill amastigotes faster.



Amastigotes ( $2 \times 10^6 \text{ ml}^{-1}$ ) were cultured with DNP for up to 4 h in amastigote culture medium. At each time point, viability was assayed by transformation efficiency.

**Figure 7.21: The effect of different concentrations of DNP on amastigote viability and ATP concentrations.**



Amastigotes ( $4 \times 10^6 \text{ ml}^{-1}$ ) were treated with RNI or DNP for up to 4 h in amastigote culture medium. At each time point viability was assayed by transformation efficiency, and the concentration of ATP in a neutralised TCA lysate was measured by luminometry.

## 7.5 Discussion

Axenicly grown amastigotes are dependent upon energy produced by their mitochondrion, since they are susceptible to several mitochondrial toxins - sodium azide (Figure 7.1), FCCP (Figure 7.2) and DNP (Figure 7.3).

The toxicity of RNI on amastigotes correlates with inhibition of the mitochondrial function (Figure 7.13). The rate at which oxygen was consumed, and the amount of uptake of Rh123 are both measures of the function of the mitochondrion. Both of these were inhibited by toxic concentrations of RNI (Figure 7.5 and Figure 7.13)

RNI produced from SNAP inhibit oxygen consumption by amastigotes. This suggests that the electron transport chain is inhibited. Many of the RNI can rapidly cycle between a protonated neutral membrane-permeable form and an unprotonated ionic form (eg  $\text{NO}_2^-$  and  $\text{HONO}$ ,  $\text{NO}^-$  and  $\text{HNO}$ ,  $\text{ONOO}^-$  and  $\text{HONOO}$ ), which means that it is conceivable that RNI were inhibiting the mitochondrion by uncoupling the membrane. However, since oxygen uptake was inhibited by RNI, the inhibition of the electron transport chain is also probably a significant factor in the inhibition of ATP synthesis by RNI.

Inhibition of oxygen consumption by SNAP (Figure 7.5), and inhibition of Rh123 uptake by acidified sodium nitrite (Figure 7.13) indicates that the mitochondrion can be inhibited by RNI produced from a variety of sources. Therefore the toxic mechanism I have been studying is not peculiar to the acidified nitrite system.

SNAP uses up oxygen in the medium (Figure 7.5), and it is possible that the decrease in oxygen tension may contribute to the toxicity of RNI. However, the inhibition of oxygen uptake by SNAP in our system is not due to SNAP competing for oxygen with

amastigotes, since below 1 mM SNAP, there is an overall decrease in oxygen consumption by the mixture of amastigotes and SNAP.

*In vivo*, however, the oxygen tension is likely to be much lower since the concentration of amastigotes is higher, and there is little vascularisation of the lesion. In this instance, the decrease in oxygen concentration caused by RNI may be a significant factor in RNI toxicity.

Rh123 is concentrated in the mitochondrion. This was confirmed by fluorescence microscopy in which the basket-like structure of the mitochondrion could clearly be seen. Unfortunately, since Rh123 cannot be fixed in amastigotes, it was not possible to photograph this phenomenon.

Uptake of 13  $\mu$ M Rh123 for 6 min by amastigotes is in the range where more Rh123 uptake leads to more fluorescence (Figure 7.7). At low concentrations of RNI, Rh123 fluorescence does not increase. It is therefore unlikely that RNI are increasing the uptake of Rh123 to such an extent that auto-quenching by Rh123 causes the decrease in fluorescence. So the inhibition of fluorescence by RNI is due to an inhibition of Rh123 uptake, probably because of an inhibition of the mitochondrial membrane potential.

Inhibition of both Rh123 uptake and the decrease in the concentration of ATP caused by RNI and DNP is very quick (Figure 7.9, Figure 7.18, and Figure 7.21). This contrasts with the slow killing by RNI, suggesting that the amastigotes can survive for up to a few hours with low levels of ATP.

Amastigotes do not have another energy source from which they can produce enough ATP to rescue themselves after their mitochondrion has been inhibited (Figure

7.18 and Figure 7.19). If they did, then they would be able to maintain their ATP levels for longer during treatment with RNI.

Amastigotes are not able to maintain their ATP levels if their mitochondrion has been uncoupled with DNP (Figure 7.21). This suggests that they are dependent on their mitochondrion for production of enough ATP to survive.

The time course of killing of amastigotes by RNI and DNP is similar - in the range of a few hours (Figure 7.21). There is a quick inhibition of the mitochondrion, and a fast drop in ATP levels, followed by slower death. This suggests that if the only thing that RNI did was to decrease the mitochondrial membrane potential, then the same kinetics of killing would be seen as were presented here.

The mechanism of RNI inhibition of mitochondrial function in amastigotes is open for speculation. However, in organisms as diverse as *E. coli* and mammalian cells, RNI inhibit the mitochondrion by ligation of nitric oxide to the iron in the iron-sulphur centres of the cytochromes (26,221,222). The inhibition of the cytochromes is fast and reversible.

In amastigotes, the toxicity of RNI is also fast and reversible and involves inhibition of electron transport flux. It is reversible since washing off the RNI allows the amastigotes to transform to promastigotes. The cytochromes are evolutionarily some of the best conserved proteins, and the iron-sulphur centres are open to ligation in the same way as *E. coli* and mammalian cells. The toxic mechanism is therefore probably the same in amastigotes as it is in these other systems.

In conclusion, the mitochondrion is an important early target of RNI.

## **8. General discussion**

The results presented in this thesis have provided additional information on viability assays for *L. m. mexicana* amastigotes, macrophage toxicity to amastigotes, the interaction of RNI with other macrophage defence mechanisms, the response of amastigotes to RNI, and the *in vitro* targets of RNI. However, the main thrust of the results is that the most likely mechanism for RNI killing *L. m. mexicana* amastigotes is the inhibition of the mitochondrion, and not direct damage to DNA or to GIPLs. The relevance of the results to these different processes is now discussed.

### 8.1 Viability assays.

The fact that the [<sup>3</sup>H]-thymidine assay worked for *L. m. mexicana* amastigotes indicates that axenic amastigotes do not synthesise all of the pyrimidine used in DNA synthesis. Some eukaryotic protozoa, eg *Plasmodium* species, live in an environment with such a low pyrimidine concentration that they rely totally on synthesis of their own pyrimidines, and have lost the thymidine uptake pathways (223). However, *Leishmania* promastigotes have retained the ability to salvage pyrimidines as well as synthesise them *de novo*, and although little is known about amastigote pyrimidine metabolism, they do contain at least some of the necessary enzymes for synthesis as well as salvage (244,245).

However, the ability of *L. m. mexicana* amastigotes to take up thymidine is poor compared to mammalian cells and *E. coli*, since incubation of the parasite for 24 h in 1  $\mu$ Ci [<sup>3</sup>H]-thymidine was required to get between  $1 \times 10^3$  and  $20 \times 10^3$  cpm incorporated (Figure 3.1). This compares with the standard protocol of a 6 h pulse of [<sup>3</sup>H]-thymidine for immune system cells to get up to  $300 \times 10^3$  cpm incorporated (see for example (224)). The parasites therefore may rely more heavily on synthesis rather than uptake for their thymidine.

It is possible that variations in the rate of pyrimidine synthesis were responsible for the variability in the [ $^3\text{H}$ ]-thymidine uptake of amastigotes. The [ $^3\text{H}$ ]-thymidine uptake assay may not therefore directly relate to amastigote proliferation, but may also reflect changes in the ratio of *de novo* pyrimidine synthesis to pyrimidine uptake.

The [ $^3\text{H}$ ]-thymidine assay also does not distinguish between chromosomal DNA and kinetoplast DNA. The kinetoplast is an unusually large amount of mitochondrial DNA, composed of minicircles and maxicircles (5). The amount of DNA in the kinetoplast is variable (225), and may account for at least some of the DNA synthesis detected by the assay.

The [ $^3\text{H}$ ]-thymidine assay also does not distinguish between DNA repair and *de novo* DNA synthesis. Since the nick translation reaction revealed that the protocol for labelling mammalian cell DNA labelled control parasite DNA extremely efficiently (Figure 6.4), it is possible that amastigote DNA contains many nicks or double strand breaks in it. This being so, DNA repair may account for much of the [ $^3\text{H}$ ]-thymidine taken up by amastigotes.

Despite these *caveats*, toxicity measured by the [ $^3\text{H}$ ]-thymidine assay occurs in the same concentration range of RNI as toxicity measured by transformation efficiency (Figure 5.2). Hence it is an effective assay for the detection of RNI toxicity. However, it is not necessarily effective for other drugs. For instance, a drug that stimulated *de novo* pyrimidine synthesis may decrease readings from the [ $^3\text{H}$ ]-thymidine assay, but increase the rate of synthesis of DNA, and hence increase parasite growth.

The transformation assay produced very variable results in terms of numbers of promastigotes produced per amastigote between experiments. However, within each experiment, the efficiency of transformation between replicates was similar, indicating

that different treatments could reasonably be compared within each experiment. In the experiments presented here, the final promastigote concentration after transformation never exceeded  $2 \times 10^7 \text{ ml}^{-1}$ , which means that the promastigotes had never reached the top end of the assay. Thus the assay was suitable for measuring the viability of the parasites within the concentrations at which we were working.

## 8.2 J774 toxicity to amastigotes.

J774 cells are able to kill amastigotes by an L-arginine dependent mechanism (Figure 5.1). This mechanism is not the inhibition of uptake of other cationic amino acids, since the effects of L-NMMA were reversible by the addition of excess L-arginine. Nor was the mechanism likely to be the production of  $\text{H}_2\text{O}_2$ , since L-NMMA does not inhibit the oxidative burst (81). The toxicity, however, did correlate with the production of RNI.

There are other L-arginine dependent killing mechanisms, though. For instance, lysosomes contain short peptides called defensins (189). These molecules are similar in structure to bacterial toxin molecules, and are present at extremely high concentrations in lysosomes ( $20\text{-}100 \text{ mg ml}^{-1}$ ). They are rich in arginine residues, and the positive charge provided by arginine in the sequence is essential to their function. A positive charge on arginine residues is maintained by protonation of the side chain, which will be preferred in acidic conditions. It is known that the maintenance of acidity is important in the toxicity of macrophages to *L. major* (130). Whether the production of defensins is inhibited by a reduction in the L-arginine concentration, or whether there is an enzyme in the regulation of their synthesis that is affected by L-NMMA is unknown, and deserves further study.

Nevertheless, it seems probable that RNI are involved since macrophages are capable of producing toxic concentrations of RNI. Attack on external targets can be

inhibited by haemoglobin (66), myoglobin/ascorbate or  $\text{FeSO}_4$ /ascorbate (153). These systems were designed to mop up RNI, and are unlikely to affect defensins. In addition, the target of macrophage toxicity is the mitochondrial complexes I and II in tumour cells (152), which is more consistent with toxicity due to RNI than due to defensins, which should affect the permeability of the outer membrane of the target rather than the mitochondrion. Since RNI are therefore a toxic mechanism of macrophages to other cells, it is plausible that they are important in macrophage toxicity to *Leishmania*.

### 8.3 The interaction of other PV toxins with RNI

RNI and  $\text{H}_2\text{O}_2$  do not affect the toxicity of one another (Figure 4.5). This is surprising since they can interact (30), and both  $\text{H}_2\text{O}_2$  and  $\text{O}_2^-$  synergised with RNI in the killing of *E. coli* (226), while  $\text{O}_2^-$  also inhibited RNI toxicity to mammalian cells (199,227). It is possible that at very different concentrations of  $\text{H}_2\text{O}_2$  or RNI, or in different media, they could react to produce enough peroxynitrite to increase the oxidative capacity, and therefore the toxicity, of RNI. However, below the toxic concentrations, neither affected the toxicity of the other to *L. m. mexicana* amastigotes, and at higher concentrations, both were toxic on their own.

ROI do not need to be added to the system for them to influence the effect of RNI. Since RNI inhibit superoxide dismutase and cytochrome c oxidase (159), RNI can lead to an increase in ROI concentration internally in the amastigote. The ROI would be produced by the partially inhibited mitochondrial electron transport chain, and would therefore be in the ideal position for the resultant peroxynitrite to oxidise the labile iron in the  $[\text{4Fe4S}]^{2+}$  clusters of the electron transport chain proteins.

Indeed, this is a more likely scenario than that in which ROI produced by the macrophage attacked the amastigote directly since superoxide and peroxynitrite are negatively charged, and cannot cross membranes to reach the parasite. Protonation in acidic pH, to neutralise their negative charge, will not allow them to cross the membrane either, since protonation catalyses their breakdown.

#### **8.4 Amastigote defence mechanisms against RNI.**

Murine macrophages can produce sufficient RNI to kill amastigotes of *L. m. mexicana* (Figure 5.1). It is interesting that despite the importance that RNI play in murine immunity to leishmaniasis, amastigotes have not developed resistance to them compared to *E. coli* (Figure 4.12) or promastigotes of *L. m. mexicana* (Figure 4.6 and Figure 4.7). This is not because it is impossible for a cell to become resistant, since *Mycobacterium intracellulare* (46), *M. avium* (50) and *Brucella abortus* (202) are not killed by RNI produced by macrophages. Culturing amastigotes in low levels of RNI for up to three days did not induce resistance (Figure 4.13), indicating that the lack of resistance is unlikely to be a temporary downregulation of expression of a resistance mechanism in BALB/c mice that are not producing much RNI (68). Axenically cultured *L. m. mexicana* amastigotes are simply susceptible to RNI.

It is possible, though, that *in vitro* cultured amastigotes are not the same as lesion amastigotes, and the time it took to assay the toxicity of RNI meant that they had sufficiently transformed to this *in vitro* form to lose their resistance to RNI. Lesion amastigotes may therefore still be resistant to RNI. In addition, to compare the susceptibility of amastigotes and promastigotes to RNI required culturing the two life cycle stages in the same medium for 24 h. This was sufficient time for promastigotes to convert to amastigotes at pH 5.5 and 32°C, and amastigotes to convert to promastigotes at

pH 6.5 and 28°C, it is possible that the experimental design meant that only the most susceptible transformation intermediates in both cultures were being compared, and not the susceptibility of true promastigotes and amastigotes.

Further reasons for believing that resistance may occur *in vivo* and not *in vitro* comes from the mechanisms by which resistance to RNI may be mediated. They could include the uptake of iron, concentration of sulphhydryl groups, or the production of a neutralising concentration of ROI. *In vivo*, if an amastigote could actively accumulate iron or sulphhydryl containing amino acids, it could become resistant to RNI. However, *in vitro*, the iron and sulphhydryl groups are already present in the medium which accounts for a much greater proportion of the volume of culture than the amastigotes themselves. Thus the accumulation of sulphhydryl groups or iron by the parasite is unlikely to alter the total number of these molecules that are available to mop up RNI.

The parasite could, however, alter the groups that bind to the iron or the sulphhydryl centres. For instance, nitroso adducts of thiol groups in proteins are more stable than nitroso adducts of free cysteine (27,161), so synthesis of cysteine-rich proteins may protect the parasite against RNI attack. Amastigotes synthesise large amounts of cysteine proteases whose function has yet to be determined (24,228), though they are necessary for amastigote transformation to promastigotes (229). Because of the high concentration of thiol groups in culture medium, their function in mopping up RNI would not be detectable. *In vivo*, though, their accumulation may be very important for protection, as would synthesis of glutathione or trypanothione (208). The chemical state of iron is also important for its activity since myoglobin alone is not very effective at mopping up RNI, but myoglobin kept in the ferrous state by ascorbate is effective (153)

The surface of amastigotes is covered with GPIs (183,227,230,246), which contain long carbohydrate chains. Peroxynitrite reacts with sugars, as does superoxide, so these molecules may play a protective role against peroxynitrite.

There is, however, no evidence to suggest that amastigotes are able to survive an RNI attack from a macrophage. If a macrophage can be activated to produce RNI, then it will kill *Leishmania* (Table 1.3). The defence mechanisms of *Leishmania* appear to concentrate on inhibiting the induction of a  $T_H1$  response rather than trying to defend the parasite against an RNI attack. For instance, *L. major* infected macrophages preferentially provide help for  $T_H2$  type cells (38).

A paradoxical quirk of *L. major* is that it may subvert the host immune response by allowing itself to be killed by RNI. Promastigotes of this species of parasite enter the macrophage “quietly”, preventing the macrophage from releasing IL-12 and thereby inducing a  $T_H1$  response in resistant mice (201). However, amastigotes enter “noisily”, allowing a protective  $T_H1$  response to develop around the outside of a lesion. This prevents the parasite from disseminating and incapacitating the host, which may allow the host to come into contact with more sandflies. BALB/c mice are unable to produce a  $T_H1$  response even after production of IL-12 (201), thereby explaining the dissemination of *L. major* in this strain of mouse.

However, *L. m. mexicana* amastigotes and promastigotes both enter murine macrophages silently (Locksley,R.M. personal communication), thereby always stimulating a  $T_H2$  type response. Compared to *L. major*, lesions in BALB/c mice from *L. m. mexicana* grow slower and disseminate through this susceptible host more slowly (compare 68 to 247). There may therefore be pathways other than the induction of a  $T_H1$  or  $T_H2$  type immune response that account for the different rates of disease progression.

Another way that parasites can evade RNI is to infect cells that do not produce RNI. Dendritic cells can harbour *L. major*, and are unable to produce RNI (20,21,231). After resistant mice have cleared an infection, it is possible to inhibit RNI production and reactivate the disease (232). There is evidence to suggest that parasites inside dendritic cells are protected from RNI produced by macrophages (21). Since up to 70 % of amastigotes are found inside cells that are negative for known macrophage markers (232), this may be a significant immune evasion mechanism.

If the *in vitro* experiments do reflect the *in vivo* situation, *L. m. mexicana* may not have developed resistance because this strain is a human parasite that is normally self-healing in some mouse strains (247). *L. m. mexicana* forms disseminating lesions in BALB/c mice, while five out of six strains of this species formed lesions that began to regress in C57Bl/6 mice (247). The normal reservoirs for *L. m. mexicana* are forest rodents in rural areas and dogs in urban areas (1,5). Human macrophages do not produce RNI as efficiently as mice so it would be interesting to compare the RNI production capabilities of the dogs and rodents that form the natural reservoirs with laboratory rodents.

Amastigotes are not more resistant to RNI than J774 cells either (Figure 4.8 and Figure 4.9), but it is not known whether murine macrophages can kill amastigotes without killing themselves. Since RNI can induce apoptosis in some macrophages (192), these cells appear to be programmed to kill themselves in response to RNI, and may not need to kill the amastigotes without committing suicide.

#### 8.4.1 The kinetics of toxicity.

RNI are cytotoxic to amastigotes. They do not just inhibit parasite proliferation, they also kill the parasite at the same time (Figure 5.2). They can take several hours to kill amastigotes *in vitro* (Figure 5.3). Unfortunately it is not yet possible to compare this to the time course of killing in a macrophage since it is impossible to detect which cells are producing RNI in a given population at a given time. Not only does the expression of iNOS not always correlate with production of detectable RNI (233), but it is difficult to tell whether a particular macrophage contains amastigotes without killing the macrophage. This makes it difficult to identify individual cells that are producing RNI, and the cells in which parasites were dying, in order to identify how long parasites were exposed to RNI for. It is also not known whether a homogeneous population of cells produces RNI in synchrony after stimulation, or whether each cell produces a short burst of a high concentration of RNI, and the gradual accumulation of RNI in the medium is due to changes in the number of cells that are releasing RNI.

In addition, the rate at which RNI become detectable in solution depends on the balance of reactions in which they react with iron, sulphhydryl groups, and oxygen. NO bound to iron may still be toxic to amastigotes, but it will not be detectable in the Griess reaction. The same applies to nitrosothiols. This makes it difficult to determine the rate at which even a population of macrophages produces RNI.

## 8.5 The mechanism of killing.

RNI did not cause apoptosis in parasites since the DNA does not ladder (Figure 6.13), the chromatin did not condense in the same way as an apoptotic mammalian cell (Figure 5.7), and the parasites had no ATP (Figure 7.18) or a mitochondrial electron potential (Figure 7.9) necessary to drive the synthesis of new proteins required for apoptosis.

Necrosis is a much more likely candidate for the toxic mechanism. Necrosis is usually caused by an inhibition of the mitochondrion (188), which prevents the cell from maintaining its osmotic balance, and leads to a disruption of intracellular structures, especially the mitochondrion. This is what was observed in electron micrographs of amastigotes treated with RNI (Figure 5.7).

That a major target of RNI should be the amastigote mitochondrion is not surprising. It has long been known that *L. tropica*, *L. b. braziliensis*, and *L. donovani* are dependent on their mitochondrion for energy, since they are susceptible to toxins such as cyanide (234). However, there have been indications that the electron transport chain of *L. donovani* promastigotes is different from the mammalian system. For instance oxygen consumption is not inhibited by rotenone (a standard inhibitor of complex I of the electron transport chain), and ~30% of the respiration was insensitive to low concentrations of cyanide (248). Oxygen uptake was totally inhibited in these promastigotes by thenoyltrifluoroacetone, suggesting that they do have a complex II in their transport chain which is required for oxygen consumption.

This work confirmed that amastigotes are susceptible to DNP, sodium azide, and FCCP, all of which are mitochondrion-specific toxins. In addition, the inhibition of the mitochondrion by RNI correlates well with the toxicity of RNI (Figure 7.13), as does the

toxicity of DNP to the mitochondrion (Figure 7.14). It is therefore likely that mitochondrial energy production is a major target of RNI.

Higher concentrations of RNI kill amastigotes faster, and inhibit ATP production faster above the concentration at which one could detect inhibition of the mitochondrion with Rh123 (Figure 7.19 and Figure 7.20). This may be due to RNI inhibiting certain components of the glycolytic pathway, for instance glyceraldehyde-3-phosphate dehydrogenase (165). However, it may also be that the Rh123 assay is not sensitive enough to detect the low mitochondrial electron potential that is left. This could be because the pump that removes Rh123 from the mitochondrion (218) pumps the drug out faster than it is accumulated when the membrane potential is low. This theory is supported by the fact that increasing the concentration of DNP above that at which it maximally inhibits Rh123 assay also kills amastigotes faster and lowers the concentration of ATP faster (Figure 7.21).

That amastigotes are reliant on the membrane potential for maintenance of viability assumes that the mechanism of action of DNP is solely the uncoupling of the mitochondrial membrane (249). If this is true then inhibition of ATP production by the mitochondrion is sufficient to account for the toxicity of RNI. DNP will reduce the NADH:NAD ratio by uncoupling the mitochondrion, while RNI should increase this ratio by inhibiting complexes I and II. Since the kinetics of the two toxins are reasonably similar, this implies that the mechanism of killing may be the same, which fits with the inhibition of ATP production rather than changes in the NADH:NAD ratio.

It may be that the unusual organisation of the glycolytic enzymes into glycosomes (235) in amastigotes may cause them to be susceptible to the  $H^+$ -permeability caused by DNP. Furthermore, since amastigotes are grown in an acidic medium, DNP could work

by uncoupling the proton gradient across the parasites' outer membrane. This would probably occur at the same concentration of DNP as the uncoupling of the mitochondrial membrane. Perhaps the correlation of inhibition of ATP production with toxicity is therefore a spurious side effect of this type of toxicity.

#### 8.6 *In vivo* relevance.

The importance of the mitochondrion in amastigote survival is surprising since a lesion has very little vascularisation, and the concentration of amastigotes in the lesion is extremely high. One would therefore expect the oxygen tension in the lesion to be very low, and if the amastigotes are totally dependent on aerobic respiration, it is surprising that they can survive under such conditions.

It is possible that the cultured amastigotes are not identical to lesion amastigotes, and that the cultured amastigotes are dependent on their mitochondrion, while lesion amastigotes are not. In support of this, amastigotes grown *in vitro* from *L. m. mexicana* are often bigger after one day in culture than lesion amastigotes. Also, the culture system used provides most of its energy in carbohydrate form - very high concentrations of glucose, with fatty acids only in low abundance. Amastigotes are particularly efficient at using fatty acids as energy sources, and upregulate their  $\beta$ -oxidation pathway, while down-regulating their glycolytic enzymes compared to promastigotes (236). It has been suggested that amastigotes in a lesion are better described as in a membrane syncytium derived from macrophage membranes than as in macrophages themselves, which would provide the amastigotes with a good energy source if they were to use lipids. This means that the major energy production systems of amastigotes in a lesion and *in vitro* may be completely different, and inhibition of the mitochondrion may not be lethal to a lesion amastigote.

It is possible, therefore, that amastigotes *in vivo* are killed by RNI in a very different way to *in vitro*. However, there was a  $10^3$ -fold difference between the toxic concentrations of RNI (Figure 3.11) and the concentrations required to deglycosylate GIPLs (Figure 6.2) or damage DNA (Figure 6.14). This large difference would suggest that the deamination reactions are still unlikely to be important *in vivo*.

Mitochondrial inhibition by RNI is primarily through the inhibition of complexes I and II of the mitochondrial electron transport chain in tumour cells (153) and *E. coli* (226). It is highly likely that a similar mechanism is true of amastigotes. Enzymes of the electron transport chain are some of the best evolutionarily conserved proteins. Complexes I and II contain an active  $[4Fe4S]^{2+}$  centre, whose iron atom is labile if it is oxidised by RNI. The toxicity of RNI is reversible since it is possible to wash off the RNI and the amastigotes recover sufficiently to transform to promastigotes efficiently. This is consistent with the short term inhibition of mitochondrial function seen in macrophages which is presumed to be caused by ligation of the iron in complexes I and II (153).

### **8.7 RNI inhibition of DNase in serum.**

The inhibition of the DNase activity is a very preliminary finding. It is not known what DNases are present in serum so their structure and possible inhibition mechanism is the subject of pure speculation. Though the concentration of RNI necessary for complete inhibition of the activity in a four hour assay was extremely high (Figure 6.15), *in vivo* production of RNI may involve different ratios of the different RNI, and may be able to target the particular DNase. Biological effects may also be seen if the DNase activity is only partially inhibited.

This inhibition has several important implications. Firstly, in the autoimmune disease, systemic lupus erythematosus, anti-dsDNA antibodies may be pathogenic (237). Since RNI are present in an initial inflammatory lesion, they may prolong the half life of DNA that is released from necrotic cells, thereby allowing the formation of anti-DNA antibodies, thereby contributing to the disease.

In addition, DNA released from necrotic cells will still be bound to histones. DNA from apoptotic cells forms ladders on ethidium bromide gels because the linker DNA between the histones is particularly susceptible to DNase digestion (188). The serum DNase activity is strong enough to digest all the DNA that is released from necrotic cells, whether it is bound to histones or not. So normally, all the DNA from necrotic cells is digested quickly. Since RNI can inhibit this DNase activity, in certain instances it may inhibit the DNase activity only sufficiently for the DNase to create a ladder rather than digesting all the DNA. The kinetics of this inhibition are totally open to speculation, but in some circumstances, RNI may be expected to create DNA ladders from a necrotic rather than an apoptotic population of cells.

In an inflammatory lesion, the production of RNI may prolong the half life of released DNA for long enough to allow neighbouring cells to take up the DNA and express peptides coded by it in conjunction with MHC-I. The success of DNA vaccines in the induction of protective immunity against *Leishmania* (238,239), as well as many viruses (240,241), suggests that this may provide a mechanism for long term production of immunity.

## 8.8 Chemical targets of RNI in *Leishmania*.

In correlation with the rate constants for the reaction of RNI with amine groups, sulphhydryl groups and iron, the two processes examined that involve deamination reactions, ie damage to DNA and GIPLs, are not likely to be significant in the toxicity of RNI. The concentrations of RNI required to cause damage were so much higher than those required to kill amastigotes that they are likely to be insignificant reactions.

Slight alterations in the type of RNI to which the DNA is exposed are also unlikely to make these reactions important. Altering the pH only affected the rate of deamination of guanine by less than two-fold (171), while there needs to be almost a 1000-fold increase in the rate before DNA or GIPLs are affected significantly. Amino acids are also unable to compete for nitrosylation of sulphhydryl groups unless they contain a sulphhydryl group themselves (31). It is therefore unlikely that these deamination reactions are important *in vivo*.

The nick translation reaction did not detect direct damage to DNA by RNI (Figure 6.14). The sort of damage that occurred at extremely high concentrations of RNI was much more consistent with a deamination reaction, which led to less labelling of the DNA, and with a cross-linking reaction that prevented the DNA from leaving the wells of the ethidium bromide gel. *In vivo*, however, deamination of the DNA causes the strands to stop base-pairing properly (171), and the resulting deaminated base is unstable in the double helix (175). In acidic solution, improperly base-paired DNA can lose its purines, becoming apurinated (175). Apurinated DNA can be attacked by basic species such as histones, or basic amino acids to break the DNA strand (242). This would allow extra labelling of DNA by nick translation. The rate of deamination is very variable, and can be affected by base sequence, the structure of the histones, the pH, the salt and the amino

acid concentration (171). It is therefore possible that such a mechanism could occur in mammalian cells and not in parasite cells. Because of all these factors, it would be completely impossible to mimic such a situation *in vitro* to make proper comparisons of the rate of killing to the rate of damage.

### 8.9 RNI production by acidified nitrite.

The system for RNI production by acidification of nitrite in amastigote culture medium has several major advantages over production of RNI by all the other available mechanisms. For instance, it produces a constant amount of RNI that is still toxic 24 h later (Figure 3.13), while NO gas bubbled through medium has a very short half life (33), and S-nitrosothiols in solution also have a very short half life and their breakdown is catalysed unpredictably in biological solutions by transition metal ions (28). Unfortunately, acidified nitrite is not suitable for assaying the effects of RNI in medium designed for mammalian cells, since the amount of sodium nitrite required to get the concentrations of RNI used here at pH 7.4 is in the molar range. Not only is that at the bounds of solubility for sodium nitrite, but it is also likely to be toxic due to osmolarity considerations.

Though acidified nitrite is better than most methods for producing RNI, it is important to note that the toxic mechanism in the system described here may not be the same as the *in vivo* toxic mechanism. RNI produced in this system is produced by the reverse reaction to the *in vivo* situation. *In vitro*, the sodium nitrite anion is protonated to become nitrous acid, which reacts with sulphhydryl groups, iron centres, molecular oxygen and amine groups to produce all the RNI. *In vivo*, RNI are produced by NOS converting L-arginine to L-citrulline and either NO or NO<sup>•</sup>. The rate of production of the different RNI is likely to be different in the two situations, and is also likely to be greatly affected

by the difference in the protein, peptide, oxygen and salt concentrations, as well as the redox potential and the concentration of parasites. These other factors make it impossible to mimic the *in vivo* situation *in vitro*. However, the acidification of nitrite is the most effectively controllable method available for *in vitro* production of RNI.

There is evidence that the important RNI species are those that are favoured by acidic conditions since acidification of the vacuole correlates with toxicity (130). In addition, it is possible to inhibit RNI toxicity by the addition of small thiol containing molecules (31), suggesting that S-nitroso-cysteine or S-nitroso-glutathione are unlikely to be important toxic molecules themselves, though they may be involved in the transport of RNI across membranes. Peroxynitrite is possibly important, especially as the toxicity of acidified nitrite correlates with inhibition of the mitochondrion, which may be more strongly inhibited by peroxynitrite than nitric oxide (155,156). If this had been the case, though, we would have expected to see a significant change in the toxicity when RNI were mixed with  $H_2O_2$ , since peroxynitrite would have been the most likely candidate to have been affected by this reaction.

However, it need not be peroxynitrite produced outside the amastigote that is important, since RNI inhibition of the electron transport chain may lead to greater production of superoxide, which may then react with RNI to form peroxynitrite. This is a more likely scenario, since the negatively charged peroxynitrite would probably find it difficult to cross the dense sugar matrix surrounding amastigotes and the membrane barrier, and not reach the mitochondrion.

## 8.10 Future experiments

The most important question to be answered is "Is the inhibition of the mitochondrion an important factor in RNI toxicity *in vivo*?" A new derivative of Rh123 called Mitofluor Green FM, that has recently come on the market may help to answer the question (217). This derivative is a fluorescent dye that is also driven into the mitochondrion by the membrane potential, but unlike Rh123 it is fixable *in situ* with agents such as formaldehyde. Injection of the dye into a lesion in CBA mice may label parasites with functional mitochondria. It may be possible to find examples of parasites that had inhibited mitochondria, possibly in macrophages that surrounded the lesion.

It may also be possible to detect formation of iron-nitrosyl complexes by electron spin resonance(243) from macrophages that surrounded the lesion. It would, however, not be possible to assign the resonant frequencies to mitochondrial proteins from amastigotes, because it would be unlikely that the frequencies would be sufficiently different from the mammalian frequencies.

Failing that, it may be possible to determine whether a macrophage can clear itself of an infection without killing itself, using a quantitative analysis of the number of infected macrophages in a culture over a time course. However, even if a population of macrophages was infected, and after stimulation there were live, uninfected macrophages, it would be possible to argue that since *in vitro* infection experiments never produce 100 % of the macrophages being infected, the uninfected macrophages may never have been infected and never produced RNI, and so were able to divide more efficiently than the infected macrophages. Since certain *Leishmania* products are able to activate RNI production in synergy with IFN $\gamma$ , this would be a reasonable scenario.

## 9. References

1. Modabber, F. 1992. Leishmaniasis. In "TDR Eleventh Programme Report". World Health Organisation, Geneva. 77-87.
2. Walton, B. C. 1987. American cutaneous and mucocutaneous leishmaniasis. In "The Leishmaniases". Academic Press Ltd, London. 637-664.
3. Adler, S. and M. Ber. 1941. The transmission of *Leishmania tropica* by the bite of *Phlebotomus papatasi*. *Indian Journal of Medical Research* 29:803-909.
4. Shortt, H. E., R. O. A. Smith, C. S. Swaminath, and K. V. Krishnan. 1931. Transmission of Kala-azar by the bite of *Phlebotomine argentipes*. *Indian Journal of Medical Research* 18:1373-1375.
5. Anonymous 1987. Trypanosomes and related organisms. In "Parasitic Protozoa". Kreier, J. P. and J. R. Baker Eds. Allen & Unwin, Winchester, Massachusetts. 43 pp.
6. Marsden, P. D. 1997. Leishmaniasis. *New England Journal of Medicine* 300:350-352.
7. Bryceson, A. D. M. 1969. Diffuse cutaneous leishmaniasis in Ethiopia. I. The clinical and histological features of the disease. *Transactions of the Royal Society of Tropical Medicine and Hygiene* 63:708-737.
8. Convit, J., M. E. Pinardi, and A. J. Rondón. 1972. Diffuse cutaneous leishmaniasis: A disease due to an immunological defect of the host. *Transactions of the Royal Society of Tropical Medicine and Hygiene* 66:603-610.
9. Preiser, W., B. Cacopardo, L. Nigro, J. Braner, A. Nunnari, H. W. Doerr, and B. Weber. 1996. Immunological findings in HIV-*Leishmania* coinfection. *Intervirology* 39:285-288.
10. Solano, J. G., C. S. Sanchez, S. M. Romero, B. G. Perez, F. J. E. Parra, R. V. Garcia, and M. PerezGuillermo. 1996. Visceral leishmaniasis of atypical location in immunodepressed patients: A report of two cases. *International Journal of Surgical Pathology* 3:241-245.

11. Gallego, M. A., A. Aguilar, S. Plaza, J. M. Gomez, F. Burgos, J. L. Agud, J. Marco, and C. Garcia. 1996. Kaposi's sarcoma with an intense parasitization by *Leishmania*. *Cutis* 57:103-105.
12. Dauden, E., P. F. Penas, L. Rios, M. Jimenez, J. Fraga, J. Alvar, and A. GarciaDiez. 1996. Leishmaniasis presenting as a dermatomyositis-like eruption in AIDS. *Journal of the American Academy of Dermatology* 35:316-319.
13. Modabber, F. 1990. Development of vaccines against leishmaniasis. *Scandinavian Journal of Infectious Diseases, Supplement* 22:72-78.
14. Modabber, F. 1995. Vaccines against leishmaniasis. *Annals of Tropical Medicine and Parasitology* 89:83-88.
15. McSorley, S. J., L. Proudfoot, C. A. O'Donnell, and F. Y. Liew. 1996. Immunology of murine leishmaniasis. *Clinics in Dermatology* 14:451-464.
16. Chang, K. P. 1983. Cellular and molecular mechanisms of intracellular symbiosis in leishmaniasis. *International Review of Cytology* 14:267-305.
17. Bray. 1974. *Leishmania*. *Annual Review of Microbiology* 28:189-217.
18. Chang, K. P. and Fish. 1997. *In vitro* cultivation of protozoa pathogenic to man and domestic animals. CRC Press, Boca Raton, Florida.
19. Chang, K. P. 1978. *Leishmania* infection of human skin fibroblasts *in vitro*: absence of phagolysosomal fusion after induced phagocytosis of promastigotes, and their intracellular transformation. *American Journal of Tropical Medicine and Hygiene* 27:1084-1096.
20. Moll, H., S. Flohe, and M. Rollinghoff. 1995. Dendritic cells in *Leishmania major*-immune mice harbor persistent parasites and mediate an antigen-specific T cell immune response. *European Journal of Immunology* 25:693-699.
21. Moll, H., S. Flohe, and C. Blank. 1995. Dendritic cells seclude *Leishmania* parasites that persist in cured mice - A role in the maintenance of T-cell memory? *Advances in Experimental Medicine and Biology* 378:507-509.

22. Lanzer, M., U. Gross, and H. Moll. 1997. Mechanisms of parasite persistence and immune evasion. *Parasitology Today* 13:1-3.
23. Bates, P. A. 1993. Axenic culture of *Leishmania* amastigotes. *Parasitology Today* 9:143-146.
24. Bates, P. A., C. D. Robertson, L. Tetley, and G. H. Coombs. 1992. Axenic cultivation and characterization of *Leishmania mexicana* amastigote-like forms. *Parasitology* 105:193-202.
25. Bates, P. A. 1994. Complete developmental cycle of *Leishmania mexicana* in axenic culture. *Parasitology* 108:1-9.
26. Nathan, C. 1992. Nitric oxide as a secretory product of mammalian cells. *FASEB Journal* 6:3051-3064.
27. Feelish, M. 1991. The biochemical pathways of nitric oxide formation from nitrovasodilators: Appropriate choice of exogenous NO donors and aspects of preparation and handling of aqueous NO solutions. *Journal of Cardiovascular Pharmacology* 17:S25-S33.
28. Butler, A. R., F. W. Flitney, and D. L. H. Williams. 1995. NO, nitrosonium ions, nitroxide ions, nitrosothiols and iron-nitrosyls in biology: A chemist's perspective. *Trends in Pharmacological Sciences* 16:18-22.
29. Stamler, J. S. 1994. Redox signaling: Nitrosylation and related target interactions of nitric oxide. *Cell* 78:931-936.
30. Stamler, J. S., D. J. Singel, and J. Loscalzo. 1992. Biochemistry of nitric oxide and its redox-activated forms. *Science* 258:1898-1902.
31. Wink, D. A., R. W. Nims, J. F. Darbyshire, D. Christodoulou, I. Hanbauer, G. W. Cox, F. Laval, J. Laval, J. A. Cook, M. C. Krishna, W. G. DeGraff, and J. B. Mitchell. 1994. Reaction kinetics for nitrosation of cysteine and glutathione in aerobic nitric oxide solutions at neutral pH. Insights into the fate and physiological effects of

- intermediates generated in the NO/O<sub>2</sub> reaction. *Chemical Research in Toxicology* 7:519-525.
32. Marletta, M. A., P. S. Yoon, R. Iyengar, C. D. Leaf, and J. S. Wishnok. 1988. Macrophage oxidation of L-arginine to nitrite and nitrate: Nitric oxide is an intermediate. *Biochemistry (USA)* 27:8706-8711.
33. Archer, S. 1993. Measurement of nitric oxide in biological models. *FASEB Journal* 7:349-360.
34. Kelm, M. and J. Schrader. 1990. Control of coronary vascular tone by nitric oxide. *Circulation Research* 66:1561-1575.
35. Nathan, C. and Q. W. Xie. 1994. Nitric oxide synthases: Roles, tolls, and controls. *Cell* 78:915-918.
36. Nathan, C. and Q. W. Xie. 1994. Regulation of biosynthesis of nitric oxide. *Journal of Biological Chemistry*. 269:13725-13728.
37. Sands, W. A., V. Bulut, A. Severn, D. Xu, and F. Y. Liew. 1994. Inhibition of nitric oxide synthesis by interleukin-4 may involve inhibiting the activation of protein kinase C epsilon. *European Journal of Immunology* 24:2345-2350.
38. Chakkalath, H. R. and R. G. Titus. 1994. *Leishmania major*-parasitized macrophages augment T<sub>H</sub>2-type T cell activation. *Journal of Immunology*. 153:4378-4387.
39. Cho, H. J., Q. W. Xie, J. Calaycay, R. A. Mumford, K. M. Swiderek, T. D. Lee, and C. Nathan. 1992. Calmodulin is a subunit of nitric oxide synthase from macrophages. *Journal of Experimental Medicine* 176:599-604.
40. Buchmuller-Rouiller, Y., S. B. Corradin, and J. Mael. 1992. Macrophage activation for intracellular killing as induced by a Ca<sup>2+</sup> ionophore. Dependence on L-arginine-derived nitrogen oxidation products. *Biochemical Journal* 284:387-392.
41. Buchmuller-Rouiller, Y., S. B. Corradin, and J. Mael. 1991. Macrophage activation for intracellular killing is induced by a Ca<sup>2+</sup> ionophore. *Journal of Immunology*. 146:217-223.

42. Green, S. J. and C. A. Nacy. 1993. Antimicrobial and immunopathologic effects of cytokine-induced nitric oxide synthesis. *Current Opinion in Infectious Diseases* 6:384-396.
43. Nussler, A., J. C. Drapier, L. Renia, S. Pied, F. Miltgen, M. Gentilini, and D. Mazier. 1991. L-Arginine-dependent destruction of intrahepatic malaria parasites in response to tumor necrosis factor and/or interleukin 6 stimulation. *European Journal of Immunology* 21:227-230.
44. Mellouk, S., S. J. Green, C. A. Nacy, and S. L. Hoffman. 1991. IFN- $\gamma$  inhibits development of *Plasmodium berghei* exoerythrocytic stages in hepatocytes by an L-arginine-dependent effector mechanism. *Journal of Immunology*. 146:3971-3976.
45. Croen, K. D. 1993. Evidence for an antiviral effect of nitric oxide. Inhibition of herpes simplex virus type 1 replication. *Journal of Clinical Investigation* 91:2446-2452.
46. Doi, T., M. Ando, T. Akaike, M. Suga, K. Sato, and H. Maeda. 1993. Resistance to nitric oxide in *Mycobacterium avium* complex and its implication in pathogenesis. *Infection and Immunity* 61:1980-1989.
47. Adams, L. B., S. G. Franzblau, Z. Vavrin, J. B. Hibbs Jr, and J. L. Krahenbuhl. 1991. L-arginine-dependent macrophage effector functions inhibit metabolic activity of *Mycobacterium leprae*. *Journal of Immunology*. 147:1642-1646.
48. Isobe, K. I. and I. Nakashima. 1993. Nitric oxide production from a macrophage cell line: Interaction with autologous and allogeneic lymphocytes. *Journal of Cellular Biochemistry* 53:198-205.
49. Drapier, J. C., H. Hirling, J. Wietzerbin, P. Kaldy, and L. C. Kuhn. 1993. Biosynthesis of nitric oxide activates iron regulatory factor in macrophages. *EMBO Journal* 12:3643-3649.
50. Bermudez, L. E. 1993. Differential mechanisms of intracellular killing of *Mycobacterium avium* and *Listeria monocytogenes* by activated human and murine macrophages. The role of nitric oxide. *Clinical and Experimental Immunology* 91:277-281.

51. Forray, M. I., S. Angelo, C. A. R. Boyd, and R. Deves. 1995. Transport of nitric oxide synthase inhibitors through cationic amino acid carriers in human erythrocytes. *Biochemical Pharmacology* 50:1963-1968.
52. Vespa, G. N. R., F. Q. Cunha, and J. S. Silva. 1994. Nitric oxide is involved in control of *Trypanosoma cruzi*-induced parasitemia and directly kills the parasite in vitro. *Infection and Immunity* 62:5177-5182.
53. Fehsel, K., A. Jalowy, S. Qi, V. Burkart, B. Hartmann, and H. Kolb. 1993. Islet cell DNA is a target of inflammatory attack by nitric oxide. *Diabetes* 42:496-500.
54. Assreuy, J., F. Q. Cunha, M. Epperlein, A. NoronhaDutra, C. A. O'Donnell, F. Y. Liew, and S. Moncada. 1994. Production of nitric oxide and superoxide by activated macrophages and killing of *Leishmania major*. *European Journal of Immunology* 24:672-676.
55. Sternberg, J., N. Mabbott, I. Sutherland, and F. Y. Liew. 1994. Inhibition of nitric oxide synthesis leads to reduced parasitemia in murine *Trypanosoma brucei* infection. *Infection and Immunity* 62:2135-2137.
56. Baydoun, A. R. and G. E. Mann. 1994. Selective targeting of nitric oxide synthase inhibitors to system  $\gamma^+$  in activated macrophages. *Biochemical and Biophysical Research Communications* 200:726-731.
57. Peterson, D. A., D. C. Peterson, S. Archer, and E. K. Weir. 1992. The non specificity of specific nitric oxide synthase inhibitors. *Biochemical and Biophysical Research Communications* 187:797-801.
58. Hoffman, R. A., J. M. Langrehr, S. M. Wren, K. E. Dull, S. T. Ildstad, S. A. McCarthy, and R. L. Simmons. 1993. Characterization of the immunosuppressive effects of nitric oxide in graft vs host disease. *Journal of Immunology*. 151:1508-1518.
59. Hoffman, R. A., J. M. Langrehr, K. E. Dull, S. A. McCarthy, M. L. Jordan, and R. L. Simmons. 1994. Macrophage synthesis of nitric oxide in the mouse mixed leucocyte reaction. *Transplant Immunology* 2:313-320.

60. Isobe, K. I. and I. Nakashima. 1992. Feedback suppression of staphylococcal enterotoxin-stimulated T-lymphocyte proliferation by macrophages through inductive nitric oxide synthesis. *Infection and Immunity* 60:4832-4837.
61. Amber, I. J., J. B. Hibbs Jr, R. R. Taintor, and Z. Vavrin. 1988. The L-arginine dependent effector mechanism is induced in murine adenocarcinoma cells by culture supernatant from cytotoxic activated macrophages. *Journal of Leukocyte Biology* 43:187-192.
62. Green, S. J., M. S. Meltzer, J. B. Hibbs Jr, and C. A. Nacy. 1990. Activated macrophages destroy intracellular *Leishmania major* amastigotes by an L-arginine-dependent killing mechanism. *Journal of Immunology*. 144:278-283.
63. Granger, D. L., J. B. Hibbs Jr, J. R. Perfect, and D. T. Durack. 1990. Metabolic fate of L-arginine in relation to microbistatic capability of murine macrophages. *Journal of Clinical Investigation* 85:264-273.
64. Mael, J., A. Ransijn, and Y. Buchmuller-Rouiller. 1991. Killing of *Leishmania* parasites in activated murine macrophages is based on an L-arginine-dependent process that produces nitrogen derivatives. *Journal of Leukocyte Biology* 49:73-82.
65. Palmer, R. M. J., A. G. Ferrige, and S. Moncada. 1987. Nitric oxide release accounts for the biological activity of endothelium-derived relaxing factor. *Nature* 327:524-526.
66. Mabbott, N. A., I. A. Sutherland, and J. M. Sternberg. 1994. *Trypanosoma brucei* is protected from the cytostatic effects of nitric oxide under *in vivo* conditions. *Parasitology Research* 80:687-690.
67. Liew, F. Y., S. Millott, C. Parkinson, R. M. J. Palmer, and S. Moncada. 1990. Macrophage killing of *Leishmania* parasite *in vivo* is mediated by nitric oxide from L-arginine. *Journal of Immunology*. 144:4794-4797.
68. Evans, T. G., L. Thai, D. L. Granger, and J. B. Hibbs Jr. 1993. Effect of *in vivo* inhibition of nitric oxide production in murine leishmaniasis. *Journal of Immunology*. 151:907-915.

69. Wei, X. Q., I. G. Charles, A. Smith, J. Ure, G. J. Feng, F. P. Huang, D. Xu, W. Muller, S. Moncada, and F. Y. Liew. 1995. Altered immune responses in mice lacking inducible nitric oxide synthase. *Nature* 375:408-411.
70. Ding, A. H., C. F. Nathan, and D. J. Stuehr. 1988. Release of reactive nitrogen intermediates and reactive oxygen intermediates from mouse peritoneal macrophages: Comparison of activating cytokines and evidence for independent production. *Journal of Immunology*. 141:2407-2412.
71. Liew, F. Y., Y. Li, D. Moss, C. Parkinson, M. V. Rogers, and S. Moncada. 1991. Resistance to *Leishmania major* infection correlates with the induction of nitric oxide synthase in murine macrophages. *European Journal of Immunology* 21:3009-3014.
72. Amber, I. J., J. B. Hibbs Jr, R. R. Taintor, and Z. Vavrin. 1988. Cytokines induce an L-arginine-dependent effector system in nonmacrophage cells. *Journal of Leukocyte Biology* 44:58-65.
73. Denis, M. 1991. Tumor necrosis factor and granulocyte macrophage-colony stimulating factor stimulate human macrophages to restrict growth of virulent *Mycobacterium avium* and to kill avirulent *M. avium*: Killing effector mechanism depends on the generation of reactive nitrogen intermediates. *Journal of Leukocyte Biology* 49:380-387.
74. Stuehr, D. J. and M. A. Marletta. 1987. Induction of nitrite/nitrate synthesis in murine macrophages by BCG infection, lymphokines, or interferon-gamma. *Journal of Immunology*. 139:518-525.
75. Cunha, F. Q., S. Moncada, and F. Y. Liew. 1992. Interleukin-10 (IL-10) inhibits the induction of nitric oxide synthase by interferon-gamma in murine macrophages. *Biochemical and Biophysical Research Communications* 182:1155-1159.
76. Wu, J., F. Q. Cunha, F. Y. Liew, and W. Y. Weiser. 1993. IL-10 inhibits the synthesis of migration inhibitory factor and migration inhibitory factor-mediated macrophage activation. *Journal of Immunology*. 151:4325-4332.

77. Nelson, B. J., P. Ralph, S. J. Green, and C. A. Nacy. 1991. Differential susceptibility of activated macrophage cytotoxic effector reactions to the suppressive effects of transforming growth factor-beta1. *Journal of Immunology*. 146:1849-1857.
78. Bogdan, C., S. Stenger, M. Rollinghoff, and W. Solbach. 1991. Cytokine interactions in experimental cutaneous leishmaniasis. Interleukin 4 synergizes with interferon-gamma to activate murine macrophages for killing of *Leishmania major* amastigotes. *European Journal of Immunology* 21:327-333.
79. Green, S. J., R. M. Crawford, J. T. Hockmeyer, M. S. Meltzer, and C. A. Nacy. 1990. *Leishmania major* amastigotes initiate the L-arginine-dependent killing mechanism in IFN $\gamma$ -stimulated macrophages by induction of tumor necrosis factor- $\alpha$ 1. *Journal of Immunology*. 145:4290-4297.
80. Liew, F. Y., Y. Li, and S. Millott. 1990. Tumour necrosis factor (TNF- $\alpha$ ) in leishmaniasis. II. TNF- $\alpha$ - induced macrophage leishmanicidal activity is mediated by nitric oxide from L-arginine. *Immunology* 71:556-559.
81. Liew, F. Y., Y. Li, and S. Millott. 1990. Tumor necrosis factor- $\alpha$  synergizes with IFN- $\gamma$  in mediating killing of *Leishmania major* through the induction of nitric oxide. *Journal of Immunology*. 145:4306-4310.
82. Roach, T. I. A., A. F. Kiderlen, and J. M. Blackwell. 1991. Role of inorganic nitrogen oxides and tumor necrosis factor  $\alpha$  in killing *Leishmania donovani* amastigotes in gamma interferon- lipopolysaccharide-activated macrophages from Lsh(s) and Lsh(r) congenic mouse strains. *Infection and Immunity* 59:3935-3944.
83. Buchmuller-Rouiller, Y., S. Betz-Corradin, and J. Mauel. 1992. Differential effects of prostaglandins on macrophage activation induced by calcium ionophore A23187 or IFN- $\gamma$ . *Journal of Immunology*. 148:1171-1175.
84. Proudfoot, L., A. V. Nikolaev, G. J. Feng, X. Q. Wei, M. A. J. Ferguson, J. S. Brimacombe, and F. Y. Liew. 1996. Regulation of the expression of nitric oxide synthase and leishmanicidal activity by glycoconjugates of *Leishmania*

- lipophosphoglycan in murine macrophages. *Proceedings of the National Academy of Science USA* 93:10984-10989.
85. Severn, A., D. Xu, J. Doyle, L. M. C. Leal, C. A. O'Donnell, S. J. Brett, D. W. Moss, and F. Y. Liew. 1993. Pre-exposure of murine macrophages to lipopolysaccharide inhibits the induction of nitric oxide synthase and reduces leishmanicidal activity. *European Journal of Immunology* 23:1711-1714.
86. Proudfoot, L., C. A. O'Donnell, and F. Y. Liew. 1995. Glycoinositolphospholipids of *Leishmania major* inhibit nitric oxide synthesis and reduce leishmanicidal activity in murine macrophages. *European Journal of Immunology* 25:745-750.
87. Mosmann, T. R., H. Cherwinski, M. W. Bond, and et al. 1986. Two types of murine helper T cell clone. I. Definition according to profiles of lymphokine activities and secreted proteins. *Journal of Immunology*. 136:2348-2357.
88. Mosmann, T. R. and R. L. Coffman. 1989. TH1 and TH2 cells: Different patterns of lymphokine secretion lead to different functional properties. *Annual Review of Immunology* 7:145-173.
89. Liew, F. Y. and C. A. O'Donnell. 1993. Immunology of leishmaniasis. *Advances in Parasitology* 32:161-259.
90. Pearson, R. D. and R. T. Steigbigel. 1980. Mechanism of lethal effect of human serum upon *Leishmania donovani*. *Journal of Immunology*. 125:2195-2201.
91. Handman, E. and G. F. Mitchell. 1985. Immunization with *Leishmania* receptor for macrophages protects mice against cutaneous leishmaniasis. *Proceedings of the National Academy of Science USA* 82:5910-5914.
92. Anderson, S., J. R. David, and D. McMahon Pratt. 1983. In vivo protection against *Leishmania mexicana* mediated by monoclonal antibodies. *Journal of Immunology*. 131:1616-1618.
93. Debons-Guillemin, M. C., I. Vouldoukis, A. Roseto, and et al. 1986. Inhibition in vivo of both infective *Leishmania major* and *L. mexicana amazonensis* mediated by a

single monoclonal antibody. *Transactions of the Royal Society of Tropical Medicine and Hygiene* 80:258-260.

94. Olobo, J. O., E. Handman, J. M. Curtis, and G. F. Mitchell. 1980. Antibodies to *Leishmania tropica* promastigotes during infection in mice of various genotypes. *Australian Journal of Experimental Biology and Medical Science* 58:595-601.
95. Howard, J. G., S. Nicklin, C. Hale, and F. Y. Liew. 1982. Prophylactic immunization against experimental leishmaniasis: I. Protection induced in mice genetically vulnerable to fatal *Leishmania tropica* infection. *Journal of Immunology*. 129:2206-2212.
96. Hale, C. and J. G. Howard. 1981. Immunological regulation of experimental cutaneous leishmaniasis. 2. Studies with Biozzi high and low responder lines of mice. *Parasite Immunology* 3:45-55.
97. Scott, P., P. Natovitz, and A. Sher. 1986. B lymphocytes are required for the generation of T cells that mediate healing of cutaneous leishmaniasis. *Journal of Immunology*. 137:1017-1021.
98. Titus, R. G., I. Muller, P. Kimsey, A. Cerny, R. Behin, R. M. Zinkernagel, and J. A. Louis. 1991. Exacerbation of experimental murine cutaneous leishmaniasis with CD4+ *Leishmania major*-specific T cell lines or clones which secrete interferon- $\gamma$  and mediate parasite-specific delayed-type hypersensitivity. *European Journal of Immunology* 21:559-567.
99. Sacks, D. L., P. A. Scott, R. Asofsky, and F. A. Sher. 1984. Cutaneous leishmaniasis in anti-IgM-treated mice: Enhanced resistance due to functional depletion of a B cell-dependent T cell involved in the suppressor pathway. *Journal of Immunology*. 132:2072-2077.
100. Mitchell, G. F., J. M. Curtis, E. Handman, and I. F. C. McKenzie. 1980. Cutaneous leishmaniasis in mice: disease patterns in reconstituted nude mice of several genotypes infected with *Leishmania tropica*. *Australian Journal of Experimental Biology and Medical Science* 58:521-532.

101. Preston, P. M., R. L. Carter, and E. Leuchars. 1972. Experimental cutaneous leishmaniasis. III. Effects of thymectomy on the course of infection CBA mice with *Leishmania tropica*. *Clinical and Experimental Immunology* 10:337-357.
102. Preston, P. M. and D. C. Dumonde. 1976. Experimental cutaneous leishmaniasis. V. Protective immunity in subclinical and self-healing infection in the mouse. *Clinical and Experimental Immunology* 23:126-138.
103. Liew, F. Y., J. G. Howard, and C. Hale. 1984. Prophylactic immunization against experimental leishmaniasis. III. Protection against fatal *Leishmania tropica* infection induced by irradiated promastigotes involves Lyt-1+2- T cells that do not mediate cutaneous DTH. *Journal of Immunology*. 132:456-461.
104. Liew, F. Y., C. Hale, and J. G. Howard. 1982. Immunologic regulation of experimental cutaneous leishmaniasis. V. Characterization of effector and specific suppressor T cells. *Journal of Immunology*. 128:1917-1922.
105. Howard, J. G., C. Hale, and F. Y. Liew. 1981. Immunological regulation of experimental cutaneous leishmaniasis. IV. Prophylactic effect of sublethal irradiation as a result of abrogation of suppressor T cell generation in mice genetically susceptible to *Leishmania tropica*. *Journal of Experimental Medicine* 153:557-568.
106. Titus, R. G., R. Ceredig, J. C. Cerottini, and J. A. Louis. 1985. Therapeutic effect of anti-L3T4 monoclonal antibody GK1.5 on cutaneous leishmaniasis in genetically-susceptible BALB/c mice. *Journal of Immunology*. 135:2108-2144.
107. Behforouz, N. C., C. D. Wenger, and B. A. Mathison. 1986. Prophylactic treatment of BALB/c mice with cyclosporine A and its analog B-5-49 enhances resistance to *Leishmania major*. *Journal of Immunology*. 136:3067-3075.
108. Titus, R. G., G. C. Lima, H. D. Engers, and J. A. Louis. 1984. Exacerbation of murine cutaneous leishmaniasis by adoptive transfer of parasite-specific helper T cell populations capable of mediating *Leishmania major*-specific delayed-type hypersensitivity. *Journal of Immunology*. 133:1594-1600.

109. Titus, R. G., M. Marchand, T. Boon, and J. A. Louis. 1985. A limiting dilution assay for quantifying *Leishmania major* in tissues of infected mice. *Parasite Immunology* 7:545-555.
110. Heinzl, F. P., M. D. Sadick, B. J. Holaday, R. L. Coffman, and R. M. Locksley. 1989. Reciprocal expression of interferon gamma or interleukin 4 during the resolution or progression of murine leishmaniasis. Evidence for expansion of distinct helper T cell subsets. *Journal of Experimental Medicine* 169:59-72.
111. Heinzl, F. P., M. D. Sadick, S. S. Mutha, and R. M. Locksley. 1991. Production of interferon gamma, interleukin 2, interleukin 4, and interleukin 10 by CD4+ lymphocytes in vivo during healing and progressive murine leishmaniasis. *Proceedings of the National Academy of Science USA* 88:7011-7015.
112. Scott, P., P. Natovitz, R. L. Coffman, E. Pearce, and A. Sher. 1988. Immunoregulation of cutaneous leishmaniasis. T cell lines that transfer protective immunity or exacerbation belong to different T helper subsets and respond to distinct parasite antigens. *Journal of Experimental Medicine* 168:1675-1684.
113. Holaday, B. J., M. D. Sadick, Z. E. Wang, S. L. Reiner, F. P. Heinzl, T. G. Parslow, and R. M. Locksley. 1991. Reconstitution of *Leishmania* immunity in severe combined immunodeficient mice using Th1- and Th2-like cell lines. *Journal of Immunology*. 147:1653-1658.
114. Belosevic, M., D. S. Finbloom, P. H. Van der Meide, M. V. Slayter, and C. A. Nacy. 1989. Administration of monoclonal anti-IFN- $\gamma$  antibodies in vivo abrogates natural resistance of C3H/HeN mice to infection with *Leishmania major*. *Journal of Immunology*. 143:266-274.
115. Sadick, M. D., F. P. Heinzl, B. J. Holaday, R. T. Pu, R. S. Dawkins, and R. M. Locksley. 1990. Cure of murine leishmaniasis with anti-interleukin 4 monoclonal antibody. Evidence for a T cell-dependent, interferon gamma-independent mechanism. *Journal of Experimental Medicine* 171:115-127.

116. Coffman, R. L., K. Varkila, P. Scott, and R. Chatelain. 1991. Role of cytokines in the differentiation of CD4<sup>+</sup> T-cell subsets in vivo. *Immunological Reviews* 189-207.
117. Leal, L. M. C. C., D. W. Moss, R. Kuhn, W. Muller, and F. Y. Liew. 1993. Interleukin-4 transgenic mice of resistant background are susceptible to *Leishmania major* infection. *European Journal of Immunology* 23:566-569.
118. Swihart, K., U. Fruth, N. Messmer, K. Hug, R. Behin, S. Huang, G. Del Giudice, M. Aguet, and J. A. Louis. 1995. Mice from a genetically resistant background lacking the interferon gamma receptor are susceptible to infection with *Leishmania major* but mount a polarized T helper cell 1-type CD4<sup>+</sup> T cell response. *Journal of Experimental Medicine* 181:961-971.
119. Wang, Z. E., S. L. Reiner, S. Zheng, D. K. Dalton, and R. M. Locksley. 1994. CD4<sup>+</sup> effector cells default to the Th2 pathway in interferon gamma- deficient mice infected with *Leishmania major*. *Journal of Experimental Medicine* 179:1367-1371.
120. Satoskar, A., H. Bluethmann, and J. Alexander. 1995. Disruption of the murine interleukin-4 gene inhibits disease progression during *Leishmania mexicana* infection but does not increase control of *Leishmania donovani* infection. *Infection and Immunity* 63:4894-4899.
121. Kopf, M., F. Brombacher, G. Kohler, G. Kienzle, K. H. Widmann, K. Lefrang, C. Humborg, B. Ledermann, and W. Solbach. 1996. IL-4-deficient Balb/c mice resist infection with *Leishmania major*. *Journal of Experimental Medicine* 184:1127-1136.
122. NobenTrauth, N., P. Kropf, and I. Muller. 1996. Susceptibility to *Leishmania major* infection in interleukin-4-deficient mice. *Science* 271:987-990.
123. Buchmuller-Rouiller, Y. and J. Mael. 1986. Correlation between enhanced oxidative metabolism and leishmanicidal activity in activated macrophages from healer and nonhealer mouse strains. *Journal of Immunology*. 136:3884-3890.

124. Alexander, J. 1981. *Leishmania mexicana*: Inhibition and stimulation of phagosome-lysosome fusion in infected macrophages. *Experimental Parasitology* 52:261-270.
125. Alexander, J. and K. Vickerman. 1975. Fusion of host cell secondary lysosomes with the parasitophorous vacuoles of *Leishmania mexicana*-infected macrophages. *J. Protozool.* 22:502-508.
126. Rabinovitch, M., G. Topper, P. Cristello, and A. Rich. 1985. Receptor-mediated entry of peroxidases into the parasitophorous vacuoles of macrophages infected with *Leishmania mexicana amazonensis*. *Journal of Leukocyte Biology* 37:247-261.
127. Green, S. J., S. Mellouk, S. L. Hoffman, M. S. Meltzer, and C. A. Nacy. 1990. Cellular mechanisms of nonspecific immunity to intracellular infection: Cytokine-induced synthesis of toxic nitrogen oxides from L-arginine by macrophages and hepatocytes. *Immunology Letters* 25:15-19.
128. Russell, D. G., S. Xu, and P. Chakraborty. 1992. Intracellular trafficking and the parasitophorous vacuole of *Leishmania mexicana*-infected macrophages. *Journal of Cell Science* 103:1193-1210.
129. Lang, T., R. Hellio, P. M. Kaye, and J. C. Antoine. 1994. *Leishmania donovani*-infected macrophages: Characterization of the parasitophorous vacuole and potential role of this organelle in antigen presentation. *Journal of Cell Science* 107:2137-2150.
130. Buchmuller-Rouiller, Y., S. B. Corradin, J. Smith, and J. Mael. 1994. Effect of increasing intravesicular pH on nitrite production and leishmanicidal activity of activated macrophages. *Biochemical Journal* 301:243-247.
131. Rockett, K. A., M. M. Awburn, W. B. Cowden, and I. A. Clark. 1991. Killing of *Plasmodium falciparum* in vitro by nitric oxide derivatives. *Infection and Immunity* 59:3280-3283.
132. Gyan, B., M. TroyeBlomberg, P. Perlmann, and A. Bjorkman. 1994. Human monocytes cultured with and without interferon-gamma inhibit *Plasmodium*

- falciparum parasite growth in vitro via secretion of reactive nitrogen intermediates. *Parasite Immunology* 16:371-375.
133. Denicola, A., H. Rubbo, D. Rodriguez, and R. Radi. 1993. Peroxynitrite-mediated cytotoxicity to *Trypanosoma cruzi*. *Archives of Biochemistry and Biophysics* 304:279-286.
134. Chan, J., Y. Xing, R. S. Magliozzo, and B. R. Bloom. 1992. Killing of virulent *Mycobacterium tuberculosis* by reactive nitrogen intermediates produced by activated murine macrophages. *Journal of Experimental Medicine* 175:1111-1122.
135. Tarr, H. L. A. 1941. Bacteriostatic Action of Nitrates. *Nature* 3727:417-418.
136. James, S. L. and J. Glaven. 1989. Macrophage cytotoxicity against schistosomula of *Schistosoma mansoni* involves arginine-dependent production of reactive nitrogen intermediates. *Journal of Immunology*. 143:4208-4212.
137. Granger, D. L., J. B. Hibbs Jr, J. R. Perfect, and D. T. Durack. 1988. Specific amino acid (L-arginine) requirement for the microbiostatic activity of murine macrophages. *Journal of Clinical Investigation* 81:1129-1136.
138. James, S. L. and J. B. Hibbs Jr. 1990. The role of nitrogen oxides as effector molecules of parasite killing. *Parasitology Today* 6:303-305.
139. Goureau, O., M. Lepoivre, and Y. Courtois. 1992. Lipopolysaccharide and cytokines induce a macrophage-type of nitric oxide synthase in bovine retinal pigmented epithelial cells. *Biochemical and Biophysical Research Communications* 186:854-859.
140. Galea, E., D. L. Feinstein, and D. J. Reis. 1992. Induction of calcium-independent nitric oxide synthase activity in primary rat glial cultures. *Proceedings of the National Academy of Science USA* 89:10945-10949.
141. Stadler, J., T. R. Billiar, R. D. Curran, D. J. Stuehr, J. B. Ochoa, and R. L. Simmons. 1991. Effect of exogenous and endogenous nitric oxide on mitochondrial

respiration of rat hepatocytes. *American Journal of Physiology - Cell Physiology* 260:C910-C916.

142. Nussler, A. K., M. Di Silvio, T. R. Billiar, R. A. Hoffman, D. A. Geller, R. Selby, J. Madariaga, and R. L. Simmons. 1992. Stimulation of the nitric oxide synthase pathway in human hepatocytes by cytokines and endotoxin. *Journal of Experimental Medicine* 176:261-264.
143. McInnes, I. B., B. P. Leung, M. Field, X. Q. Wei, F. P. Hueng, R. D. Sturrock, A. Kinninmonth, J. Weidner, R. Mumford, and F. Y. Liew. 1996. Production of nitric oxide in the synovial membrane of rheumatoid and osteoarthritis patients. *Journal of Experimental Medicine* 184:1519-1524.
144. Geller, D. A., C. J. Lowenstein, R. A. Shapiro, A. K. Nussler, M. Di Silvio, S. C. Wang, D. K. Nakayama, R. L. Simmons, S. H. Snyder, and T. R. Billiar. 1993. Molecular cloning and expression of inducible nitric oxide synthase from human hepatocytes. *Proceedings of the National Academy of Science USA* 90:3491-3495.
145. Schneemann, M., G. Schoedon, S. Hofer, N. Blau, L. Guerrero, and A. Schaffner. 1993. Nitric oxide synthase is not a constituent of the antimicrobial armature of human mononuclear phagocytes. *Journal of Infectious Diseases* 167:1358-1363.
146. Padgett, E. L. and S. B. Prueett. 1992. Evaluation of nitrite production by human monocyte-derived macrophages. *Biochemical and Biophysical Research Communications* 186:775-781.
147. Vouldoukis, I., P. A. Becherel, V. Riveros-Moreno, M. Arock, O. da Silva, P. Debre, D. Mazier, and M. Djavad Mossalayi. 1997. Interleukin-10 and interleukin-4 inhibit intracellular killing of *Leishmania infantum* and *Leishmania major* by human macrophages by decreasing nitric oxide generation. *European Journal of Immunology* 27:860-865.
148. Murray, H. W. and D. M. Cartelli. 1983. Killing of intracellular *Leishmania donovani* by human mononuclear phagocytes. Evidence for oxygen-dependent and -independent leishmanicidal activity. *Journal of Clinical Investigation* 72:32-44.

149. Murray, H. W., B. Y. Rubin, and C. D. Rothermel. 1983. Killing of intracellular *Leishmania donovani* by lymphokine-stimulated human mononuclear phagocytes. Evidence that interferon-gamma is the activating lymphokine. *Journal of Clinical Investigation* 72:1506-1510.
150. Cillari, E., G. Vitale, F. Arcolco, P. D'Agostino, C. Mocciaro, G. Gambino, R. Malta, G. Stassi, C. Giordano, S. Milano, and S. Mansueto. 1995. *In vivo* and *in vitro* cytokine profiles and mononuclear cell subsets in Sicilian patients with active visceral leishmaniasis. *Cytokine* 7:740-745.
151. Hogg, N., R. J. Singh, and B. Kalyanaraman. 1996. The role of glutathione in the transport and catabolism of nitric oxide. *FEBS Letters* 382:223-228.
152. Granger, D. L. and A. L. Lehninger. 1982. Sites of inhibition of mitochondrial electron transport in macrophage-injured neoplastic cells. *Journal of Cell Biology* 95:527-535.
153. Stuehr, D. J. and C. F. Nathan. 1989. Nitric oxide: A macrophage product responsible for cytostasis and respiratory inhibition in tumor target cells. *Journal of Experimental Medicine* 169:1543-1555.
154. Drapier, J. C. and J. B. Hibbs Jr. 1986. Murine cytotoxic activated macrophages inhibit aconitase in tumor cells. Inhibition involves the iron-sulfur prosthetic group and is reversible. *Journal of Clinical Investigation* 78:790-797.
155. Hausladen, A. and I. Fridovich. 1994. Superoxide and peroxynitrite inactivate aconitases, but nitric oxide does not. *Journal of Biological Chemistry*. 269:29405-29408.
156. Castro, L., M. Rodriguez, and R. Radi. 1994. Aconitase is readily inactivated by peroxynitrite, but not by its precursor, nitric oxide. *Journal of Biological Chemistry*. 269:29409-29415.
157. Verniquet, F., J. Gaillard, M. Neuberger, and R. Douce. 1991. Rapid inactivation of plant aconitase by hydrogen peroxide. *Biochemical Journal* 276:643-648.

158. Wink, D. A., Y. Osawa, J. F. Darbyshire, C. R. Jones, S. C. Eshenaur, and R. W. Nims. 1993. Inhibition of cytochromes P<sub>450</sub> by nitric oxide and a nitric oxide-releasing agent. *Archives of Biochemistry and Biophysics* 300:115-123.
159. Khatsenko, O. G., S. S. Gross, A. B. Rifkind, and J. R. Vane. 1993. Nitric oxide is a mediator of the decrease in cytochrome P450-dependent metabolism caused by immunostimulants. *Proceedings of the National Academy of Science USA* 90:11147-11151.
160. Assreuy, J., F. Q. Cunha, F. Y. Liew, and S. Moncada. 1993. Feedback inhibition of nitric oxide synthase activity by nitric oxide. *British Journal of Pharmacology* 108:833-837.
161. Stamler, J. S., D. I. Simon, J. A. Osborne, M. E. Mullins, O. Jaraki, T. Michel, D. J. Singel, and J. Loscalzo. 1992. S-nitrosylation of proteins with nitric oxide: Synthesis and characterization of biologically active compounds. *Proceedings of the National Academy of Science USA* 89:444-448.
162. Stamler, J. S., O. Jaraki, J. Osborne, D. I. Simon, J. Keaney, J. Vita, D. Singel, C. R. Valeri, and J. Loscalzo. 1992. Nitric oxide circulates in mammalian plasma primarily as an S-nitroso adduct of serum albumin. *Proceedings of the National Academy of Science USA* 89:7674-7677.
163. Jia, L., C. Bonaventura, and J. S. Stamler. 1995. S-Nitrosohemoglobin: A new transport function of arterial erythrocytes involved in regulation of blood pressure. *Endothelium* 3:S6 (Abstract)
164. Lander, H. M., P. K. Sehajpal, and A. Novogrodsky. 1993. Nitric oxide signaling: A possible role for G proteins. *Journal of Immunology*. 151:7182-7187.
165. Vedia, L. M., B. McDonald, B. Reep, B. Brune, M. Di Silvio, T. R. Billiar, and E. G. Lapetina. 1992. Nitric oxide-induced S-nitrosylation of glyceraldehyde-3-phosphate dehydrogenase inhibits enzymatic activity and increases endogenous ADP-ribosylation. *Journal of Biological Chemistry*. 267:24929-24932.

166. Stamler, J. S., D. J. Simon, O. Jaraki, J. A. Osborne, S. Francis, M. Mullins, D. Singel, and J. Loscalzo. 1992. S-nitrosylation of tissue-type plasminogen activator confers vasodilatory and antiplatelet properties on the enzyme. *Proceedings of the National Academy of Science USA* 89:8087-8091.
167. Abate, C., L. Patel, I. I. I. Rauscher FJ, and T. Curran. 1990. Redox regulation of Fos and Jun DNA-binding activity in vitro. *Science* 249:1157-1161.
168. Matthews, J. R., C. H. Botting, M. Panico, H. R. Morris, and R. T. Hay. 1996. Inhibition of NF- $\kappa$ B DNA binding by nitric oxide. *Nucleic Acids Research* 24:2236-2242.
169. Laval, F. and D. A. Wink. 1994. Inhibition by nitric oxide of the repair protein, O6-methylguanine- DNA-methyltransferase. *Carcinogenesis* 15:443-447.
170. Arnette, D. R. and J. S. Stamler. 1995. NO<sup>+</sup>, NO<sup>•</sup>, and NO<sup>-</sup> donation by S-nitrosothiols: Implications for regulation of physiological functions by S-nitrosylation and acceleration of disulfide formation. *Archives of Biochemistry and Biophysics* 318:279-285.
171. Orgel, L. E. 1963. The Chemical Basis of Mutation. *Advances in Enzymology* 27:289-346.
172. Routledge, M. N., D. A. Wink, L. K. Keefer, and A. Dipple. 1993. Mutations induced by saturated aqueous nitric oxide in the pSP189 supF gene in human Ad293 and E. Coli MBM7070 cells. *Carcinogenesis* 14:1251-1254.
173. Routledge, M. N., F. J. Mirsky, D. A. Wink, L. K. Keefer, and A. Dipple. 1994. Nitrite-induced mutations in a forward mutation assay: Influence of nitrite concentration and pH. *Mutation Research - Genetic Toxicology* 322:341-346.
174. Routledge, M. N., D. A. Wink, L. K. Keefer, and A. Dipple. 1994. DNA sequence changes induced by two nitric oxide donor drugs in the supF assay. *Chemical Research in Toxicology* 7:628-632.

175. Nguyen, T., D. Brunson, C. L. Crespi, B. W. Penman, J. S. Wishnok, and S. R. Tannenbaum. 1992. DNA damage and mutation in human cells exposed to nitric oxide *in vitro*. *Proceedings of the National Academy of Science USA* 89:3030-3034.
176. Moriguchi, M., L. R. Manning, and J. M. Manning. 1992. Nitric oxide can modify amino acid residues in proteins. *Biochemical and Biophysical Research Communications* 183:598-604.
177. Beckman, J. S., H. Ischiropoulos, L. Zhu, M. Van der Woerd, C. Smith, J. Chen, J. Harrison, J. C. Martin, and M. Tsai. 1992. Kinetics of superoxide dismutase- and iron-catalyzed nitration of phenolics by peroxynitrite. *Archives of Biochemistry and Biophysics* 298:438-445.
178. Lepoivre, M., F. Fieschi, J. Coves, L. Thelander, and M. Fontcave. 1991. Inactivation of ribonucleotide reductase by nitric oxide. *Biochemical and Biophysical Research Communications* 179:442-448.
179. Lepoivre, M., J. M. Flaman, and Y. Henry. 1992. Early loss of the tyrosyl radical in ribonucleotide reductase of adenocarcinoma cells producing nitric oxide. *Journal of Biological Chemistry*. 267:22994-23000.
180. Lepoivre, M., J. M. Flaman, P. Bobe, G. Lemaire, and Y. Henry. 1994. Quenching of the tyrosyl free radical of ribonucleotide reductase by nitric oxide. Relationship to cytostasis induced in tumor cells by cytotoxic macrophages. *Journal of Biological Chemistry*. 269:21891-21897.
181. Rubbo, H., R. Radi, M. Trujillo, R. Telleri, B. Kalyanaraman, S. Barnes, M. Kirk, and B. A. Freeman. 1994. Nitric oxide regulation of superoxide and peroxynitrite-dependent lipid peroxidation. Formation of novel nitrogen-containing oxidized lipid derivatives. *Journal of Biological Chemistry*. 269:26066-26075.
182. Munday, R. and C. C. Winterbourn. 1989. Reduced glutathione in combination with superoxide dismutase as an important biological antioxidant defence mechanism. *Biochemical Pharmacology* 38:4349-4352.

183. Ferguson, M. A. J. 1992. Glycosyl-phosphatidylinositol membrane anchors: The tale of a tail. *Biochemical Society Transactions* 20:243-256.
184. Yim, C. Y., N. R. Bastian, J. C. Smith, J. B. Hibbs Jr, and W. E. Samlowski. 1993. Macrophage nitric oxide synthesis delays progression of ultraviolet light- induced murine skin cancers. *Cancer Research* 53:5507-5511.
185. Nathan, C. F. and J. B. Hibbs Jr. 1991. Role of nitric oxide synthesis in macrophage antimicrobial activity. *Current Opinion in Immunology* 3:65-70.
186. Ziche, M., L. Morbidelli, E. Masini, S. Amerini, H. J. Granger, C. A. Maggi, P. Geppetti, and F. Ledda. 1994. Nitric oxide mediates angiogenesis in vivo and endothelial cell growth and migration *in vitro* promoted by substance P. *Journal of Clinical Investigation* 94:2036-2044.
187. Lander, H. M., P. Sehajpal, D. M. Levine, and A. Novogrodsky. 1993. Activation of human peripheral blood mononuclear cells by nitric oxide- generating compounds. *Journal of Immunology*. 150:1509-1516.
- 188.. Anonymous 1996. Cytotoxic Effector Cells. "In Advanced Immunology" Male, D., A. Cooke, M. Owen, J. Trowsdale, and B. Champion Eds. Mosby, London, England. 15.1-15.13.
189. Roitt, I. 1994. Essential Immunology. Blackwell Science, Oxford.
190. Kaneto, H., J. Fujii, Han Geuk Seo, K. Suzuki, T. A. Matsuoka, M. Nakamura, H. Tatsumi, Y. Yamasaki, T. Kamada, and N. Taniguchi. 1995. Apoptotic cell death triggered by nitric oxide in pancreatic beta- cells. *Diabetes* 44:733-738.
191. Fehsel, K., K. D. Kroncke, K. L. Meyer, H. Huber, V. Wahn, and V. KolbBachofen. 1995. Nitric oxide induces apoptosis in mouse thymocytes. *Journal of Immunology*. 155:2858-2865.
192. Sandoval, M., X. J. Zhang, X. Liu, E. E. Mannick, D. A. Clark, and M. J. S. Miller. 1997. Peroxynitrite-induced apoptosis in T84 and RAW 264.7 cells: Attenuation by L-Ascorbic acid. *Free Radical Biology and Medicine* 22:489-495.

193. Mitrovic, B., L. J. Ignarro, H. V. Vinters, M. A. Akers, J. Schmid, C. Uittenbogaart, and J. E. Merrill. 1995. Nitric oxide induces necrotic but not apoptotic cell death in oligodendrocytes. *Neuroscience* 65:531-539.
194. Bonfoco, E., D. Krainc, M. Ankarcrona, P. Nicotera, and S. A. Lipton. 1995. Apoptosis and necrosis: Two distinct events induced, respectively, by mild and intense insults with N-methyl-D-aspartate or nitric oxide/superoxide in cortical cell cultures. *Proceedings of the National Academy of Science USA* 92:7162-7166.
195. CharriautMarlangue, C., I. Margaill, F. Borrega, M. Plotkine, and Y. BenAri. 1996. N(G)-Nitro-L-arginine methyl ester reduces necrotic but not apoptotic cell death induced by reversible focal ischemia in rat. *European Journal of Pharmacology* 310:137-140.
196. Radi, R., M. Rodriguez, L. Castro, and R. Telleri. 1994. Inhibition of mitochondrial electron transport by peroxynitrite. *Archives of Biochemistry and Biophysics* 308:89-95.
197. Miles, A. M., D. S. Bohle, P. A. Glassbrenner, B. Hansert, D. A. Wink, and M. B. Grisham. 1996. Modulation of superoxide-dependent oxidation and hydroxylation reactions by nitric oxide. *Journal of Biological Chemistry*. 271:40-47.
198. Kiderlen, A. F. and P. M. Kaye. 1990. A modified colorimetric assay of macrophage activation for intracellular cytotoxicity against Leishmania parasites. *Journal of Immunological Methods* 127:11-18.
199. Wink, D. A., I. Hanbauer, M. C. Krishna, W. DeGraff, J. Gamson, and J. B. Mitchell. 1993. Nitric oxide protects against cellular damage and cytotoxicity from reactive oxygen species. *Proceedings of the National Academy of Science USA* 90:9813-9817.
200. Kaye, P. M., N. J. Rogers, A. J. Curry, and J. C. Scott. 1994. Deficient expression of co-stimulatory molecules on Leishmania-infected macrophages. *European Journal of Immunology* 24:2850-2854.

201. Reiner, S. L., S. Zheng, Z. E. Wang, L. Stowring, and R. M. Locksley. 1994. *Leishmania* promastigotes evade interleukin 12 (IL-12) induction by macrophages and stimulate a broad range of cytokines from CD4+ T cells during initiation of infection. *Journal of Experimental Medicine* 179:447-456.
202. Jiang, X., B. Leonard, R. Benson, and C. L. Baldwin. 1993. Macrophage control of *Brucella abortus*: Role of reactive oxygen intermediates and nitric oxide. *Cellular Immunology* 151:309-319.
203. Berens, R. L., R. Brun, and S. M. Krassner. 1976. A simple monophasic medium for axenic culture of haemoflagellates. *Journal of Parasitology* 62:360-365.
204. Churchill, T. A., C. J. Green, and B. J. Fuller. 1995. Protective properties of amino acids in liver preservation: Effects of glycine and a combination of amino acids on anaerobic metabolism and energetics. *Journal of Hepatology* 23:720-726.
205. Strehler, B. L. 1974. Adenosine 5'-triphosphate and creatine phosphate. Determination with Luciferase. *Methods of Enzymatic Analysis*. H. U. Bergmeyer, editor. Academic Press, 2112-2126.
206. Sambrook, J., E. F. Fritsch, and T. Maniatis. 1989. *Molecular Cloning - a laboratory manual*. Cold Spring Harbor Laboratory Press, New York.
207. Chen, M., S. B. Christensen, J. Blom, E. Lemmich, L. Nadelmann, K. Fich, T. G. Theander, and A. Kharazmi. 1993. Licochalcone A, a novel antiparasitic agent with potent activity against human pathogenic protozoan species of *Leishmania*. *Antimicrobial Agents and Chemotherapy* 37:2550-2556.
208. Fairlamb, A. H. 1989. Novel biochemical pathways in parasitic protozoa. *Parasitology* 99:S93-S112.
209. Daubener, W., S. Nockemann, M. Gutsche, and U. Hadding. 1995. Heparin inhibits the antiparasitic and immune modulatory effects of human recombinant interferon-gamma. *European Journal of Immunology* 25:688-692.

210. Green, S. J., L. F. Scheller, M. A. Marletta, M. C. Seguin, F. W. Klotz, M. Slayter, B. J. Nelson, and C. A. Nancy. 1994. Nitric Oxide: Cytokine-regulation of nitric oxide in host resistance to intracellular pathogens. *Immunology Letters* 43:87-94.
211. Bogle, R. G., A. R. Baydoun, J. D. Pearson, and G. E. Mann. 1996. Regulation of L-arginine transport and nitric oxide release in superfused porcine aortic endothelial cells. *Journal of Physiology* 490:229-241.
212. Ingram, 1939. The endogenous respiration of *bacillus aureus*. II. The effect of salts on the rate of absorption of oxygen. *Journal of Bacteriology* 38:613
213. Adams, L. B., J. B. Hibbs Jr, R. R. Taintor, and J. L. Krahenbuhl. 1990. Microbiostatic effect of murine-activated macrophages for *Toxoplasma gondii*. Role for synthesis of inorganic nitrogen oxides from L- arginine. *Journal of Immunology*. 144:2725-2729.
214. Stadler, J., R. D. Curran, J. B. Ochoa, B. G. Harbrecht, R. A. Hoffman, R. L. Simmons, and T. R. Billiar. 1991. Effect of endogenous nitric oxide on mitochondrial respiration of rat hepatocytes *in vitro* and *in vivo*. *Archives of Surgery* 126:186-191.
215. Murphy, K. M., A. B. Heimberger, and D. Y. Loh. 1990. Induction by antigen of intrathymic apoptosis of CD4+CD8+TCR(lo) thymocytes *in vivo*. *Science* 250:1720-1723.
216. Shapiro, R. and S. H. Pohl. 1968. The reaction of ribonucleosides with nitrous acid. side products and kinetics. *Biochemistry* 7:448-455.
217. Handbook of Fluorescent Probes and Research Chemicals 1996. R. P. Haugland, editor. Molecular probes Inc. 585-589.
218. Miyauchi, S., M. Komatsubara, and N. Kamo. 1992. In archaebacteria, there is a doxorubicin efflux pump similar to mammalian P-glycoprotein. *Biochimica et Biophysica Acta - Biomembranes* 1110:144-150.

219. Darzynkiewicz, Z., L. StaianoCoico, and M. R. Melamed. 1981. Increased mitochondrial uptake of rhodamine 123 during lymphocyte stimulation. *Proceedings of the National Academy of Science USA* 78:2383-2387.
220. Wiese, M. and U. Seydel. 1995. Monitoring of drug effects on cultivable mycobacteria and *Mycobacterium leprae* via the determination of their adenylate energy charges (AEC). *Journal of Microbiological Methods* 24:65-80.
221. Lancaster JR Jr, J. M. Langrehr, H. A. Bergonia, N. Murase, R. L. Simmons, and R. A. Hoffman. 1992. EPR detection of heme and nonheme iron-containing protein nitrosylation by nitric oxide during rejection of rat heart allograft. *Journal of Biological Chemistry*. 267:10994-10998.
222. Welter, R., L. Yu, and C. A. Yu. 1996. The effects of nitric oxide on electron transport complexes. *Archives of Biochemistry and Biophysics* 331:9-14.
223. Sherman, I. W. 1979. Biochemistry of *Plasmodium* (malarial parasites). *Microbiological Reviews* 43:453-495.
224. Eun Ah Cho, M. P. Riley, A. L. Sillman, and H. Quill. 1993. Altered protein tyrosine phosphorylation in anergic  $T_H1$  cells. *Journal of Immunology*. 151:20-28.
225. Lee, S. T., C. Tarn, and K. P. Chang. 1993. Characterization of the switch of kinetoplast DNA minicircle dominance during development and reversion of drug resistance in *Leishmania*. *Mol. Biochem. Parasitol.* 58:187-203.
226. Pacelli, R., D. A. Wink, J. A. Cook, M. C. Krishna, W. DeGraff, N. Friedman, M. Tsokos, A. Samuni, and J. B. Mitchell. 1995. Nitric oxide potentiates hydrogen peroxide-induced killing of *Escherichia coli*. *Journal of Experimental Medicine* 182:1469-1479.
227. Wink, D. A., I. Hanbauer, F. Laval, J. A. Cook, M. C. Krishna, and J. B. Mitchell. 1994. Nitric oxide protects against the cytotoxic effects of reactive oxygen species. *Annals of the New York Academy of Sciences* 738:265-278.

228. Robertson, C. D. and G. H. Coombs. 1992. Stage-specific proteinases of *Leishmania mexicana mexicana* promastigotes. *FEMS Microbiology Letters* 94:127-132.
229. Coombs, G. H., D. T. Hart, and J. Capaldo. 1982. Proteinase inhibitors as antileishmanial agents. *Transactions of the Royal Society of Tropical Medicine and Hygiene* 76:660-663.
230. Proudfoot, L., P. Schneider, M. A. J. Ferguson, and M. J. McConville. 1995. Biosynthesis of the glycolipid anchor of lipophosphoglycan and the structurally related glycoinositolphospholipids from *Leishmania major*. *Biochemical Journal* 308:45-55.
231. Blank, C., C. Bogdan, C. Bauer, K. Erb, and H. Moll. 1996. Murine epidermal Langerhans cells do not express inducible nitric oxide synthase. *European Journal of Immunology* 26:792-796.
232. Stenger, S., N. Donhouse, H. Thüring, M. Röllinghoff, and C. Bogdan. 1996. Reactivation of latent leishmaniasis by inhibition of inducible nitric oxide synthase. *Journal of Experimental Medicine* 183:1501-1514.
233. del Pozo, V., E. de Arruda-Chaves, B. de Andres, B. Cardaba, A. Lopez-Farre, S. Gallardo, I. Cortegano, L. Vidarte, A. Jurado, J. Sastre, P. Palomino, and C. Lahoz. 1997. Eosinophils transcribe and translate messenger RNA for inducible nitric oxide synthase. *Journal of Immunology*. 158:859-864.
234. von Brand, T. and E. M. Johnson. 1947. A comparative study of the effect of cyanide on the respiration of some trypanosomidae. *Journal of Cellular and Comparative Physiology* 29:33-49
235. Fairlamb, A. H. and F. R. Opperdoes. 1986. Carbohydrate metabolism in African trypanosomes, with special reference to the glycosome. In "Carbohydrate metabolism in cultured cells". M. J. Morgan, editor. Plenum Publishing Corporation, 183-224.
236. Blum, J. J. 1993. Intermediary metabolism of *Leishmania*. *Parasitology Today* 9:118-122.

237. Smeenk, R. J. T., J. H. M. Berden, and A. J. G. Swaak. 1996. dsDNA autoantibodies. In "Autoantibodies". J. B. Pcter and Y. Shoenfeld, editors. Elsevier Science, 227-236.
238. Xu, D. and F. Y. Liew. 1994. Genetic vaccination against leishmaniasis. *Vaccine* 12:1534-1536.
239. Xu, D. and F. Y. Liew. 1995. Protection against leishmaniasis by injection of DNA encoding a major surface glycoprotein, gp63, of *L. major*. *Immunology* 84:173-176.
240. Waite, G. J. and D. P. McManus. 1995. Nucleic acids: Vaccines of the future. *Parasitology Today* 11:113-116.
241. Pardoll, D. M. and A. M. Beckerleg. 1995. Exposing the immunology of naked DNA vaccines. *Immunity* 3:165-169.
242. Lindahl, T. and A. Andersson. 1972. Rate of chain breakage at apurinic sites in double stranded DNA. *Biochemistry* 11:3618-3623.
243. Bastian, N. R., C. Y. Yim, J. B. Hibbs Jr, and W. F. Samlowski. 1994. Induction of iron-derived EPR signals in murine cancers by nitric oxide. Evidence for multiple intracellular targets. *Journal of Biological Chemistry*. 269:5127-5131.
244. Berens, R.L., E.C. Krug and J. J. Marr. 1995. Purine and pyrimidine metabolism. In "Biochemistry and Molecular Biology of Parasites" Academic Press Ltd., London. 89-119.
245. Hassan, H. F. and G. H. Coombs. 1988. Purine and pyrimidine metabolism in parasitic protozoa. *FEMS Microbiology Reviews* 54:47-84.
246. McConville, M. J., P. Schneider, L. Proudfoot, C. Masterson and M. A. J. Ferguson. 1994. The developmental regulation and biosynthesis of GPI-related structures in *Leishmania* parasites. *Brazilian Journal of Medical and Biological Research* 27:139-144.

247. Monroy-Ostria, A., I. Fuentes-Fraga, C. Garcia-Flores, and L. Favila-Castillo. 1994. Infection of BALB/c, C57Bl/6 mice and F1 hybrid CB6F1 mice with strains of *Leishmania mexicana* isolated from Mexican patients with localized or diffuse cutaneous leishmaniasis. *Archives of Medical Research* 25:401-406.
248. Santhamma, K. R., A. Bhaduri. 1995. Characterization of the respiratory chain of *Leishmania donovani* promastigotes. *Molecular and Biochemical Parasitology* 75:43-53.
249. van Dam, K. and E. C. Slater. 1967. A suggested mechanism of uncoupling of respiratory chain phosphorylation. *Proceedings of the National Academy of Science USA* 58:2015-2019.



1950  
MAY 10 1950  
LIBRARY